



## **Turnover and transport of greenhouse gases in a Danish wetland**

### **Effects of water level changes and plant-mediated gas transport on N<sub>2</sub>O production, consumption and emission dynamics**

Jørgensen, Christian Juncher

*Publication date:*  
2011

*Document version*  
Early version, also known as pre-print

*Citation for published version (APA):*  
Jørgensen, C. J. (2011). *Turnover and transport of greenhouse gases in a Danish wetland: Effects of water level changes and plant-mediated gas transport on N<sub>2</sub>O production, consumption and emission dynamics.*



# Turnover and transport of greenhouse gases in a Danish wetland

Effects of water level changes and plant-mediated gas transport on  $N_2O$  production, consumption and emission dynamics

PhD Thesis  
Christian Juncher Jørgensen  
Academic advisor: Bo Elberling



# **Turnover and transport of greenhouse gases in a Danish wetland**

-

**Effects of water level changes and plant-mediated gas  
transport on N<sub>2</sub>O production, consumption and emission  
dynamics**

PhD thesis by  
**Christian Juncher Jørgensen**  
September 2011

Supervisor  
Prof. Bo Elberling

Department of Geography and Geology  
The PhD School of Science, Faculty of Science  
University of Copenhagen  
Denmark.



**PhD Thesis**

Christian Juncher Jørgensen

Academic supervisor

Prof. Bo Elberling

Department of Geography and Geology

Faculty of Science, University of Copenhagen

Denmark

September 2011

**Front cover**

Gas flux measurements at the Maglemeden field site.

Photography and cover art by Kent Pørksen.

## Preface

This PhD thesis consists of a synopsis and the following four papers listed according to the date of publication:

Paper 1 - Askaer, L., Elberling, B., Friberg, T., *Jørgensen C.J.*, Hansen B.U (2011) **Plant-mediated CH<sub>4</sub> transport and C gas dynamics quantified in-situ in a *Phalaris arundinacea*-dominant wetland**, Plant and Soil, Vol. 43, pp. 287-301. (Accepted 07-01-2011)

Paper 2 - Elberling, B., Askaer, L., *Jørgensen, C.J.*, Joensen, H.P., Kuhl, M., Glud, R.N., Lauritsen, F.R. (2011) **Linking Soil O<sub>2</sub>, CO<sub>2</sub>, and CH<sub>4</sub> Concentrations in a Wetland Soil: Implications for CO<sub>2</sub> and CH<sub>4</sub> Fluxes**, Environmental Science & Technology, Vol. 45, pp. 3393-3399 (Accepted 24-02-2011)

Paper 3 - *Jørgensen, C.J.*, Struwe, S., Elberling, B. (2011) **Temporal trends in N<sub>2</sub>O flux dynamics in a Danish wetland – effects of plant-mediated gas transport of N<sub>2</sub>O and O<sub>2</sub> following changes in water level and soil mineral-N availability**, Global Change Biology, doi:10.1111/j.1365-2486.2011.02485.x. (Accepted 15-06-2011)

Paper 4 - *Jørgensen, C.J.* and Elberling, B. (2011) **Flooding-induced N<sub>2</sub>O production, consumption and emission dynamics in wetland soil**, Submitted to Global Change Biology 22-08-2011.

The PhD study was conducted in the period May 2008 to September 2011 with primary funding from the Faculty of Science, University of Copenhagen, Denmark. The main focus of this PhD study is to establish new and improved knowledge on spatiotemporal aspects in N-transformation processes leading to production, consumption and emission of nitrous oxide (N<sub>2</sub>O) in a Danish wetland, with a vantage point of the academic disciplines of soil science and physical geography. The research activities were supported and carried out in close cooperation with research on oxygen (O<sub>2</sub>) availability and carbon gas dynamics of carbon dioxide (CO<sub>2</sub>) and methane (CH<sub>4</sub>) conducted within the framework of “**Oxygen availability controlling the dynamics of buried organic carbon pools and greenhouse gas emissions**” and paved the way for the on-going research project “**Nitrous oxide dynamics: The missing links between controls on subsurface N<sub>2</sub>O production/consumption and net atmospheric emissions**” both funded by the Danish Natural Science Research Council (PI: B.E.).

## Resumé

Natural wetlands act as both sources and sinks of greenhouse gases such as carbon dioxide (CO<sub>2</sub>), methane (CH<sub>4</sub>) and nitrous oxide (N<sub>2</sub>O) from the soil to the atmosphere. Production and consumption of these gases in the soil are controlled by a series of highly dynamic and interrelated processes involving plants, soil and microorganisms. These processes are regulated by different physio-chemical drivers such as soil moisture content, soil temperature, nutrient and oxygen (O<sub>2</sub>) availability. In wetlands, the position of the free standing water level (WL) influences the spatiotemporal variation in these drivers, thereby influencing the net emission or uptake of greenhouse gas.

In this PhD thesis the complex aspects in the exchange of N<sub>2</sub>O across the soil-atmosphere is investigated with special focus on the spatiotemporal variations in drivers for N<sub>2</sub>O production and consumption in the soil and their relation to observed flux patterns. It is demonstrated how the seasonal variations in N<sub>2</sub>O emissions are linked to the subsurface concentrations of N<sub>2</sub>O at the capillary fringe above the WL by regulating the apparent diffusion rates of oxygen (O<sub>2</sub>) into the soil which availability regulates sequential nitrification-denitrification processes in the soil.

It is shown that fast acting N-transformation processes both produce and consume large concentration of N<sub>2</sub>O over short distances in response to rapid WL variations, and that these processes are crucial for explaining the spatiotemporal variation in observed net N<sub>2</sub>O dynamics.

Similarly, plant-mediated gas transport by the subsurface aerating macrophyte *Phalaris arundinacea* played a major part in regulating and facilitating emissions of greenhouse gases across the soil-atmosphere interface.

It is concluded that the spatiotemporal distribution of dominating N<sub>2</sub>O producing and consuming processes below the surface, in combination with the variations in the diffusive exchange rates due to soil water content and apparent diffusivity, control the magnitude and timing of N<sub>2</sub>O emissions to the atmosphere in close connection with the plant-mediated gas transport. It is evident, that the inclusion of the aboveground biomass in these types of flux measurements is essential to avoid significant underestimations of net N<sub>2</sub>O fluxes, whereas an inadequate sampling frequency or non-uniform temporal coverage could impose an undesirable bias to the net flux estimates.

## Sammendrag

Naturlige vådområder er i stand til at både frigive og optage kuldioxid (CO<sub>2</sub>), metan (CH<sub>4</sub>) og lattergas (N<sub>2</sub>O), der alle fungerer som drivhusgasser i atmosfæren. Produktion og forbrug af disse drivhusgasser i jordsystemer er reguleret af flere dynamiske og indbyrdes afhængige processer, hvor samspillet mellem jordforhold, plantevækst og mikrobiel aktivitet spiller en væsentlig rolle. Processerne er styret af forskellige fysiske og kemiske regulatorer såsom jordvandsindhold, jordtemperatur, næringsstof- og ilttilgængelighed, hvis tidlige og rumlige indflydelse på gasfluksdynamikken selv er styret af sæsonvariationer i dybden til det terrænnære sekundære grundvandspejl.

Et af hovedformålene i denne PhD afhandling er at kvantificere den rumlige og tidlige dynamik i produktionen og forbruget af N<sub>2</sub>O i et uopdyrket dansk vådområde, og relatere denne dynamik til sæsonmæssige frigivelser og/eller optag af N<sub>2</sub>O. En tæt sammenhæng blev demonstreret mellem de sæsonmæssige variationer i N<sub>2</sub>O frigivelser og dybdefordelingen af lattergaskoncentrationer i området ved det kapillære grænselag umiddelbart over det frie vandspejl. Det blev demonstreret, at tidlige variationer i den effektive diffusionrate er et styrende parameter for iltnedtrængningen gennem dette kapillære grænselag, hvilket påvirker koblede nitrifikation-denitrifikations processer i jordsystemet.

En særdeles hurtig respons på hurtige vandspejlsændringer blev vist gældende for processerne der styrer produktionen og forbruget af N<sub>2</sub>O i jorden, hvilket har stor betydning for den rumlige og tidlige variation i frigivelserne af den dannede N<sub>2</sub>O. Det blev derudover påvist, at vådbundsplanten *Phalaris arundinacea*, der er karakteriseret ved at have luftfyldt aerenkym-væv, spillede en afgørende rolle for gas transporten ved at fungere som passiv luftvej for N<sub>2</sub>O i frigivelsen fra jord til atmosfære.

Det konkluderes, at den tidlige og rumlige variation i de processer der regulerer produktionen og forbruget af N<sub>2</sub>O i jorden, sammen med plantetransport og de tidlige variationer i effektive diffusionsrater i forbindelse med ændringer i jordvandsindholdet, er styrende faktorer for både størrelsesordenen og den tidlige fordeling i udvekslingen af N<sub>2</sub>O mellem jorden og atmosfæren. Det konkluderes desuden, at inkludering af den overjordiske plantebiomasse er nødvendig for at undgå markante underestimeringer af N<sub>2</sub>O frigivelserne, samt at en for sporadisk målefrekvens i fluksmålinger vil kunne medføre en u hensigtsmæssig påvirkning af det samlede nettoresultat.





# CONTENTS

<b>1 - INTRODUCTION .....</b>	<b>1</b>
<b>2 - N<sub>2</sub>O DYNAMICS IN NATURAL WETLANDS.....</b>	<b>3</b>
2.1 SUBSURFACE CONTROLS OF N <sub>2</sub> O PRODUCTION, CONSUMPTION AND EMISSION	4
2.1.1 <i>Effects of water level on production, consumption and emission rates</i>	5
2.1.2 <i>Effects of soil temperature on activity and emission rates</i>	6
2.1.3 <i>Effects of O<sub>2</sub> availability for N-transformation processes</i>	6
2.1.4 <i>Plant-soil interactions on N-transformation</i>	8
2.2 GAS TRANSPORT MECHANISMS ACROSS THE SOIL-ATMOSPHERE INTERFACE	10
2.3 POTENTIAL ECOSYSTEM PERTUBATIONS OF LAND-USE AND CLIMATE CHANGE	11
2.4 STUDY OBJECTIVE	12
<b>3 - FIELD SITE AND SELECTED METHODOLOGY.....</b>	<b>13</b>
3.1 THE MAGLEMOSEN FIELD SITE	13
3.2 O <sub>2</sub> METHODOLOGY	16
3.3 N <sub>2</sub> O METHODOLOGY	17
3.4 MICROSENSOR N <sub>2</sub> O AND O <sub>2</sub> METHODOLOGY	19
<b>4 - RESEARCH PAPER SUMMARIES.....</b>	<b>21</b>
4.1 SUMMARY OF PAPER 1	21
4.2 SUMMARY OF PAPER 2	22
4.3 SUMMARY OF PAPER 3	23
4.4 SUMMARY OF PAPER 4	24
<b>5 - CONCLUSIONS AND OUTLOOK.....</b>	<b>25</b>
5.1 GAS TRANSPORT MECHANISMS ACROSS THE SOIL-ATMOSPHERE INTERFACE	
5.2 SPATIOTEMPORAL N <sub>2</sub> O FLUX DYNAMICS IN RELATION TO SEASONAL WL VARIATIONS	26
5.3 FLOODING INDUCED N <sub>2</sub> O EMISSIONS	27
5.4 SUBSURFACE GAS DYNAMICS IN RESPONSE TO WATER LEVEL VARIATIONS	28
5.5 SUBSURFACE PRODUCTION AND COMSUMPTION DYNAMICS	31
5.6 GREENHOUSE GAS BUDGETS AND POTENTIAL CLIMATIC FEEDBACKS	32
5.7 APPLIED SCOPE AND PERSPECTIVES	34
<b>6 - ACKNOWLEDGEMENTS.....</b>	<b>35</b>
<b>7 - REFERENCE LIST.....</b>	<b>37</b>
<b>APPENDIX 1 - ERRATA FOR PAPER 1</b>	<b>47</b>
<b>APPENDIX 2 - THE PHD THESIS - RULES AND REQUIREMENTS</b>	<b>49</b>
<b>APPENDIX 3 - CO-AUTHOR STATEMENTS</b>	<b>51</b>
<b>ANNEX I-IV .....</b>	<b>57</b>



# 1 - Introduction

Natural wetlands are found in all climatic zones on Earth from the arctic tundra to tropical wetlands and act as half-way worlds between terrestrial and aquatic ecosystems with specific characteristics from each (Gopal and Ghosh, 2008). Natural wetlands accumulate and store large amounts of reactive carbon (C) and nitrogen (N) due to slow decomposition rates of buried soil organic matter (SOM) when the soils are oxygen (O<sub>2</sub>) depleted. Natural wetland ecosystems modify the amounts of important greenhouse gases in the atmosphere by acting as either sources or sinks of these gases across the soil-atmosphere interface. A huge variety of microorganisms in wetland soils have the ability to mobilize and transform the buried C and N pools with resulting production and consumption of carbon dioxide (CO<sub>2</sub>), methane (CH<sub>4</sub>) and nitrous oxide (N<sub>2</sub>O) in the soil. Depending on the environmental soil conditions, a net exchange of these greenhouse gases can occur across the soil-atmosphere interface with different climatic impacts.

N<sub>2</sub>O is an important greenhouse gas with a lifetime of approximately 114 years in the atmosphere and a global warming potential of approximately 298 times that of carbon dioxide (CO<sub>2</sub>) (IPCC, 2007). In recent years, emissions of N<sub>2</sub>O has received increasing attention due to its role in both global warming (IPCC, 2007) and the destruction of stratospheric ozone (Chipperfield, 2009; Ravishankara *et al.* 2009). Terrestrial emissions of N<sub>2</sub>O across the soil-atmosphere take place from both natural and agricultural ecosystems. Over the last 150 years, the average atmospheric concentration of N<sub>2</sub>O has increased from ~270 ppbv in the preindustrial era to ~320 ppbv today (IPCC, 2007; Davidson, 2009) primarily due to the use if agricultural fertilizers.

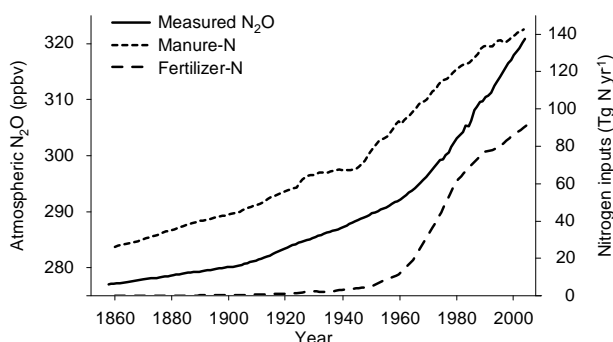


**Figure 1** Historical reconstruction of atmospheric N<sub>2</sub>O concentrations and annual input of agricultural N to terrestrial ecosystems. (Modified from Davidson, 2009)

While agricultural land areas are the largest source of terrestrial N<sub>2</sub>O emissions, natural wetlands have been documented as significant sources of N<sub>2</sub>O to the atmosphere (Regina *et al.* 1996a; Aerts

and Ludwig, 1997; Liikanen and Martikainen, 2003; Bedard-Haughn *et al.* 2006; Zhu *et al.* 2008; Dinsmore *et al.* 2009; Repo *et al.* 2009; Danevcic *et al.* 2010; Pennock *et al.* 2010). However, detailed knowledge on the dynamics of both the spatiotemporal variability on an hourly or sub-diurnal time scale and environmental drivers of seasonal N<sub>2</sub>O emissions have been limited by the relative scarce numbers of field studies in natural wetlands using in high-resolution sampling frequency strategies (Rochette and Eriksen-Hamel, 2008).

It is therefore still an open question whether the future changes in the thermal and hydrological state of natural wetlands will lead to larger net sink or net source scenarios (Arneth *et al.* 2010; Cantarel *et al.* 2011). Improved knowledge on spatiotemporal greenhouse gas dynamics is relevant for understanding the natural feedback of greenhouse gas exchange across the soil-atmosphere interface from wetlands under both current and future climatic conditions as well as providing the basis for improved modelling of future climate change (Smith, 1997). The quantification of processes controlling gas exchange across the soil-atmosphere interface requires improved knowledge at a high spatiotemporal resolution about the physical mass transfer properties of the soil system and the complex biogeochemical interactions in plant-soil-microbe processes and plant-mediated gas transport. Uncertainty exists on the role of plants for conveying N<sub>2</sub>O across the soil-atmosphere interface. How this gas exchange responds to fast acting environmental drivers is poorly understood and efforts using near-continuous measurements in highest possible temporal resolution are needed to capture the real-time dynamics of these gas transport mechanism. Also, uncertainty exists on how the spatial zonation of N<sub>2</sub>O producing and consuming processes is linked to temporal variations in process drivers and surface emissions. Resolving this uncertainty could involve micro-scale measurements of both physical mass transfer properties and gas concentration profiles leading to production rate modelling of subsurface gas dynamics and surface emissions. Only by coupling subsurface processes to emissions under fluctuating soil moisture conditions will the mechanisms regulating greenhouse gas emissions from wetland soils clarified.

This PhD thesis addresses the knowledge gap on how the spatiotemporal N<sub>2</sub>O emission dynamics from a natural non-managed Danish wetland overgrown with the subsurface aerating macrophyte *Phalaris arundinacea* is linked to subsurface N-transformation processes, and how these respond to variations in environmental process drivers following seasonal variations in the water level. This particular wetland type was chosen since it represents an ecosystem which is prone to significant future modifications following perturbations of the general water balance and temperature regime.

## 2 - N<sub>2</sub>O dynamics in natural wetlands

Conditions favouring N<sub>2</sub>O production in wetland soils are sensitive to seasonal and interannual weather patterns which affect the soil moisture content, position of the water level (WL) - defined as the depth from the surface to the free-standing position of the secondary groundwater body closest to the surface - and seasonal growth pattern of subsurface aerating wetland macrophytes, such as *Phalaris arundinacea*. Together these parameters regulate O<sub>2</sub> transport into the soil and determine both the timing and the location of anoxic zones and thereby the nature of N-transformation processes and N<sub>2</sub>O production, consumption and emission. Following global warming these conditions will be subject to changes potentially affecting net N<sub>2</sub>O fluxes from the soil to the atmosphere.

A conceptual model of plant-soil-microbe interactions involved in the N<sub>2</sub>O dynamics in a natural wetland ecosystem with *P. arundinacea* as dominating plant cover is shown in Figure 2 with boxed grey numbers indicating zone of relevance for the following sub-chapters.

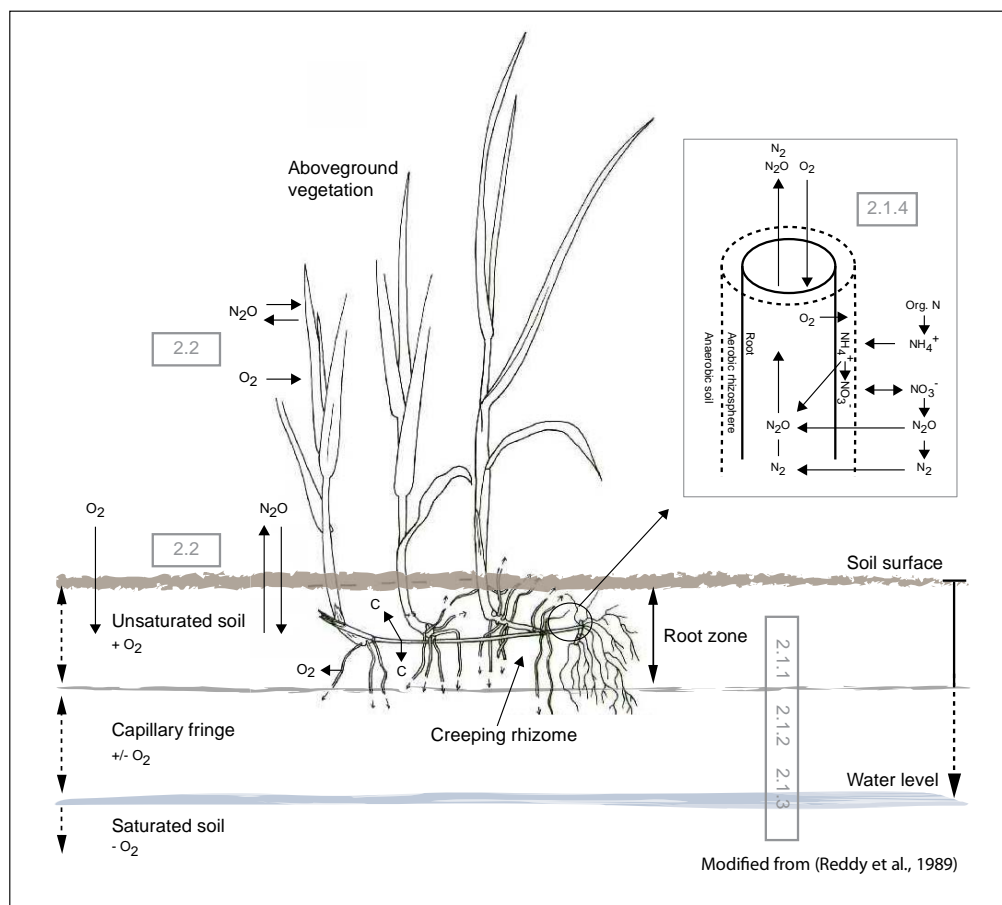


**Figure 2** Conceptual model of relevant plant-soil-microbe interactions. Insert shows processes involved in sequential nitrification-denitrification in the root zone. Subsurface O<sub>2</sub> availability in the soil is influenced by O<sub>2</sub> diffusion across the soil surface and O<sub>2</sub> loss from the plant roots, from which exudation of C compounds also occurs. N<sub>2</sub>O emissions occur as fluxes across the soil-atmosphere interface and by plant-mediated gas transport. The seasonally variable position of the WL and capillary fringe above it are indicated by dotted arrows.



The potential N<sub>2</sub>O reduction capacity of microorganisms in the soil and root zone can under certain conditions produce sub-ambient N<sub>2</sub>O concentrations, creating a negative flux gradient into the soil which then functions as a net sink of atmospheric N<sub>2</sub>O. The conditions promoting N<sub>2</sub>O consumption in the soil and the environmental drivers for N<sub>2</sub>O deposition from the atmosphere to the soil are yet to be consistently identified. While denitrification is considered the most important process for N<sub>2</sub>O uptake, the roles of NO<sub>3</sub><sup>-</sup> availability, soil pH, temperature and soil moisture as well as O<sub>2</sub> pressure are much less clear (Chapuis-Lardy *et al.* 2007; Vieten *et al.* 2008).

## **2.1 Subsurface controls of N<sub>2</sub>O production, consumption and emission**

Production and consumption of N<sub>2</sub>O in soil occurs primarily through the microbial processes of aerobic nitrification and anaerobic denitrification (Robertson and Tiedje, 1987; Firestone and Davidson, 1989). Dominance of these processes are linked to soil moisture content and O<sub>2</sub> availability in the soil, as well as the presence of labile N and carbon (C) in the soil (Davidson, 1991; Skiba and Smith, 2000; Liikanen and Martikainen, 2003; Andersen and Petersen, 2009). The soil moisture content affects both the diffusion rates of dissolved species and soil gases, the amount of dissolved N<sub>2</sub>O in the soil solution, the rate of microbial N<sub>2</sub>O production and consumption and the amplitude of diurnal soil temperature variations (Blackmer *et al.* 1982; Clough *et al.* 2005). Similarly, the availability of O<sub>2</sub> in the subsoil controls where and when both gaseous intermediate and terminal reaction products will be produced and consumed in the soil profile.

The diffusive exchange of N<sub>2</sub>O across the soil-atmosphere interface is greatly enhanced when the position of the capillary fringe above the WL moves down through the root zone and increasing numbers of previously water-filled macropores become air-filled. This promotes improved diffusive mass loss through the root zone porosity and decreases the residence time of N<sub>2</sub>O in subsoil which lowers the potential for full reduction of N<sub>2</sub>O to N<sub>2</sub> (Clough *et al.* 2005; Chapuis-Lardy *et al.* 2007) The improved potential for subsoil oxygenation via air-filled macropores will, in combination with plant mediated O<sub>2</sub> release to the root zone, stimulate nitrification of NH<sub>4</sub><sup>+</sup> to NO<sub>3</sub><sup>-</sup> in the presence of labile carbon exudates from the plant roots (Edwards *et al.* 2006). This can potentially increase N<sub>2</sub>O production rates or even lead to N<sub>2</sub>O reductase inhibition at the higher O<sub>2</sub> pressures at the capillary fringe (Betlach and Tiedje, 1981), resulting in a concentration build up of N<sub>2</sub>O, which could be emitted to the atmosphere. To complicate matters, certain subsurface aerating wetland macrophytes can modify N-transformation processes and N<sub>2</sub>O emissions by actively providing the

N-transforming microorganisms in the soil profile with O<sub>2</sub> and labile organic C compounds (van Noordwijk *et al.* 1998; Bastviken *et al.* 2005), as well as transporting the soil gases across the soil-atmosphere interface through aerenchymous plant tissue (Reddy *et al.* 1989; Yu and Chen, 2009). In combination, these drivers make up a complex system of both synergistic and antagonistic interrelated processes, producing net N<sub>2</sub>O emission patterns which are likely to vary significantly over space and time.

### 2.1.1 Effects of water level on production, consumption and emission rates

Wetlands are characterized by having the free standing water level (WL) close to the surface and near saturated soil moisture conditions during extended periods of the year resulting in high accumulation rates of organic C and N. Soil moisture is a key regulator for diffusion of O<sub>2</sub> into the soil by lowering the diffusion rate of O<sub>2</sub> by a factor 10<sup>4</sup> (Meronigal *et al.* 2003). Natural lowering of the WL increases the air-filled porespace fraction and improves the O<sub>2</sub> availability in near-surface layers, which affects the decomposition rates of soil organic matter and the transformation rates of soil mineral-N. Minor changes in the total content and distribution of soil water films influences the effective diffusion rates of O<sub>2</sub> giving rise to the formation of anaerobic microsites within an otherwise oxidized soil matrix (Strong and Fillery, 2002; Vieten *et al.* 2009). When wetland soils are flooded the rate of respiratory O<sub>2</sub> demand by soil microbes typically outweighs the rate of diffusive influx of atmospheric O<sub>2</sub> to the soil resulting in the formation of anaerobic soil conditions (Meronigal *et al.* 2003).

Seasonal variations in soil moisture and subsurface O<sub>2</sub> availability following WL fluctuations are strong determinants for soil conditions determining N<sub>2</sub>O production, consumption and transport, thereby exerting a major control on these processes in the soil (Heincke and Kaupenjohann, 1999; Clough *et al.* 2005). The existence of a delicate N<sub>2</sub>O regulatory mechanism influenced by the position of the WL has been demonstrated in a number of studies with contrasting results in terms of the effects of lowered water levels on N<sub>2</sub>O emission (Martikainen *et al.* 1993; Kliewer and Gilliam, 1995; Regina *et al.* 1996b; Velthof *et al.* 1996; Aerts and Ludwig, 1997; Regina *et al.* 1999; Glatzel *et al.* 2008; Jungkunst *et al.* 2008; Dinsmore *et al.* 2009; Danevcic *et al.* 2010; Berglund and Berglund, 2011).

Rapid natural shifts from naturally drained to fully flooded soil moisture conditions in wetland soil limit subsurface O<sub>2</sub> availability and provide improved conditions for N<sub>2</sub>O production via denitrification by depletion of the soil NO<sub>3</sub><sup>-</sup> pool followed by N<sub>2</sub>O emissions. However, the duration and magnitude of these flooding induced N<sub>2</sub>O emissions remain unclear and the temporal linkages between the surface emission dynamics of N<sub>2</sub>O in response to both slow and rapid changes in WL and subsurface N<sub>2</sub>O concentrations need to be determined for determining the potential role of future increased flooding intensity on net annual N<sub>2</sub>O emissions.

### *2.1.2 Effects of soil temperature on activity and emission rates*

Like most other biological processes, the rates of N<sub>2</sub>O production and consumption increase with increasing temperatures. The rate changes as a consequence of raising the temperature 10°C for these processes (Q<sub>10</sub> coefficient) are typically a factor 2-3, but coefficients up to 9 have been demonstrated (Skiba and Smith, 2000; Maag and Vinther, 1996; Blackmer *et al.* 1982). However, the links between predictable temperature dependent reaction rates increases and surface emissions are not necessarily straight-forward and contrasting effects of soil temperature on surface emissions rates of N<sub>2</sub>O have been reported (Blackmer *et al.* 1982; Skiba and Smith, 2000; Müller *et al.* 2004; Smith, 1997; Martikainen *et al.* 1993; Flechard *et al.* 2005). If variations in soil temperatures are to have an unambiguous effect on microbial activity rates and N<sub>2</sub>O emissions, the soil moisture conditions have to be within a certain range. If the soil is either suboptimally dry or excessively wet, the temperature stimulated activity rates may be retarded due to moisture stress and O<sub>2</sub> depletion (Laiho, 2006) indicating that the net effects of climate change on N<sub>2</sub>O emissions will have to be investigated in the combined changes of the temperature regime energy and water balance.

### *2.1.3 Effects of O<sub>2</sub> availability for N-transformation processes*

Microbial C and N transformation processes in peat soil governing the production and consumption of N<sub>2</sub>O are sensitive to the availability of both O<sub>2</sub> and inorganic nutrients for microbial growth (Aerts and Ludwig, 1997; Bollmann and Conrad, 1998; Khalil *et al.* 2004) and linked to the decomposition of soil organic matter and release of previously occluded NH<sub>4</sub><sup>+</sup> (Laiho, 2006). The O<sub>2</sub> dependency of N transformation processes that lead to N<sub>2</sub>O production has been extensively documented in the scientific literature over the past decades. For example, it is evident that, when the processes are studied in isolation, O<sub>2</sub> concentrations above a certain threshold will inhibit both denitrification of NO<sub>3</sub><sup>-</sup> to N<sub>2</sub> and dissimilatory NO<sub>3</sub><sup>-</sup> reduction to NH<sub>4</sub><sup>+</sup> (DNRA) with resulting

concentration build up of N<sub>2</sub>O in the soil. Similarly, when O<sub>2</sub> availability is unrestricted, rapid transformation of NH<sub>4</sub><sup>+</sup> to NO<sub>3</sub><sup>-</sup> via nitrification is likely going to happen if nitrifying bacteria are present, with production of N<sub>2</sub>O as reaction intermediate. Several comprehensive reviews of potentially relevant N-transformation processes which might promote the formation of N<sub>2</sub>O in the soil are available in the literature, e.g. (Parkin and Tiedje, 1984; Tiedje *et al.* 1983; Betlach and Tiedje, 1981; Firestone *et al.* 1980; Robertson and Tiedje, 1987; Smith and Patrick Jr, 1983; Khalil *et al.* 2004; Bollmann and Conrad, 1998; Wrage *et al.* 2001; Megonigal *et al.* 2003). A common trait for most of these O<sub>2</sub> sensitive N-transformation processes is, that the presence or absence of O<sub>2</sub> itself is not the agent which facilitates the actual N-transformation, but its availability regulates the microbial expression of relevant catalyzing enzymes needed to get the electron transfers happening at any significant rate (Firestone *et al.* 1980; Betlach and Tiedje, 1981; Tiedje *et al.* 1983; Korner and Zumft, 1989; Dendooven and Anderson, 1994; Bollmann and Conrad, 1998; Baek and Shapleigh, 2005).

Knowledge on the O<sub>2</sub> sensitivity of individual processes under controlled conditions is highly valuable for understanding the fundamental processes of N<sub>2</sub>O production and consumption in soil isolates. In field scale investigations where the level of complexity increases with the number of interrelated and interacting processes taking place more or less simultaneously, it will be highly challenging to predict open system N<sub>2</sub>O dynamics by the sum of the isolated process responses. For example, when conditions in the root zone of certain wetland macrophytes alternate between oxic and anoxic conditions the production of N<sub>2</sub>O is controlled by sequential nitrification-denitrification reactions (Patrick and Reddy, 1976; Smith and Patrick Jr, 1983; Firestone and Davidson, 1989; Bodelier *et al.* 1996). In these reactions, NH<sub>4</sub><sup>+</sup> from the anaerobic zone of the soil diffuses into the oxic part of the root zone, where it is either taken up by the plants or oxidized into NO<sub>3</sub><sup>-</sup>, which can be taken up by the plants or diffuses into the adjacent anaerobic zones where it is denitrified into N<sub>2</sub> (Reddy *et al.* 1989) or reduced into N<sub>2</sub>O if soil conditions are suboptimal for full denitrification (Firestone and Davidson, 1989; Davidson, 1991).

The net N<sub>2</sub>O output from the sequential reactions are coupled to competition between plant-microbe O<sub>2</sub> and NO<sub>3</sub><sup>-</sup> demand, which is modified by rhizodeposition of labile organic C compounds and radial oxygen loss from plant roots (Kaye and Hart, 1997; Engelaar *et al.* 1995; Rubinigg *et al.* 2002; Jones *et al.* 2004; Sasikala *et al.* 2009). These interactions may lead to highly contrasting redox-conditions in the soil within a spatial scale of few hundred μm, resulting in the formation of

anaerobic microsites, where conditions for the production of N<sub>2</sub>O are especially favourable. Such N<sub>2</sub>O hotspots are especially pronounced near sources of organic carbon such as roots or detritus and leads to notorious high spatial variation in N<sub>2</sub>O production and consumption rates (Megonigal *et al.* 2003).

#### 2.1.4 Plant-soil interactions on N-transformation

Many wetland plants possess characteristics which allow them to survive periodic flooding and the accompanying changes in soil chemistry when O<sub>2</sub> is depleted. Upon flooding, plants are not only faced by the lowered diffusive influx rates of atmospheric O<sub>2</sub>, but also a substantial demand for O<sub>2</sub> by roots, soil micros and other reductants in the soil (Pezeshki, 2001). Many wetland plants, e.g. *Phalaris arundinacea*, have developed aerenchymous tissue in the roots, stems and leaves which facilitates transport of O<sub>2</sub> to the roots needed for aerobic respiration and oxidation of reducing compounds in the rhizosphere (Brix and Sorrell, 1996; Colmer, 2003; Cook and Knight, 2003; Kercher and Zedler, 2004; Sasikala *et al.* 2009). In this way, roots and rhizomes obtain O<sub>2</sub> via plant internal gas transport of atmospheric or photosynthetically produced O<sub>2</sub> (Armstrong *et al.* 1994; Wiessner *et al.* 2002).

In wetlands, labile organic carbon is supplied by root exudation by plant roots and is used as carbon and energy source for a wide number of heterotrophic bacteria (Jones *et al.* 2004). The availability of labile carbon is known to be a rate limiting factor for both denitrification and overall O<sub>2</sub> consumption rates (Megonigal *et al.* 2003; Bastviken *et al.* 2005). Depending on plant species and growth stage, an average of 10-25% of the photosynthetically assimilated C may be translocated to the roots and exuded to the surrounding soil in concentrations as high as 15-20 mg L<sup>-1</sup> (Zhu and Sikora, 1995; Edwards *et al.* 2006). As the C assimilation rate in photosynthesis is dependent on the amount of incoming solar radiation in the photosynthetically active radiation spectrum (PAR spectrum), it is likely that root exudation rates of organic C compounds are linked to variations in incoming PAR radiation, with the potential of modifying O<sub>2</sub> availability and N<sub>2</sub>O production/consumption processes when these are rate limited by C availability.

O<sub>2</sub> regulated mineral N-transformation via sequential or coupled nitrification-denitrification in the root zone have been demonstrated for a number of different aquatic macrophytes (Patrick and Reddy, 1976; Reddy *et al.* 1989; Kuenen and Robertson, 1994; Engelaar *et al.* 1995; Russow *et al.*



2000; Kirk and Kronzucker, 2005). Since the process of O<sub>2</sub> release from the roots is, at least partially, light driven (Wiessner *et al.* 2002), it is likely that the rate of the nitrification-denitrification sequence could exhibit strong diurnal variations in response to changes in incoming solar radiation. In addition to functioning as a zone of ongoing transformation of NH<sub>4</sub><sup>+</sup> and NO<sub>3</sub><sup>-</sup> into various N-containing soil gases, the root zone can act as diffusion or reduction barrier to N<sub>2</sub>O present in deeper layers in the soil profile, if the denitrifying activity rates are sufficiently high or the residence time in the root zone sufficiently long.

Although not yet documented for *P. arundinacea* and therefore somewhat speculative, it has been hypothesized that plants may produce N<sub>2</sub>O in vivo during N assimilation (Yu and Chen, 2009). For plants to assimilate N into amino acid and proteins they need to convert NO<sub>3</sub><sup>-</sup> taken up by the roots from the soil solution into NH<sub>4</sub><sup>+</sup>. One theory is that N<sub>2</sub>O emitted from plant leaves can be generated in the process of nitrite (NO<sub>2</sub><sup>-</sup>) reduction to NH<sub>4</sub><sup>+</sup> in the chloroplasts, with N<sub>2</sub>O as potential intermediate product (Dean and Harper, 1986; Smart and Bloom, 2001; Hakata *et al.* 2003). Accumulation of NO<sub>2</sub><sup>-</sup> during NO<sub>3</sub><sup>-</sup> assimilation could be a cause of N<sub>2</sub>O production and release, by which toxic NO<sub>2</sub><sup>-</sup> is removed (Yu and Chen, 2009). Since the expression of NO<sub>3</sub><sup>-</sup> reductase genes is light-dependent and light energy is involved in the assimilation of NO<sub>3</sub><sup>-</sup> in plants (Yu and Chen, 2009), it is likely that the temporal dynamics of plant internally produced N<sub>2</sub>O could exhibit a strong diurnal variation in response to changes in incoming solar radiation functioning in parallel with photosynthesis. To complicate matters even more, it has been suggested that certain plants, by some undefined mechanism, may absorb N<sub>2</sub>O directly from the atmosphere (Lensi and Chalamet, 1981; Chen *et al.* 1997; Yu and Chen, 2009; Li *et al.* 2011), in a process which could be affected by variations in soil moisture content (Li *et al.* 2011).

Wetland plants such as *P. arundinacea* function as important “ecological engineers” (Tanner, 2001) by regulating the diurnal variations in input of both O<sub>2</sub> and labile organic C into the root zone where important N-transformation processes take place. Still, the temporal nature and variation of these plant and soil interactions and their net implications for seasonal variations in N<sub>2</sub>O emission dynamics are still open questions. Answers to these questions are highly relevant for predicting changes in N<sub>2</sub>O emissions from natural wetlands in response to future changes in seasonal WL dynamics and plant growth of subsurface aerating macrophytes affecting subsurface aeration, SOM decomposition and nutrient availability for both plants and N<sub>2</sub>O producers and consumers in the soil.

## **2.2 Gas transport mechanisms across the soil-atmosphere interface**

Gases can be transported between terrestrial ecosystems and the atmosphere in several ways. The most intensively described transport mechanism pathway is the diffusive exchange between gases in the soil and gases in the atmosphere, where the gas exchange and gas movement within the soil profile follow the concentration gradient as described by Fick's first law of diffusion (Stumm and Morgan, 1996; Borggaard and Elberling, 2007). In recent years, the role of plant-mediated trace gas exchange between the soil and the atmosphere has received increasingly more attention as it becomes evident that plants may significantly affect gas emission rates (Lensi and Chalamet, 1981; Mosier *et al.* 1990; Armstrong *et al.* 1996; Chen *et al.* 1997; Chang *et al.* 1998; Rusch and Rennenberg, 1998; Reddy *et al.* 1989; Müller, 2003; Rückauf *et al.* 2004; Garnet *et al.* 2005; Pihlatie *et al.* 2005; Cheng *et al.* 2007; Yu and Chen, 2009; Li *et al.* 2011).

Transport of N<sub>2</sub>O between the soil and the atmosphere by terrestrial plants is believed to occur via two major pathways: (1) N<sub>2</sub>O transport in the gas phase through plant internal airspaces in the aerenchyma and (2) transport of dissolved N<sub>2</sub>O in the liquid phase through the transpiration stream (Chang *et al.* 1998; Müller, 2003; Yu and Chen, 2009). Plant-mediated gas transport through the aerenchyma can be driven both by molecular diffusion along the concentration gradient and by pressurized light-enhanced convective through-flow (Armstrong and Armstrong, 1990; Brix *et al.* 1994; Shannon *et al.* 1996; Colmer, 2003; Sorrell and Brix, 2003). Both plant mediated transport mechanisms are sensitive to variations in incoming solar radiation. Variations in stomatal conductance is the primary control on gas transport by molecular diffusion, where the plants can be compared to a light sensitive valve which open or closes in response to the degree of incoming PAR (Joabsson *et al.* 1999). This valve like mechanism could produce more or less pronounced diurnal variations in the timing and magnitude of plant mediated gas fluxes.

In the case of light-enhanced convective through-flow, emission peaks are typically observed following the rapid onset of daylight where the soil gases are flushed from the stem and rhizome air space, where it had accumulated during the dark hours (Garnet *et al.* 2005; Armstrong and Armstrong, 1990). Irrespective of the plant-internal gas transport mechanism, plant-mediated gas transport can promote elevated and highly variable soil gas emissions over time and space by means of rapid gas exchange, when the potential CH<sub>4</sub> oxidizing or N<sub>2</sub>O reducing capacities of the root zone is bypassed.

### **2.3 Potential ecosystem perturbations of land-use and climate change**

Long term increases in variations in air and soil temperature will not only affect the rates of microbial C and N transformations in the soil (Conant *et al.* 2011; Larsen *et al.* 2011), but also the successional changes in the composition of the vegetation and length of active growing season (Martikainen *et al.* 1993; Laiho, 2006). Changes in species composition of wetland plant will affect the water balance due to alterations in seasonal water consumption and evapotranspiration, changing the conditions for subsoil aeration and transport of dissolved substances as well as imposing increased moisture stress to soil ecosystems. How these changes will influence future N<sub>2</sub>O sink or source dynamics is largely unknown but appear increasingly relevant to quantify, in the light of increasing number of wetland restorations and constructed wetlands with the introduction of subsurface aerating wetland plants such as *P. arundinacea* as biofuel crops in northern wetlands (Zhu and Sikora, 1995; Katterer *et al.* 1998; Rückauf *et al.* 2004; Adams and Galatowitsch, 2005; Hyvoenen *et al.* 2009; Maltais-Landry *et al.* 2009; Smeets *et al.* 2009; Jin *et al.* 2010).

In northern Europe, future climate change is predicted to change towards longer and drier warm periods with a change in precipitation patterns where periods with increased temperature and little precipitation are interrupted by more intensive precipitation events (IPCC, 2007; Energistyrelsen, 2008). How these changes will actually manifest themselves are a matter of controversy, but it seems plausible that future changes in precipitation patterns will result in an amplification of seasonal WL dynamics in non-managed wetlands (Kim *et al.* 2008) compared to what is currently observed. Whether this potential amplification of seasonal WL dynamics and increased flooding frequency will lead to higher N<sub>2</sub>O emissions from natural wetlands, thereby acting as a positive feedback to climate change is difficult to predict without an improved understanding of the spatiotemporal dynamics of current N<sub>2</sub>O emissions in response to seasonal and episodic WL fluctuations.

## **2.4 Study objectives**

The microbial N transformation processes which govern the production and consumption of N<sub>2</sub>O in the soil are sensitive to the combined influences from a complex and interrelated system of processes where plant-soil-microbe relations modifies both reaction rates and gas fluxes across the soil-atmosphere interface. In the search for a better understanding of the links between the current spatiotemporal variability in N<sub>2</sub>O surface emissions and subsurface N-transformation processes in response to a fluctuating water level under both current and future climatic conditions this PhD thesis aims to:

- (1) Determine the main transport mechanisms of gas across the soil-atmosphere interface in a non-managed Danish wetland with a dominating vegetation cover of *Phalaris arundinacea* (paper 1, 2 & 3).
- (2) Relate the spatiotemporal dynamics in current N<sub>2</sub>O flux patterns in response to seasonal changes in the water level (paper 3 & 4)
- (3) Evaluate the temporal nature and total contribution of flooding induced N<sub>2</sub>O emissions to net annual N<sub>2</sub>O emissions from a non-managed Danish wetland (paper 4).
- (4) Explore the linkages between subsurface gas concentrations of O<sub>2</sub>, N<sub>2</sub>O, and dissolved mineral-N in response to seasonal water level variations (paper 2, 3 & 4).
- (5) Quantify and model the subsurface O<sub>2</sub> and N<sub>2</sub>O production and consumption dynamics over time at different soil depths using: (i) observed in situ gas concentrations and apparent gas diffusivity measurements (paper 2), (ii) high-resolution microsensors profiles of subsurface N<sub>2</sub>O and O<sub>2</sub> concentrations in a controlled laboratory flooding experiment (paper 4) and (iii) soil sample incubation (paper 3).
- (6) Quantify the net annual greenhouse gas budget for CO<sub>2</sub>, CH<sub>4</sub> and N<sub>2</sub>O relevant for evaluating the climatic impacts and potential positive feedbacks to climate change of the annual N<sub>2</sub>O flux budget and flooding induced N<sub>2</sub>O emissions (paper 1, 4)

## 3 - Field site and selected methodology

### 3.1 The Maglemosen field site

The Maglemosen experimental site is a non-managed minerotrophic wetland located approximately 20 km north of Copenhagen, Denmark (55°51'N, 12°32'E). In the Atlantic Period, ~8.800 to ~5.000 before present, the area was covered by the Littorina Sea. At approximately 5.000 years ago, a slow uplift of the land-area caused the shallow inlet fjord to close at its eastern fringe creating a shallow freshwater lake which turned into an overgrown wetland as organic detritus accumulated as peat (Fig. 3.1). The average elevation at the experimental field site is approximately 2.5 m above m.s.l.

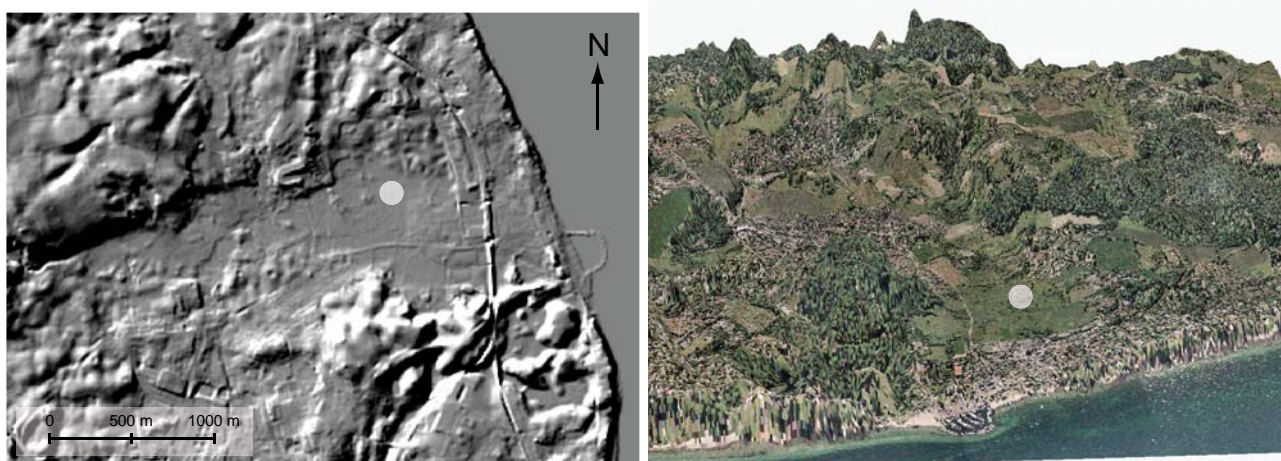


**Figure 3.1** Digital hillshade model indicating the extent of the Maglemosen basin (left) and pseudo-3D visualization of the wetland and its surroundings (right; 15 time vertical exaggeration). The location of the experimental site is shown by a grey dot.

Histosols cover the majority of the area with peat depths ranging from 0-3 m. According to USDA soil taxonomy, the soil can be classified as a Fibric Haplohemist with udic soil moisture regime and mesic temperature regime. The average peat thickness is approximately 45 to 55 cm with the main root zone occupying the upper 25-30 cm. Soil porosity in the peat layers ranges from 70 to 80% by volume. Bulk density decreases gradually from 0.25 at the surface to 0.40 g cm<sup>-3</sup> at 60 cm depth. The peat total organic C content ranges from 23 to 29%, while total N ranges from 1.8 to 2.4% resulting in peat C:N ratios of 10 to 12 (Fig. 3.2). At a depth of approximately 60 cm the sediment changes from peat to carbonate rich organic silt extending to ~80 cm below the surface. The organic material in the top 0.6 m of the peat soil was deposited during the filling up of the freshwater lake by plant detritus. Radiocarbon dating of macrofossils from the top soil layers have showed that the upper 30 cm of peat has been deposited within the last 40 years, with an average recent accumulation rate of 730 g C m<sup>-2</sup> yr<sup>-1</sup> (Paper 1).



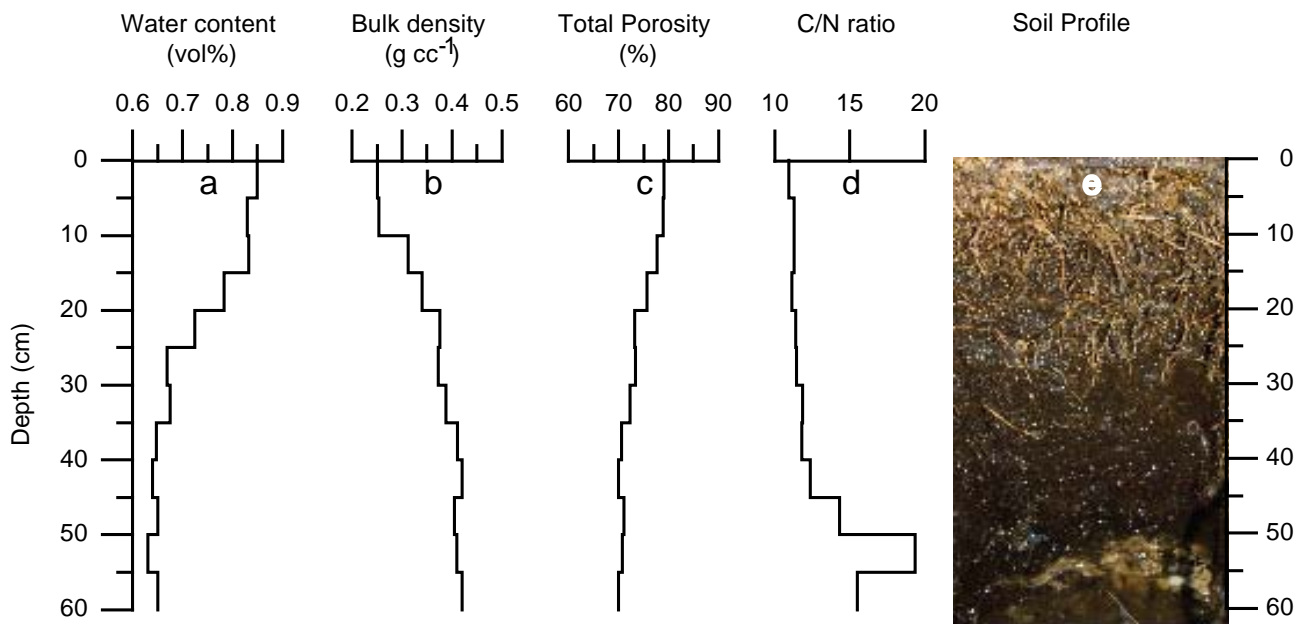


Figure 3.2 Overview of soil properties and soil profile picture (Sample date: 05-03-2010): (a) Soil moisture profile (vol %) under fully flooded conditions, (b) Bulk density profile ( $\text{g cc}^{-1}$ ), (c) Calculated total porosity (%), (d) C/N ratio and (e) picture of soil profile. The upper 50-55 cm is dominated by peat deposits with the main root zone occupying the top 25-30 cm. Carbonate rich organic silt is the dominating deposit at a depth of 55-60 cm.

Mean annual air temperature at the field site is approximately  $8\text{ }^{\circ}\text{C}$ . Figure 3.3 shows a 7 days moving average of the air temperature in the period March 2007 to August. The duration of the growing season in the individual years, defined as a 7 day moving average of daily air temperature  $> 5\text{ }^{\circ}\text{C}$  (Jin *et al.* 2010), can be seen as the part of temperature graph above the  $5\text{ }^{\circ}\text{C}$  isoline (dotted grey line).

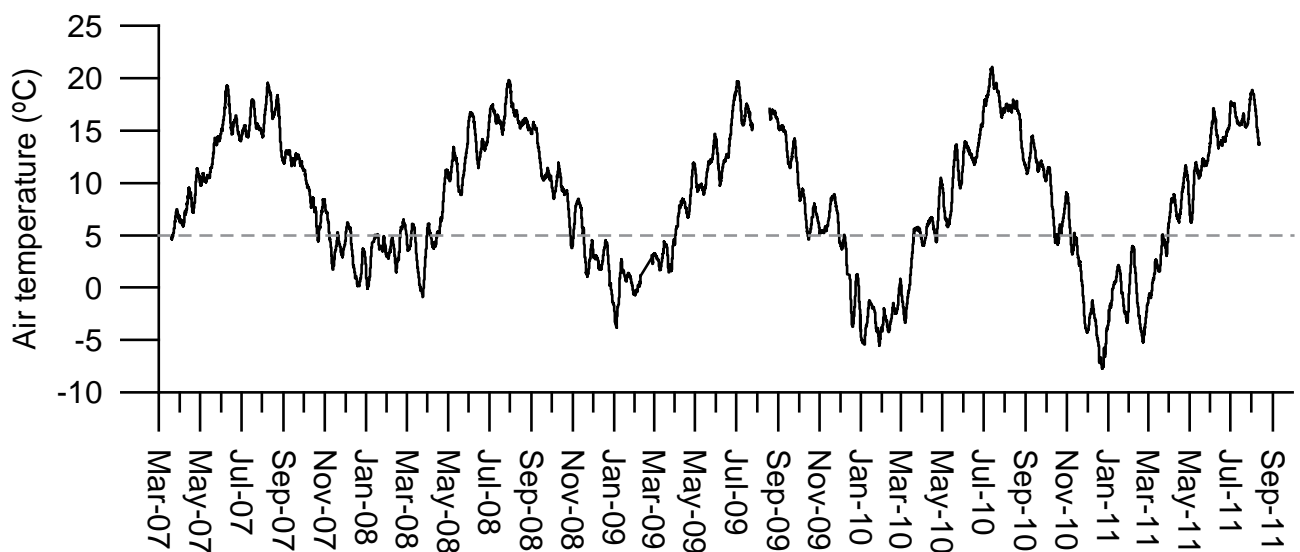


Figure 3.3 Seven days moving average of measured air temperature (2m) in the period March 2007 to August 2011.

The maximum annual amplitude of the WL has been measured to be approximately 100 cm in the period since continuous logging was started in July 2008 (Fig. 3.4). Normal average annual precipitation is 618 mm (1960-1990 normal period, Danish Meteorological Institute) with large annual and seasonal variations. Liquid precipitation has been measured at the Maglemosen field site since July 2008 (Fig. 3.4). Maximum daily precipitation in the Maglemosen data record was 129 mm on 14<sup>th</sup> August 2010.

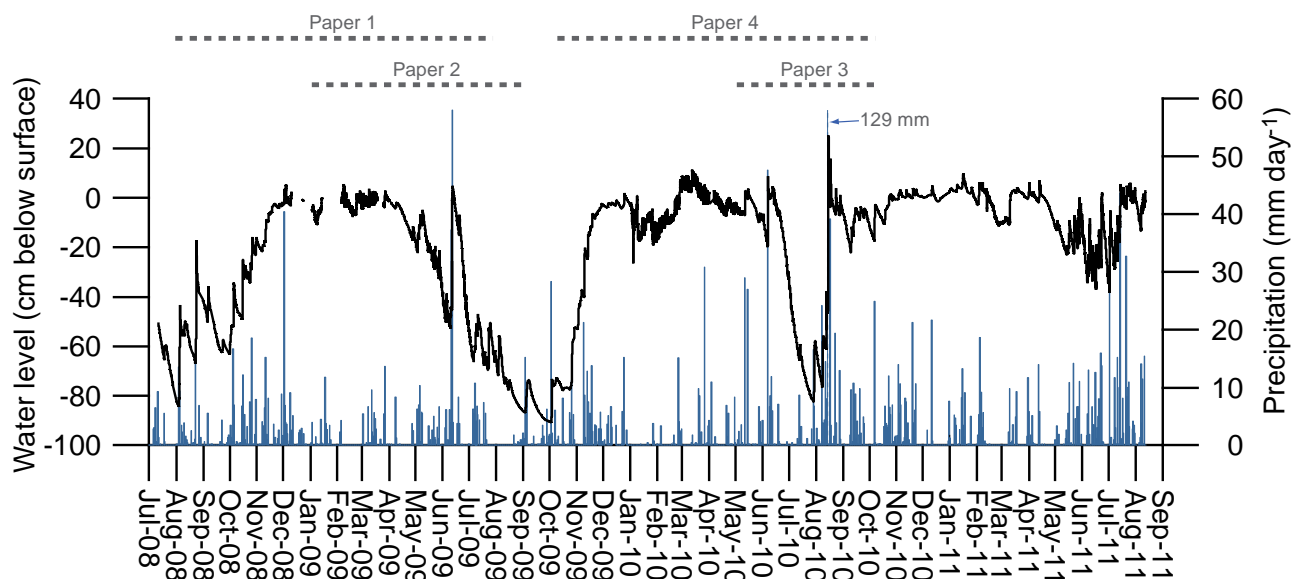


Figure 3.4 Position of the free standing water level and daily liquid precipitation in the period 07-2008 to 08-2011. (Note: Precipitation in water equivalents from snow fall is not included). Investigation periods of each of the 4 research papers are shown by dotted grey lines above main graphs.

### 3.2 O<sub>2</sub> methodology

Measurements of subsurface O<sub>2</sub> concentrations were conducted using permanently buried oxygen probes in which a sensor foil on the tip of an optical fibre is excited by light in the blue wave spectrum whereby it emits light in the red wave spectrum. When O<sub>2</sub> is present at the sensor tip the energy of the excited molecule is transferred by collision with O<sub>2</sub> instead as being emitted as return light (PreSens GmbH; [www.presens.de](http://www.presens.de); Germany). The amount of emitted light can be converted to an O<sub>2</sub> concentration using a modified Stern-Volmer equation after correction for depth-specific soil temperature at the time of measurement.

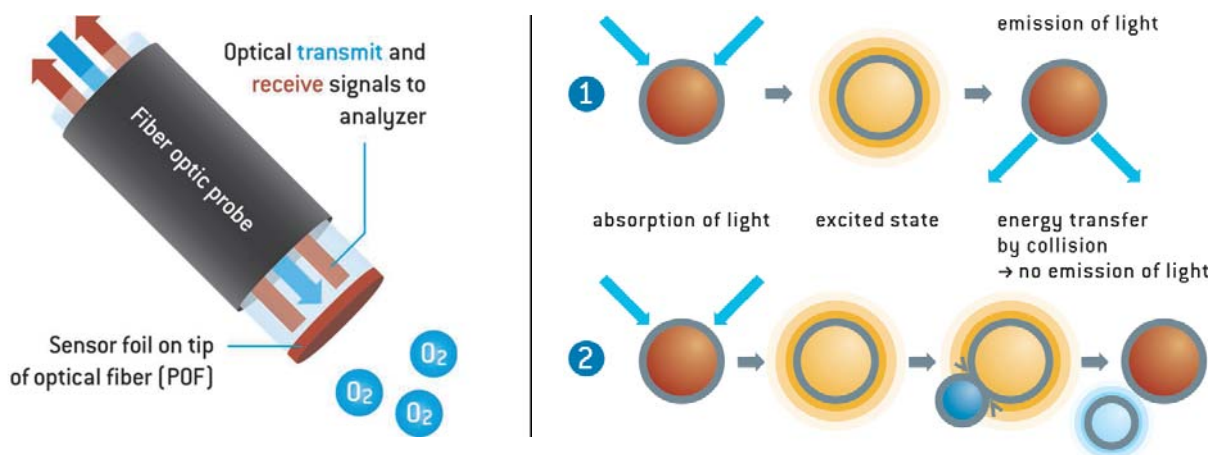


Figure 3.5 Operating principle of oxygen probe (see explanation in-text; source: [www.presens.de](http://www.presens.de))

The technique is non-consuming, robust and offers real-time high-temporal resolution measurement (sampling frequency > 1 min) but offers limited information about spatial heterogeneity in soil aeration or anaerobic microsites under changing soil water conditions, i.e. as could be detected by 2-D planar optodes (Askaer *et al.* 2010).

### 3.3 N<sub>2</sub>O flux methodology

Automated closed static chamber methodology was used for the measurements of the gas exchange of CO<sub>2</sub>, CH<sub>4</sub> and N<sub>2</sub>O across the soil-atmosphere interface in order to obtain near continuous temporal resolution of the flux estimates. The methodology has been proven in a variety of ecosystems and climatic zones with known strengths and weaknesses (Loftfield *et al.* 1992; Velthof and Oenema, 1995; Ambus and Robertson, 1998; Yamulki and Jarvis, 1999; Flessa *et al.* 2002; Flechard *et al.* 2005; Holst *et al.* 2008; Akiyama *et al.* 2009; Yao *et al.* 2009; Wolf *et al.* 2010)

The flux chambers were constructed from transparent 6 mm polycarbonate sheets and permanently installed in steel frames in an area with a uniform stand of *P. arundinacea*, at an average elevation of 2.5 m above mean sea level. The chambers were fitted with both inlet and outlet tube connectors. During measurements, air from the chamber headspace was from the chamber to the gas analysers in a closed and pressure tight loop at approximately 2.5 L min<sup>-1</sup>. After the chamber lid had been closed, the air volume inside the closed chamber headspace was circulated using a 12 volt fan to prevent build up of concentration gradients of the measured gasses across the height of the chambers (Fig. 3.6).

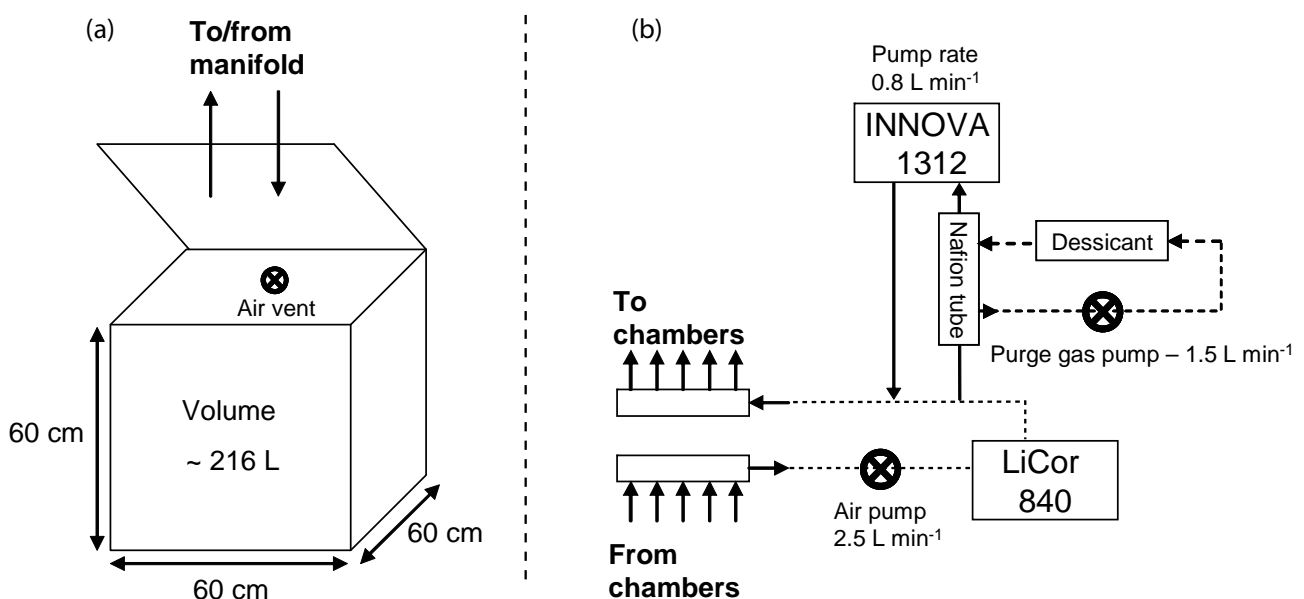


Figure 3.6 Simplified sketch of the automated flux chamber system. (a): Flux chamber dimension without extender. (b): Flow path of sample gases.

For the N<sub>2</sub>O study, five chambers were closed one at a time in a fixed sequence with one chamber being closed for 55 min followed by an open period of 4 hrs. In this way, chamber specific flux estimates could be obtained with a 5 hour temporal resolution. Real-time concentrations of N<sub>2</sub>O, CO<sub>2</sub> and water vapour (H<sub>2</sub>O) were determined using both a non-dispersive infrared gas analyser (LI-840, LiCor, Lincoln, USA) and an in-line photoacoustic trace gas analyzer (INNOVA 1312, LumaSense Technology Inc, Denmark) similar to other automated N<sub>2</sub>O flux measurements studies (Ambus and Robertson, 1998; Yamulki and Jarvis, 1999; Flechard *et al.* 2005). Simultaneous measurements of CO<sub>2</sub> and H<sub>2</sub>O concentrations were performed by both the LI-840 and the INNOVA 1312 to achieve a 30 sec temporal resolution of CO<sub>2</sub> concentrations by the LI-840, providing an indirect and independent CO<sub>2</sub> control on the status of the low concentration measurements (nL L<sup>-1</sup> region) of N<sub>2</sub>O by the photoacoustic gas analyser. Gas concentrations of H<sub>2</sub>O, CO<sub>2</sub> and N<sub>2</sub>O in the chamber headspace were determined every 4 minutes with the INNOVA (sample integration time of 50 sec for each gas) with corrections made for water vapour and CO<sub>2</sub> interferences. To stabilize the water vapour pressure in the measurement cell, the sample gas was dried prior to analysis using a non-interfering Nafion dryer (MD110, PermaPure Inc., US) with continuous purging of dry air.

Surface flux estimates of N<sub>2</sub>O were calculated using quadratic regression to account for potential non-linearity in the headspace gas increase over 30 minutes providing a more accurate estimate of N<sub>2</sub>O fluxes while returning the same estimate as the linear regression model in case of perfect linearity in headspace concentration increase/decrease (Wagner *et al.* 1997).

### 3.4 Microsensor $N_2O$ and $O_2$ methodology

Vertical concentration profiles of  $N_2O$ ,  $O_2$  and apparent diffusivity were measured in the soil columns using commercial microsensors with an outside tip diameter of 100-200  $\mu m$  (Unisense, Denmark). The sensors were mounted side by side on a motorized micromanipulator and connected to a picoammeter (PA2000, Unisense, Denmark)(Fig 3.7). The use of microsensors offers ultra-high spatial resolution (<10  $\mu m$  if desired) concentration profiles with minimum disturbance to the soil.

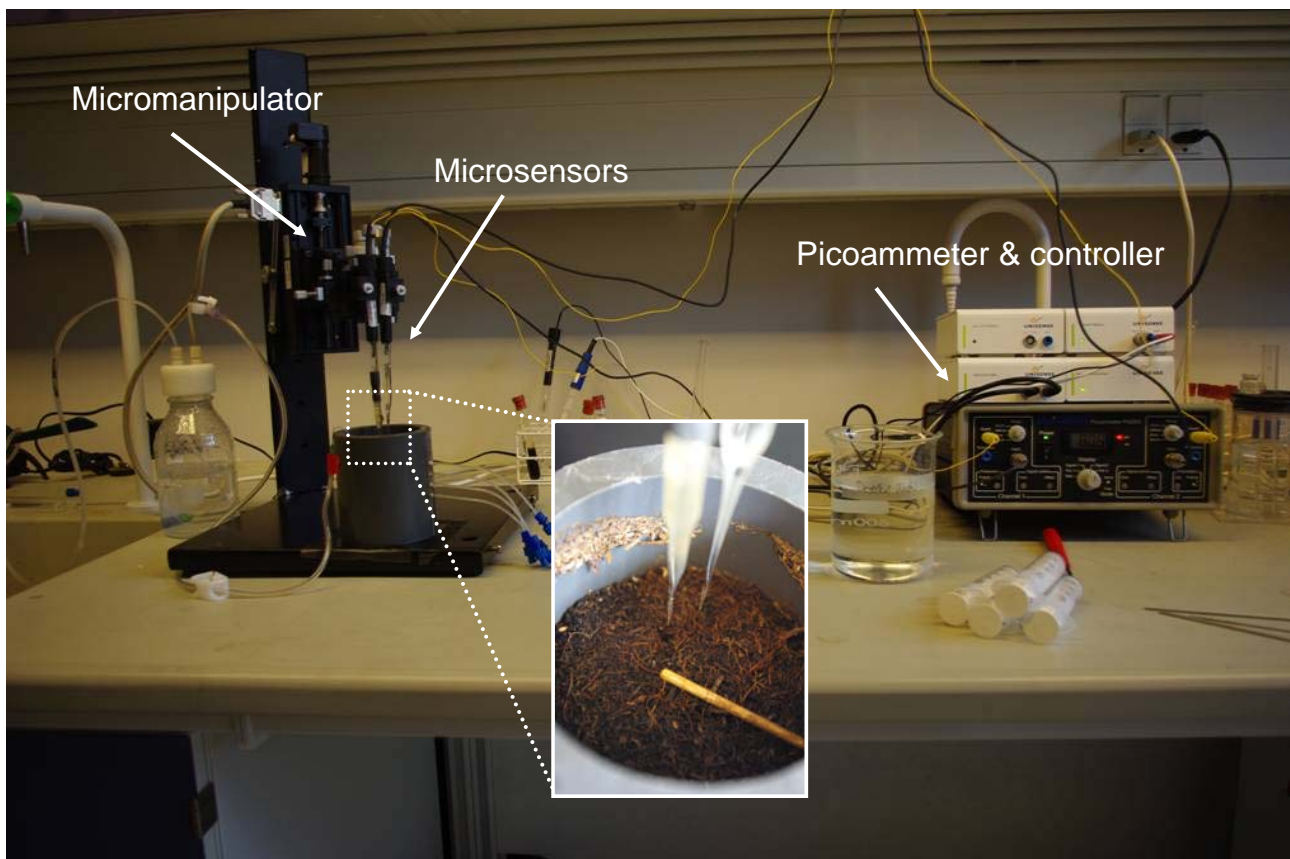


Figure 3.7 Picture of microsensor setup.

The numerical model PROFILE (Berg *et al.* 1998) was used to analyse measured  $N_2O$ ,  $O_2$  concentration profiles and apparent diffusivity. PROFILE calculates the rate of production and consumption as a function of depth, assuming that the concentration depth profiles represent steady state conditions. The procedure involves finding a series of least square fits for the measured concentration profile, followed by comparisons of these fits through statistical F-testing. This approach leads to an objective selection of the simplest consumption profile that reproduces the measured concentration profile. The model has been successfully tested against analytical solutions describing the transport and consumption of  $O_2$  in sediment pore water (Berg *et al.* 1998) and used to model the production and consumption of  $N_2O$  in soil (Elberling *et al.* 2010).



## 4 - Research paper summaries

### 4.1 Summary of Paper 1

**Title** “Plant-mediated CH<sub>4</sub> transport and C gas dynamics quantified in-situ in a *Phalaris arundinacea* dominant wetland”

#### **Introduction**

In this paper we investigate the temporal flux dynamics of CO<sub>2</sub> and CH<sub>4</sub> gases across the soil-atmosphere interface in order to determine both the dominating gas transport mechanisms and the potential role of plant-mediated gas transport from *P. arundinacea*. Results are used to calculate the net annual C-gas emission budgets in response to seasonal variations in soil temperature, soil moisture and the position of the free-standing water level, and used as benchmark for designing the N<sub>2</sub>O flux measurement strategy and evaluating the climatic feedback of the corresponding N<sub>2</sub>O emissions.

#### **Research highlights**

- An average of ~70% of total ecosystem CH<sub>4</sub> emissions was plant-mediated.
- Temporal flux patterns showed no diurnal signature of light-enhanced convective gas transport indicating that the plant-mediated gas transport was driven by passive diffusion.
- CH<sub>4</sub> fluxes were highest during periods of high WL, whereas surface emissions were below the detection limits when the WL was below 30 cm from the surface.
- The presence of an oxidized root zone where CH<sub>4</sub> could be oxidized to CO<sub>2</sub> was observed when WL was below 30 cm from the surface.
- Average annual net CO<sub>2</sub> fixation of approximately 620 g CO<sub>2</sub>-C m<sup>-2</sup> yr<sup>-1</sup>.
- Annual net CH<sub>4</sub> emission of approximately 2 g CH<sub>4</sub>-C m<sup>-2</sup> yr<sup>-1</sup>.
- Converted to CO<sub>2</sub>-equivalents, approximately 3%\* of the net annually sequestered C is returned to the atmosphere as CH<sub>4</sub>.

\* = see errata in appendix 1



## 4.2 Summary of Paper 2

**Title** “Linking O<sub>2</sub>, CO<sub>2</sub> and CH<sub>4</sub> dynamics in a wetland at contrasting water levels”

### **Introduction**

In this paper we investigate the spatiotemporal trends in soil gas dynamics and greenhouse gas emissions following changes in near-surface apparent diffusivity, microscale O<sub>2</sub> dynamics and plant-mediated gas transport in response to marked changes in the position of the WL. Since the spatial distribution of subsurface O<sub>2</sub> concentrations is a key parameter for determining the location of high activity zones for both C and N transformation in the soil, variations in the mass transfer rates of O<sub>2</sub> in response to WL variations is likely to govern the subsurface zonation of ongoing production and consumption of CH<sub>4</sub> (as well as N<sub>2</sub>O), ultimately leading to net surface emission or deposition of greenhouse gas. PROFILE modelling of soil production and consumption profiles based on high resolution data inputs were used to elucidate the effect of time-dependent changes in apparent diffusivity following WL variations.

### **Research highlights**

- ➔ A strong temporal effect on effective diffusivity following flooding was observed and apparent diffusivity rates decreased by a factor 8 over three months after flooding due to the gradual replacement of trapped soil air by soil water
- ➔ The length and degree of drainage before flooding is important for the time needed to reach stable apparent diffusivity values after flooding.
- ➔ When spatiotemporal variations in soil and depth specific apparent diffusivity are taken into account, the linkage between subsurface gas concentrations under drained soil condition and surface fluxes can be roughly predicted by simple gas diffusion.
- ➔ Under flooded conditions O<sub>2</sub> transport occurred mainly by other means than simple diffusion across the soil-atmosphere interface and near-surface O<sub>2</sub> levels were linked to plant-mediated O<sub>2</sub> transport and O<sub>2</sub> release from roots.
- ➔ When the WL was below 40cm, CH<sub>4</sub> fluxes were negative indicating root zone oxidation of CH<sub>4</sub> and net CH<sub>4</sub> uptake.

### 4.3 Summary of Paper 3

**Title** “Temporal trends in N<sub>2</sub>O flux dynamics in a Danish wetland – effects of plant-mediated gas transport of N<sub>2</sub>O and O<sub>2</sub> following changes in water level and soil mineral-N availability”

#### **Introduction**

In this paper we investigate the temporal dynamics of N<sub>2</sub>O fluxes in a non-managed Danish wetland by near-continuous flux measurements over an entire growing season of a subsurface aerating macrophytes *Phalaris arundinacea*. By applying high temporal resolution methodology on both gas exchange across the soil-atmosphere interface and below ground environmental drivers, we were able to link the temporal variability in hourly measured gas fluxes to seasonal variations in subsurface N<sub>2</sub>O concentrations and O<sub>2</sub> availability following changes in the position of the WL. Results highlight the potential importance of plant-mediated gas transport of N<sub>2</sub>O and O<sub>2</sub> for belowground N-transformation processes and surface emissions of N<sub>2</sub>O.

#### **Research highlights**

- N<sub>2</sub>O fluxes across the soil-atmosphere interface showed surprisingly high temporal variability with marked changes in flux magnitude and flux direction within hours.
- Patterns in N<sub>2</sub>O flux dynamics were associated with diurnal variations in PAR radiation
- Significant N<sub>2</sub>O emissions were measured directly from the vegetation canopy of *P. arundinacea*.
- *P. arundinacea* has the ability to mediate gas transport of N<sub>2</sub>O from the root zone to the atmosphere and thereby bypassing the diffusive gas transport through the soil.
- N<sub>2</sub>O emissions are related to the presence of N<sub>2</sub>O in the upper 35 cm of the soil profile corresponding to the main root zone
- N<sub>2</sub>O sink activity was linked to N<sub>2</sub>O consumption in the root zone.
- Seasonal variations in subsurface N<sub>2</sub>O concentrations were directly linked to the position of the WL and O<sub>2</sub> availability at the capillary fringe above the WL.
- Correlation between diurnal variations in subsurface O<sub>2</sub> concentrations and incoming solar radiation in the PAR spectrum indicates the potential importance of plant-driven subsoil aeration for N-transformation processes in the root zone.

## 4.4 Summary of Paper 4

**Title** “Flooding-induced N<sub>2</sub>O production, consumption and emission dynamics in wetland soil”

### Introduction

In this paper we investigate the spatiotemporal aspects of rapid water level changes on the production, consumption and emission of N<sub>2</sub>O. Rapid flooding of naturally drained peat may lead to hotspot production and pulse emission of N<sub>2</sub>O. The duration of these emissions pulses will most likely depend on the N-availability in the soil at the time of flooding, the rate of O<sub>2</sub> depletion/oxygenation in the hours and days after flooding, and the relative magnitude and zonation of N<sub>2</sub>O producing and consuming processes in the subsoil. If the magnitude of such emission pulses are large but the duration short, substantial N<sub>2</sub>O emissions could have been overlooked in previous low-temporal resolution studies resulting in a general underestimation of N<sub>2</sub>O emissions to the atmosphere. On the other hand, if the flooding-induced fluxes are low the risk of significant positive feedback to climate change following intensified flooding/drainage dynamics would be minimized.

### Research highlights

- The majority of net annual N<sub>2</sub>O emission budget of ~0.74 kg N<sub>2</sub>O-N ha<sup>-1</sup> yr<sup>-1</sup> occurred during the growing season of *Phalaris arundinacea*.
- Flooding-induced N<sub>2</sub>O emission pulses were observed when soil conditions in the upper 30 cm had been oxidized for more than 2-3 weeks and constituted ~2.5% of the net annual N<sub>2</sub>O emission.
- Highest subsurface N<sub>2</sub>O concentrations were observed at the capillary fringe -5 to 40 cm above the WL.
- Main emission periods were observed in periods where the WL and maximum subsurface N<sub>2</sub>O concentration were located in the root zone of *P. arundinacea*.
- Net N<sub>2</sub>O sink activity counterbalancing ~6.4 % of net annual emission was observed during mid-summer when the WL was low.
- N<sub>2</sub>O production and consumption profiles reveal sequential N<sub>2</sub>O production and consumption capacities of more than 500 nmol cm<sup>-3</sup> in less than 24 hours.
- Approximately 0.5-2.5% of soil NO<sub>3</sub><sup>-</sup> were emitted as N<sub>2</sub>O when plant roots were removed, while increasing to ~33% when aerenchymous roots were present, highlighting the importance of plant-mediation for the transport of N<sub>2</sub>O across the soil-atmosphere interface

## 5 - Conclusions and outlook

### 5.1 Gas transport mechanisms across the soil-atmosphere interface

Net exchange of greenhouse gases across the soil-atmosphere interface was measured from a non-managed natural Danish wetland as both gas fluxes between the soil and the atmosphere (paper 1 & 2) and via plant-mediated gas transport (papers 1-4). Several independent relations showed that diffusive gas transport was the governing transport mechanism: (i) the linkage between subsurface gas concentrations and surface fluxes could be roughly predicted by simple gas diffusion when soil and depth specific variations in apparent diffusivity were taken into account (paper 1), (ii) no diurnal emission signature specific to light-enhanced convective throughflow were observed in the field scale flux measurements (paper 1 & 3) and (iii) the relative proportion of soil ecosystem fluxes versus total ecosystem fluxes showed that ~30% of the total CH<sub>4</sub> emissions could be ascribed to Fickian diffusion across the soil-atmosphere interface (paper 1 & 2).

While diffusive exchange of gases across the soil-atmosphere interface would be the expected transport mechanism, one of the main novelties presented in this PhD thesis is the important role of plant-mediated transport for net emission of N<sub>2</sub>O. This transport mechanism was demonstrated directly by application of a plant-only flux chamber by which emissions of N<sub>2</sub>O could be measured from the leaf sheets of *P. arundinacea* (paper 3). More in-direct evidence of plant-mediated gas transport was found in (i) the observed difference between soil ecosystem fluxes and total ecosystem fluxes (paper 1), (ii) the suppressed surface emissions when gas transport takes place through the bulk soil matrix as opposed to when plants were included (paper 2), (iii) the significant correlation between O<sub>2</sub> concentrations in the root zone and incoming radiation in the PAR spectrum (paper 3), (iv) the apparent light-regulation of N<sub>2</sub>O emissions, both in the plant-only experiment and in temporal dynamics in field emissions (paper 3) and (v) by the decrease in relative proportion of NO<sub>3</sub><sup>-</sup> emitted as N<sub>2</sub>O after soil flooding when the plants were excluded (paper 4).

It is concluded that *P. arundinacea* has the ability to facilitate N<sub>2</sub>O transport from the root zone to the atmosphere and thereby effectively by-passing the soil and root zone and their associated lower diffusion rates and higher N<sub>2</sub>O consumption potential (paper 3&4). However, additional experiments are needed to resolve the complexity of the interrelated biogeochemical processes governing the plant-mediated gas transport mechanisms, potential transport drivers and seasonal

timing. Adding to the complexity, N<sub>2</sub>O production during N-assimilation within the above-ground biomass of certain higher plants has been hypothesized (Yu and Chen, 2009). The potential ramifications of this leaf internal N<sub>2</sub>O production or consumption in *P. arundinacea* could be a parallel N<sub>2</sub>O source and sink system detached from the soil and belowground biomass, modifying the net N<sub>2</sub>O fluxes from this type of wetland ecosystem. Despite these uncertainties, our results show that plant-mediated gas transport of N<sub>2</sub>O by *P. arundinacea* is an important process to include when measuring net ecosystem emissions of N<sub>2</sub>O. It is evident, that the inclusion of the aboveground biomass in these types of flux measurements is essential to avoid significant underestimations of net N<sub>2</sub>O fluxes, whereas an inadequate sampling frequency or non-uniform temporal coverage could impose an undesirable bias to the net flux estimates.

## **5.2 Spatiotemporal N<sub>2</sub>O flux dynamics in relation to seasonal water level variations**

Near-continuous measurement of N<sub>2</sub>O fluxes showed high temporal variations in both magnitude and direction of N<sub>2</sub>O fluxes on both a shorter time scale (daily to weekly time spans) and over longer periods (time span of the entire growing season to annual budget). Periods of different temporal N<sub>2</sub>O flux dynamics could be distinguished by the seasonal position of the WL. In general, the N<sub>2</sub>O fluxes were characterized by positive N<sub>2</sub>O fluxes lower than 25 µg N<sub>2</sub>O-N m<sup>-2</sup> hr<sup>-1</sup> during periods with near-surface WL while the magnitudes of the N<sub>2</sub>O fluxes were measured to increase in response to a falling WL. When the position of the WL was below 50 cm, a period with significant negative fluxes (N<sub>2</sub>O uptake) was observed with pronounced diurnal flux dynamics (paper 3). Field profiles of seasonal N<sub>2</sub>O concentration profiles systematically showed N<sub>2</sub>O concentration peaks at the capillary fringe between the position of the WL and the oxidized soil layers above (paper 4), similar to the observation by (Velthof *et al.* 1996; Jungkunst *et al.* 2008). Periods with positive fluxes of N<sub>2</sub>O during the illuminated hours of the day were observed when maximum concentrations of N<sub>2</sub>O were located within 30-40 cm below the surface corresponding to the vertical extend of the root zone (paper 3&4). In the period characterized by net N<sub>2</sub>O sink activity (paper 3&4), the direction of the N<sub>2</sub>O fluxes shifted within a few hours from net emission during the illuminated hours to net sink during the dark hours indicating a light-related control on N<sub>2</sub>O emission dynamics. With the exception of a few weeks in early summer 2009 with one of the chambers showing 5-8 times higher values than the remaining four chambers (paper 3), the spatial variation between the five chambers was less than 25% of the daily average N<sub>2</sub>O emissions and

most likely a result of a close to identical elevation, hydrology, soil temperature, vegetation cover and peat thickness in all of the five chambers.

### **5.3 Flooding induced N<sub>2</sub>O emissions**

Two natural flooding events were observed at the field site during the measurement period where high precipitation events caused the WL to rise in the range of 25-70 cm within 6 hours (paper 4). In both flooding events the WL rise caused complete water saturation of the soil with standing water above the surface in the hours following the flooding peak. Contrasting temporal N<sub>2</sub>O emission patterns were associated with each of the flooding events. In the first flooding event where the WL rose from -20 cm to 5 cm above the surface, fairly steady N<sub>2</sub>O emissions of ~90 µg N<sub>2</sub>O-N m<sup>-2</sup> hr<sup>-1</sup> ceased when the WL reached the surface (paper 4). In contrast, a pronounced N<sub>2</sub>O emission pulse was observed ~16 hours after the rapid WL rise from - 50cm to 20 cm above the surface at the second flooding events. The duration of the emission pulse was ~12 hours with emission rates in the order of 25-250 µg N<sub>2</sub>O-N m<sup>-2</sup> hr<sup>-1</sup> (paper 4).

A very high spatiotemporal dynamics on N<sub>2</sub>O production, consumption and emission rates were observed following laboratory flooding of root zone peat samples. After an initial lag phase of approximately 4-6 hours, N<sub>2</sub>O concentrations increased with increasing depth below the surface. Concentration increases were observed at all depths until maximum concentrations (C<sub>max</sub>) were measured between 15 and 26 hours after flooding depending on the soil depth. After C<sub>max</sub>, a net decrease in N<sub>2</sub>O concentrations were observed until concentrations went below the detection limit ~ 42 hours after flooding (paper 4). Production and consumption profiles, as modelled by PROFILE, show net N<sub>2</sub>O production over the measured soil profile in the time period of concentration increases and net consumption over the measured profile when concentrations decreased. The temporal development of the surface emissions of N<sub>2</sub>O from the experimental soil columns correlated with the subsurface N<sub>2</sub>O concentration development in the top soil of the experimental soil columns. This indicates that it is not necessarily the absolute subsurface N<sub>2</sub>O concentrations which control the surface emissions, but rather the zonation below the surface and the dominance and reaction rates of N<sub>2</sub>O production or consumption in the overlying soil layers which regulates N<sub>2</sub>O emissions across the soil-atmosphere interface.

An important difference between field and laboratory conditions is the presence or absence of the above-ground biomass and aerenchymous roots and rhizosphere. These differences are likely reflected in the marked difference between laboratory and field ratios of the potential denitrification product emitted as N<sub>2</sub>O after soil flooding (i.e. the stoichiometric N fraction of potential NO<sub>3</sub><sup>-</sup> reduction measured as N<sub>2</sub>O before/after flooding). When the aerenchymous roots were removed in the laboratory experiment, approximately 0.5-2.5% of the initial soil NO<sub>3</sub><sup>-</sup> present at the time of flooding was being emitted as N<sub>2</sub>O, which is in the same proportions as (Kliewer and Gilliam, 1995) who found this fraction to be approximately 2% (paper 4). Under natural field conditions this fraction could be up to 1/3 of the initial NO<sub>3</sub><sup>-</sup> concentration present in the soil profile before and after flooding under natural field conditions (paper 4), highlighting the potential importance of plant-mediated gas transport for the net annual N<sub>2</sub>O emission budget across the soil-atmosphere interface (paper 4).

#### ***5.4 Subsurface gas dynamics in response to water level variations***

O<sub>2</sub> availability in wetland soil is a controlling factor for the production, consumption and potential emission of the major greenhouse gases from the soil to the atmosphere. Depth specific apparent diffusivity values of O<sub>2</sub> in the soil are affected by small changes in the soil moisture content and distribution of water and air in the porespace of the soil. Non-linear temporal aspect of soil moisture changes on gas exchange were observed in the apparent diffusivity measurements normalized to 10°C in newly saturated peat layers, where an initial values of approximately 10 times the diffusivity in water ( $1.57 \times 10^{-5} \text{ cm}^2 \text{ s}^{-1}$ ) are observed to decrease by a factor 8 during the first 3 months after flooding (paper 1). These changes over time occur as trapped soil air is gradually replaced by water, decreasing the total soil gas volume and/or creating less connected air spaces in the peat matrix. Repeated measurements of such time-dependent changes in the apparent diffusivity indicate that the time and degree of drainage before flooding is important for the mass transfer properties of gases across the soil-atmosphere interface (paper 1). Longer and more extensive drainage resulted in higher apparent diffusivity values upon flooding and a longer time was required to reach to reach constant values (paper 1). These observations are relevant for the prediction of redox sensitive N-transformations in the soil, since spatiotemporal variations O<sub>2</sub> availability control where and when both gaseous intermediate and terminal reaction products will be produced, consumed or lost from the soil profile.

In wetlands with low external nitrogen inputs (i.e. atmospheric deposition as primary N input), the rate of subsoil N<sub>2</sub>O production from both nitrification and denitrification is primarily dependent on N-mineralization (Smith, 1997) in which organic N is mineralized into NH<sub>4</sub><sup>+</sup> in the absence of O<sub>2</sub>, which can then be nitrified into NO<sub>3</sub><sup>-</sup> in the presence of O<sub>2</sub>, for further reduction into N<sub>2</sub>O and/or N<sub>2</sub> under O<sub>2</sub> depleted soil conditions. It was found that a temporal requirement for NO<sub>3</sub><sup>-</sup> concentrations to accumulate above a few mg kg<sup>-1</sup> was a period of prolonged soil oxygenation as observed in the highest NO<sub>3</sub><sup>-</sup> concentrations at a depth of 20-30 cm below the surface in the weeks following O<sub>2</sub> penetration into these previously anoxic soil layers in late July and early August 2010 (paper 3). Weekly concentration profiles of subsurface N<sub>2</sub>O concentrations normalized to the position of the WL showed maximum N<sub>2</sub>O concentrations at the capillary fringe -5 to 40 cm above the WL (paper 3&4) indicating that the position of the WL could impose a lower boundary for significant N<sub>2</sub>O accumulation to occur due to very limited O<sub>2</sub> availability favouring full reduction of N<sub>2</sub>O to N<sub>2</sub> if the appropriate enzymes are expressed (Korner and Zumft, 1989). Since denitrification in peat is often limited by NO<sub>3</sub><sup>-</sup> availability (Regina *et al.* 1996b), increased nitrification in the periods of falling WL and increased O<sub>2</sub> penetration depths under future climatic conditions may lead to increased NO<sub>3</sub><sup>-</sup> availability in both the bulk soil and at the capillary fringe.

Existence of a complex temporal aspect of O<sub>2</sub> penetration depth versus the position of the WL was observed. In both the early and late season, the O<sub>2</sub> penetration depth was closely delineated by the position of the WL when this was located within the upper 20 cm of the soil profile. In contrast, an anaerobic soil volume up to 40 cm above the WL was observed in mid-season were a combination of restricted subsoil aeration in the unsaturated zone due to relative high soil moisture contents in the peat and high respiratory O<sub>2</sub> consumption by soil microorganisms which is stimulated due to higher mid-season soil temperatures (Smith, 1980) caused the apparently aerated soil volume (as would be the standard interpretation of the measured soil moisture contents) to become O<sub>2</sub> depleted (paper 3).

The significant relationship between diurnal variations in O<sub>2</sub> concentrations in the root zone and incoming solar radiation in the PAR spectrum (paper 3) highlights the potential importance and added complexity of plant-driven oxygenation of the rhizosphere on root zone N-transformation and the associated controls on coupled nitrification/denitrification processes. How this process affects the kinetics of the coupled N-transformation sequence over time is unclear. It has been suggested that O<sub>2</sub> transported into the soil by aerenchymatous plants could maintain a small nitrifying



population even under waterlogged conditions so that the population is ready to become active and increase upon lowering of the water table (Regina *et al.* 1999).

A high degree of spatiotemporal complexity in subsurface O<sub>2</sub> distribution in response to soil flooding and drainage was demonstrated in an experiment, where the subsurface O<sub>2</sub> distribution following controlled drainage and rewetting was determined by use of planar optode measurements in peat columns from the same study site (Askaer *et al.* 2010). Here the development of several anaerobic soil volumes within an aerobic soil matrix was measured in the hours and days following drainage, emphasizing the role of soil heterogeneity for subsurface gas transport via a dynamic macropore system created by soil development, macrofauna and flora, all of which facilitated varying degrees of preferential flow of water and O<sub>2</sub> in response to changes in soil moisture content at the capillary fringe above the WL (Askaer *et al.* 2010). Similar heterogeneous O<sub>2</sub> distribution dynamics at the capillary fringe is likely to develop during WL variations at the field scale (see also paper 3 & 4 for O<sub>2</sub> profiles), where the soil matrix would be preferentially aerated via air-filled macropores, while soil micropores and sites of high respiration would remain anaerobic producing highly contrasting redox conditions and N-transformation processes over very short spatial distances.

In combination with plant-transported O<sub>2</sub> into the root zone, the extent and duration of soil oxygenation following a natural lowering of the WL influenced N-transformation as measured in increasing concentrations of extractable NO<sub>3</sub><sup>-</sup> after prolonged periods of oxic soil conditions in the root zone (paper 3). In relation to flooding-induced N<sub>2</sub>O emissions, a temporal trend is apparent in which a period of prolonged and more extensive drainage is required for an emission pulse to form after flooding (paper 4). So even though the variations in the seasonal position of the WL may be a key determinant for soil moisture content at the capillary fringe (paper 3), and thereby for the environmental drivers N<sub>2</sub>O production and surface emissions, the absolute position of the WL and measurements of soil moisture content are inadequate predictors of the spatiotemporal changes in subsurface O<sub>2</sub> availability and N<sub>2</sub>O emissions under seasonally fluctuating positions of the WL due to the non-linear effect of temporal changes in apparent diffusivity following flooding and drainage (paper 1). This conclusion may be a possible explanation to some of the contrasting results in terms of lowered water levels on N<sub>2</sub>O emission (see section “2.1.1 Effects of water level and soil moisture variations”) where site specific differences in physio-chemical soil properties, wetland hydrology, composition of the microbial N-transforming communities or spatiotemporal issues involved with

the duration and degree drainage/flooding cycles may produce a contrasting net result despite an apparent similarity in WL movement.

### **5.5 Subsurface production and consumption dynamics**

Incubation experiments of potential N<sub>2</sub>O consumption capacities (paper 3) and PROFILE modelling of subsurface production and consumption rates (paper 4) demonstrated large N<sub>2</sub>O consumption capacities in soil samples from both within and below the root zone. Results show that the measured net consumption of N<sub>2</sub>O in the subsoil under certain conditions can consume very large quantities of N<sub>2</sub>O giving rise to negative flux gradients across the soil-atmosphere interface resulting in net sink capacity of atmospheric N<sub>2</sub>O. According to the measured potential N<sub>2</sub>O consumption capacities (paper 3), the net N<sub>2</sub>O sink effect would be largest in the top soil and rhizosphere through which all N<sub>2</sub>O produced at deeper soil depths will have to pass before being emitted, unless gas transport through plants occur (paper 3).

In the period characterized by nocturnal N<sub>2</sub>O sink activity (paper 3&4), soil moisture contents in the top soil were at a seasonal low with oxic soil condition in the top 40 cm and soil temperature at a seasonal high. The main drivers of N<sub>2</sub>O uptake is still an unresolved question (Chapuis-Lardy *et al.* 2007), but it has previously been reported that hypoxic or anoxic micro sites may form in even well-aerated soils, and provide a sink for N<sub>2</sub>O diffusing through the gas-filled pore space (Vieten *et al.* 2009). Also, N<sub>2</sub>O uptake by plants have been suggested as a net N<sub>2</sub>O sink, especially when soil moisture is low (Li *et al.* 2011). Taken together with the measured N<sub>2</sub>O consumption capacities at various depths in the soil profile (paper 3&4), it seems likely that N<sub>2</sub>O consumption processes in the root zone can explain or account for the observed net N<sub>2</sub>O uptake during mid-summer, when aerated conditions in top soil facilitates a faster diffusive exchange of atmospheric N<sub>2</sub>O to anoxic microsites in the soil where a further reduction to N<sub>2</sub> can occur.

It is conceivable that during the period with nocturnal sink activity, emissions of N<sub>2</sub>O produced at the capillary fringe deeper in the soil profile could be emitted primarily via plant transport which is stimulated or even regulated by variations in incoming light. Under these conditions the majority of the N<sub>2</sub>O emissions would occur during the day-time and level of during night, while the N<sub>2</sub>O sink activity in the top soil could occur at all times during both the day and night. Since net emissions are always the resulting net product of combined N<sub>2</sub>O production and consumption, this dynamic

balance could produce positive net fluxes during the illuminated hours of the time if net emissions were greater than net consumptions while the opposite would be true during the dark hours of the day. Explanations for the seasonal variations in N<sub>2</sub>O emission patterns in response to WL changes are likely related to N-transformation processes and N<sub>2</sub>O production and consumption within the root zone. It follows that the deeper the locations of the capillary fringe, the longer the path of diffusion from the soil depth of formation of the diffusion path to the atmosphere will be, yielding a longer residence time promoting higher probability for full reduction to N<sub>2</sub> as also described in (Clough *et al.* 2005).

It is concluded that the spatiotemporal distribution of dominating N<sub>2</sub>O producing and consuming processes below the surface, in combination with the variations in the diffusive exchange rates due to soil water content and apparent diffusivity, control the magnitude and timing of N<sub>2</sub>O emissions to the atmosphere in close connection with the plant-mediated gas transport mechanism which also stimulates sequential nitrification-denitrification in the root zone. It does therefore not appear to be the total amount of N<sub>2</sub>O in the subsoil which controls the magnitude and timing of the surface emissions, but rather the zonation of the N<sub>2</sub>O below the surface, and just as importantly, the dominance and reaction rates of N<sub>2</sub>O production or consumption in the overlying soil layers and adjacency to plant roots.

## **5.6 Greenhouse gas budgets and potential climatic feedbacks**

The net annual greenhouse gas budgets was calculated on basis of daily net emissions to encompass the high temporal variability in the seasonal flux dynamics and render an average of net seasonal with minimum interpretational bias (Velthof and Oenema, 1995) (paper 4). Measurements of net ecosystem exchange (NEE) of CO<sub>2</sub> show an average net C fixation (C sink) of ~620 g CO<sub>2</sub>-C m<sup>-2</sup> yr<sup>-1</sup> (paper 1). Net annual emission of CH<sub>4</sub> were estimated to be ~2 g CH<sub>4</sub>-C m<sup>-2</sup> yr<sup>-1</sup> (paper 1), while net annual emissions of N<sub>2</sub>O were estimated to be ~0.074 g N<sub>2</sub>O-N m<sup>-2</sup> yr<sup>-1</sup> (paper 4). When the net annual emissions of CH<sub>4</sub> and N<sub>2</sub>O are converted into CO<sub>2</sub>-equivalents according to their relative global warming potentials (GWP) (see appendix 1) it shows that the annual CH<sub>4</sub> emissions counterbalances ~3% of net annual CO<sub>2</sub> fixation, while the relatively low net annual N<sub>2</sub>O emissions counterbalances ~1.5 % of net annual CO<sub>2</sub> fixation due to the high GWP of N<sub>2</sub>O (paper 4). Flooding-induced N<sub>2</sub>O emissions were observed when the soil was rapidly flooded after a 3 week period of natural drainage and top soil oxygenation. Cumulative flooding-induced N<sub>2</sub>O emissions

constituted ~2.5% of the total annual N<sub>2</sub>O emission budget, while the mid-summer period of net daily N<sub>2</sub>O sink activity counterbalance ~6.4% of the annual N<sub>2</sub>O emission budget.

Future changes in the seasonal WL dynamics with longer periods of drought may produce longer periods of oxidized soil conditions during the summer months. This could influence the rates of N-transformation and NO<sub>3</sub><sup>-</sup> availability, with the potential result of greater subsoil production rates of N<sub>2</sub>O if the soil moisture conditions and O<sub>2</sub> availability favours the production of N<sub>2</sub>O. On the other hand, improved conditions for plant growth and microbial respiration under warmer and more nutrient rich conditions as well as elevated CO<sub>2</sub> pressures may counterbalance the accelerated N-mineralization rate by increased resource competition for mineral-N between plants and soil microbes or increased rates of DNRA, increasing the current net N<sub>2</sub>O sink capacity when N-availability is limited (paper 3). In this way, future intensifications in high frequency fluctuations in the position of the surface near WL may cause increased seasonal net emissions, while slower fluctuations in the WL may have the opposite effect.

Results presented in this PhD thesis show that both the timing and magnitude of current and future N<sub>2</sub>O emission from natural wetlands are strongly influenced by the concentration and location of N<sub>2</sub>O and O<sub>2</sub> in the subsoil, which is determined by a combination of plant growth and seasonal groundwater level dynamics. While periods of different net N<sub>2</sub>O emission dynamics were distinguished by the seasonal position of the WL, this driver could not explain the contrasting flux dynamics on a diurnal to weekly time scale indicating that the linkages between subsurface N<sub>2</sub>O concentration and surface flux dynamics are more complex. The results presented in this work emphasize the risk of substantial underestimations of net N<sub>2</sub>O fluxes from wetland ecosystems if the sampling frequency is too low, or if the plant-transported N<sub>2</sub>O contribution is omitted and stress the importance for gas flux measurements on a high spatiotemporal resolution.

## 5.7 Applied scope and perspectives

In Denmark, many natural wetlands, e.g. Store Åmosen on western Zealand, have been drained and utilized for agricultural and peat extraction purposes over the past century. During this process, many important archaeological discoveries of buried organic artefacts have been made providing many unique insights into the history of the late Stone Age culture approximately 6.000-8.000 year ago (Noe-Nygaard, 1995). In recent years, wetland restoration of previously drained areas in Store Åmosen has been proposed as a method for *in-situ* conservation of these buried organic artefacts as well as providing improved conditions for wild-life protection and increased biodiversity. Typically, wetland restoration strategies involve blocking of the drainage system allowing the position of the surface near water level (WL) to follow the seasonal variations as would be observed in a non-managed natural counterpart.

Wetland restoration of formerly drained and fertilized peat soil may result in rapid colonization of former agricultural areas by aerenchymous wetland plants and altered emissions of important greenhouse gases such as N<sub>2</sub>O and CH<sub>4</sub> (Glatzel *et al.* 2008; Hunter and Faulkner, 2001; Stadmark *et al.* 2009) similar to the results of other water table management strategies which enhance denitrification, e.g. in constructed wetland for wastewater treatment (Kliwer and Gilliam, 1995; Zhu and Sikora, 1995; Tanner, 2001; Mayo and Bigambo, 2005; Scholz, 2006; Picek *et al.* 2007; Inamori *et al.* 2008; Maltais-Landry *et al.* 2009). Therefore, when planning wetland restoration strategies a solid understanding of current emission dynamics from natural wetland ecosystems with a seasonally fluctuating WL would be required to assess the climatic impacts of altering the net greenhouse gas budgets following the land use change, whether it will result in greater net emissions or net sinks of carbon dioxide (CO<sub>2</sub>), methane (CH<sub>4</sub>) and nitrous oxide (N<sub>2</sub>O)

Research on the spatiotemporal dynamics in greenhouse gas dynamics in Danish wetlands could also provide valuable knowledge on the temporal nature of C and N transformation and gas flux dynamics in less accessible parts of the world, i.e. arctic wetlands and peatlands with aerenchymous macrophytes, thereby offering a best-estimate of potential future changes in greenhouse gas emissions from these areas and their potential natural feedbacks to climate change.

## **6 - Acknowledgements**

The making of this PhD thesis has not been possible without the help and support by a large number of great people. Warm and heartfelt thanks goes to all field assistants, technicians, co-authors, research group members as well as past and present colleagues and friends! Also thanks to Joshua Schimel at The University of California, Santa Barbara, for great inspiration and useful discussions during my visit at UCSB in the autumn and winter of 2010.

Special thanks to my academic supervisor Professor Bo Elberling for all your inspiring encouragement, support and criticism and for many great discussions, not to mention all the awesome field trips and journeys into the Arctic. It's been one hell of a ride!

Very special thanks to my darling wife Trine for your endless patience and support and to Frederik and Clara for being there and keeping matters in their right perspectives. I love you all!

September 2011 - Christian Juncher Jørgensen



## 7 - Reference list

- Adams CR, Galatowitsch SM (2005) Phalaris arundinacea (reed canary grass): Rapid growth and growth pattern in conditions approximating newly restored wetlands. *Ecoscience*, **12**, 569-573.
- Aerts R, Ludwig F (1997) Water-table changes and nutritional status affect trace gas emissions from laboratory columns of peatland soils. *Soil Biology & Biochemistry*, **29**, 1691-1698.
- Akiyama H, Hayakawa A, Sudo S, Yonemura S, Tanonaka T, Yagi K (2009) Automated sampling system for long-term monitoring of nitrous oxide and methane fluxes from soils. *Soil Science and Plant Nutrition*, **55**, 435-440.
- Ambus P, Robertson GP (1998) Automated near-continuous measurement of carbon dioxide and nitrous oxide fluxes from soil. *Soil Science Society of America Journal*, **62**, 394-400.
- Andersen AJ, Petersen SrO (2009) Effects of C and N availability and soil-water potential interactions on N<sub>2</sub>O evolution and PLFA composition. *Soil Biology and Biochemistry*, **41**, 1726-1733.
- Armstrong J, Armstrong W (1990) Light-Enhanced Convective Throughflow Increases Oxygenation in Rhizomes and Rhizosphere of Phragmites-Australis (Cav) Trin Ex Steud. *New Phytologist*, **114**, 121-128.
- Armstrong J, Armstrong W, Beckett PM, Halder JE, Lythe S, Holt R, Sinclair A (1996) Pathways of aeration and the mechanisms and beneficial effects of humidity- and Venturi-induced convections in Phragmites australis (Cav) Trin ex Steud. *Aquatic Botany*, **54**, 177-197.
- Armstrong W, Brandle R, Jackson MB (1994) Mechanisms of Flood Tolerance in Plants. *Acta Botanica Neerlandica*, **43**, 307-358.
- Arneeth A, Harrison SP, Zaehle S, et al (2010) Terrestrial biogeochemical feedbacks in the climate system. *Nature Geoscience*, **3**, 525-532.
- Askaer L, Elberling B, Glud RN, Kuhl M, Lauritsen FR, Joensen HP (2010) Soil heterogeneity effects on O<sub>2</sub> distribution and CH<sub>4</sub> emissions from wetlands: In situ and mesocosm studies with planar O<sub>2</sub> optodes and membrane inlet mass spectrometry. *Soil Biology and Biochemistry*, **42**, 2254-2265.
- Baek SH, Shapleigh JP (2005) Expression of Nitrite and Nitric Oxide Reductases in Free-Living and Plant-Associated Agrobacterium tumefaciens C58 Cells. *Applied and Environmental Microbiology*, **71**, 4427-4436.
- Bastviken SK, Eriksson PG, Premrov A, Tonderski K (2005) Potential denitrification in wetland sediments with different plant species detritus. *Ecological Engineering*, **25**, 183-190.
- Bedard-Haughn A, Matson AL, Pennock DJ (2006) Land use effects on gross nitrogen mineralization, nitrification, and N<sub>2</sub>O emissions in ephemeral wetlands. *Soil Biology & Biochemistry*, **38**, 3398-3406.



- Berg P, Risgaard-Petersen N, Rysgaard S (1998) Interpretation of measured concentration profiles in sediment pore water. *Limnology and Oceanography*, **43**, 1500-1510.
- Berglund Í, Berglund K (2011) Influence of water table level and soil properties on emissions of greenhouse gases from cultivated peat soil. *Soil Biology and Biochemistry*, **43**, 923-931.
- Betlach MR, Tiedje JM (1981) Kinetic Explanation for Accumulation of Nitrite, Nitric-Oxide, and Nitrous-Oxide During Bacterial Denitrification. *Applied and Environmental Microbiology*, **42**, 1074-1084.
- Blackmer AM, Robbins SG, Bremner JM (1982) Diurnal Variability in Rate of Emission of Nitrous-Oxide from Soils. *Soil Science Society of America Journal*, **46**, 937-942.
- Bodelier PLE, Libochant JA, Blom CWPM, Laanbroek HJ (1996) Dynamics of nitrification and denitrification in root-oxygenated sediments and adaptation of ammonia-oxidizing bacteria to low-oxygen or anoxic habitats. *Applied and Environmental Microbiology*, **62**, 4100-4107.
- Bollmann A, Conrad R (1998) Influence of O<sub>2</sub> availability on NO and N<sub>2</sub>O release by nitrification and denitrification in soils. *Global Change Biology*, **4**, 387-396.
- Borggaard OK, Elberling B (2007) *Pedological Biogeochemistry*. Department of Natural Sciences and Department of Geography and Geology, University of Copenhagen, Copenhagen, Denmark.
- Brix H, Lorenzen B, Morris JT, Schierup HH, Sorrell BK (1994) Effects of Oxygen and Nitrate on Ammonium Uptake Kinetics and Adenylate Pools in Phalaris-Arundinacea l and Glyceria-Maxima (Hartm) Holmb. *Proceedings of the Royal Society of Edinburgh Section B-Biological Sciences*, **102**, 333-342.
- Brix H, Sorrell BK (1996) Oxygen stress in wetland plants: Comparison of de-oxygenated and reducing root environments. *Functional Ecology*, **10**, 521-526.
- Cantarel AA, Bloor JM, Deltroy N, Soussana JF (2011) Effects of Climate Change Drivers on Nitrous Oxide Fluxes in an Upland Temperate Grassland. *Ecosystems*, **14**, 223-233.
- Chang C, Janzen HH, Cho CM, Nakonechny EM (1998) Nitrous oxide emission through plants. *Soil Science Society of America Journal*, **62**, 35-38.
- Chapuis-Lardy L, Wrage N, Metay A, Chotte JL, Bernoux M (2007) Soils, a sink for N<sub>2</sub>O? A review. *Global Change Biology*, **13**, 1-17.
- Chen GX, Huang GH, Huang B, Yu KW, Wu J, Xu H (1997) Nitrous oxide and methane emissions from soil-plant systems. *Nutrient Cycling in Agroecosystems*, **49**, 41-45.
- Cheng XL, Peng RH, Chen JQ, et al (2007) CH<sub>4</sub> and N<sub>2</sub>O emissions from *Spartina alterniflora* and *Phragmites australis* in experimental mesocosms. *Chemosphere*, **68**, 420-427.
- Chipperfield M (2009) ATMOSPHERIC SCIENCE Nitrous oxide delays ozone recovery. *Nature Geoscience*, **2**, 742-743.
- Clough TJ, Sherlock RR, Rolston DE (2005) A review of the movement and fate of N<sub>2</sub>O in the subsoil. *Nutrient Cycling in Agroecosystems*, **72**, 3-11.

- Colmer TD (2003) Long-distance transport of gases in plants: a perspective on internal aeration and radial oxygen loss from roots. *Plant Cell and Environment*, **26**, 17-36.
- Conant RT, Ryan MG, Ågren GI, et al (2011) Temperature and soil organic matter decomposition rates – synthesis of current knowledge and a way forward. *Global Change Biology*, DOI: 10.1111/j.1365-2486.2011.02496.x.
- Cook FJ, Knight JH (2003) Oxygen transport to plant roots: Modeling for physical understanding of soil aeration. *Soil Science Society of America Journal*, **67**, 20-31.
- Danevcic T, Mandic-Mulec I, Stres B, Stopar D, Hacin J (2010) Emissions of CO<sub>2</sub>, CH<sub>4</sub> and N<sub>2</sub>O from Southern European peatlands. *Soil Biology & Biochemistry*, **42**, 1437-1446.
- Davidson EA (1991) Fluxes of Nitrous Oxide and Nitric Oxide from Terrestrial ecosystems. In: *Microbial Production and Consumption of Greenhouse Gases: Methane, Nitrogen Oxides, and Halomethanes* (eds Rogers JE, Whitman WB), pp. 219-235. American Society of Microbiology, Washington, D.C.
- Davidson EA (2009) The contribution of manure and fertilizer nitrogen to atmospheric nitrous oxide since 1860. *Nature Geoscience*, **2**, 659-662.
- Dean JV, Harper JE (1986) Nitric-Oxide and Nitrous-Oxide Production by Soybean and Winged Bean During the In vivo Nitrate Reductase Assay. *Plant Physiology*, **82**, 718-723.
- Dendooven L, Anderson JM (1994) Dynamics of reduction enzymes involved in the denitrification process in pasture soil. *Soil Biology and Biochemistry*, **26**, 1501-1506.
- Dinsmore KJ, Skiba UM, Billett MF, Rees RM (2009) Effect of water table on greenhouse gas emissions from peatland mesocosms. *Plant and Soil*, **318**, 229-242.
- Edwards KR, Cizkova H, Zemanova K, Santruckova H (2006) Plant growth and microbial processes in a constructed wetland planted with *Phalaris arundinacea*. *Ecological Engineering*, **27**, 153-165.
- Elberling B, Christiansen HH, Hansen BU (2010) High nitrous oxide production from thawing permafrost. *Nature Geoscience*, **3**, 332-335.
- Energistyrelsen (2008) Tilpasning til fremtidens klima i Danmark - om regeringens strategi for klimatilpasning. pp. 1-10.
- Engelaar WMHG, Symens JC, Laanbroek HJ, Blom CWPM (1995) Preservation of Nitrifying Capacity and Nitrate Availability in Waterlogged Soils by Radial Oxygen Loss from Roots of Wetland Plants. *Biology and Fertility of Soils*, **20**, 243-248.
- Firestone MK, Davidson EA (1989) Microbiological Basis of NO and N<sub>2</sub>O Production and Consumption in Soil. *Exchange of Trace Gases Between Terrestrial Ecosystems and the Atmosphere*, **47**, 7-21.
- Firestone MK, Firestone RB, Tiedje JM (1980) Nitrous Oxide from Soil Denitrification: Factors Controlling its Biological Production. *Science*, **208**, 749-751.

- Flechard CR, Neftel A, Jocher M, Ammann C, Fuhrer J (2005) Bi-directional soil/atmosphere N<sub>2</sub>O exchange over two mown grassland systems with contrasting management practices. *Global Change Biology*, **11**, 2114-2127.
- Flessa H, Ruser R, Schilling R, Lofthfield N, Munch JC, Kaiser EA, Beese F (2002) N<sub>2</sub>O and CH<sub>4</sub> fluxes in potato fields: automated measurement, management effects and temporal variation. *Geoderma*, **105**, 307-325.
- Garnet KN, Megonigal JP, Litchfield C, Taylor J (2005) Physiological control of leaf methane emission from wetland plants. *Aquatic Botany*, **81**, 141-155.
- Glatzel S, Forbrich I, Kruger C, Lemke S, Gerold G (2008) Small scale controls of greenhouse gas release under elevated N deposition rates in a restoring peat bog in NW Germany. *Biogeosciences*, **5**, 925-935.
- Gopal B, Ghosh D (2008) Natural Wetlands. In: *Encyclopedia of Ecology* (eds Sven EJ, Brian F), pp. 2493-2504. Academic Press, Oxford.
- Hakata M, Takahashi M, Zumft W, Sakamoto A, Morikawa H (2003) Conversion of the nitrate nitrogen and nitrogen dioxide to nitrous oxides in plants. *Acta Biotechnologica*, **23**, 249-257.
- Heincke M, Kaupenjohann M (1999) Effects of soil solution on the dynamics of N<sub>2</sub>O emissions: a review. *Nutrient Cycling in Agroecosystems*, **55**, 133-157.
- Holst J, Liu C, Yao Z, Brueggemann N, Zheng X, Giese M, Butterbach-Bahl K (2008) Fluxes of nitrous oxide, methane and carbon dioxide during freezing-thawing cycles in an Inner Mongolian steppe. *Plant and Soil*, **308**, 105-117.
- Hunter RG, Faulkner SP (2001) Denitrification potentials in restored and natural bottomland hardwood wetlands. *Soil Science Society of America Journal*, **65**, 1865-1872.
- Hyvoenen NP, Huttunen JT, Shurpali NJ, Tavi NM, Repo ME, Martikainen PJ (2009) Fluxes of nitrous oxide and methane on an abandoned peat extraction site: Effect of reed canary grass cultivation. *Bioresource Technology*, **100**, 4723-4730.
- Inamori R, Wang Y, Yamamoto T, Zhang J, Kong H, Xu K, Inamori Y (2008) Seasonal effect on N<sub>2</sub>O formation in nitrification in constructed wetlands. *Chemosphere*, **73**, 1071-1077.
- IPCC (2007) *The Physical Science Basis. Contribution of Working Group I to the Fourth Assessment Report of the Intergovernmental Panel on Climate Change*. Cambridge University Press, Cambridge.
- Jin T, Shimizu M, Marutani S, Desyatkin AR, Iizuka N, Hata H, Hatano R (2010) Effect of chemical fertilizer and manure application on N<sub>2</sub>O emission from reed canary grassland in Hokkaido, Japan. *Soil Science and Plant Nutrition*, **56**, 53-65.
- Joabsson A, Christensen TRj, Walløen B (1999) Vascular plant controls on methane emissions from northern peatforming wetlands. *Trends in Ecology & Evolution*, **14**, 385-388.
- Jones DL, Hodge A, Kuzyakov Y (2004) Plant and mycorrhizal regulation of rhizodeposition. *New Phytologist*, **163**, 459-480.

- Jungkunst HF, Flessa H, Scherber C, Fiedler S (2008) Groundwater level controls CO<sub>2</sub>, N<sub>2</sub>O and CH<sub>4</sub> fluxes of three different hydromorphic soil types of a temperate forest ecosystem. *Soil Biology and Biochemistry*, **40**, 2047-2054.
- Katterer T, Andren O, Pettersson R (1998) Growth and nitrogen dynamics of reed canarygrass (*Phalaris arundinacea* L.) subjected to daily fertilization and irrigation in the field. *Field Crops Research*, **55**, 153-164.
- Kaye JP, Hart SC (1997) Competition for nitrogen between plants and soil microorganisms. *Trends in Ecology & Evolution*, **12**, 139-143.
- Kercher SM, Zedler JB (2004) Flood tolerance in wetland angiosperms: a comparison of invasive and noninvasive species. *Aquatic Botany*, **80**, 89-102.
- Khalil K, Mary B, Renault P (2004) Nitrous oxide production by nitrification and denitrification in soil aggregates as affected by O<sub>2</sub> concentrations. *Soil Biology & Biochemistry*, **36**, 687-699.
- Kim SY, Lee SH, Freeman C, Fenner N, Kang H (2008) Comparative analysis of soil microbial communities and their responses to the short-term drought in bog, fen, and riparian wetlands. *Soil Biology and Biochemistry*, **40**, 2874-2880.
- Kirk GJD, Kronzucker HJ (2005) The potential for nitrification and nitrate uptake in the rhizosphere of wetland plants: A modelling study. *Annals of Botany*, **96**, 639-646.
- Kliwer BA, Gilliam JW (1995) Water-Table Management Effects on Denitrification and Nitrous-Oxide Evolution. *Soil Science Society of America Journal*, **59**, 1694-1701.
- Korner H, Zumft WG (1989) Expression of Denitrification Enzymes in Response to the Dissolved-Oxygen Level and Respiratory Substrate in Continuous Culture of *Pseudomonas-Stutzeri*. *Applied and Environmental Microbiology*, **55**, 1670-1676.
- Kuenen JG, Robertson LA (1994) Combined nitrification-denitrification processes. *FEMS Microbiology Reviews*, **15**, 109-117.
- Laiho R (2006) Decomposition in peatlands: Reconciling seemingly contrasting results on the impacts of lowered water levels. *Soil Biology & Biochemistry*, **38**, 2011-2024.
- Larsen KS, ANDRESEN LC, BEIER CLAU, et al (2011) Reduced N cycling in response to elevated CO<sub>2</sub>, warming, and drought in a Danish heathland: Synthesizing results of the CLIMAITE project after two years of treatments. *Global Change Biology*, **17**, 1884-1899.
- Lensi R, Chalamet A (1981) Absorption of Nitrous-Oxide by Shoots of Maize. *Plant and Soil*, **59**, 91-98.
- Li J, Lee X, Yu Q, Tong X, Qin Z, Macdonald B (2011) Contributions of agricultural plants and soils to N<sub>2</sub>O emission in a farmland. *Biogeosciences Discuss.*, **8**, 5505-5535.
- Liikanen A, Martikainen PJ (2003) Effect of ammonium and oxygen on methane and nitrous oxide fluxes across sediment-water interface in a eutrophic lake. *Chemosphere*, **52**, 1287-1293.

- Loftfield NS, Brumme R, Beese F (1992) Automated Monitoring of Nitrous-Oxide and Carbon-Dioxide Flux from Forest Soils. *Soil Science Society of America Journal*, **56**, 1147-1150.
- Maag M, Vinther FP (1996) Nitrous oxide emission by nitrification and denitrification in different soil types and at different soil moisture contents and temperatures. *Applied Soil Ecology*, **4**, 5-14.
- Maltais-Landry G, Maranger R, Brisson J, Chazarenc F (2009) Greenhouse gas production and efficiency of planted and artificially aerated constructed wetlands. *Environmental Pollution*, **157**, 748-754.
- Martikainen PJ, Nykanen H, Crill P, Silvola J (1993) Effect of A Lowered Water-Table on Nitrous-Oxide Fluxes from Northern Peatlands. *Nature*, **366**, 51-53.
- Mayo AW, Bigambo T (2005) Nitrogen transformation in horizontal subsurface flow constructed wetlands I: Model development. *Physics and Chemistry of the Earth*, **30**, 658-667.
- Megonigal JP, Hines ME, Visscher PT (2003) Anaerobic Metabolism: Linkages to Trace Gases and Aerobic Processes. In: *Treatise on Geochemistry* (eds Heinrich DH, Karl KT), pp. 317-424. Pergamon, Oxford.
- Mosier AR, Mohanty SK, Bhadrachalam A, Chakravorti SP (1990) Evolution of Dinitrogen and Nitrous-Oxide from the Soil to the Atmosphere Through Rice Plants. *Biology and Fertility of Soils*, **9**, 61-67.
- Müller C (2003) Plants affect the in situ N<sub>2</sub>O emissions of a temperate grassland ecosystem. *Journal of Plant Nutrition and Soil Science-Zeitschrift für Pflanzenernährung und Bodenkunde*, **166**, 771-773.
- Müller C, Stevens RJ, Laughlin RJ, Jäger HJ (2004) Microbial processes and the site of N<sub>2</sub>O production in a temperate grassland soil. *Soil Biology & Biochemistry*, **36**, 453-461.
- Noe-Nygaard N (1995) Ecological, sedimentary, and geochemical evolution of the late-glacial to postglacial Åmose lacustrine basin, Denmark. *Fossils & Strata*, **37**.
- Parkin TB, Tiedje JM (1984) Application of a soil core method to investigate the effect of oxygen concentration on denitrification. *Soil Biology and Biochemistry*, **16**, 331-334.
- Patrick WH, Reddy KR (1976) Nitrification-Denitrification Reactions in Flooded Soils and Water Bottoms - Dependence on Oxygen-Supply and Ammonium Diffusion. *Journal of Environmental Quality*, **5**, 469-472.
- Pennock D, Yates T, Bedard-Haughn A, Phipps K, Farrell R, McDougal R (2010) Landscape controls on N<sub>2</sub>O and CH<sub>4</sub> emissions from freshwater mineral soil wetlands of the Canadian Prairie Pothole region. *Geoderma*, **155**, 308-319.
- Pezeshki SR (2001) Wetland plant responses to soil flooding. *Environmental and Experimental Botany*, **46**, 299-312.
- Picek T, Cízková H, Dusek J (2007) Greenhouse gas emissions from a constructed wetland - Plants as important sources of carbon. *Ecological Engineering*, **31**, 98-106.

- Pihlatie M, Ambus P, Rinne J, Pilegaard K, Vesala T (2005) Plant-mediated nitrous oxide emissions from beech (*Fagus sylvatica*) leaves. *New Phytologist*, **168**, 93-98.
- Ravishankara AR, Daniel JS, Portmann RW (2009) Nitrous Oxide (N<sub>2</sub>O): The Dominant Ozone-Depleting Substance Emitted in the 21st Century. *Science*, 1176985.
- Reddy KR, Patrick WH, Lindau CW (1989) Nitrification-Denitrification at the Plant Root-Sediment Interface in Wetlands. *Limnology and Oceanography*, **34**, 1004-1013.
- Regina K, Nykanen H, Silvola J, Martikainen PJ (1996a) Fluxes of nitrous oxide from boreal peatlands as affected by peatland type, water table level and nitrification capacity. *Biogeochemistry*, **35**, 401-418.
- Regina K, Silvola J, Martikainen PJ (1999) Short-term effects of changing water table on N<sub>2</sub>O fluxes from peat monoliths from natural and drained boreal peatlands. *Global Change Biology*, **5**, 183-189.
- Regina K, Nykänen H, Silvola J, Martikainen P (1996b) Fluxes of nitrous oxide from boreal peatlands as affected by peatland type, water table level and nitrification capacity. *Biogeochemistry*, **35**, 401-418.
- Repo ME, Susiluoto S, Lind SE, et al (2009) Large N<sub>2</sub>O emissions from cryoturbated peat soil in tundra. *Nature Geosci*, **2**, 189-192.
- Robertson GP, Tiedje JM (1987) Nitrous oxide sources in aerobic soils: Nitrification, denitrification and other biological processes. *Soil Biology and Biochemistry*, **19**, 187-193.
- Rochette P, Eriksen-Hamel NS (2008) Chamber measurements of soil nitrous oxide flux: Are absolute values reliable? *Soil Science Society of America Journal*, **72**, 331-342.
- Rubinigg M, Stulen I, Elzenga JTM, Colmer TD (2002) Spatial patterns of radial oxygen loss and nitrate net flux along adventitious roots of rice raised in aerated or stagnant solution. *Functional Plant Biology*, **29**, 1475-1481.
- Rückauf U, Augustin J, Russow R, Merbach W (2004) Nitrate removal from drained and reflooded fen soils affected by soil N transformation processes and plant uptake. *Soil Biology and Biochemistry*, **36**, 77-90.
- Rusch H, Rennenberg H (1998) Black alder (*Alnus glutinosa* (L.) Gaertn.) trees mediate methane and nitrous oxide emission from the soil to the atmosphere. *Plant and Soil*, **201**, 1-7.
- Russow R, Sich I, Neue HU (2000) The formation of the trace gases NO and N<sub>2</sub>O in soils by the coupled processes of nitrification and denitrification: results of kinetic <sup>15</sup>N tracer investigations. *Chemosphere - Global Change Science*, **2**, 359-366.
- Sasikala S, Tanaka N, Wah HSYW, Jinadasa KBSN (2009) Effects of water level fluctuation on radial oxygen loss, root porosity, and nitrogen removal in subsurface vertical flow wetland mesocosms. *Ecological Engineering*, **35**, 410-417.
- Scholz M (2006) Constructed wetlands. In: *Wetland Systems to Control Urban Runoff (First Edition)* pp. 91-110. Elsevier, Amsterdam.

- Shannon RD, White JR, Lawson JE, Gilmour BS (1996) Methane efflux from emergent vegetation in peatlands. *Journal of Ecology*, **84**, 239-246.
- Skiba U, Smith KA (2000) The control of nitrous oxide emissions from agricultural and natural soils. *Chemosphere - Global Change Science*, **2**, 379-386.
- Smart DR, Bloom AJ (2001) Wheat leaves emit nitrous oxide during nitrate assimilation. *Proceedings of the National Academy of Sciences*, **98**, 7875-7878.
- Smeets EMW, Bouwmanw LF, Stehfest E, van Vuuren DP, Posthuma A (2009) Contribution of N<sub>2</sub>O to the greenhouse gas balance of first-generation biofuels. *Global Change Biology*, **15**, 1-23.
- Smith CJ, Patrick Jr WH (1983) Nitrous oxide emission as affected by alternate anaerobic and aerobic conditions from soil suspension enriched with ammonium sulfate. *Soil Biology & Biochemistry*, **15**, 693-697.
- Smith KA (1980) A Model of the Extent of Anaerobic Zones in Aggregated Soils, and Its Potential Application to Estimates of Denitrification. *Journal of Soil Science*, **31**, 263-277.
- Smith KA (1997) The potential for feedback effects induced by global warming on emissions of nitrous oxide by soils. *Global Change Biology*, **3**, 327-338.
- Sorrell BK, Brix H (2003) Effects of water vapour pressure deficit and stomatal conductance on photosynthesis, internal pressurization and convective flow in three emergent wetland plants. *Plant and Soil*, **253**, 71-79.
- Stadmark J, Seifert AG, Leonardson L (2009) Transforming meadows into free surface water wetlands: Impact of increased nitrate and carbon loading on greenhouse gas production. *Atmospheric Environment*, **43**, 1182-1188.
- Strong DT, Fillery IRP (2002) Denitrification response to nitrate concentrations in sandy soils. *Soil Biology and Biochemistry*, **34**, 945-954.
- Stumm W, Morgan JJ (1996) *Aquatic Chemistry - Chemical Equilibria and Rates in Natural Waters*. John Wiley & Sons, New York.
- Tanner CC (2001) Plants as ecosystem engineers in subsurface-flow treatment wetlands. *Water Science and Technology*, **44**, 9-17.
- Tiedje JM, Sexstone AJ, Myrold DD, Robinson JA (1983) Denitrification: ecological niches, competition and survival. *Antonie van Leeuwenhoek*, **48**, 569-583.
- van Noordwijk M, Martikainen P, Bottner P, Cuevas E, Rouland C, Dhillion SS (1998) Global change and root function. *Global Change Biology*, **4**, 759-772.
- Velthof GL, Brader AB, Oenema O (1996) Seasonal variations in nitrous oxide losses from managed grasslands in The Netherlands. *Plant and Soil*, **181**, 263-274.
- Velthof GL, Oenema O (1995) Nitrous oxide fluxes from grassland in the Netherlands .1. Statistical analysis of flux-chamber measurements. *European Journal of Soil Science*, **46**, 533-540.

- Vieten B, Conen F, Neftel A, Alewell C (2009) Respiration of nitrous oxide in suboxic soil. *European Journal of Soil Science*, **60**, 332-337.
- Vieten B, Conen F, Seth B, Alewell C (2008) The fate of N<sub>2</sub>O consumed in soils. *Biogeosciences*, **5**, 129-132.
- Wagner SW, Reicosky DC, Alessi RS (1997) Regression models for calculating gas fluxes measured with a closed chamber. *Agronomy Journal*, **89**, 279-284.
- Wiessner A, Kusch P, Stottmeister U (2002) Oxygen release by roots of *Typha latifolia* and *Juncus effusus* in laboratory hydroponic systems. *Acta Biotechnologica*, **22**, 209-216.
- Wolf B, Zheng X, Bruggemann N, et al (2010) Grazing-induced reduction of natural nitrous oxide release from continental steppe. *Nature*, **464**, 881-884.
- Wrage N, Velthof GL, van Beusichem ML, Oenema O (2001) Role of nitrifier denitrification in the production of nitrous oxide. *Soil Biology and Biochemistry*, **33**, 1723-1732.
- Yamulki S, Jarvis SC (1999) Automated chamber technique for gaseous flux measurements: Evaluation of a photoacoustic infrared spectrometer-trace gas analyzer. *Journal of Geophysical Research-Atmospheres*, **104**, 5463-5469.
- Yao ZS, Zheng XH, Xie BH, et al (2009) Comparison of manual and automated chambers for field measurements of N<sub>2</sub>O, CH<sub>4</sub>, CO<sub>2</sub> fluxes from cultivated land. *Atmospheric Environment*, **43**, 1888-1896.
- Yu K, Chen G (2009) Nitrous Oxide Emissions from Terrestrial Plants: Observations, Mechanisms and Implications. In: *Nitrous Oxide Emissions Research Progress* (eds Sheldon AI, Barnbart EP), pp. 85-104. Nova Science Publishers.
- Zhu R, Liu Y, Ma J, Xu H, Sun L (2008) Nitrous oxide flux to the atmosphere from two coastal tundra wetlands in eastern Antarctica. *Atmospheric Environment*, **42**, 2437-2447.
- Zhu T, Sikora FJ (1995) Ammonium and nitrate removal in vegetated and unvegetated gravel bed microcosm wetlands. *Water Science and Technology*, **32**, 219-228.





## Appendix 1 - Errata for paper 1

### Calculation of Carbon Dioxide Equivalent (CDE)

Global warming potential (GWP) for CH<sub>4</sub> = 25 & N<sub>2</sub>O = 298 according to 100 year lifetime scenario (IPCC, 2007)

CDE = Mass of greenhouse gas (g) x GWP

CDE compensation = emission fraction of GHG emission compared to C assimilation x GWP

Erroneous calculation of CDE as written in Paper 1 based on molecular C content:

Annual C assimilation as CO<sub>2</sub>-C = 620 g CO<sub>2</sub>-C m<sup>-2</sup> yr<sup>-1</sup>

Annual C emission as CH<sub>4</sub>-C = 2 g CH<sub>4</sub>-C m<sup>-2</sup> yr<sup>-1</sup>

Annual CDE compensation - CH<sub>4</sub> emissions = (2/620) g C m<sup>-2</sup> yr<sup>-1</sup> x 25 x 100 = 8 %

Correct calculation of CDE based on weight of entire molecule

Annual C assimilation as CO<sub>2</sub> = 620 g CO<sub>2</sub>-C m<sup>-2</sup> yr<sup>-1</sup> x (44/12) = 2274 g CO<sub>2</sub> m<sup>-2</sup> yr<sup>-1</sup>

Annual C emission as CH<sub>4</sub> = 2 g CH<sub>4</sub>-C m<sup>-2</sup> yr<sup>-1</sup> x (16/12) = 2.67 g CH<sub>4</sub> m<sup>-2</sup> yr<sup>-1</sup>

Annual N emission as N<sub>2</sub>O = 0.074 g N<sub>2</sub>O-N m<sup>-2</sup> yr<sup>-1</sup> x (44/28) = 0.116 g N<sub>2</sub>O m<sup>-2</sup> yr<sup>-1</sup>

Annual CH<sub>4</sub> emission in CDE = 2.67 g CH<sub>4</sub> m<sup>-2</sup> yr<sup>-1</sup> x 25 = 67 g m<sup>-2</sup> yr<sup>-1</sup>

Annual N<sub>2</sub>O emission in CDE = 0.116 g N<sub>2</sub>O m<sup>-2</sup> yr<sup>-1</sup> x 298 = 35 g m<sup>-2</sup> yr<sup>-1</sup>

Annual CDE compensation - CH<sub>4</sub> emissions = ((67/2274) g m<sup>-2</sup> yr<sup>-1</sup> x 100) x 25 ≈ 3.0 %

Annual CDE compensation - N<sub>2</sub>O emissions = ((35/2274) g m<sup>-2</sup> yr<sup>-1</sup> x 100) x 298 ≈ 1.5 %



## Appendix 2 - The PhD thesis - rules and requirements

(Source “<http://www.science.ku.dk/phd/student/during/thesis/>”)

The PhD thesis is, in essence, an account of the research work, results and implications of the PhD project. The thesis should be written by the PhD student only, but under due supervision by the supervisor(s).

### General requirements

1. The PhD thesis cannot be submitted by a group, each thesis must have one author only.
2. Master theses and other evaluated assignments cannot be resubmitted as a PhD thesis. However, such work can form a starting point for a PhD thesis, but cannot comprise the bulk of the thesis.
3. The PhD thesis should be written in English, but theses in Danish can be accepted if the subject area tradition justifies this.
4. The PhD thesis must be written as a monograph, or as a synopsis with attached paper manuscripts or published papers (see below).

### Required elements in a monograph

1. A title page with correct affiliations. In addition to names and local affiliations such as the Department, the following affiliations should be included at the title page: The PhD School of Science, Faculty of Science, University of Copenhagen, Denmark.
2. A summary (resumé) of the thesis and a Danish translation of the abstract (or vice versa if the main language in the thesis is Danish).
3. A short abstract suitable for databases etc.
4. Thesis objectives.
5. A description of the thesis subject in relation to the existing knowledge within that research field.
6. A description of the research work carried out during the PhD project (materials, methods and results).
7. A summarising discussion.
8. Conclusions and perspectives for future research within the field.
9. References.
10. If the monograph is based on one or more papers without a broad overview of the research field, a section giving an overview on the current state of the research within that field with future perspectives should be included.

### Required elements in a synopsis

1. A title page with correct affiliations. In addition to names and local affiliations such as the Department, the following affiliations should be included at the title page: The PhD School of Science, Faculty of Science, University of Copenhagen, Denmark.
2. A summary (resumé) of the thesis and a Danish translation of the abstract (or vice versa if the main language in the thesis is Danish).
3. A short abstract suitable for databases etc.
4. Thesis objectives.
5. A description of the thesis subject in relation to the existing knowledge within that research field.
6. An overview of the results presented in the attached papers/manuscripts in relation to the existing international knowledge within that field.
7. Conclusions and perspectives for future research within the field.
8. References.
9. Manuscripts or published papers enclosed as annexes to the synopsis (see below).

## **Co-author statements and authorship rules**

All papers/manuscripts with multiple authors enclosed as annexes to a PhD thesis synopsis should contain a co-author statement, stating the PhD student's contribution to the paper (use the "Co-author statement" form found [here](#)). The Vancouver Convention authorship guidelines (see <http://www.icmje.org/>) apply at the University of Copenhagen.

## **Confidentiality**

Parts of a PhD thesis can be treated as confidential if the interests of a collaborating company or institution warrant confidentiality. However, the evaluation of the PhD thesis and the award of the PhD degree can only be based on the public part of the thesis. This part must constitute an independent thesis in itself.

The official opinion on the PhD studies by the supervisor should be based on the entire PhD programme. The assessment committee bases the evaluation of the thesis on the public part. Likewise, the PhD defence will only include the public parts of the thesis.

If a PhD thesis contains material which is a part of a patent application, the publication of the thesis and the PhD defence can be postponed by agreement between the PhD student, the external partners and the PhD School of Science. A patent application must be filed as soon as possible during the PhD programme and should not cause unnecessary delays of the PhD defence.

**Appendix 3 - Co-author statements**



### Declaration of co-authorship

**Name:**  **Civ. Reg. No. (CPR No.):**

**Department:**  **E-mail:**

**Principal supervisor:**  **Supervisor's e-mail:**

**Position of supervisor:**

**Title of PhD thesis:**

**This co-authorship declaration applies to the following paper:**

**The student's contribution to the paper:**

Signatures of co-authors:		
Date	Name	Signature
10/8-2011	Louise Askaer	<i>L. Askaer</i>
12/8-2011	Bo Elberling	<i>Bo Elberling</i>
12/8-2011	Thomas Friberg	<i>Thomas Friberg</i>
16/8-2011	Birger Ulf Hansen	<i>Birger Ulf Hansen</i>



## Declaration of co-authorship

**Name:**  **Civ. Reg. No. (CPR No.):**

**Department:**  **E-mail:**

**Principal supervisor:**  **Supervisor's e-mail:**

**Position of supervisor:**

**Title of PhD thesis:**

**This co-authorship declaration applies to the following paper:**

Linking Soil O<sub>2</sub>, CO<sub>2</sub>, and CH<sub>4</sub> Concentrations in a Wetland Soil: Implications for CO<sub>2</sub> and CH<sub>4</sub> Fluxes

**The student's contribution to the paper:**

Data analysis, illustrations and paper writing

Signatures of co-authors:		
Date	Name	Signature
12/8-2011	Bo Elberling	<i>Bo Elberling</i>
19/8-2011	Louise Askaer	<i>L. Askaer</i>
11/8-2011	Hans P. Joensen /	<i>Hans P. Joensen</i>
10/8-2011	Michael Kühl	<i>Michael Kühl</i>
10/8-2011	Ronnie Glud	<i>Ronnie Glud</i>
11/8-2011	Frants R. Lauritsen	<i>Frants R. Lauritsen</i>





## Declaration of co-authorship

<b>Name:</b>	Christian Juncher Jørgensen	<b>Civ. Reg. No. (CPR No.):</b>	130976
<b>Department:</b>	Geography and Geology	<b>E-mail:</b>	cjj@geo.ku.dk
<b>Principal supervisor:</b>	Bo Elberling	<b>Supervisor's e-mail:</b>	be@geo.ku.dk
<b>Position of supervisor:</b>	Professor		

**Title of PhD thesis:** Turnover and transport of greenhouse gases in a Danish wetland -Effects of water level changes and plant-mediated gas transport on N<sub>2</sub>O production, consumption and emission dynamics

**This co-authorship declaration applies to the following paper:**

Temporal trends in N<sub>2</sub>O flux dynamics in a Danish wetland – effects of plant-mediated gas transport of N<sub>2</sub>O and O<sub>2</sub> following changes in water level and soil mineral-N availability

**The student's contribution to the paper:**

All principal aspects including field work, data analysis, illustrations and paper writing

Signatures of co-authors:		
Date	Name	Signature
12/8-2011	Bo Elberling	
16/8-2011	Sten Struwe	

## Declaration of co-authorship

**Name:**  **Civ. Reg. No. (CPR No.):**

**Department:**  **E-mail:**

**Principal supervisor:**  **Supervisor's e-mail:**


**Position of supervisor:**

**Title of PhD thesis:**

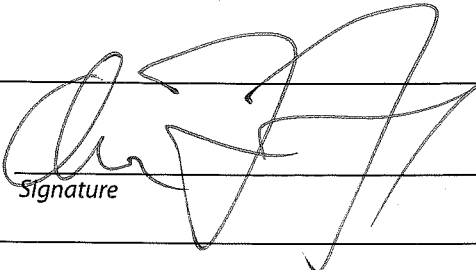
**This co-authorship declaration applies to the following paper:**

**The student's contribution to the paper:**

**Signatures of co-authors:**

Date	Name	Signature
12/8-2011	Bo Elberling	



PhD student:  Signature	Date: <input type="text" value="11/08-2011"/>
---	---

**A copy must be sent to the Department.**

**When completed, the form with signatures must be forwarded by e-mail, preferably in PDF format, to:**

E-mail: [PhD@science.ku.dk](mailto:PhD@science.ku.dk)

*PhD School at the Faculty of Science,  
University of Copenhagen,  
Tagensvej 16, DK-2200 Copenhagen N.*

**Annex I-IV**





# Annex I







# Plant-mediated CH<sub>4</sub> transport and C gas dynamics quantified in-situ in a *Phalaris arundinacea*-dominant wetland

Louise Askaer · Bo Elberling · Thomas Friborg ·  
Christian J. Jørgensen · Birger U. Hansen

Received: 15 September 2010 / Accepted: 7 January 2011 / Published online: 1 February 2011  
© Springer Science+Business Media B.V. 2011

**Abstract** Northern peatland methane (CH<sub>4</sub>) budgets are important for global CH<sub>4</sub> emissions. This study aims to determine the ecosystem CH<sub>4</sub> budget and specifically to quantify the importance of *Phalaris arundinacea* by using different chamber techniques in a temperate wetland. Annually, roughly 70±35% of ecosystem CH<sub>4</sub> emissions were plant-mediated, but data show no evidence of significant diurnal variations related to convective gas flow regardless of season or plant growth stages. Therefore, despite a high percentage of aerenchyma, *P. arundinacea*-mediated CH<sub>4</sub> transport is interpreted to be predominantly passive. Thus, diurnal variations are less important in contrast to wetland vascular plants facilitating convective gas flow. Despite of plant-dominant CH<sub>4</sub> transport, net CH<sub>4</sub> fluxes were low (−0.005–0.016 μmol m<sup>−2</sup> s<sup>−1</sup>) and annually less than 1% of the annual C-CO<sub>2</sub> assimilation. This is considered a result of an effective root zone oxygenation resulting in increased CH<sub>4</sub>

oxidation in the rhizosphere at high water levels. This study shows that although CH<sub>4</sub>, having a global warming potential 25 times greater than CO<sub>2</sub>, is emitted from this *P. arundinacea* wetland, less than 9% of the C sequestered counterbalances the CH<sub>4</sub> emissions to the atmosphere. It is concluded that *P. arundinacea*-dominant wetlands are an attractive C-sequestration ecosystem.

**Keywords** Plant-mediated CH<sub>4</sub> flux · Automated closed static chambers · Diurnal variation · *Phalaris arundinacea*

## Introduction

In wetland ecosystems, the rate of photosynthetic production of organic matter exceeds decomposition (Clymo 1983). Wetlands are important carbon (C) sinks holding 20–30% of the global terrestrial carbon pool (Gorham 1991). C sink capacity is sensitive to changes in hydrological conditions driven by both land use and climate change. Carbon dioxide (CO<sub>2</sub>) is the main end product of aerobic organic matter decomposition under oxic conditions, while methane (CH<sub>4</sub>) is the main end product of anaerobic decomposition under anoxic conditions after the depletion of alternative electron acceptors. Due to the prevalence of anoxic conditions in wet ecosystems, natural wetlands are at present the single largest CH<sub>4</sub> source (IPCC 2007) and Northern

---

Responsible Editor: Eric J.W. Visser.

**Electronic supplementary material** The online version of this article (doi:10.1007/s11104-011-0718-x) contains supplementary material, which is available to authorized users.

---

L. Askaer · B. Elberling (✉) · T. Friborg ·  
C. J. Jørgensen · B. U. Hansen  
Department of Geography and Geology,  
University of Copenhagen,  
Øster Voldgade 10,  
1350 Copenhagen K, Denmark  
e-mail: be@geo.ku.dk



peatlands alone emit more than 12% of the global total CH<sub>4</sub> emissions (Wuebbles and Hayhoe 2002). Therefore, wetland ecosystems are of great interest in a global change perspective as CH<sub>4</sub> has a 25 times greater global warming potential than CO<sub>2</sub> on a 100-year time horizon (IPCC 2007).

The majority of wetland vascular plants have aerenchyma, an internal gas-space ventilation system to provide aeration for submerged organs in anoxic peat (Joabsson et al. 1999). Under anoxic conditions the aerenchyma can facilitate the transport of CH<sub>4</sub> from roots in the anaerobic zone to the atmosphere, by-passing the aerobic, methane-oxidizing peat layers (Whalen 2005). Studies of *P. arundinacea* have shown a very high percentage of aerenchyma and Kercher and Zedler (2004) found that, *P. arundinacea* had the highest levels of internal root airspace among seventeen different wetland plant species. There are two major mechanisms involved in plant-mediated transport of CH<sub>4</sub> to the atmosphere; 1) molecular diffusion and 2) convective gas flow (Joabsson et al. 1999). Molecular diffusion is a passive transport mechanism driven by the respiratory uptake of oxygen (O<sub>2</sub>) by plants, which creates a diffusion gradient that draws O<sub>2</sub> from the atmosphere to roots and rhizomes. This is accompanied by an upward diffusion of CH<sub>4</sub> from the rhizosphere to the atmosphere via aerenchyma down the concentration gradient (Brix et al. 1992). In contrast, convective flow is an active mechanism driven by differences in temperature or water-vapour pressure between the internal air spaces in plants and the surrounding atmosphere (Brix et al. 1992). Differences in temperature or water-vapour are primarily created by diurnal atmospheric temperature variations. These differences generate a pressure gradient that drives gas flow from leaves to rhizome and then vent back to the atmosphere through old leaves or horizontal rhizomes connected to other shoots (Brix et al. 1992). To our knowledge, CH<sub>4</sub> and O<sub>2</sub> transport pathways in *P. arundinacea* have not been reported and their ability to produce static internal gas pressure differentials producing internal convective airflows as well as their resistance to airflow at the stem-rhizome junction are still unclear. A study of internal pressurization and convective gas flow in emergent freshwater macrophytes by Brix et al. (1992) summarises that macrophytes growing predominantly in very shallow water or on wet soil do not produce a significant

convective through-flow. Therefore, passive CH<sub>4</sub> transport by molecular diffusion may be the dominant process in *P. arundinacea* as water levels in the area seldom increase above the peat surface at the investigated field site. However, stands of *Phragmites australis* are found within similar conditions in the study area, and they are well documented for their convective gas flow (Brix et al. 1992; Grünfeld and Brix 1999; Armstrong and Armstrong 1991). It has previously been shown that 80–90% of CH<sub>4</sub> effluxes from wetlands occur through plants containing aerenchymous tissue (Lai 2009). Therefore, CH<sub>4</sub> emissions from wetland ecosystems are strongly influenced by the type of plants present, the dominant transport mechanisms and hence the potential for CH<sub>4</sub> transport to the atmosphere.

Previous studies of CH<sub>4</sub> fluxes from various wetland vegetation types e.g. *Carex lasiocarpa* and *Typha latifolia* L. have shown distinct diurnal CH<sub>4</sub> emission patterns (Ding et al. 2004; Mikkilä et al. 1995; Whiting and Chanton 1996), and Mikkilä et al. (1995) concluded that short daytime measurements of CH<sub>4</sub> fluxes could result in an underestimation of the CH<sub>4</sub> emission, amounting to ~25% for Swedish mire types. In relation to sampling strategies and calculating greenhouse gas budgets and potential feedbacks to climate change, it is highly relevant to quantify the diurnal variation throughout the year from a *P. arundinacea*-dominated wetland. This is especially important in light of increasing numbers of wetland restorations, more frequently flooded areas and the introduction of perennial invasive wetland plant species such as *P. arundinacea* as biofuel crops in northern wetlands. In Denmark alone, 8,000 ha of wetland reconstruction are projected in an effort to remove 1,100 tN from the soil system each year (Danish Ministry of Economic and Business Affairs 2009). Furthermore, the European Union have set a general target that 20% of energy used should be based on renewable energy sources by 2020 (Commission of the European Communities 2007). *P. arundinacea* is a potential crop for bio-energy (Adler et al. 2007) resulting in rapidly increasing cultivation areas in northern territories. In Finland alone, *P. arundinacea* is projected to take up 100,000 ha by 2012 (Hyvönen et al. 2009).

The main objective of this study is to determine the importance of *P. arundinacea* on ecosystem CH<sub>4</sub> fluxes by (1) evaluating the dominant transport

mechanism through *P. arundinacea* and (2) quantifying the net C—greenhouse gas budget of a *P. arundinacea*-dominant wetland. Here, in-situ measurements include high temporal resolution automated closed static chambers and weekly manual static chamber measurements of CH<sub>4</sub> and CO<sub>2</sub> fluxes. Flux measurements were combined with subsurface measurements of gas concentrations, temperature and water level, to assess the link between subsurface CH<sub>4</sub> production and consumption. Furthermore, the CH<sub>4</sub> transport pathways to the atmosphere are assessed from the high temporal resolution automated chamber measurements. We hypothesise that *P. arundinacea* is effective in C sequestration although the high percentage of aerenchyma may result in high levels of CH<sub>4</sub> transfer from anoxic soil layers to the atmosphere bypassing oxic layers and thereby reducing soil CH<sub>4</sub> oxidation potentials. High CH<sub>4</sub> emissions may counteract the CO<sub>2</sub> sequestered from the atmosphere and thus the C sequestration potential in a global change perspective. Throughout this manuscript, positive ecosystem fluxes (effluxes) represent emissions to the atmosphere while negative ecosystem fluxes represent an uptake.

## Materials and methods

### Site characteristics

The study site is situated in a temperate wetland area, Maglemeden (roughly 0.6 km<sup>2</sup>), formed through the retreat of an ancient inlet near Vedbæk about 20 km north of Copenhagen, Denmark (55°51'N, 12°32'E) (Supporting Figure 1S, online). The climate is characterised by a mean annual temperature of 8 °C and a mean annual precipitation of 613 mm (normal for 1961–1990 Danish Meteorological Institute, [www.dmi.dk](http://www.dmi.dk)). The peat depths range from 3 m at the deepest points to roughly 0.5 m at the margins of which the top 50 cm is a terrestrial peat deposit. The study site is located in a non-managed *P. arundinacea*-dominated area of the wetland. In order to reduce the impact on the area during weekly measuring campaigns, 20 m of boardwalks were constructed on 3 m long pillars installed vertically into the peat roughly 10 months prior to measurements. All measurements were made within reach of these boardwalks.

### Vegetation characteristics

The graminoid wetland site is dominated by *Phalaris arundinacea* (>95%) while *Poa trivialis* and *Juncus effesus* are found in isolated stands. *P. arundinacea*, is an invasive, perennial grass, which reproduces by seed and spreads by creeping rhizomes. At the site, growth begins in early spring (March) dominated by vertical growth to roughly 2 m within 5–7 weeks and then expands horizontally. The annual life cycle for *P. arundinacea* has been divided into seven stages (according to Wisconsin Reed Canary Grass Management Working Group 2009) and are used consistently in this paper as follows (months in brackets indicate approx. timing specific to Maglemeden): dormancy (October–February), initial sprouting (either from a rhizome or seed) (March/April), tillering and initial growth peak (May), flowering (June), seed shattering (July/August), mid-summer dormancy (stems lodge and may grow parallel to the ground) (August), and second growth peak (root and rhizome development) (August/September).

### Soil analyses

Volume specific (100 cm<sup>3</sup>) soil samples were taken from 2, 5, 10, 20, 30, 40 and 60 cm below the surface in 3 replicate core profiles. Flowers and seeds of terrestrial plants (*Chenopodium*) and shells of marine snails (*Hydrobia ventrosa*) were selected for AMS <sup>14</sup>C analyses and analysed according to Bennike et al. (1994). The soil pH was measured in-situ in all samples (Metrohm 704 Pocket pH meter). The soil samples were dried at 60 °C for 3 days to obtain soil bulk density. Total carbon was measured on a CS500-analyser (ELTRA GmbH, Germany). Total nitrogen was determined on an Elemental Determinator (Leco). Peat samples from 10 depths were analyzed by solid-state <sup>13</sup>C nuclear magnetic resonance (NMR) according to Knicker and Skjemstad (2000) (Appendix S1, online).

### Environmental parameters

A meteorological station was constructed to monitor air temperature at 2 m height (Campbell Scientific 107 Temperature probe), wind speed (A100R anemometer), wind direction (W200P Potentiometer wind vane) relative humidity, radiation and soil temperature at

depths 0, 10, 20, 30, 40, 50, 60, 70 cm at 30 min intervals. Photosynthetically active radiation (PAR) was calculated from incoming short wave radiation (SI) using the equation:  $PAR = -0.04 + 0.47 \cdot SI$  where both PAR and SI are given in  $MJ\ m^{-2}\ d^{-1}$  according to Papaioannou et al. (1993). Barometric pressure and precipitation data were obtained from a meteorological station (WS2310 weather station) within a 5 km radius. The ground water level was monitored by a pressure transducer (Druck PDCR 1830 Series) installed in a 2.5 m long perforated plastic tube. In order to ensure a correct measurement of the water table height unaffected by peat swelling and shrinking, the pressure transducer was fastened to a crossbar between two 3 m long metal rods installed 2.6 m into the peat. Replicate water level tubes installed at each of the Automated Closed Static (ACS) chambers were manually measured weekly.

#### Automated closed static (ACS) chambers—Total ecosystem flux

Net ecosystem exchange (NEE) and ecosystem  $CH_4$  flux was measured continuously in 3 replicate ACS Plexiglas (~80% of the PAR transmission) chambers (690 mm×690 mm×500 mm+extensions of heights 500 mm and 1200 mm) (Supporting Figure 2S, online). A lid (750 mm×730 mm) was constructed and fitted to the chamber with two large and robust plastic hinges. The lid was motorised (Linak A/S, S3010-0050010) and a rubber gasket attached to the top of the chamber ensured air tightness. The chambers were permanently installed at the soil surface on a metal rim inserted 25 cm into the soil to ensure one dimensional gas transport between the soil and the chamber. Chambers were installed in one representative isolated stand of *P. arundinacea* with regard to vegetation composition and cover, topographical elevation and stand density. The lid was

open for 20 min between measurements and closed for a total of 6 min during measurements. The chamber was continuously vented and air was mixed during measurements using a standard computer fan. During measurements, air samples were transported through 10-m long 0.5-mm inner diameter (id) (0.9 mm outer diameter (od)) R.S. 293-2000 tubing from the chamber, first into a LiCor  $CO_2/H_2O$  Gas Analyzer (Li-840, LiCor, Lincoln, USA) and thereafter into a High Accuracy Methane Analyzer (Los Gatos Research, Inc., CA, USA) and back into the chamber. The setup was powered by a 12 V power cable from an outlet 200 m away. During measurements, concentrations of both  $CO_2$  and  $CH_4$  were measured at 30 sec intervals. Measurements were logged through a CR1000 Wiring panel to a Campbell CFM100 Compact flash memory module. The  $CO_2$  flux measurements made when  $PAR < 50\ \mu mol\ photon\ m^{-2}\ s^{-1}$  were defined as ecosystem respiration ( $R_{eco}$ ) as with no incoming PAR the fluxes measured during the night should represent the respiring components of the system (Ruimy et al. 1995). The effects of the chambers at full height (2.45 m) on the natural exchange of  $CH_4$  from the soil was validated at two campaign measurements. No significant differences in  $CO_2$  and  $CH_4$  concentrations within the chamber compared to outside the chamber, indicating sufficient ventilation between measurements (Table 1). The influence of the Plexiglas chamber on the soil temperature at 5 and 10 cm of depth showed no significant difference at a 95% confidence interval ( $p > 0.05$ ) from simultaneous temperatures measured outside the chamber. However, as only 80% of the PAR passes through the Plexiglas, C sequestration may be underestimated. This has not been taken into account in the following study but PAR transmission is in a similar range as observed before using chambers (e.g. Roehm and Roulet 2003).

**Table 1** Chamber ventilation validation by measuring profiles of  $CH_4$  and  $CO_2$  concentrations at 3 heights inside each open chamber and in free air

Sample height	0.4 m		1.2 m		1.8 m	
	$CO_2$	$CH_4$	$CO_2$	$CH_4$	$CO_2$	$CH_4$
Chamber nr.						
1	231.2	2.22	267.7	2.71	290.8	2.35
2	288.4	2.68	186.7	1.91	223.1	2.59
3	248.3	2.08	229.2	1.96	218.6	1.99
Mean ( $\pm$ SD)	256.0 $\pm$ 29.4	2.33 $\pm$ 0.31	227.9 $\pm$ 40.6	2.19 $\pm$ 0.45	244.2 $\pm$ 40.4	2.31 $\pm$ 0.30
Natural	254.0	2.28	261.7	2.34	281.4	2.31

## Manual closed static (MCS) chambers—soil ecosystem flux

Soil ecosystem  $\text{CH}_4$  flux was measured weekly using 3 replicate MCS chambers from which replicate gas samples were withdrawn by syringe for Gas Chromatography (GC) analyses of  $\text{CH}_4$  within 24 hrs. Chambers were constructed of a closed-end CHA Type plumbing coupling id: 110 mm which could be securely fitted on the base column. The total volume of the chamber was on average 0.5 L, dependent on the height of the soil in the base collar. Actual heights were measured for each measurement and the volumes calculated were used in the flux calculations. Before the chamber was attached to the base collar, a gas sample was taken in the centre of the base collar. Thereafter, the chamber was attached and the chamber headspace was sampled three times at 15 min intervals. Samples (10 ml) were taken in a plastic syringe and ejected into a 2.5 ml glass injection flask with an 11 mm collar resulting in a flushing of 7.5 ml through an inserted outlet syringe needle. A septa lid consisting of Polyisobutylene was fitted to the injection flask with an 11 mm aluminium capsule using a tong (reference nr. LP 11090831, WH 224100030, LP11060006, ML 33022 Mikrolab Aarhus A/S). Samples were analyzed within 24 h using a Shimadza GC 2014 with back flush system. Methane was analysed with a Mol Sive 5A 80/100 mesh (1/8"×1 m) column connected to an FID detector. As samples were extracted by syringe, compensation air was simultaneously drawn into the chamber through a 10 cm 1 mm id pressure equilibrium tube. The sample withdrawal was roughly 6% of the total air in the chamber. Before each measurement the chamber air was mixed carefully by slowly pumping 5 ml (1% of total sample) air out of the chamber and into the chamber again using the syringe. Volumetric soil water content in 0–5 cm depth was manually measured using a Theta Probe Soil Moisture Sensor (ML2x, Delta-T Devices Ltd, Cambridge, UK) and soil temperatures in 2 cm and 5 cm depth were measured simultaneously at each of the 3 replicate chambers. Using the MCS chambers, gas samples are obtained from the soil ecosystem in the *P. arundinacea*-dominated area. Although eliminating above-ground plant biomass and thereby the rhizosphere and its related processes are considered

comparable to those found below the ACS chambers e.g. organic acid excretion and  $\text{CH}_4$  oxidation (Fig. 1). The volumetric soil water content in 0–5 cm depth was monitored manually using a Theta Probe Soil Moisture Sensor (ML2x, Delta-T Devices Ltd, Cambridge, UK) in 50 replicates. Soil temperatures at 2 cm and 5 cm depth were measured in 10 replicates.

## Depth specific gas sampling using silicone probes

Depth specific soil  $\text{CH}_4$  and  $\text{CO}_2$  concentrations were measured weekly at depths 5, 10, 20 and 50 cm using probes constructed from silicone tubing as described by Kammann et al. (2001). Each probe consisted of 1.3 m of tubing (id 10 mm, wall thickness 3 mm) giving a total probe volume of 100 ml closed with a rubber septa at both ends. The tubing was rolled into a coil and fixed by wire. A 0.92 mm (id) stainless steel tube was inserted through the outer septa of the probe to connect the silicone probe in the soil with the soil surface (1 ml dead volume per meter steel tube). The end of the steel tube was fitted with a three-way stopcock to enable the soil air to be sampled undisturbed from the soil surface. Soil gas samples were taken with 60 ml plastic syringes and handled and analyzed in the same manner as gas samples from the MCS chambers. The silicon probes were installed in the peat soil by pre-cutting a 20 cm×3 cm semicircular cavity in a soil pit wall. Probes were

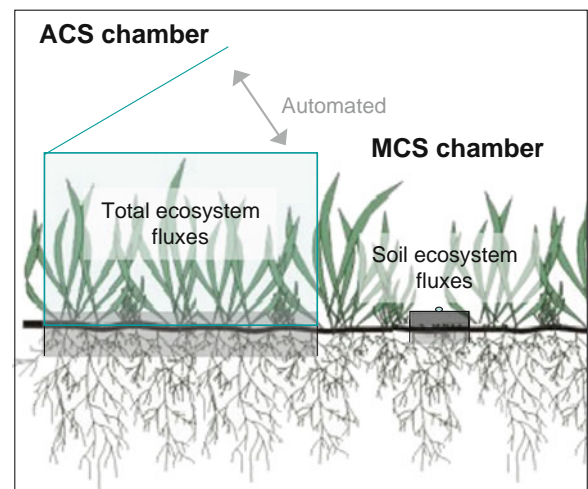


**Fig. 1** Schematic illustration of the difference between total ecosystem flux and soil ecosystem flux measured by ACS chambers and MCS chambers

inserted into each cavity and the soil was seen to close around the probe after insertion. The pit was refilled with soil, horizon by horizon.

### Analytical procedures

Measurements from the ACS chambers during a closure period were analyzed using Eq. 1. The concentration change over time ( $\Delta C/\Delta t$ ) was analyzed by linear regression. Both  $\text{CO}_2$  and  $\text{CH}_4$  fluxes were calculated from sample concentrations measured after chamber closure over 4.5 min. The measurements were temperature and pressure-corrected according to Eq. 1.

$$F_c = \frac{(\Delta C/\Delta t)Vp}{RTA} \quad (1)$$

Where  $\Delta C$  is the change in concentration in ppm,  $\Delta t$  is the change time in seconds,  $V$  is the volume of air in the chamber in  $\text{m}^3$ ,  $p$  is the atmospheric pressure during measurement time in atm,  $R$  is the ideal gas constant in  $\text{m}^3 \text{atm mol}^{-1} \text{K}^{-1}$ ,  $T$  is the temperature in the chamber in Kelvin and  $A$  is the basal area of the chamber in  $\text{m}^2$ . A significance test was made to remove flux measurements where  $p > 0.1$ . Roughly 25% of  $\text{CH}_4$  measurements and 8% of  $\text{CO}_2$  measurements were removed due to lack of linearity resulting from chamber lid malfunctions, power and thus pump and analyser malfunctions or fluxes close or equal to zero. The significance test could in theory result in an underestimation of  $\text{CH}_4$  effluxes as ebullition events resulting in non-linear increases in concentrations are removed. Tokida et al. (2007) state that an estimated 50–64% of total  $\text{CH}_4$  fluxes in northern peatlands may

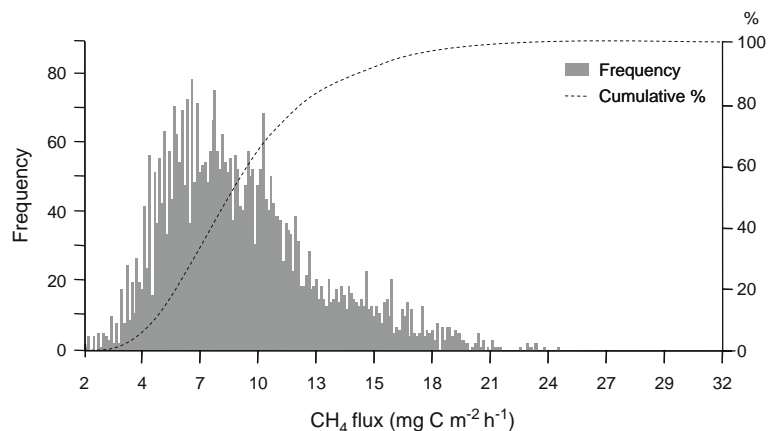
be emitted by ebullition. A frequency histogram was constructed for  $\text{CH}_4$  fluxes to evaluate the importance of ebullition on net  $\text{CH}_4$  fluxes according to Ström et al. 2005. Fluxes were normally distributed and no marked frequency peaks were noted (Fig. 2). However, data is skewed towards higher fluxes in line with periods with a high water level.

The significance test furthermore results in the removal of all  $\text{CH}_4$  and NEE measurements where the flux is  $\sim 0$ . For NEE measurements this is during reversal of flux direction between night and day. We acknowledge this error, however, as it has no effect on the C budget as the flux  $\sim 0$  this error is not accounted for. A similar but less selective significance test was made to remove measurement series where  $p > 0.25$  for samples taken from the MCS chambers due to less degrees of freedom. Contour plots of subsurface  $\text{CH}_4$  concentrations have been constructed by kriging using Surfer Version 8.05 (Surface Mapping System, Golden Software Inc.). Correlation analyses have been made using Pearson correlation. Correlation and multiple regression analyses have been carried out using SPSS 18.0. The temperature dependence of soil respiration is assessed by the increase in reaction rate per  $10^\circ \text{C}$  ( $Q_{10}$ ).

### Results

Soil characteristics can be seen in Table 2. Further information is found in Askaer et al. (2010). The peat-deposited SOC (0–30 cm depth) amounts to  $29 \text{ kg m}^{-2}$  thereby resulting in a recent mean accumulation rate of  $730 \pm 175 \text{ gC m}^{-2} \text{ yr}^{-1}$ . The peat-deposited SOC

**Fig. 2**  $\text{CH}_4$  flux histogram for chamber 3 (Jan–April 2008)





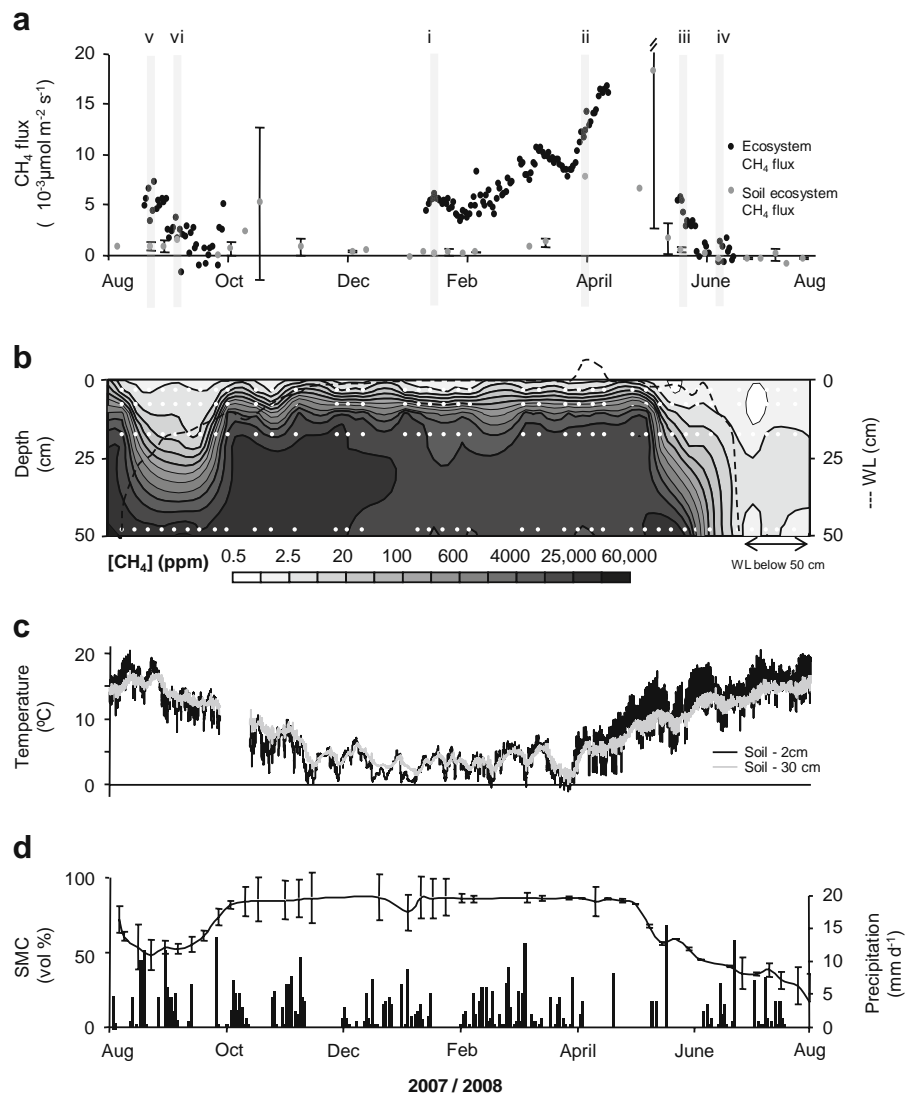
(0–50 cm depth) amounts to  $47 \text{ kg m}^{-2}$  thereby resulting in a longer term mean accumulation rate of  $\sim 76 \pm 18 \text{ g C m}^{-2} \text{ yr}^{-1}$  over the past  $\sim 600$  years.

### CH<sub>4</sub> fluxes and depth-specific CH<sub>4</sub> concentrations

Daily average ecosystem and soil CH<sub>4</sub> fluxes from August 2007 to August 2008 are shown in Fig. 3a. The mean annual water level in this period was  $-11 \text{ cm}$ , with a range of 6.5 cm above the surface to  $-81 \text{ cm}$  below the surface (Fig. 3b). The water level was near the soil surface from November until May 2008 where the near soil surface water content and temperature, fluctuated around 80% vol. and  $3^\circ \text{C}$

(Fig. 3c–d). A significant correlation was found between water level and surface soil moisture content ( $r^2=0.63$ ,  $p<0.01$ ,  $n=55$ ). Ecosystem CH<sub>4</sub> emissions were highest during periods where high water level coincided with high soil temperatures during April–May (Fig. 3a–d). Ecosystem CH<sub>4</sub> fluxes ranged from  $-0.005$  to  $0.017 \mu\text{mol CH}_4 \text{ m}^{-2} \text{ s}^{-1}$  and soil CH<sub>4</sub> fluxes ranged from  $-0.0009$  to  $0.018 \mu\text{mol CH}_4 \text{ m}^{-2} \text{ s}^{-1}$  over the measurement period. A significant correlation was found between the available overlapping data on ecosystem CH<sub>4</sub> emissions measured by ACS chambers and soil fluxes measured by MCS chambers (Fig. 4), showing that soil fluxes amounted to  $32 \pm 22\%$  of the ecosystem flux

**Fig. 3** **a** Daily average CH<sub>4</sub> fluxes measured by automatic chambers (black circle) and static chambers (white circle) calculated by linear regression. Missing data is due to problems with the electrical supply to the automatic chambers or datalogging unit. **b** Contour map of depth specific soil CH<sub>4</sub> concentrations and water level (WL). The contour map is constructed from weekly measurements from 5, 10, 20 and 50 cm depth (measurement frequency is shown as white dots). **c** Soil temperatures at 2 and 30 cm depths ( $^\circ\text{C}$ ). **d** Daily precipitation (mm), and soil surface moisture content (vol %). Error bars show 1 SD from the mean. Roman letters and grey boxes signify high temporal resolution measurement periods shown on Fig. 7



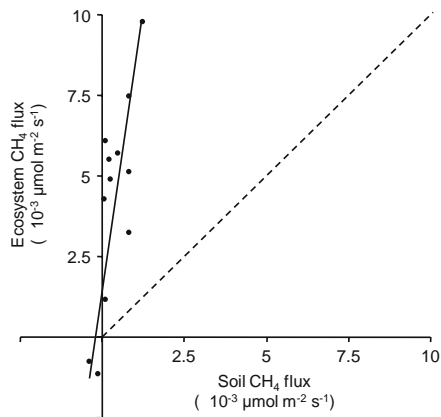
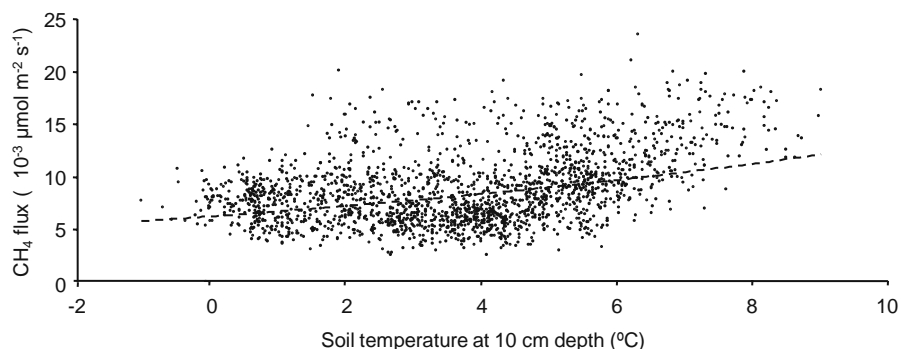


**Fig. 4** Soil CH<sub>4</sub> flux versus ecosystem CH<sub>4</sub> flux. Best fit line  $y=5.2198x+0.0024$  ( $r^2=0.5847$ ,  $n=12$ ). The dashed line shows the 1:1 relationship

( $y=5.22x+0.0024$ ,  $r^2=0.6$ ,  $n=12$ ,  $p=0.004$ ). The ecosystem CH<sub>4</sub> fluxes did not correlate significantly with atmospheric or soil temperatures. However, 15% of the variation in ecosystem CH<sub>4</sub> flux could be explained by the soil temperature at -10 cm depth when the water level was constant (~0 cm) from January–April (Fig. 5). During this period, the  $Q_{10}$  equalled 2.1. Ecosystem CH<sub>4</sub> fluxes correlated significantly with the water level, explaining 18% of the variation in the CH<sub>4</sub> flux throughout the year ( $r=0.43$ ,  $n=7051$ ,  $p=0.00$ ). No soil CH<sub>4</sub> effluxes were measured at water levels below 30 cm.

Depth-specific subsurface CH<sub>4</sub> concentrations were highest at 50 cm depth and decreased towards the surface (Fig. 3b). Highest concentrations of up to 6% CH<sub>4</sub> were found in October–December 2007 and May 2008 when the water level was near the surface and temperatures were ~10 °C. Lowest CH<sub>4</sub> concentrations were measured during the dry months of

**Fig. 5** Hourly average ecosystem CH<sub>4</sub> fluxes from January to April (2008) versus soil temperature at 10 cm depth. The water level was constant at or above 0 cm during this period. Exponential line (dashed) of the best fit:  $y=0.0061e^{0.0748x}$  ( $r^2=0.15$  and  $Q_{10}=2.1$ )



September 2007, and June and July 2008 when peat layers down to 20 cm depth had CH<sub>4</sub> concentrations below atmospheric CH<sub>4</sub> concentrations resulting in CH<sub>4</sub> soil uptake (Fig. 3a).

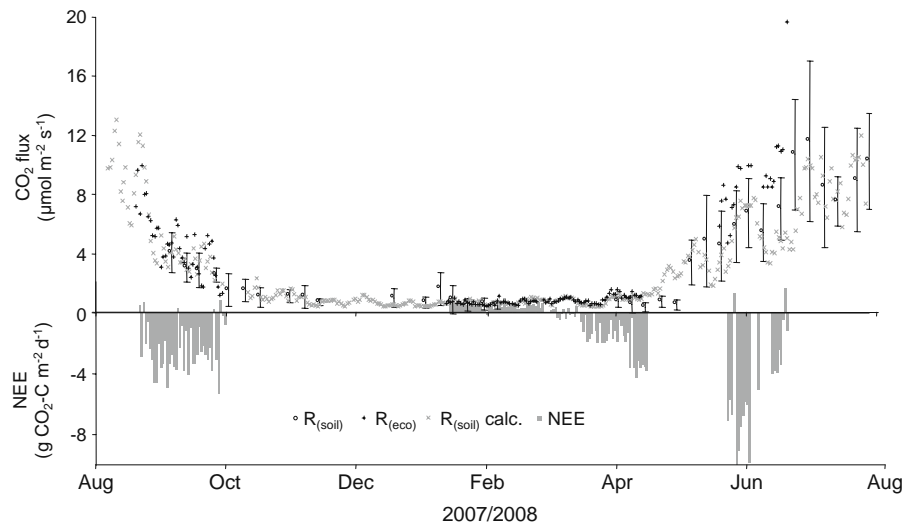
#### Net ecosystem exchange and ecosystem respiration

Net ecosystem exchange (NEE) of CO<sub>2</sub> was negative (net uptake) during the growing season and positive (net emission) during the non-growing season. NEE varied from  $-9.96$  g CO<sub>2</sub>-C m<sup>-2</sup> d<sup>-1</sup> in May to  $0.93$  g CO<sub>2</sub>-C m<sup>-2</sup> d<sup>-1</sup> in February (Fig. 6). Ecosystem respiration measured by the ACS chambers during the night (PAR <50 μmol photon m<sup>-2</sup> s<sup>-1</sup>) showed a significant correlation with temperature ( $p<0.01$ ), explaining 69% of the variation in night respiration measurements. An exponential regression equation made between mean daily ecosystem respiration measurements and soil surface temperatures (-2 cm) was used to calculate mean daily ecosystem respiration throughout the year ( $y = e^{-1.325+0.21x}$ ). Including the water level in a multiple regression analyses did not improve the significance, most probably due to a high autocorrelation between temperature and water level. Thus large autocorrelation also results in an apparent higher than expected  $Q_{10}$  ( $Q_{10}=8$ ) for soil ecosystems, which are usually in the range 1.3–3.3 (Reich and Schlesinger 1992).

#### Diurnal variation in ecosystem CH<sub>4</sub> flux at different growth stages

During dormancy the water level was ~0 cm and there was no evidence of diurnal variation in CH<sub>4</sub> (Fig. 7a). Average soil temperatures increased with soil depth ranging from  $3.4\pm 0.3$  °C at the surface (-2 cm) to

**Fig. 6** Daily NEE (bars), mean hourly ecosystem respiration (+) and calculated ecosystem respiration (×)



4.5±0.1 °C at 50 cm depth with limited diurnal variations. The average CH<sub>4</sub> flux was 0.0052±0.0018 μmol m<sup>-2</sup> s<sup>-1</sup> and there was no significant correlation with any environmental parameters (Table 3). During sprouting, when the water table was still ~0 cm, mean CH<sub>4</sub> fluxes were 0.0101±0.0030 μmol m<sup>-2</sup> s<sup>-1</sup> and showed no distinct diurnal variation although a positive correlation ( $r=0.2$ ) was found with soil surface temperature ( $p=0.096$ ). In contrast to winter soil temperatures, soil temperatures during sprouting decreased with soil depth, ranging from 6.5±1.0 °C at the soil surface (-2 cm) to 4.4±0.3 °C at -50 cm depth. Temperature oscillations were clearly dampened with increased soil depth (Fig. 7). During the initial growth peak (Fig. 7c), the water level was at ~0 cm and mean CH<sub>4</sub> fluxes were significantly lower than during sprouting (0.0032±0.0014 μmol m<sup>-2</sup> s<sup>-1</sup>) and had a slightly negative correlation with soil temperature at 10 cm depth ( $r=-0.4$ ,  $p=0.001$ ). CH<sub>4</sub> fluxes were significantly negatively correlated to soil temperatures at all depths although the temperature at 10 cm had the highest correlation ( $r=-0.4$ ). At the time of flowering (Fig. 7d), the water level was ~15 cm below the surface and a general CH<sub>4</sub> uptake was observed (-0.0014±0.0031 μmol m<sup>-2</sup> s<sup>-1</sup>). CH<sub>4</sub> fluxes were significantly correlated ( $r=0.23$ ,  $p=0.08$ ) with atmospheric temperature. During the second growth peak by the end of August, the water level was ~22 cm below the soil surface and atmospheric and soil temperatures were significantly higher than prior growth periods ranging from 17.7±0.6°C at the surface to 14.1±0.2°C at -50 cm depth. The mean CH<sub>4</sub> flux was 0.0053±

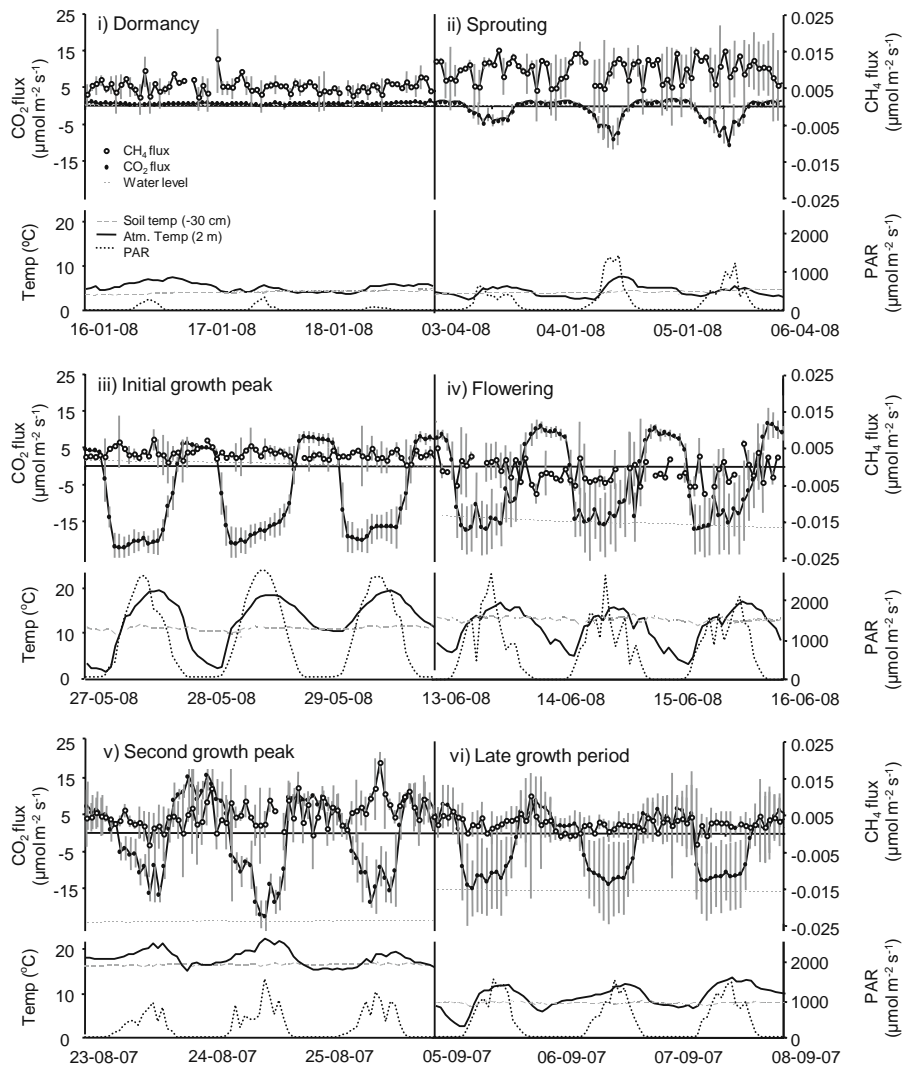
0.0036 and significant correlation was found with all soil temperatures although correlation coefficients differed markedly. The CH<sub>4</sub> flux was negatively correlated to soil temperatures above the water level (surface:  $r=-0.2$ ,  $p=0.05$  and -10 cm:  $r=-0.3$ ,  $p=0.03$ ) whereas the CH<sub>4</sub> flux was positively correlated to the soil temperature below the water level (-30 cm:  $r=0.02$ ,  $p=0.09$  and -50 cm:  $r=0.3$ ,  $p=0.03$ ). The parameter with the best correlation with the ecosystem CH<sub>4</sub> flux within the growth periods was the water level explaining up to 20% of the variation in CH<sub>4</sub> flux. The best correlation was found during the second growth period when the water level was -22.7 cm. In all situations where the water level was fluctuating within the top 30 cm, a positive correlation was found (Table 3).

#### Wetland carbon balance and global warming potential

An approximation of the carbon balance, with respect to CO<sub>2</sub> and CH<sub>4</sub> emissions and uptake of the *P. arundinacea* wetland studied, was made by extrapolation of the available measurements. Soil CH<sub>4</sub> emissions from the soil were calculated from average monthly soil ecosystem flux measurements (Fig. 8). The average available total ecosystem CH<sub>4</sub> data from the ACS chambers was used to estimate the monthly total ecosystem CH<sub>4</sub> emissions. Due to instrument failure during the months October–December 2007, data has been estimated from the relationship between soil ecosystem and total ecosystem CH<sub>4</sub> measurements during the months (January–March) as these



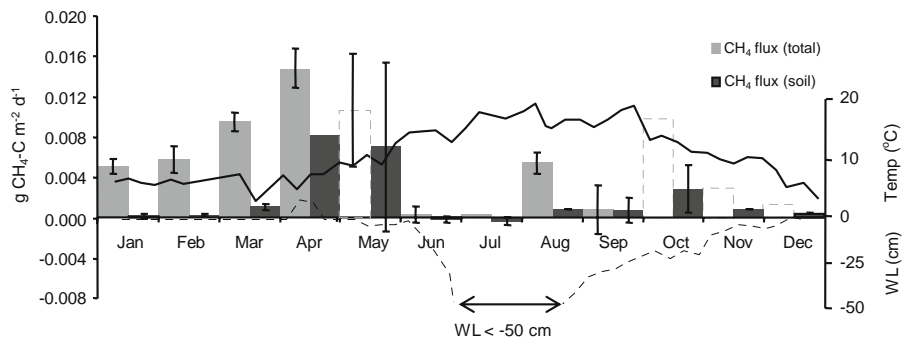
**Fig. 7** Hourly average CO<sub>2</sub> and CH<sub>4</sub> fluxes for a 3 day period during different growth stages of *Phalaris arundinacea*. All measurements have been made by automatic closed chambers. Dates on the x axis represent 0:00 am. Error bars show 1 SD from the mean, *n*=3. **a** Dormancy, **b** Sprouting, **c** Early growth season (high WL), **d** Mid growth season (low WL), **e** Late growth season. Periods are shown on Fig. 3a



months are assumed similar with respect to limited active vegetation. The CH<sub>4</sub> emission is highest during spring and early summer coinciding with high water tables. Highest emissions were measured in April with an average CH<sub>4</sub> emission of 0.015 g CH<sub>4</sub>-C m<sup>-2</sup>

d<sup>-1</sup>. During the summer CH<sub>4</sub> emissions are low and even negative coinciding with water levels below—50 cm depth. During periods with the water level below—30 cm, no CH<sub>4</sub> efflux is measured. During the winter months there is a positive NEE in the range

**Fig. 8** Monthly average ecosystem and soil CH<sub>4</sub> flux. Water table is shown by the perforated grey line and soil temperature at -10 cm depth is shown by the grey line



of  $0.75 \text{ g CO}_2\text{-C m}^{-2} \text{ d}^{-1}$  resulting from soil respiration and limited photosynthesis. Spring and summer are periods of net carbon fixation in the range  $5 \text{ g CO}_2\text{-C m}^{-2} \text{ d}^{-1}$  (Fig. 6). Measurements of NEE result in a net annual fixation of  $620 \pm 440 \text{ gC m}^{-2} \text{ yr}^{-1}$ . Approximately  $2 \text{ g CH}_4\text{-C m}^{-2}$  is annually emitted to the atmosphere. The annual release of  $\text{CH}_4$  is thus 0.3% of net annual  $\text{CO}_2$  assimilation.

## Discussion

### Site characteristics

*P. arundinacea* is an invasive, perennial wetland grass growing to a height of 2 m within the growth season producing an above-ground biomass of up to  $1.2 \text{ kg DM m}^{-2} \text{ yr}^{-1}$  (Lewandowski et al. 2003) and having a root:shoot ratio greater than 1 (Reinhardt and Galatowitsch 2005). This agrees well with the relatively large C accumulation rate ( $730 \pm 175 \text{ gC m}^{-2} \text{ yr}^{-1}$ ) calculated for Maglemeden by  $^{14}\text{C}$  analyses and results obtained from NEE measurements ( $620 \pm 440 \text{ gC m}^{-2} \text{ yr}^{-1}$ ).  $^{13}\text{C}$  NMR analyses show a depth-specific trend in labile C with a significantly higher intensity of O/N-alkyl C in the surface peat (Table 2). This is in line with the young age of the surface layers, formed within the past 25 years as well as the large annual biomass contribution.

### Seasonal and diurnal variations in ecosystem $\text{CO}_2$ concentrations and emissions

NEE measurements showed a distinct seasonality of net C uptake during the active growing season (Fig. 7b–f) and net loss of C during the non-

growing season (Fig. 7a). There were distinct seasonal and diurnal variations in ecosystem  $\text{CO}_2$  fluxes in response to PAR-driven photosynthesis giving rise to C assimilation during periods when photosynthetic  $\text{CO}_2$  uptake were larger than the sum of soil and plant respiration.

### Seasonal variations in ecosystem $\text{CH}_4$ concentrations and emissions

$\text{CH}_4$  emissions were highest from March to May because of a high water table and higher temperatures as well as a potentially larger availability of labile organic compounds from root exudates (Fig. 3) (Lai 2009). During June and July,  $\text{CH}_4$  emissions were low because of a lower water level resulting in a large oxic zone where  $\text{CH}_4$  can be oxidised to  $\text{CO}_2$  (Askaer et al. 2010). Soil  $\text{CH}_4$  contents were as high as 6% during October and November and in May during the transition from low to high and high to low ground water levels, respectively. This corresponded to high soil  $\text{CH}_4$  emissions measured by both ACS and MCS chambers (Fig. 3a–b). It was observed that from January to March when the ground water level was stable at the surface,  $\text{CH}_4$  emission increased by a factor of 2.1 with a  $10^\circ\text{C}$  increase (Fig. 5) most likely attributed to methanogens having  $Q_{10}$  values in this range according to Segers (1998).

$\text{CH}_4$  emissions measured by ACS and MCS chambers showed similar trends although effluxes measured by the MCS chambers, not containing plants, amounted to only  $32 \pm 22\%$  of the total ecosystem  $\text{CH}_4$  flux measured by the ACS chambers (Fig. 4). This indicates that  $\sim 70\%$  of the  $\text{CH}_4$  emitted from the wetland ecosystem is emitted through plants. This corresponds to earlier studies that have estimated

**Table 2** Depth specific soil properties. O/N-alkyl C is the most labile carbon compound and used as a measure of soil reactivity. One standard deviation from the mean is shown,  $n=3$

Depth (cm)	2	5	10	20	30	40	60
$^{14}\text{C}$ age	–	–	1982 AC	1974 AC	1969 AC	1400 BC	2900 BC
pH	$7.4 \pm 0.1$	$7.4 \pm 0.2$	$7.4 \pm 0.1$	$7.0 \pm 0.3$	–	$6.9 \pm 0.2$	$6.8 \pm 0.2$
C %	$27.4 \pm 9.6$	$27.3 \pm 4.8$	$25.5 \pm 3.3$	$26.5 \pm 7.6$	–	$31.6 \pm 7.7$	$22.7 \pm 7.6$
C/N	$16.9 \pm 2.3$	$15.2 \pm 1.4$	$15.0 \pm 1.2$	$15.2 \pm 1.9$	–	$17.0 \pm 3.7$	$19.8 \pm 1.7$
Bulk density ( $\text{g cm}^{-2}$ )	0.25	0.25	0.31	0.34	0.37	0.41	–
Total porosity (%)	79.15	78.87	74.01	71.71	68.93	65.69	–
O/N-alkyl C (intensity)	49.22	–	38.22	36.14	35.84	33.00	–

plant-dependent transport of CH<sub>4</sub> from a *Carex*-dominated fen in Quebec, Canada, and in an ombrotrophic peat in Michigan, USA, to account for up to 90% of the total CH<sub>4</sub> emission (Whiting and Chanton 1993).

### Diurnal variations in CH<sub>4</sub> emissions

During dormancy, dead culms of *P. arundinacea* were present and ecosystem CH<sub>4</sub> fluxes were not significantly correlated with any environmental parameters (Table 3, Fig. 7a). CH<sub>4</sub> emissions are primarily controlled by passive diffusion through the soil matrix and dead culms can facilitate a transport path with reduced friction to the atmosphere. From February to April, CH<sub>4</sub> fluxes increase markedly and, over that period, the water table is all the time near the surface and soil temperatures increase and decrease again. Some of the variations in observed CH<sub>4</sub> fluxes are linked to variations in soil temperature, but the main trend is probably due to the fact that *P. arundinacea* are growing with high percentage of aerenchyma, which facilitate an increased oxidation of CH<sub>4</sub> below-ground but also an increased passive flux of CH<sub>4</sub> to the atmosphere through the plant. During the initial growth peak in May, the significantly lower CH<sub>4</sub> flux compared to measured fluxes during sprouting was due to a decreasing water level as well as increased radial oxygen loss creating a 0.1 mm oxic zone around the growing roots (Edwards et al. 2006) of *P. arundinacea* leading to increased soil CH<sub>4</sub> oxidation (Watson et al. 1997). The CH<sub>4</sub> flux was significantly negatively correlated with soil temperatures at all soil depths due to methanotrophs situated in the oxic zones within the rhizosphere also having Q<sub>10</sub> in the range 1.8–2.9 (Whalen 2005). Potential CH<sub>4</sub> oxidation by methanotrophs is typically an order of magnitude greater than potential CH<sub>4</sub> production by methanogens (Segers 1998). Therefore, a limited oxic zone can result in the oxidation of a relatively large amount of CH<sub>4</sub>. A review of earlier studies of CH<sub>4</sub> consumption and production by Segers (1998) states that up to 90% of the produced CH<sub>4</sub> could be consumed again, either in the oxic top layer or in the oxic rhizosphere. The temperature at 10 cm depth had the highest correlation ( $r=-0.4$ ) with the CH<sub>4</sub> flux as this depth coincided with the maximum root biomass and is therefore also expected to have the largest radial oxygen loss zone. This is in line with Edwards

**Table 3** Correlation coefficients between growth stage specific ecosystem CH<sub>4</sub> flux and environmental parameters within a 3 day period corresponding to periods illustrated in Figs. 3 and 7. Correlations are made with linear regression. Temperatures are correlated with Ln(CH<sub>4</sub> flux). Significant at a 95% confidence interval ( $p<0.05$ ) is indicated by \* and significant at a 90% is indicated by \*\*. One SD from the mean is indicated ( $\pm$ ),  $n=68-71$

Parameter	Dormancy		Sprouting		Initial growth peak		Flowering		Second growth peak		Late growth season	
	mean	r	mean	r	mean	r	mean	r	mean	r	mean	r
CH <sub>4</sub>	0.01±0.00	na	0.01±0.00	na	0.00±0.00	na	0.00±0.00	–	0.01±0.00	–	0.00±0.00	–
CO <sub>2</sub>	0.57±0.22	0.07	-1.07±2.85	-0.11	-8.52±11.77**	-0.22	-3.71±10.45	-0.11	-0.38±10.15	0.07	-3.08±7.93*	0.34
PAR	33.6±75.2	-0.16	223.3±345.4	0.06	666.0±6.8	0.14	496.1±514.4	0.17	195.9±248.0	0.07	380.1±473.8	-0.17
Temp (atm)	5.50±1.00	0.08	5.80±1.70	0.15	12.37±5.50	-0.14	11.20±3.90**	0.23	18.20±1.80*	-0.16	13.20±3.80*	-0.43
Soil temp (surface)	3.40±0.30	0.18	6.50±1.00**	0.20	11.88±2.71*	-0.30	12.50±1.70	0.18	17.70±0.60	-0.24	12.30±1.40	-0.20
Soil temp (-10 cm)	4.30±0.30	0.14	6.40±0.60	0.15	11.11±1.02*	-0.40	12.70±0.80	0.07	17.70±0.40*	-0.26	12.60±0.70	-0.04
Soil temp (-30 cm)	4.00±0.30	0.10	5.40±0.40	0.15	10.25±0.45*	-0.28	12.70±0.50	0.05	16.4±0.20*	0.02	13.10±0.30	0.07
Soil temp (-50 cm)	4.50±0.10	0.10	4.40±0.30	0.16	8.81±0.47*	-0.23	10.80±0.50	0.05	14.14±0.20*	0.26	13.40±0.40	0.00
Water level	0.00±0.00	na	0.00±0.00	na	0.50±0.52*	0.27	-14.89±0.99	0.06	-22.70±0.30*	0.45	-15.90±0.20*	0.20

et al. (2006) who estimated the root volume to be a reasonable predictor of the size of the aerobic space adjacent to the roots. At the end of August, when the water level is at  $-23$  cm, after a short period of even lower water levels, ecosystem  $\text{CH}_4$  fluxes are in the range  $0.005 \pm 0.004 \mu\text{mol CH}_4 \text{ m}^{-2} \text{ s}^{-1}$  corresponding to higher soil  $\text{CH}_4$  concentrations and deeper plant roots developed during the second growth peak. A significant correlation was found between  $\text{CH}_4$  fluxes and soil temperatures at all depths although negative correlations exist above the water level and negative correlations exist below the water level. This relationship could be due to consumption above the ground water level in the oxic zone and production below the water level in the anoxic zone although this relationship was not observed during the initial growth peak where correlations between temperature and  $\text{CH}_4$  emissions at all depths were negative.

#### Summary of diurnal variations

The study of diurnal variations in  $\text{CH}_4$  emissions from *P. arundinacea* indicates that gas flow is predominantly driven by passive diffusion. If convective gas flow had been the dominant transport mechanism,  $\text{CH}_4$  emissions would be driven by diurnal atmospheric temperature variations creating differences in temperature or water-vapour pressure between the internal air spaces in the plants and the surrounding atmosphere. Differences in temperature or water-vapour pressure generate pressure gradients that drive gas flow from leaves to rhizome and then vent back to the atmosphere (Brix et al. 1992) in line with those found in wetlands vegetated by stands of e.g. *Pragmites australis*, *Carex lasiocarpa*, *Deyeuxia angustifolia*, *Typha Latifolia* (Mikkilä et al. 1995; Ding et al. 2004; Whiting and Chanton 1996). Very limited significant correlations were observed between the diurnal variations in  $\text{CH}_4$  emissions and atmospheric temperature during flowering when the correlation was positive, to the late growth season when correlations were negative (Table 3). Thus, results suggest that convective gas flow is not the primary transport mechanism although mature *P. arundinacea* may be capable of building slight pressure differentials resulting in slight  $\text{CH}_4$  transport during flowering and increased  $\text{O}_2$  transport to the rhizosphere during the second growth peak and the late growth season. This is in line with a study by Kao-

Kniffin et al. (2010) that found that amongst 7 graminoid species a stalk of *P. arundinacea* had the lowest  $\text{CH}_4$  emissions under controlled laboratory conditions. They also suggest that the large above-ground and below-ground biomass may aid in greater oxygen transport to anoxic sediments, which could stimulate  $\text{CH}_4$  consumption by rhizospheric bacteria (Brune et al. 2000).

#### Impact of *P. arundinacea* as a dominant wetland species

Despite the fact that  $\text{CH}_4$  transport through *P. arundinacea* is primarily passive,  $\sim 70 \pm 35\%$  of the  $\text{CH}_4$  emitted to the atmosphere is emitted through this wetland species. The main reason for these high *P. arundinacea*-mediated  $\text{CH}_4$  emissions are the high concentration gradients between the soil at the maximum root biomass depth ( $\sim 20$  cm) amounting, in 50% of the year, to  $\sim 14,000$  times higher concentrations than in the atmosphere. This is in the size order of  $\sim 500$  times larger than for  $\text{CO}_2$  concentration differences. Therefore, although  $\text{CO}_2$  is also passively *P. arundinacea*-mediated it has a much smaller contribution to NEE. To our knowledge no previous studies have been conducted to measure flow through this plant species. In this study, bulk soil with no influence of plants has not been studied simultaneously. This would have been interesting in order to evaluate the oxidative potential of the *P. arundinacea* rhizosphere. Previous studies have shown that *P. arundinacea*-cultivated wetlands emit less  $\text{CH}_4$  than bare wetland soils (Hyvönen et al. 2009) due to their increased  $\text{CH}_4$  oxidation potential.

In contrast to vegetation types with convective gas flow, diurnal variations in  $\text{CH}_4$  fluxes are of less importance for calculating  $\text{CH}_4$  budgets in a *P. arundinacea*-dominant wetland. Northern peatlands emit an estimated 12.2% of the global total  $\text{CH}_4$  emissions (Wuebbles and Hayhoe 2002) with emissions in the range  $5\text{--}80 \text{ mg m}^{-2} \text{ d}^{-1}$  (Blodau 2002). Average  $\text{CH}_4$  emissions from Maglemosen amounted to  $4.9 \text{ mg m}^{-2} \text{ d}^{-1}$  and are therefore low in comparison to other peatlands at similar latitudes. These low emissions are likely the result of the dry summer period where the water level is below 30 cm depth for 52 days coinciding with the period of highest temperatures where  $\text{CH}_4$  production potentials are highest, given anoxic conditions and where  $\text{CH}_4$  oxidation potentials are highest, given oxic condi-

tions. Askær et al. (2010) found that 30 cm was the threshold depth for CH<sub>4</sub> emissions in the study area implying that with water levels below 30 cm CH<sub>4</sub> is oxidised before reaching the atmosphere if transport is exclusively soil-mediated.

## Conclusions and implications

The study of diurnal variations in CH<sub>4</sub> emissions from *P. arundinacea* shows that gas flow is predominantly driven by passive diffusion. Although ~70±35% of the CH<sub>4</sub> emitted from this wetland is plant-mediated, CH<sub>4</sub> emissions from this wetland, in a global change perspective, have little importance as the mean C-sequestration rate is at least one order of magnitude higher than the CH<sub>4</sub>-C emissions. Despite the fact that CH<sub>4</sub> has a 25 times larger global warming potential than CO<sub>2</sub>, CH<sub>4</sub> causes only 8% of the C assimilated to be annulled in a global change perspective. Although this is an approximation, it is to our knowledge the first attempt at making a CH<sub>4</sub> budget for a Danish wetland ecosystem showing that *P. arundinacea*-dominated wetland ecosystems are net C sinks despite CH<sub>4</sub> emissions and despite a high potential of enhanced gas fluxes due to aerenchyma-rich plants.

Although *P. arundinacea* appears to be a desirable plant in a global warming perspective, it is also known to reduce biological diversity by homogenizing habitat structure and environmental variability (Maurer et al. 2003). Furthermore, *P. arundinacea* decreases retention time of nutrients and carbon stored in wetlands, accelerating turnover cycles and reducing the carbon sequestration capabilities characteristic of a more diverse plant community (RCG Management Working Group 2009). Therefore more factors must be taken into account when assessing the impact of *P. arundinacea* on a wetland ecosystem although appearing positive in a global change perspective.

**Acknowledgements** This study is conducted within the framework of the “Oxygen availability controlling the dynamics of buried organic carbon pools and greenhouse emissions” project financed by the Danish National Research Council (BE). We are grateful to O. Bennike (GEUS) for preparing samples for AMS <sup>14</sup>C dating, J. Heinemeier from the AMS <sup>14</sup>C dating centre at Department of Physics and Astronomy, Aarhus University and H. Knicker, Lehrstuhl für Bodenkunde, Technische Universität München for help with solid state <sup>13</sup>C NMR analyses. We further thank P. Frederiksen and J.R. Christiansen (from Forest &

Landscape Denmark, University of Copenhagen), P. Christiansen and H. Ferdinand for assistance in the field and with laboratory analyses.

## References

- Adler PR, Del Grosso SJ, Parton WJ (2007) Lifecycle assessment of net greenhouse-gas flux for bioenergy cropping systems. *Ecol Appl* 17:675–691
- Armstrong J, Armstrong W (1991) A convective through-flow of gases in *Phragmites australis* (Cav.) Trin. Ex Steud. *Aquat Bot* 39:75–88
- Askaer L, Elberling B, Glud RN et al (2010) Soil heterogeneity effects on O<sub>2</sub> distribution and CH<sub>4</sub> emissions from wetlands: in situ and mesocosm studies with planar O<sub>2</sub> optodes and membrane inlet mass spectrometry. *Soil Biol Biochem* 42(12):2254–2265
- Bennike O, Houmark-Nielsen M, Böcher J et al (1994) A multi-disciplinary macrofossil study of Middle Weichselian sediments at Kobbegård, Mon, Denmark. *Palaeogeogr Palaeoclimatol Palaeoecol* 111(1–2):1–15
- Blodau C (2002) Carbon cycling in peatlands—A review of processes and controls. *Environ Rev* 10(2):111–134
- Brix H, Sorrell BK, Orr PT (1992) Internal pressurization and convective gas flow in some emergent freshwater macrophytes. *Limnol Oceanogr* 37:1420–1433
- Brune A, Frenzel P, Cypionka H (2000) Life at the oxic–anoxic interface: microbial activities and adaptations. *FEMS Microbiol Rev* 24:691–710
- Clymo RS (1983) Peat. In: Gore AJP (ed) *Mires: Swamp, Bog, Fen and Moor. General Studies, Ecosystems of the World*, 4A. Elsevier Scientific Publishing Company, pp 159–224
- Commission of the European Communities (2007) Limiting Global Climate Change to 2 degrees Celsius. The way ahead for 2020 and beyond. Communication from The Commission to The Council, The European Parliament, The European Economic and Social Committee and the Committee of The Regions. 52007DC0002
- Danish Ministry of Economic and Business Affairs (Økonomi- og Erhvervsministeriet) (2009) Grøn Vækst. ISBN electronic edition: 978-87-92480-09-5 (in Danish)
- Ding W, Cai Z, Tsuruta H (2004) Diel variation in methane emissions from the stands of *Carex lasiocarpa* and *Deyeuxia angustifolia* in a cool temperate freshwater marsh. *Atmos Environ* 38:181–188
- Edwards KR, Cizkova H, Zemanova K et al (2006) Plant growth and microbial processes in a constructed wetland planted with *Phalaris arundinacea*. *Ecol Eng* 27:153–165
- Gorham E (1991) Northern Peatlands: role in the carbon cycle and probable responses to climatic warming. *Ecol Appl* 1:182–195
- Grünfeld S, Brix H (1999) Methanogenesis and methane emissions: effects of water table, substrate type and presence of *Phragmites australis*. *Aquat Bot* 64:63–75
- Hyvönen NP, Huttunen JT, Shurpali NJ et al (2009) Fluxes of nitrous oxide and methane on an abandoned peat extraction site: effect of reed canary grass cultivation. *Bioresour Technol* 100:4723–4730

- IPCC (2007) Climate Change 2007: The physical science basis. Contribution of Working Group I to the Fourth Assessment. Report of the Intergovernmental Panel on Climate Change. In: Solomon S, Qin D, Manning M, Chen Z, Marquis M, Averyt KB, Tignor M, Miller HL (eds) Cambridge University Press, Cambridge, United Kingdom and New York, NY, USA, pp 996
- Joabsson A, Christensen TR, Wallen B (1999) Vascular plant controls on methane emissions from northern peat forming wetlands. *Trends Ecol Evol* 14(10):385–388
- Kammann C, Grunhage L, Jager H-J (2001) A new sampling technique to monitor concentrations of CH<sub>4</sub>, N<sub>2</sub>O and CO<sub>2</sub> in air at well-defined depths in soils with varied water potential. *Eur J Soil Sci* 52:297–303
- Kao-Kniffn J, Freyreb DS, Balsera TC (2010) Methane dynamics across wetland plant species. *Aquat Bot* 93:107–113
- Kercher SM, Zedler JB (2004) Flood tolerance in wetland angiosperms: a comparison of invasive and noninvasive species. *Aquat Bot* 80:89–102
- Knicker H, Skjemstad JO (2000) Nature of organic carbon and nitrogen in physically protected organic matter of some Australian soils as revealed by solid-state <sup>13</sup>C and <sup>15</sup>N NMR spectroscopy. *Aust J Soil Res* 38:113–127
- Lai DYF (2009) Methane dynamics in Northern Peatlands: a review. *Pedosphere* 19(4):409–421
- Lewandowski I, Scurlock JMO, Lindvall E et al (2003) The development and current status of perennial rhizomatous grasses as energy crops in the US and Europe. *Biomass Bioenergy* 25:335–361
- Maurer DA, Linding-Cisneros R, Werner KJ et al (2003) The replacement of wetland vegetation by reed canary grass (*Phalaris arundinacea*). *Ecol Res* 21:116–119
- Mikkela C, Sundh I, Svensson BH et al (1995) Diurnal variation in methane emission in relation to the water table, soil temperature, climate and vegetation cover in a Swedish acid mire. *Biogeochemistry* 28:93–114
- Papaioannou G, Papanikolaou N, Retalis D (1993) Relationships of photosynthetically active radiation and shortwave irradiance. *Theor Appl Climatol* 48:23–27
- Reich JW, Schlesinger WH (1992) The global carbon dioxide flux in soil respiration and its relationship to climate. *Tellus* 44B:81–99
- Reinhardt CH, Galatowitsch SM (2005) *Phalaris arundinacea* L. (reed canary grass): rapid growth and growth pattern in conditions approximating newly restored wetlands. *Ecoscience* 12:569–573
- Roehm CL, Roulet NT (2003) Seasonal contribution of CO<sub>2</sub> fluxes in the annual C budget of a northern bog. *Glob Biogeochem Cycl* 17:1029
- Ruimy A, Jarvis PG, Baldocchi D et al (1995) CO<sub>2</sub> fluxes over plant canopies and solar radiation: a review. *Adv Ecol Res* 26:1–65
- Segers R (1998) Methane production and methane consumption: a review of processes underlying wetland methane fluxes. *Biogeochemistry* 41:23–51
- Strom L, Mastepanov M, Christensen TR (2005) Species-specific effects of vascular plants on carbon turnover and methane emissions from wetlands. *Biogeochemistry* 75(1):65–82
- Tokida T, Mizoguchi M, Miyazaki T et al (2007) Episodic release of methane bubbles from peatland during spring thaw. *Chemosphere* 70:165–171
- Watson A, Stephen KD, Nedwell DB et al (1997) Oxidation of methane in peat: kinetics of CH<sub>4</sub> and O<sub>2</sub> removal and the role of plant roots. *Soil Biol Biochem* 29:1165–1172
- Whalen SC (2005) Biochemistry of methane exchange between natural wetlands and the atmosphere. *Environ Eng Sci* 22(1):73–94
- Whiting GJ, Chanton JP (1993) Primary production control of methane emission from wetlands. *Nature* 364:794–795
- Whiting GJ, Chanton JP (1996) Control of diurnal pattern of methane emission from aquatic macrophytes by gas transport mechanisms. *Aquatic Botany* 54:237–253
- Wisconsin Reed Canary Grass Management Working Group (2009) Reed Canary Grass (*Phalaris arundinacea*). Management Guide: Recommendations for Landowners and Restoration Professionals, PUB-FR-428 2009
- Wuebbles DJ, Hayhoe K (2002) Atmospheric methane and global change. *Earth Sci Rev* 57(3):177–210



1 **Supporting information:**

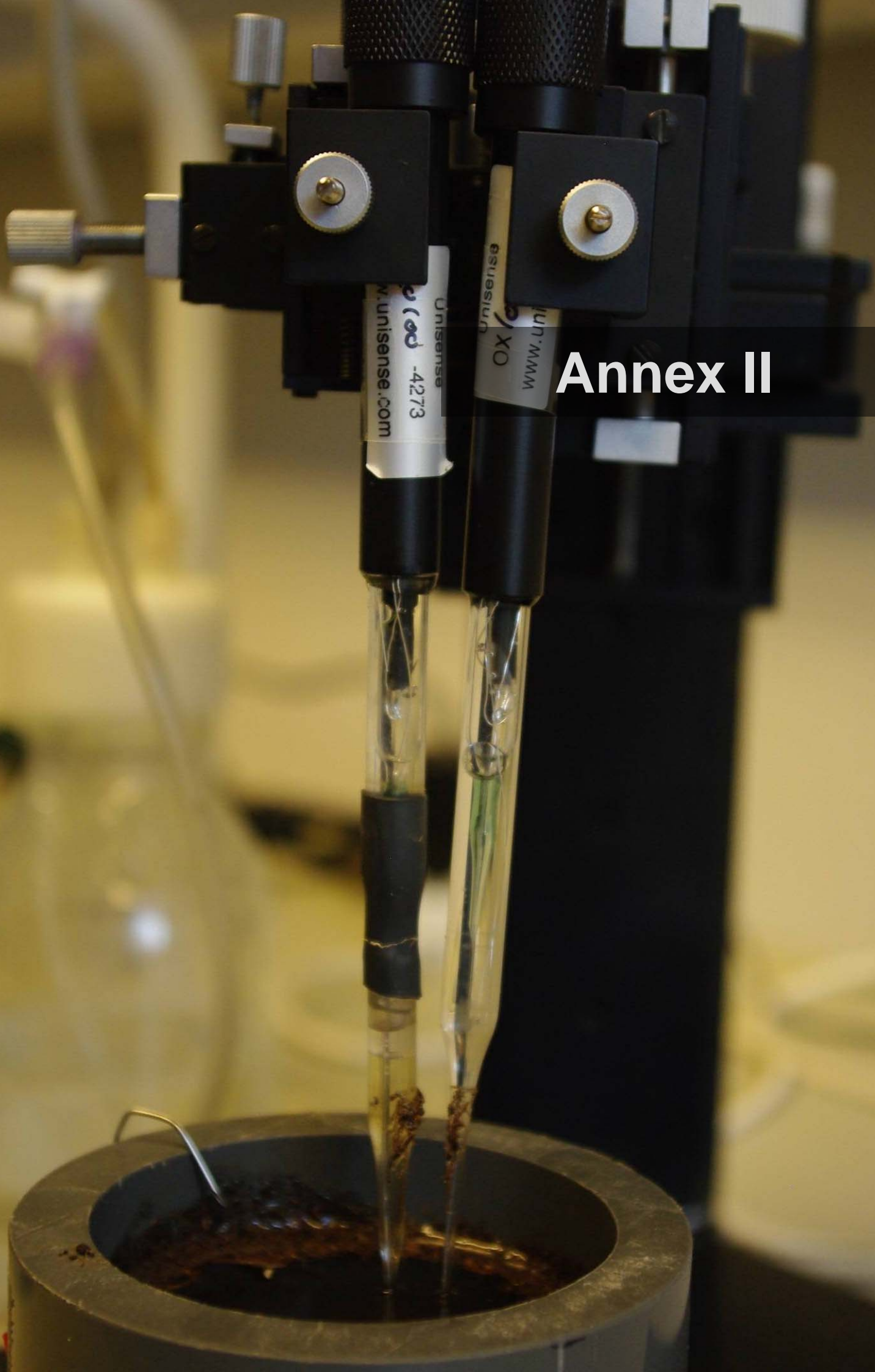
2

3 **Appendix S1** *Solid state <sup>13</sup>C NMR analysis*

4 Peat samples were prepared for solid state <sup>13</sup>C NMR analysis. Samples were freeze-dried and milled and  
5 solid-state <sup>13</sup>C NMR spectra were obtained on a Bruker DSX 200 operating at a frequency of 50.3 MHz using  
6 zirconium rotors of 7 mm OD with KEL-F-caps. The CPMAS technique was applied during magic-angle  
7 spinning of the rotor at 6.8 kHz. A contact time of 1 ms was used for all spectra. The <sup>13</sup>C-chemical shifts  
8 were calibrated to tetramethylsilane (TMS) (= 0 ppm) and were calibrated with glycine (176.04 ppm).  
9 Between 7951 and 169040 singles scans were made for each spectra. Line broadening of 50.00 Hz was used  
10 to decrease the noise by multiplying the free induction decay (FID) with an exponential function that  
11 decreases the noise but increases the line width. The relative intensity of the peaks was obtained by  
12 integration of the specific chemical shift ranges by an integration routine supplied with the instrument  
13 software.

14

# Annex II







## Linking Soil O<sub>2</sub>, CO<sub>2</sub>, and CH<sub>4</sub> Concentrations in a Wetland Soil: Implications for CO<sub>2</sub> and CH<sub>4</sub> Fluxes

Bo Elberling,<sup>†,\*</sup> Louise Askaer,<sup>†</sup> Christian J. Jørgensen,<sup>†</sup> Hans P. Joensen,<sup>†</sup> Michael Kühl,<sup>‡,§</sup> Ronnie N. Glud,<sup>||,⊥,#</sup> and Frants R. Lauritsen<sup>▽</sup>

<sup>†</sup>Department of Geography and Geology, University of Copenhagen, Copenhagen, Denmark

<sup>‡</sup>Marine Biological Laboratory, Department of Biology, University of Copenhagen, Strandpromenaden 5, DK-3000 Helsingør, Denmark

<sup>§</sup>Plant Functional Biology and Climate Change Cluster, University of Technology, Sydney PO Box 123 Broadway NSW 2007 Australia

<sup>||</sup>The Scottish Association for Marine Science, Dunstaffnage Marine Laboratory, Oban, Argyll, PA37 1QA, United Kingdom

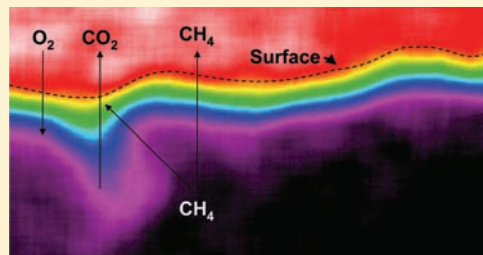
<sup>⊥</sup>Institute of Biology and Nordic Center for Earth Evolution, University of Southern Denmark, Odense M, Denmark

<sup>#</sup>Greenland Climate Research Centre, Kivioq 2, Box 570, 3900 Nuuk Greenland

<sup>▽</sup>Department of Pharmacy and Analytical Chemistry, University of Copenhagen, Universitetsparken 2, 2100 Copenhagen Ø, Denmark

### Supporting Information

**ABSTRACT:** Oxygen (O<sub>2</sub>) availability and diffusivity in wetlands are controlling factors for the production and consumption of both carbon dioxide (CO<sub>2</sub>) and methane (CH<sub>4</sub>) in the subsoil and thereby potential emission of these greenhouse gases to the atmosphere. To examine the linkage between high-resolution spatiotemporal trends in O<sub>2</sub> availability and CH<sub>4</sub>/CO<sub>2</sub> dynamics in situ, we compare high-resolution subsurface O<sub>2</sub> concentrations, weekly measurements of subsurface CH<sub>4</sub>/CO<sub>2</sub> concentrations and near continuous flux measurements of CO<sub>2</sub> and CH<sub>4</sub>. Detailed 2-D distributions of O<sub>2</sub> concentrations and depth-profiles of CO<sub>2</sub> and CH<sub>4</sub> were measured in the laboratory during flooding of soil columns using a combination of planar O<sub>2</sub> optodes and membrane inlet mass spectrometry. Microsensors were used to assess apparent diffusivity under both field and laboratory conditions. Gas concentration profiles were analyzed with a diffusion-reaction model for quantifying production/consumption profiles of O<sub>2</sub>, CO<sub>2</sub>, and CH<sub>4</sub>. In drained conditions, O<sub>2</sub> consumption exceeded CO<sub>2</sub> production, indicating CO<sub>2</sub> dissolution in the remaining water-filled pockets. CH<sub>4</sub> emissions were negligible when the oxic zone was >40 cm and CH<sub>4</sub> was presumably consumed below the depth of detectable O<sub>2</sub>. In flooded conditions, O<sub>2</sub> was transported by other mechanisms than simple diffusion in the aqueous phase. This work demonstrates the importance of changes in near-surface apparent diffusivity, microscale O<sub>2</sub> dynamics, as well as gas transport via aerenchymous plants tissue on soil gas dynamics and greenhouse gas emissions following marked changes in water level.



### INTRODUCTION

Northern wetlands store about 30% of the global subsurface organic carbon (C) pools and function as net sources of methane (CH<sub>4</sub>) with an annual release of 46 Tg CH<sub>4</sub>-C to the atmosphere.<sup>1–3</sup> Soil water content is a key regulator for diffusion of O<sub>2</sub> into the soil. Lowering the water level increases the oxygen (O<sub>2</sub>) availability in near-surface layers and accelerates decomposition rates of organic matter, increases carbon dioxide (CO<sub>2</sub>) emissions, and decreases CH<sub>4</sub> emissions due to subsurface CH<sub>4</sub> oxidation. However, highly contrasting results in terms of the effects of lowered water levels on gas emission are reported in the literature and the controlling mechanisms are unclear.<sup>4</sup> In particular, the temporal nature of the gas transport mechanism across the soil-atmosphere interface remains unresolved.<sup>5,6</sup>

Subsurface O<sub>2</sub> concentrations in wetlands have rarely been reported at high spatiotemporal scales despite the fact that O<sub>2</sub> is a key parameter for the biogeochemistry of soils and sediments.

Subsurface O<sub>2</sub> concentrations can be quantified both in the laboratory and in situ with electrochemical and optical sensors.<sup>7</sup> Most recently, 2D distributions of O<sub>2</sub> have been measured using planar optodes<sup>8–10</sup> providing novel insights into high resolution O<sub>2</sub> dynamics in a range of complex and heterogeneous marine environments.<sup>9</sup> In wetlands, detailed investigations on subsoil O<sub>2</sub> distribution are important as the transport of soil gases occurs both via diffusive transport in the pores as well as through the aerenchymous tissue of many wetland plants.<sup>11,12</sup>

The quantification of soil-atmosphere gas exchange at a high spatiotemporal resolution requires detailed knowledge about the mass transfer properties of the soil system. However, standard

**Received:** October 20, 2010

**Accepted:** February 24, 2011

**Revised:** February 13, 2011

**Published:** March 17, 2011

equations for calculating effective diffusion coefficients of wetland soils and peat are few<sup>13,14</sup> and limited by rapid changes in air-filled porosity as well as total porosity values following changes in water level. High resolution measurements of the mass transfer properties under fluctuating soil moisture conditions will potentially help clarifying the mechanisms regulating greenhouse gas emissions from wetland soils. Therefore, this work aims to (i) quantify subsurface O<sub>2</sub> dynamics in a protected Danish wetland with respect to natural water level fluctuations, and (ii) to quantify depth-specific O<sub>2</sub>, CO<sub>2</sub>, and CH<sub>4</sub> consumption/production profiles based on observed in situ gas concentrations and apparent gas diffusivity measurements using PROFILE, a simple diffusion-reaction model<sup>15</sup> for analysis of measured concentration gradients.

## MATERIALS AND METHODS

**Study Site.** The study site is situated in a temperate wetland area, Maglemosen (55°51'N, 12°32'E) formed through the retreat of an ancient inlet in Vedbæk, 20 km north of Copenhagen, Denmark (Supporting Information, SI, Figure 1S). Mean annual air temperature is 8 °C and mean annual precipitation is 613 mm (normals for 1961–1990, Danish Meteorological Institute). The wetland is characterized as a fen covering an area of roughly 0.6 km<sup>2</sup> with peat depths ranging from 0.5 to 3 m. The mean annual water level in 2007–2008 was 14 cm below the surface and ranged from 6 cm above the surface to 73 cm below the surface. The study site has not been managed for >100 years and is dominated by graminoids, mainly reed canary grass (*Phalaris arundinacea*) but also common reed (*Phragmites australis*) and different herbs.

**Field Measurements and Sampling.** Subsoil CO<sub>2</sub> and CH<sub>4</sub> concentration profiles and surface fluxes were measured on a weekly basis (January to August 2009). Ground temperature, water content, water level, and O<sub>2</sub> concentrations were logged continuously on an hourly basis. Soil CO<sub>2</sub> fluxes (microbial and root respiration) were measured using an infrared gas analyzer (LiCor 6400–09/6262 Soil CO<sub>2</sub> Flux Chamber, LiCor, Lincoln, USA) attached to a portable chamber, functioning as a dark and closed soil-flux chamber and placed on top of open preinstalled soil collars (10 cm in diameter) for 2–3 min at sites without plants within the collars. The CO<sub>2</sub> efflux was calculated on the basis of a linear increase ( $r^2 > 0.95$ ) in chamber CO<sub>2</sub> concentrations over time on 10 replicate collars. Soil CH<sub>4</sub> fluxes were measured using three replicate static collars installed to a depth of 8 cm and leaving 2 cm above the surface. These collars were closed during measurements using a closed-end CHA-type plumbing creating a total chamber volume of about 0.5 L. Headspace gas samples were extracted four times at 15-min intervals and stored in 2.5 mL glass injection flasks with polyisobutylene septa. Gas samples were analyzed for CH<sub>4</sub> within 24 h using a gas chromatography (Shimadzu GC 2014 with Back Flush system, SHIMADZU EUROPA GmbH, Duisburg, Germany) equipped with a Mol Sieve 5A 80/100 mesh (1/8" × 1 m) column connected to an FID detector.

Air in the soil pores was sampled for CO<sub>2</sub> and CH<sub>4</sub> analyses at depths of 5, 10, 20, 30, 40, 50, 60, 80, 110, and 140 cm using silicone probes as described.<sup>16,17</sup>

Oxygen (O<sub>2</sub>) concentrations were measured at in situ 5, 10, 15, 20, 25, 30, 40, 50, 60, 80, and 110 cm depth using fiber-optic O<sub>2</sub> optodes connected to a fiber-optic oxygen meter (FIBOX 3, Presens GmbH, Germany) in combination with K-type

thermocouples connected to a thermometer (RS 206–3722). Temperature readings were made with the same spatiotemporal resolution as O<sub>2</sub> in order to enable temperature compensation of the sensor signals. All sensors were linearly calibrated with a 2 point temperature and O<sub>2</sub> concentration procedure with precisions  $\leq 5\%$  of standard deviation at standard temperature and pressure. In the laboratory, electrochemical O<sub>2</sub> microsensors (OX-50, 40–60  $\mu\text{m}$  tip diameter; Unisense A/S, Aarhus, Denmark) connected to a pA meter (PA2000, Unisense A/S, Aarhus, Denmark) were used to measure O<sub>2</sub> concentrations under flooded conditions when O<sub>2</sub> penetration depths were <5 cm and in soil without plants (>0.5 m from nearest *Phalaris arundinacea*).

Volumetric soil water content was measured using soil moisture sensors (Theta Probes ML2x, Delta-T Devices Ltd., Cambridge, UK) installed in 8 depths in one profile and connected to a datalogger (Campbell, CR10X Datalogger for Measurement & Control, Campbell Scientific Ltd., Loughborough, UK). The water level was measured by a pressure sensor (PCR 1830, Druck) submerged in a 2.5 m perforated plastic tube. All installations were completed more than two months prior to measurements (see SI).

Depth and volume-specific soil samples ( $\sim 100 \text{ cm}^3$ ) were collected from pits and included all major horizons (including the litter layer). In situ pH measurements (Metrohm 704 Pocket pH meter, Metrohm Nordic, Glostrup, Denmark) were made directly with probes inserted into peat/sediment or after the addition of distilled water at depths with a soil-solution ratio of  $\sim 1:2.5$ . Bulk density was determined on the basis of the weight of dried volume-specific soil cores. Total organic carbon (TOC) was measured after acidification, using 6 M HCl to remove inorganic C using an Eltra SC-500 analyzer (ELTRA GmbH, Neuss, Germany), with an accuracy of  $\pm 0.2\%$ . Four replicate soil columns were sampled and stored in the dark at 4 °C until analysis in the laboratory. Three additional columns without living plants were sampled during winter in circular PVC columns (id:20 cm, h:60 cm), with one side removed, where a Plexiglas sheet containing a planar optode was fixed for laboratory experimental work. The soil column openings were closed with rubber-coated aluminum sheets, the upper with a large opening to ensure equilibrium with the atmosphere.

**Experimental Work.** Gas profiling using Membrane Inlet Mass Spectrometry (MIMS) and planar optode (PO) imaging were made in the dark at 10 °C after >6 months preincubation to obtain steady state conditions, and with a water level 5 cm above the peat surface. An aquarium pump was used to aerate the water column keeping it at atmospheric O<sub>2</sub> saturation. Depth-specific analyses of dissolved CH<sub>4</sub>, CO<sub>2</sub>, and Ar concentrations were done with a quadrupole mass spectrometer (QMA125, Balzers, Liechtenstein), where CH<sub>4</sub> and CO<sub>2</sub> concentrations were normalized using a two-point calibration with Ar as an internal standard. Details of the MIMS and PO setups have been described elsewhere<sup>17</sup> and are also included in the SI.

**Apparent Diffusivity.** Microscale diffusivity sensors (DF200, Unisense A/S, Aarhus, Denmark) with a tip diameter of 200  $\mu\text{m}$  were applied to measure apparent diffusivity, i.e., the bulk diffusivity in partly saturated peat and sediment by measuring concentrations of a tracer gas in an internal H<sub>2</sub> gas (at 1 atm partial pressure) reservoir within the sensor tip.<sup>18</sup> In brief, the diffusivity sensor is a hydrogen transducer in which an air volume behind a separating membrane is continuously flushed avoiding potential interference with both O<sub>2</sub> and CO<sub>2</sub>. A mathematical model has been made<sup>18</sup> which describes the sensor signal as a

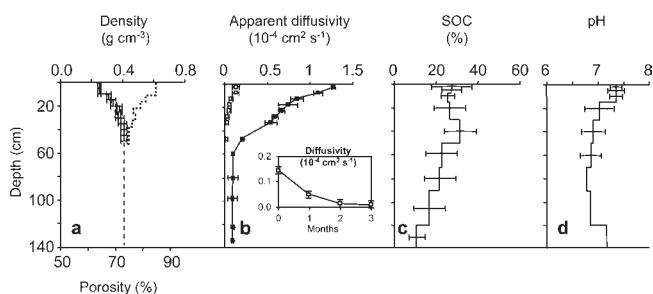


**Figure 1.** Depth specific soil properties including (a) bulk density (solid line) and porosity (dashed line) down to 50 cm; (b) in situ apparent  $O_2$  diffusivity measured under saturated conditions (open squares) and well-drained conditions (filled squares); and (c) soil organic C, (d) in situ soil pH. Bars represent one standard deviation ( $n = 4$ ). Insert in part b shows the changes in apparent  $O_2$  diffusivity measured in well-drained top peat samples (0–3 cm,  $n = 5$ ) over 3 months following flooding under laboratory conditions.

function of diffusivity and is based on a two-point calibration. Standards for calibration in this work included: (1) stagnant water, (2) 5–20 and 40–75  $\mu\text{m}$  unsorted glass beads in water, and (3) a standard moist peat sample. The apparent diffusivity of the glass beads have previously been measured in diffusion chambers<sup>18</sup> and the moist peat sample was previously measured.<sup>19</sup> In the current study, mean values ( $n = 25$ ) of apparent diffusivity for each depth interval was measured in situ under drained condition. Measurements were repeated in the laboratory using intact cores and subsequently measured again after flooding (within one week). Measurements were repeated monthly on 5 replicate cores from the well-drained top layer monthly over 3 months following core flooding. Tabulated values for the  $O_2$  solubility and diffusion coefficient<sup>20</sup> were used to calculate  $O_2$  concentrations at atmospheric saturation and the diffusivity of  $O_2$  in distilled water at 10 °C ( $1.57 \times 10^{-5} \text{ cm}^2 \text{ s}^{-1}$ ). Diffusion coefficients for  $CO_2$  and  $CH_4$  were calculated by multiplying the value for  $O_2$  by 0.7961 and 0.8495.<sup>20,21</sup>

**Oxygen Diffusion-Reaction Model.** Steady-state profile analysis was performed using the diffusion-reaction model PROFILE<sup>15</sup> providing estimates of net consumption/production rates as a function of depth using measured diffusivities and gas concentrations as input values. The diffusion-reaction model provides an objective selection of the simplest consumption/production profile that reproduces the measured concentration profiles based on Ficks' second law. On the basis of such calculated production/consumption profiles, the depth-integrated gas fluxes were estimated by PROFILE and subsequently compared to fluxes measured in situ. Boundary conditions for simulations were no flux at the bottom and atmospheric conditions at the top.

## RESULTS AND DISCUSSION

**Site Characteristics.** The wetland soil profile (SI Figures 2S, 3S) can be divided into three functional layers: A top surface 10 cm layer with recently deposited organic C with a bulk density of 0.2–0.3  $\text{g cm}^{-3}$ , a mean pH of 7.3 and a mean organic C content of 28% (Figure 1). From 10 to 50 cm, the bulk density increases to about 0.4  $\text{g cm}^{-3}$  and pH values decrease to 7. The amount of organic C within the upper 30 cm (main root zone) is 29  $\text{kg m}^{-3}$ . Below 50 cm depth, the sediment is dominated by brackish lake sediments with a decreasing organic C content.

**Apparent Diffusivity.** Apparent diffusivities measured in situ and in the laboratory (SI Figure 4S) show similar results indicating

that intact cores can be moved to the laboratory and used to represent the apparent diffusivity in the field. However, apparent diffusivity measurements across intact cores need to be made in steps to identify “edge effects” (SI Figure 5S). Extreme values in the boundary zones of  $\sim 0.5$  cm from the top/bottom indicate the physical limitation of laboratory diffusion measurements using intact cores.

Apparent diffusivity measurements (Figure 1b) normalized to 10 °C show values in newly saturated peat layers about 10 times the diffusivity in water ( $1.57 \times 10^{-5} \text{ cm}^2 \text{ s}^{-1}$ ). This is in line with previous reported peat diffusivities<sup>13</sup> and is considered a result of a small but continuous soil–air network. Repeated laboratory measurements over 3 months following saturation ( $n = 5$ ) showed that the apparent diffusivity decreased slowly by a factor of 8 (Figure 1b, insert). These changes over time occur as trapped soil air is replaced by water, decreasing the gas phase volume and/or generating less connected air spaces in the peat matrix. Similar changes have been observed for water retention caused by “wetting inhibition”,<sup>22</sup> where the phenomenon is explained by a combination of air inclusion, water-repelling films, and pore geometry alterations due to shrinkage during drying. Repeated measurements of such time-dependent changes in apparent diffusivity (Figure 1b, inserted) also indicated that also the degree of drainage before flooding is important. Longer and more extensive drainage resulted in higher apparent diffusivities upon flooding and a longer time (weeks to months) was required to reach a constant apparent diffusivity (data not shown).

Laboratory manipulations of the water level showed a marked increase in soil fauna activity following flooding. Newly created macropores for air and water flow by migrating earthworms in the top 10 cm add to the complexity of mass transfer in the peat soil.<sup>17</sup>

The combination of the above observations leads us to conclude that the position of the water level and water content measurements are inadequate predictors of temporal changes in the apparent diffusivity. Even minor changes in air-filled and total porosities following physical shrinkage or swelling of the peat can over time change the apparent diffusivity by a factor 8 after flooding.

**Temporal Variations in Gas Concentrations and Fluxes.** Measurements from January to August 2009 showed fluctuating water levels from intermittent flooding during winter followed by a general water level drawdown during summer with some interference from precipitation events (Figure 2). Water saturation followed the same pattern but remained high (>80% by saturation) throughout the summer. During winter, ground temperatures were 0–4 °C and despite flooded conditions,  $O_2$  was present in the upper 10 cm at sites with vegetation (Figure 2). In contrast, experimental work without plants showed  $O_2$  depletion within the upper 4 mm (Figure 3a). Due to warm summer air temperatures and low water levels, temperatures reached 16–20 °C in the top 30 cm and  $O_2$  levels were up to 80% air saturation within the top 40 cm. Generally, concentrations of  $CO_2$  and  $CH_4$  varied markedly over the time period with warmer conditions leading to increasing concentrations of  $CO_2$  above the water level and  $CH_4$  concentrations below the water level (Figures 2 and 3). During flooded conditions (March 3, 2009),  $CO_2$  and  $CH_4$  concentrations increased with depth to 3000 and 150  $\mu\text{M}$ , respectively (Figure 3A). Comparable concentration ranges have previously been reported from similar sites.<sup>23</sup> Fluxes of  $CO_2$  and  $CH_4$  were low in winter and increased with temperature until the early part of the growing season when near-surface oxic conditions further increased  $CO_2$  fluxes but limited  $CH_4$  fluxes. When the water level was below 40 cm, the  $CH_4$  flux was negative indicating a net



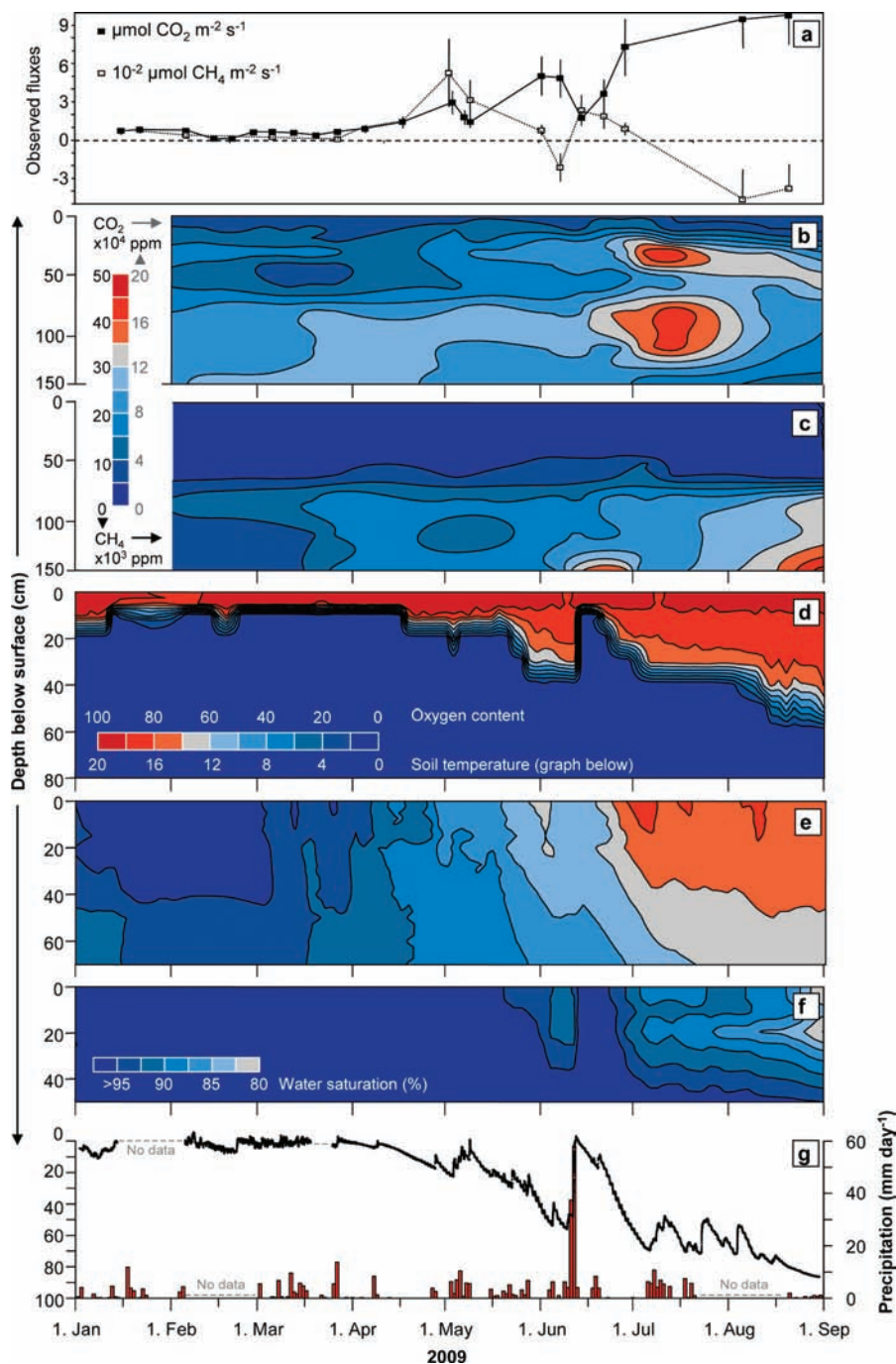


**Figure 2.** Temporal changes in subsurface conditions from January through August 2009; (a) weekly observed CO<sub>2</sub> and CH<sub>4</sub> fluxes; (b) subsurface CO<sub>2</sub> concentrations; (c) subsurface CH<sub>4</sub> concentrations; (d) subsurface O<sub>2</sub> concentrations (% air saturation); (e) ground temperatures ( $^{\circ}\text{C}$ ); (f) water contents (% saturation); and (g) water level (shown as a line) and daily precipitation (shown as bars).

uptake. These shifts in CO<sub>2</sub> and CH<sub>4</sub> fluxes and the magnitude of fluxes are within the range quantified in other Northern wetlands.<sup>3</sup>

**Modeling Soil Gas Dynamics during Steady State Field Conditions.** Concentration profiles were analyzed within two time frames assuming steady-state conditions; after months with the water level above the ground surface (0–5 cm) and after weeks with the water level fluctuating below 50 cm (Figure 2). Modeled production and consumption profiles showed that CO<sub>2</sub> and CH<sub>4</sub> were mainly produced within the upper 20 cm containing newly deposited organic material and the main rhizosphere

zone. However, these rates are lower than those reported from similar wetlands.<sup>2</sup> The CH<sub>4</sub> production profile could also be influenced by different CH<sub>4</sub> production pathways, i.e., near-surface acetate fermentation versus deeper methanogenesis from the reduction of CO<sub>2</sub> in less reactive layers.<sup>23</sup> We found maximum CH<sub>4</sub> in situ fluxes of  $0.005 \mu\text{mol CH}_4 \text{ m}^{-2} \text{ s}^{-1}$ , which were very low as compared to potential CH<sub>4</sub> production rates observed in laboratory studies, i.e.,  $0.01–10 \mu\text{mol CH}_4 \text{ m}^{-3} \text{ s}^{-1}$ .<sup>24</sup>

After a period of natural drainage and water level depths >50 cm (August 20, 2009), O<sub>2</sub> was present to a depth of 50 cm

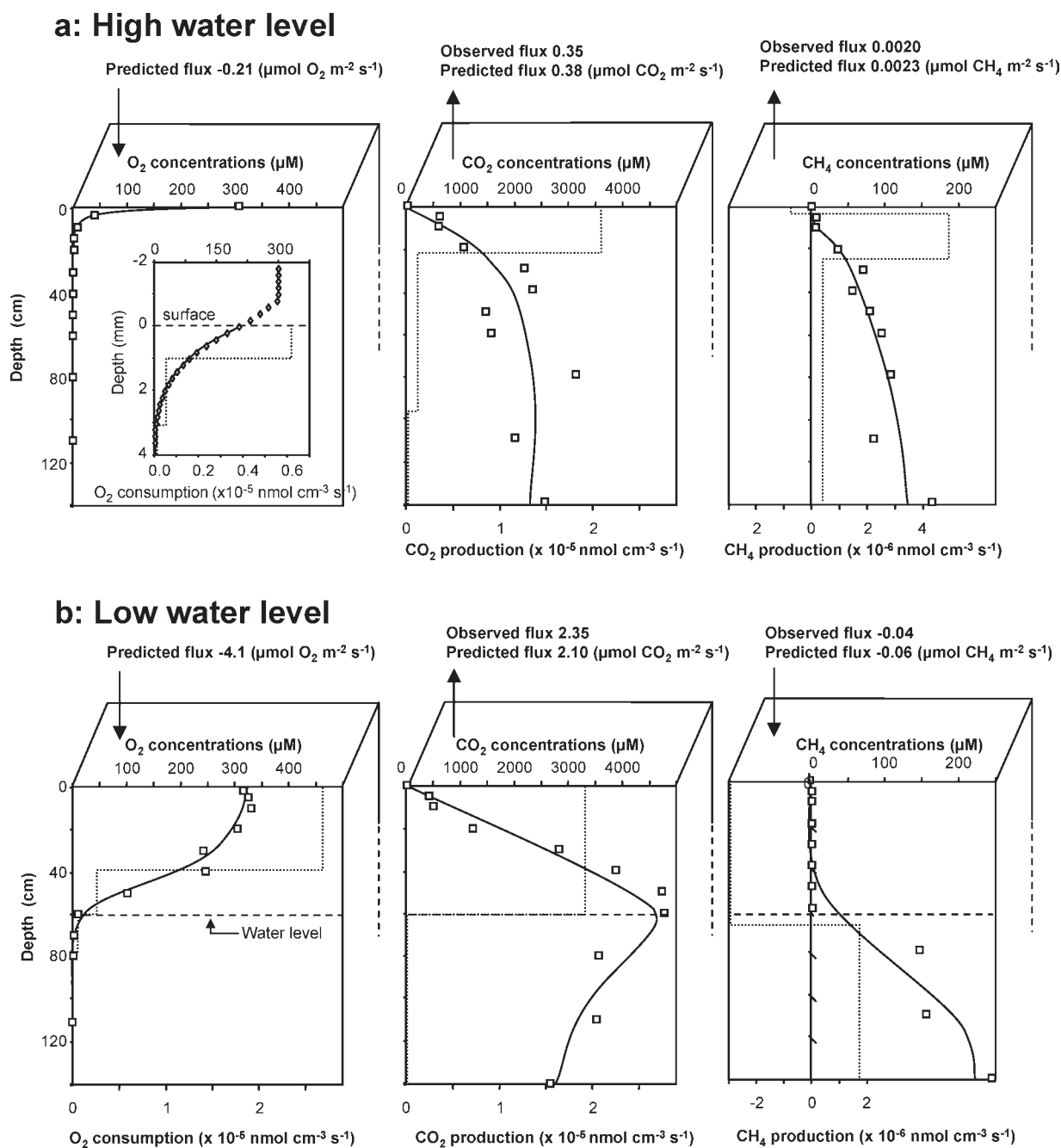


**Figure 3.** Field observed (symbols) and simulated (lines) subsurface gas concentrations at near steady state conditions: (a) cold and flooded conditions on March 20, 2009 and (b) warm and water level below 50 cm on August 20, 2009. Consumption and production profiles (dashed lines) are made using PROFILE (see Materials and Methods) and the depth-integrated net uptake or release of  $\text{CO}_2$  and  $\text{CH}_4$  are compared to in situ observed fluxes. Under flooded conditions,  $\text{O}_2$  is measured using microsensors (diamonds) and under drained conditions  $\text{O}_2$  is measured using optodes (squares).

and the  $\text{O}_2$  flux (based on PROFILE simulation) was 20 times larger than under flooded conditions. Corresponding maximal  $\text{CO}_2$  concentration (about  $4500 \mu\text{M}$ ) was also observed at 50 cm depth (Figure 3B). The total subsurface  $\text{O}_2$  flux ( $\sim 4 \mu\text{mol O}_2 \text{ m}^{-2} \text{ s}^{-1}$ ) was almost twice as high as the total surface  $\text{CO}_2$  flux according to PROFILE simulations. This could be caused by a notable amount of  $\text{CO}_2$  being dissolved in the liquid phase and transported out of the soil-ecosystem without being released to the atmosphere, in line with previous observations<sup>25</sup> and high dissolved C export rates from wetlands which is an advective transport not represented in our profiles of transport coefficients.<sup>26</sup>  $\text{CH}_4$  concentrations increased from

atmospheric levels above the water level to  $>100 \mu\text{M}$  with increasing depth. However, concentrations and production rates cannot be directly compared as the flooded conditions typically occurred during winter with low temperatures, while the drained conditions occurred during summer with markedly warmer temperatures (Figure 2). Rates estimated from our PROFILE analysis were depth-integrated and compared with observed surface fluxes in situ (Figure 3) showing reasonable agreement between observed and modeled fluxes.

**Laboratory Experiment.** Laboratory measurements of  $\text{O}_2$  by planar optode and  $\text{CO}_2/\text{CH}_4$  using a MIMS (Figure 4 and SI Figure 6S) were performed to provide data for controlled steady

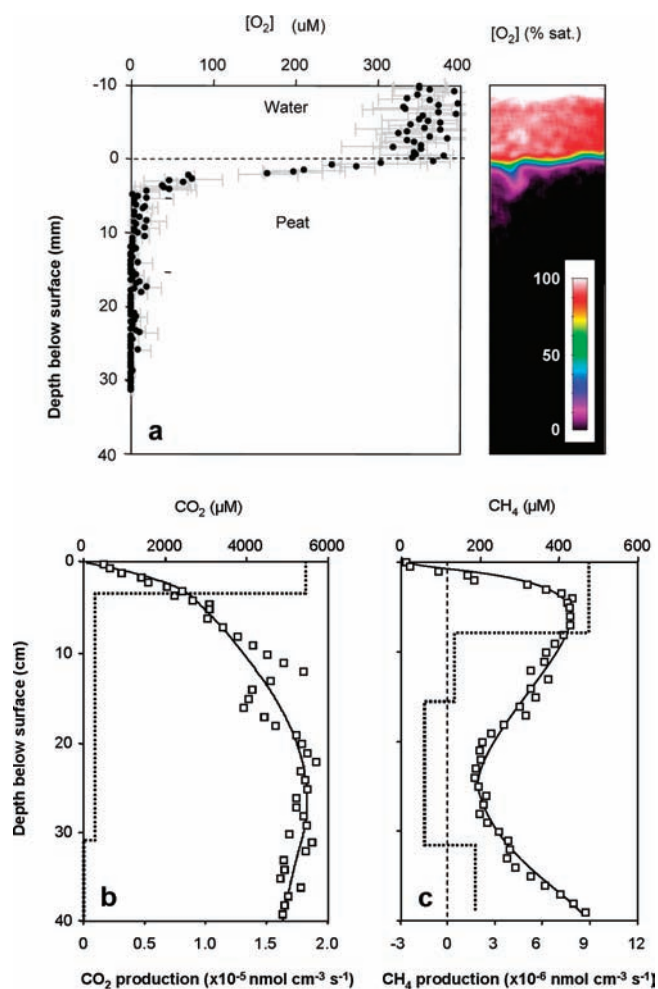


**Figure 4.** Laboratory observed (symbols) and simulated (lines) subsurface gas concentrations: (a) An image of the O<sub>2</sub> distribution using planar optodes and the mean O<sub>2</sub> concentration ( $\pm$ one standard deviation) across the entire image, (b) subsurface CO<sub>2</sub> concentrations, and (c) subsurface CH<sub>4</sub> concentrations measured by MIMS. Consumption and production profiles (dashed lines) were made using PROFILE.

state conditions and to explore links between often reported one-dimensional gas gradients and area-based flux measurements. After more than 6 months of dark incubation at 10 °C, O<sub>2</sub> penetrated down to about 4 mm (Figure 4 and SI Figure 7S) similar to results from in situ measurements in soil without active plant growth. Subsurface concentrations of both CO<sub>2</sub> and CH<sub>4</sub> were high: >5000 μM CO<sub>2</sub> and >400 μM CH<sub>4</sub> but also highly variable with depth. We speculate that such variations, particularly at 10–30 cm depth, were influenced by dead but open culms of grasses.<sup>27</sup> The flux of CH<sub>4</sub> calculated from PROFILE was 0.10 μmol CH<sub>4</sub> m<sup>-2</sup> s<sup>-1</sup>, which is about twice the mean value of measured fluxes using flux chambers in the laboratory (0.065 μmol CH<sub>4</sub> m<sup>-2</sup> s<sup>-1</sup>). This can originate in uncertainties related to the PROFILE simulations or that some CH<sub>4</sub> oxidation occurred in the well-oxidized water/sediment interface, which is not reflected in the relatively coarse depth resolution of the field profiles and consequently not accounted for in PROFILE.

We attribute the higher concentrations of CH<sub>4</sub> (and higher fluxes) measured under flooded laboratory conditions as opposed to flooded field conditions to be due to a combination of slightly

warmer conditions as well as the absence of plants in the laboratory experiment. Although plant activity is low during the initial growth stage in March, seedlings of *Phalaris arundinacea* with internal aeration through aerenchymous tissue<sup>28–30</sup> start to develop under complete water covered conditions (anoxia).

## CONCLUSIONS

This work focused on the diffusive gas dynamics in the soil air and pore water phases, which both affect the net fluxes of CO<sub>2</sub> and CH<sub>4</sub> across the soil–atmosphere interface. Our study suggests that the near-surface O<sub>2</sub> level is affected by transport linked to the presence of plants and O<sub>2</sub> release from plant roots. Analysis of concentration gradients showed that CH<sub>4</sub> oxidation can occur below the water level both under completely flooded conditions as well as for conditions with the water level well below the surface (Figure 3). The immediate oxidation of CH<sub>4</sub> by O<sub>2</sub> near the roots may explain our finding of rather low CH<sub>4</sub> emissions rates to the atmosphere through the bulk soil matrix, indicating that gas transport through plants is an important control on the overall CH<sub>4</sub> budget. Direct measurement of ecosystem CH<sub>4</sub> emissions in dynamic chambers suggest that roughly 80% of the total CH<sub>4</sub> emission at the actual study site can be mediated through plants. We conclude that the linkage between subsurface gas concentrations and surface fluxes can be roughly predicted by simple gas diffusion, but only if soil and depth specific apparent diffusivities are taken into account. We have shown that microscale patterns in time and space are more important than reported so far. In particular, this work highlights the importance of changes in near-surface time-dependent apparent diffusivity following flooding and the influence of macro fauna activity. Future measurements should include the entire ecosystem (including plants and macro fauna) as well as further studies of the microscale O<sub>2</sub> distribution in order to improve the quantification of processes linking subsurface greenhouse gas production and net gas emissions in wetlands with marked water level variations not least in a climate change context.

## ASSOCIATED CONTENT

**Supporting Information.** Seven figures provide additional information about the field site and the experimental setup. This material is available free of charge via the Internet at <http://pubs.acs.org>.

## AUTHOR INFORMATION

### Corresponding Author

\*Phone: (+45) 3532 2520; e-mail: [be@geo.ku.dk](mailto:be@geo.ku.dk).

## ACKNOWLEDGMENT

This work was conducted within the framework of the project “Oxygen Availability Controlling the Dynamics of Buried Organic Carbon Pools and Greenhouse Emissions” financed by the Danish Natural Science Research Council (PI: B.E.). We wish to thank Lars Rickelt for constructing the planar optodes and for many valuable discussions, to Gry Lyngsø and Louise Langhorn for help with fieldwork, sample collection, and laboratory analysis and very helpful journal review comments.

## REFERENCES

(1) Gorham, E. Northern peatlands: Role in the carbon cycle and probable responses to climatic warming. *Ecol. Appl.* **1991**, *1*, 182–195.



- (2) Blodau, C.; Moore, T. R. Micro-scale CO<sub>2</sub> and CH<sub>4</sub> dynamics in a peat soil during a water fluctuation and sulphate pulse. *Soil Biol. Biochem.* **2003**, *35*, 535–547, DOI: 10.1016/S0038-0717(03)00008-7.
- (3) Strack, M.; Waddington, J. M. Response of peatland carbon dioxide and methane fluxes to a water table drawdown experiment. *Global Biogeochem. Cycles* **2007**, *21*, GB1007, DOI: 10.1029/2006GB002715.
- (4) Laiho, R. Decomposition in peatlands: Reconciling seemingly contrasting results on the impacts of lowered water levels. *Soil Biol. Biochem.* **2006**, *38*(8), 2011–2024, DOI: 10.1016/j.soilbio.2006.02.017.
- (5) Wachinger, G.; Fiedler, S.; Zepp, K.; Gättinger, A.; Sommer, M.; Roth, K. Variability of soil methane production on the micro-scale: Spatial association with hot spots of organic material and Archaeal populations. *Soil Biol. Biochem.* **2000**, *32*, 1121–1130, DOI: 10.1016/S0038-0717(00)00024-9.
- (6) Le Mer, J.; Roger, P. Production, oxidation, emission, and consumption of methane by soils: A review. *Eur. J. Soil Sci.* **2001**, *37*, 25–50, DOI: 10.1016/S1164-5563(01)01067-6.
- (7) Kühn, M. Optical microsensors for analysis of microbial communities. *Environmental Microbiology. Methods Enzymol.* **2005**, *397*, 166–199, DOI: 10.1016/S0076-6879(05)97010-9.
- (8) Glud, R. N.; Ramsing, N. B.; Gundersen, J. K.; et al.; Planar optodes, a new tool for fine scale measurements of two-dimensional O<sub>2</sub> distribution in benthic communities. *Mar. Ecol.: Prog. Ser.*, **1996**, *140*, 217–226; IDS Number: VJ377.
- (9) Glud, R. N. Oxygen dynamics of marine sediments. *Mar. Biol. Res.* **2008**, *4*, 243–289, DOI: 10.1080/17451000801888726.
- (10) Kühn, M.; Polerecky, L. Functional and structural imaging of phototrophic microbial communities and symbioses. *Aquat. Microb. Ecol.* **2008**, *53*, 99–118, DOI: 10.3354/ame01224.
- (11) Armstrong, W. Oxygen diffusion from the roots of some British bog plants. *Nature* **1964**, *204*, 801–802.
- (12) Colmer, T. D. Long-distance transport of gases in plants: a perspective on internal aeration and radial oxygen loss from roots. *Plant, cell Environ.* **2003**, *26*(1), 17–36.
- (13) Stephen, K. D.; Arah, J. R. M.; Thomas, K. L.; Benstead, J.; Lloyd, D. Gas diffusion coefficient profile in peat determined by modelling mass spectrometric data: implications for gas phase distribution. *Soil Biol. Biochem.* **1998**, *30*(3), 429–431, DOI:10.1016/S0038-0717(97)00118-1.
- (14) Iiyama, I.; Hasegawa, S. Gas diffusion coefficient of undisturbed peat soils. *Soil Sci. Plant Nutr.* **2005**, *51*(3), 431–435, DOI: 10.1111/j.1747-0765.2005.tb00049.x.
- (15) Berg, P.; Risgaard-Petersen, N.; Rysgaard, S. Interpretation of measured concentration profiles in sediment pore water. *Limnol. Oceanogr.* **1998**, *43*, 1500–1510.
- (16) Kammann, C.; Grunhage, L.; Jäger, H.-J. A new sampling technique to monitor concentrations of CH<sub>4</sub>, N<sub>2</sub>O and CO<sub>2</sub> in air at well-defined depths in soils with varied water potential. *Eur. J. Soil Sci.* **2001**, *52*, 297–303, DOI: 10.1046/j.1365-2389.2001.00380.x
- (17) Askaer, L.; Elberling, B.; Glud, R. N.; Kühn, M.; Lauritsen, F. R.; Joensen, H. P. Soil heterogeneity effects on O<sub>2</sub> distribution and CH<sub>4</sub> emissions from wetlands: In situ and mesocosm studies with planar O<sub>2</sub> optodes and membrane inlet mass spectrometry. *Soil Biol. Biochem.* **2010**, *42*, 2254–2265, DOI: 10.1016/j.soilbio.2010.08.026.
- (18) Revsbech, N. P.; Nielsen, L. P.; Ramsing, N. B. A novel microsensor for determination of apparent diffusivity in sediments. *Limnol. Oceanogr.* **1998**, *43*, 986–992.
- (19) Elberling, B. Gas phase diffusion coefficients in cemented porous media. *J. Hydrol.* **1996**, *178*, 93–108.
- (20) Ramsing, N.; Gundersen, J. Seawater and gases—Tabulated physical parameters of interest to people working with microsensors in marine systems. Version 2.0. 1994, Unisense Internal Report, 16 pp.
- (21) Li, Y.-H.; Gregory, S. Diffusion of ions in seawater and deep-sea sediments. *Geochim. Cosmochim. Acta* **1974**, *38*, 703–714.
- (22) Schwärzel, K.; Renger, M.; Sauerbrey, R.; Wessolek, G. Soil physical characteristics of peat soils. *J. Plant Nutr. Soil Sci.* **2002**, *165*(4), 479–486, DOI: 10.1002/1522-2624(200208).
- (23) Hornibrook, E. R. C.; Longstaff, F. J.; Fyfe, W. S. Spatial distribution of microbial methane production pathways in temperate zone wetland soils: Stable carbon and hydrogen isotope evidence. *Geochim. Cosmochim. Acta* **1997**, *61*, 745–753, DOI: 10.1016/S0016-7037(96)00368-7.
- (24) Segers, R. Methane production and methane consumption: A review of processes underlying wetland methane fluxes. *Biogeochem.* **1998**, *41*, 23–51, DOI: 10.1023/A:1005929032764.
- (25) Iiyama, I.; Hasegawa, S. In situ CO<sub>2</sub> profiles with complementary monitoring of O<sub>2</sub> in a drained peat layer. *Soil Sci. Plant Nutr.* **2009**, *55*, 26–34, DOI: 10.1111/j.1747-0765.2008.00331.x.
- (26) Fenner, N.; Freeman, C.; Lock, M. A.; Harmens, H.; Reynolds, B.; Sparks, T. Interactions between elevated CO<sub>2</sub> and warming could amplify DOC exports from peatland catchments. *Environ. Sci. Technol.* **2007**, *41*, 3146–3152, DOI: 10.1021/es061765v.
- (27) Tanaka, N.; Yutani, K.; Aye, T.; Jinadasa, K. B. S. N. Effect of broken dead culms of *Phragmites australis* on radial oxygen loss in relation to radiation and temperature. *Hydrobiol.* **2007**, *583*, 165–172, DOI: 10.1007/s10750-006-0483-7.
- (28) Brix, H.; Lorenzen, B.; Morris, J. T.; Schierup, H. H.; Sorrell, B. K. Effect of oxygen and nitrate on ammonium uptake kinetics and adenylate pools in *Phalaris arundinacea* L. and *Glyceria maxima* (Hartm) Holmb. *Proc. R. Soc. Edinburgh* **1994**, *102B*, 333–342.
- (29) Kercher, S. M.; Zedler, J. B. Flood tolerance in wetland angiosperms: A comparison of invasive and noninvasive species. *Aquat. Bot.* **2004**, *80*, 89–102, DOI: 10.1016/j.aquabot.2004.08.003.
- (30) Askaer, L.; Elberling, B.; Jørgensen, C. J.; Friberg, T.; Hansen, B. U. Plant-mediated CH<sub>4</sub> transport and C gas dynamics quantified in situ in a *Phalaris arundinacea*-dominant wetland. *Plant Soil* **2011**, DOI: 10.1007/s11104-011-0718-x.



## Supporting information

### MATERIALS AND METHODS

**Climate station and measurements of other environmental parameters** A climate station was constructed to monitor air temperature at 2 meters height (Campbell Scientific 107 Temperature probe, Campbell Scientific Ltd., Loughborough, UK), wind speed (A100R anemometer), wind direction (W200P Potentiometer wind vane) relative humidity, radiation and soil temperature at depths 0, 10, 20, 30, 40, 50, 60, 70 cm at 30 minute intervals. Pressure and precipitation data was obtained from a climate station 5 km away. Water level was monitored by a pressure transducer (Druck PDCR 1830 Series, Campbell Scientific Ltd., Loughborough, UK) installed at a known depth in a 2.5 meter long perforated plastic tube. To avoid effects of peat swelling and shrinking on water level measurements, the pressure transducer was fixed to a 2.6 m long metal rod installed into the peat. Measurements of pH are sensitive to environmental conditions and therefore measured within 10 min after sampling and reported at 10°C. The Theta Probe Soil Moisture Sensors have been calibrated according to user Manual (v1.21, May 1999) by measuring output in depth-specific samples at three different moisture contents, disturbing it as little as possible so that it is at the same density as *in situ*.

**Experimental setup.** Mesocosm peat core samples were taken during winter to obtain dormant vegetation and high water level. After extraction the peat columns were insulated and kept in the dark to eliminate plant photosynthesis and avoid development of microphytes along the planar optode. Cores were moved into a dark climate chamber kept at 10 °C and water levels were adjusted to 5 cm above the soil surface in all cores. The cores were preincubated for 6 month to obtain steady state conditions with respect to O<sub>2</sub>, CO<sub>2</sub> and CH<sub>4</sub>. The initial water level was maintained 5 cm above the peat surface and an aquarium pump and pumice stone was used to maintain constant O<sub>2</sub> concentrations in the water above the surface. Steady state conditions were confirmed during the last week of preincubation by daily gas profiling using the MIMS and planar O<sub>2</sub> optode imaging.

**Oxygen planar optode.** The setup for 2-D O<sub>2</sub> measurements is described in detail elsewhere (1S-3S). As for other O<sub>2</sub> optodes systems, the basic principle of the planar optode is the ability of O<sub>2</sub> to act as a dynamic quencher of the luminescence of an immobilised O<sub>2</sub> indicator (4s). Here we used the O<sub>2</sub> quenchable indicator dye Ruthenium(II)-tris-4,7-diphenyl-1,10-phenanthroline (Ru-dpp) immobilized in a ~20 μm thick polystyrene layer cast onto a 0.125 mm-thick transparent polyethylene terephthalate carrier foil (Mylar, Goodfellow, UK). The indicator is excited by blue light (ex. max. 460 nm) inducing red luminescence (em. max. 610 nm), which is quenched in the presence of O<sub>2</sub>. Two planar optode foils (100 x 250 mm) were taped together (100 x 500 mm) and mounted on the inside of a plexiglass sheet glued onto the cut PVC cylinder (section 2.3.1). In the experimental setup, excitation light was supplied by blue light-emitting diodes (LED) (λ = 470 nm) illuminating the sensor foil from behind through the Plexiglas and the Mylar foil. Images of the O<sub>2</sub> dependent luminescence were obtained with a cooled gate-able charge coupled device (CCD) camera (SensiCam Sensimod, PCO Computer Optics, Germany) equipped with a 25 mm/1.4 Nikon wide-angle lens. All O<sub>2</sub> images were obtained without ambient light.

The camera and LED's were part of a modular luminescence lifetime imaging system (MOLLI) for image acquisition and processing (2S). A "by area average" two-point calibration was performed at 100 % and 0 % air saturation to enable image calibrations using a modified Stern-Volmer equation (5S). The obtained O<sub>2</sub> images covered an area of 70 x 50 mm (CCD camera chip size 640 x 480 pixel). More details about optical O<sub>2</sub> imaging, sensor materials, measuring and calibration routines are given elsewhere (1S-4S, 6S).

**Membrane Inlet Mass Spectrometry (MIMS)** Depth-specific analyses of dissolved CH<sub>4</sub> concentrations were carried out using a MIMS similar to that original developed by (7S). A detailed description of the method and the MIMS probe itself is found in (8S). Our probe was a 50 cm long stainless steel probe (3.2 mm o.d, 1.6 mm i.d.) fitted with a 20 mm long narrow tip (1.6 o.d., 1.0 mm i.d) in one end and attached to the mass spectrometer at the other end via a 50 cm long flexible metal bellow. The narrow tip was closed in the end and had a 0.5 mm orifice drilled 1 cm from the end. The orifice was covered with a microporous polypropylene membrane (CELGARD 2502, Hoechst Celanese, Charlotte, NC) that was 50 μm thick, has an effective pore size of 0.075 μm and a 45% porosity. In contrast to the silicone rubber membranes used

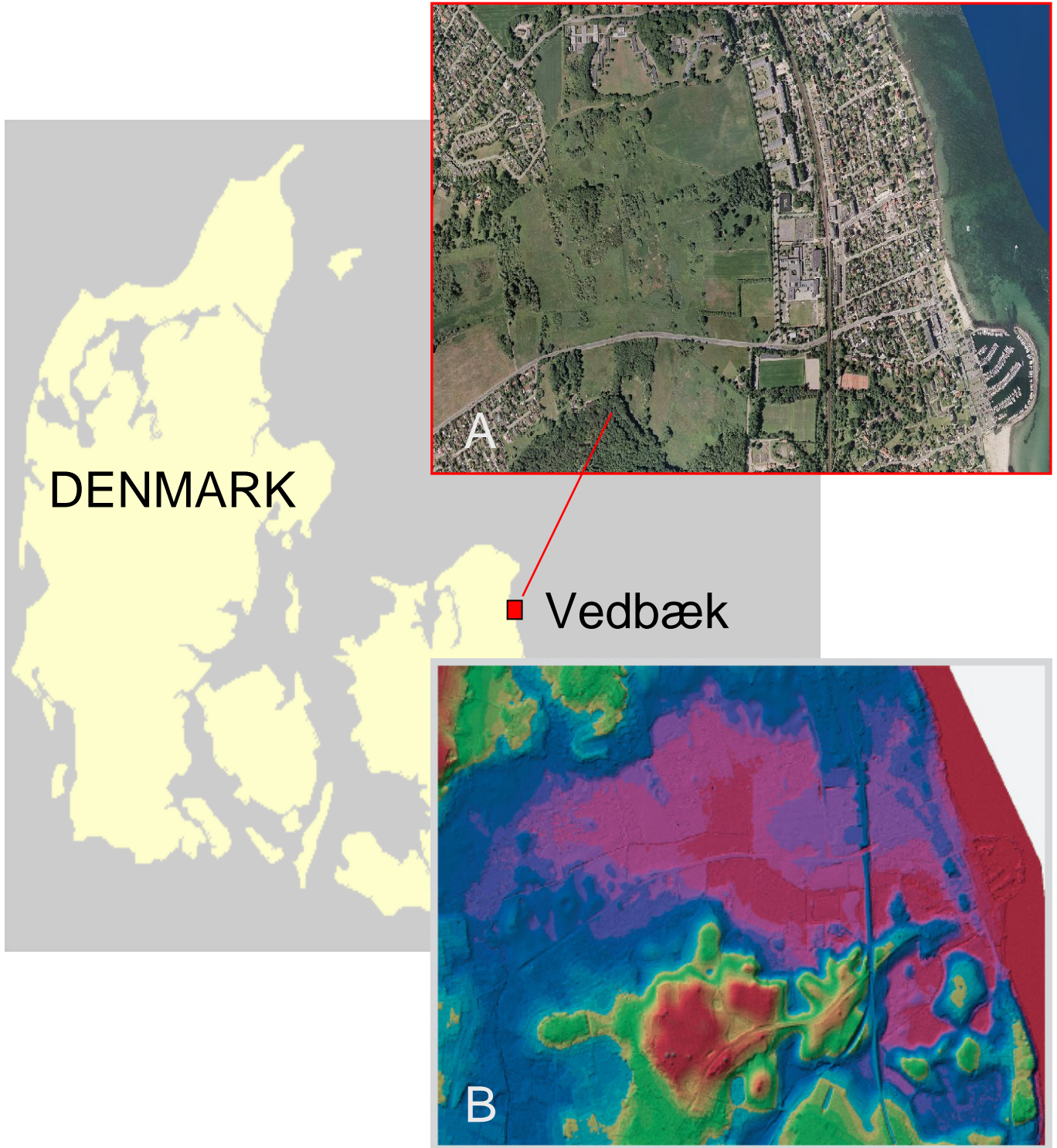
previous (7S, 8S), this type of membrane does not result in a highly preferential transport of gases as compared to water through the membrane; instead all compounds pass the membrane at a comparable rate (9). The missing enrichment of gases as compared to water is compensated by a 50-100 times higher flux of water and gas through the membrane into the probe and the mass spectrometer. With the membrane probe inserted in water a total pressure inside the mass spectrometer below  $1 \cdot 10^{-5}$  torr is obtained, which corresponds to a maximal liquid (water and gases) consumption rate of 1 nL/s for our mass spectrometer system. The mass spectrometer was a quadrupole mass spectrometer (QMA 125, Balzers, Lichtenstein).

#### **Supporting references:**

- (S1) Glud, R. N.; Ramsing, N.B.; Gundersen *et al.* Planar optodes, a new tool for fine scale measurements of two-dimensional O<sub>2</sub> distribution in benthic communities. *Marine Ecology Progress Series*, **1996**, *140*, 217-226.
- (S2) Holst, G.; Kohls, O.; Klimant, I. *et al.* A modular luminescence lifetime imaging system for mapping oxygen distribution in biological samples. *Sensors and Actuators*, **1998**, *B51*, 163-170.
- (S3) Holst, G.; Franke, U.; Grunwald, B. Transparent oxygen optodes in environmental applications at fine scale as measured by luminescence lifetime imaging. Proceedings of SPIE – volume 4576. International Society of Optical Engineering, Advanced Environmental Sensing Technology **2002**, *II*, 138-148.
- (S4) Kühl, M.; Polerecky, L. Functional and structural imaging of phototrophic microbial communities and symbioses. *Aquatic Microbial Ecology* **2008**, *53*, 99-118.
- (S5) Klimant, I.; Meyer, V.; Kühl, M. Fiber-optic oxygen microsensors, a new tool in aquatic biology. *Limnol. Oceanogr.* **1995**, *40*, 1159-1165.

- (S6) Glud, R. N.; Tengberg, A.; Köhl, M. *et al.* An *in situ* instrument for planar O<sub>2</sub> optode measurements at benthic interfaces. *Limnol. Oceanogr.* **2001**, *46*, 2073-2080.
- (S7) Bernstead, J.; Lloyd, D. Direct mass spectrometric measurement of gases in peat cores. *FEMS Microbiol. Ecol.* **1994**, *13*, 233-240.
- (S8) Sheppard, S. K.; Lloyd, D. Direct mass spectrometric measurement of gases in soil monoliths. *J. Microbiol. Methods*, **2002**, *50*, 175-188.
- (S9) Lauritsen, F. R.; Choudhury, T. K.; Dejarme, L. E. *et al.* Microporous membrane introduction mass spectrometry with solvent chemical ionization and glow discharge for the direct detection of volatile organic compounds in aqueous solution. *Anal. Chim. Acta*, **1992**, *266*, 1-12.

## Supporting information (figures)



**Supporting figure 1.** A: Location map of the study site *Maglemosen* near Vedbæk in Denmark and B: Digital elevation model of the same area using aerial laser scan technique. The reddish colours indicate the area below 7 m above the present sea level.





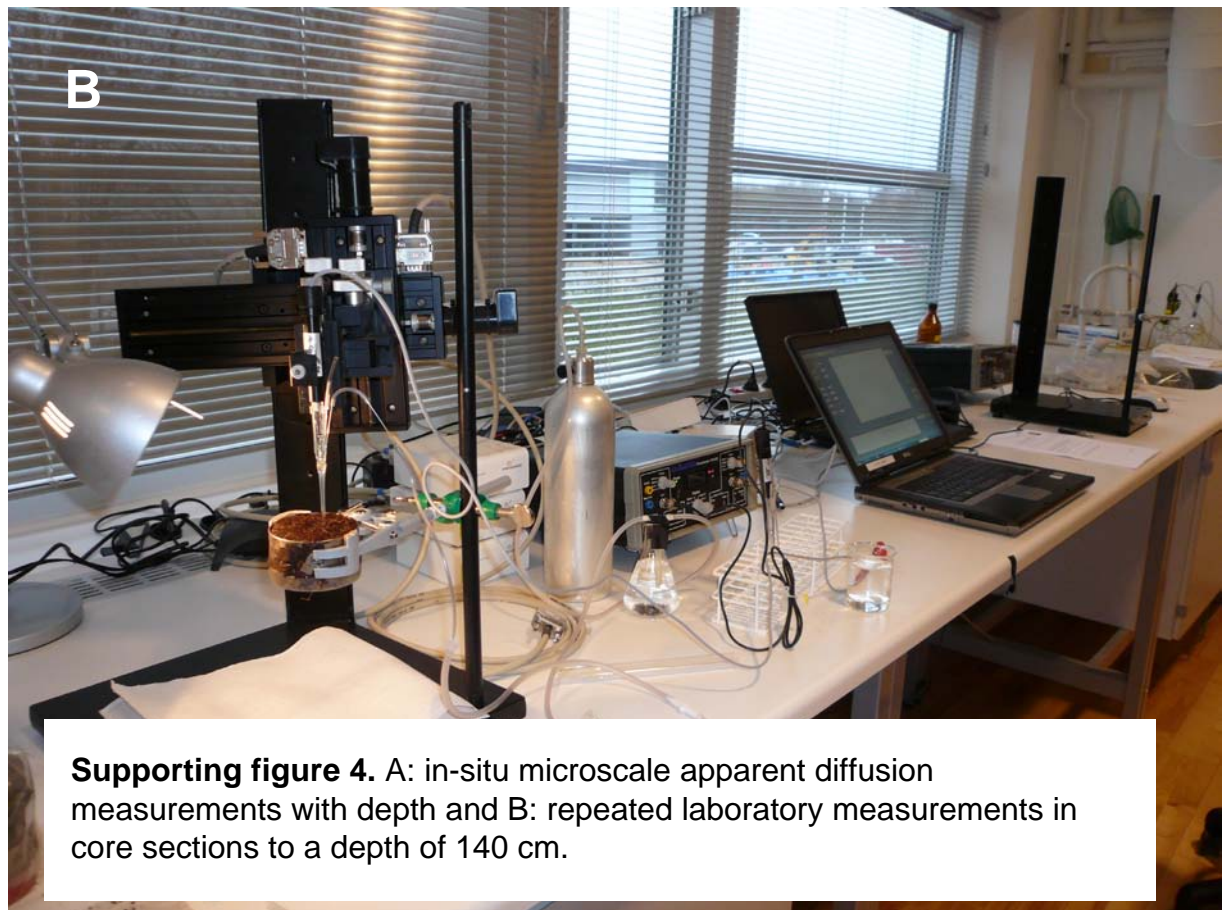
**Supporting figure 2.** A typical profile to a depth of 1.2 m dominated by the upper peat layer of 45-50 cm thickness.





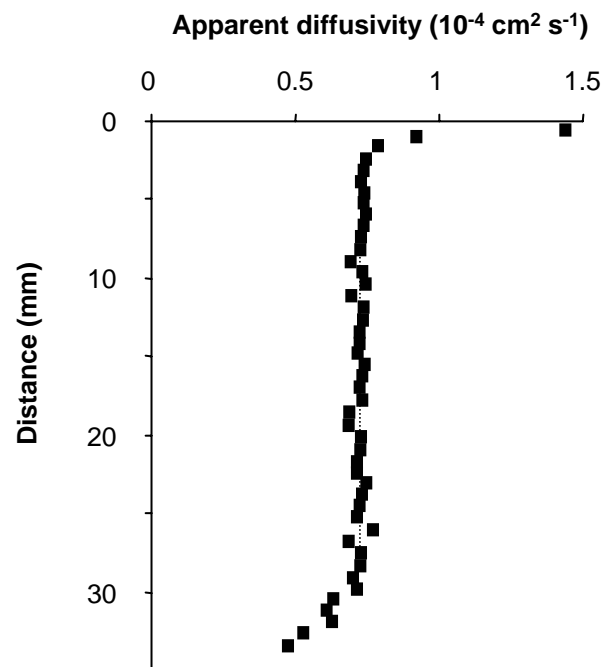
**Supporting figure 3.** Top 1 meter profile from Maglemosen, Vedbæk, showing the marked in top 50-55 cm peat overlying 15 cm carbonate rich gytje and organic rich brackish lake sediment. Inserted picture B shows details of the top 20 cm consisting of up to 16% living roots by weight.





**Supporting figure 4.** A: in-situ microscale apparent diffusion measurements with depth and B: repeated laboratory measurements in core sections to a depth of 140 cm.

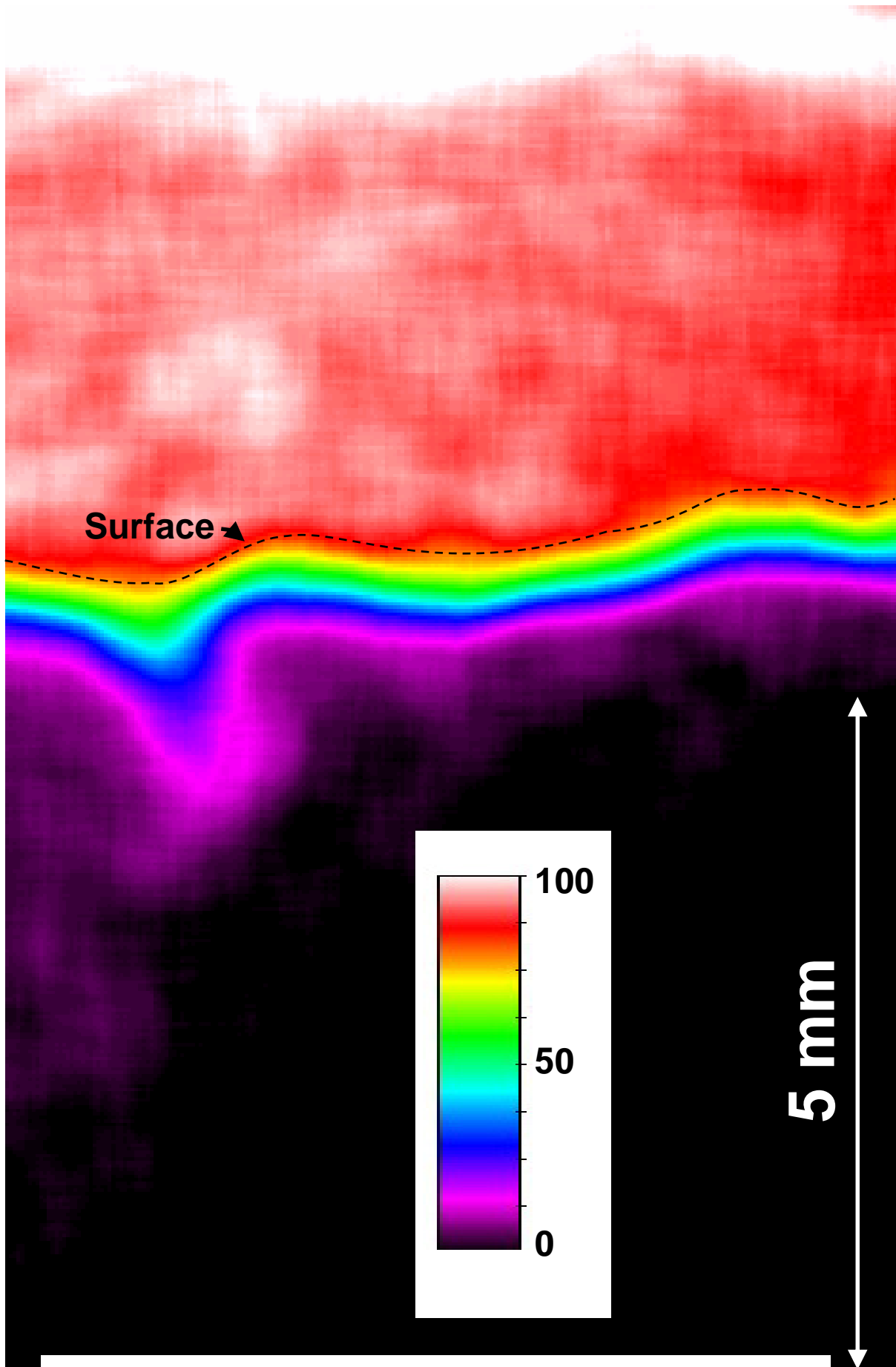




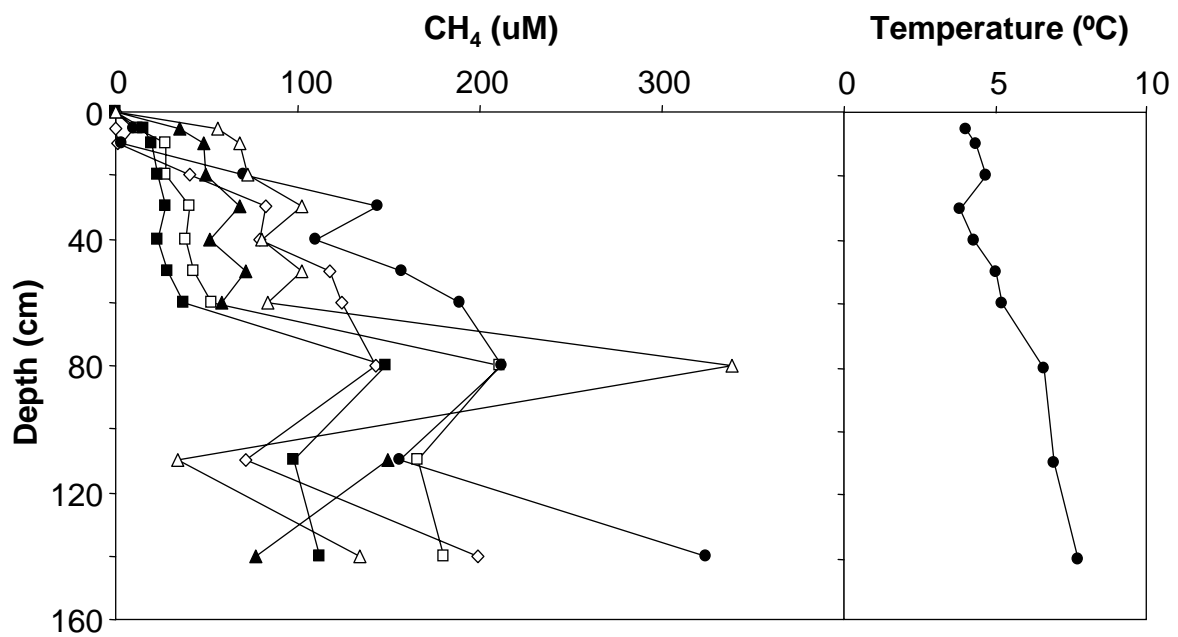
**Supporting figure 5.** Laboratory microscale apparent diffusion measurements with depth measured across one peat core over 3.5 cm showing “edge effects” and the importance of stepwise measurements and not bulk core measurements. The dash line represent the mean value of measurements across the central 2 cm.



**Supporting figure 6.** Laboratory measurements of subsurface gas concentrations using Membrane Inlet Mass Spectrometry (MIMS) and planar optode (PO). Measurements and images were made in dark and at 10°C after collected cores of 50 cm in length were kept saturated over more than 6 months.



**Supporting figure 7.** Enlarged picture of Figure 4a showing details of the oxygen distribution (0 – 100 % atm. saturation) near the surface during flooded conditions after steady state conditions have been reached



**Supporting figure 8.** *In-situ* subsurface CH<sub>4</sub> concentrations measured in 3 profiles twice over one week during stable water table (5 cm above the surface) by the end of march 2009. The figure illustrates the spatial variability in profiles within 100 m in a homogeneous vegetation site and shifts in concentrations level probably due to water flow during the most stable period during the year.







**Annex III**





# Temporal trends in N<sub>2</sub>O flux dynamics in a Danish wetland – effects of plant-mediated gas transport of N<sub>2</sub>O and O<sub>2</sub> following changes in water level and soil mineral-N availability

CHRISTIAN JUNCHER JØRGENSEN\*, STEN STRUWE† and BO ELBERLING\*,

\*Department of Geography and Geology, University of Copenhagen, Øster Voldgade 10, DK1350 Copenhagen, Denmark, †Section of Microbiology, Department of Biology, University of Copenhagen, Sølvgade 83H, DK1307 Copenhagen, Denmark

## Abstract

Temporal trends of N<sub>2</sub>O fluxes across the soil–atmosphere interface were determined using continuous flux chamber measurements over an entire growing season of a subsurface aerating macrophyte (*Phalaris arundinacea*) in a nonmanaged Danish wetland. Observed N<sub>2</sub>O fluxes were linked to changes in subsurface N<sub>2</sub>O and O<sub>2</sub> concentrations, water level (WL), light intensity as well as mineral-N availability. Weekly concentration profiles showed that seasonal variations in N<sub>2</sub>O concentrations were directly linked to the position of the WL and O<sub>2</sub> availability at the capillary fringe above the WL. N<sub>2</sub>O flux measurements showed surprisingly high temporal variability with marked changes in fluxes and shifts in flux directions from net source to net sink within hours associated with changing light conditions. Systematic diurnal shifts between net N<sub>2</sub>O emission during day time and deposition during night time were observed when max subsurface N<sub>2</sub>O concentrations were located below the root zone. Correlation ( $P < 0.001$ ) between diurnal variations in O<sub>2</sub> concentrations and incoming photosynthetically active radiation highlighted the importance of plant-driven subsoil aeration of the root zone and the associated controls on coupled nitrification/denitrification. Therefore, *P. arundinacea* played an important role in facilitating N<sub>2</sub>O transport from the root zone to the atmosphere, and exclusion of the aboveground biomass in flux chamber measurements may lead to significant underestimations on net ecosystem N<sub>2</sub>O emissions. Complex interactions between seasonal changes in O<sub>2</sub> and mineral-N availability following near-surface WL fluctuations in combination with plant-mediated gas transport by *P. arundinacea* controlled the subsurface N<sub>2</sub>O concentrations and gas transport mechanisms responsible for N<sub>2</sub>O fluxes across the soil–atmosphere interface. Results demonstrate the necessity for addressing this high temporal variability and potential plant transport of N<sub>2</sub>O in future studies of net N<sub>2</sub>O exchange across the soil–atmosphere interface.

**Keywords:** denitrification, N<sub>2</sub>O sink, N<sub>2</sub>O source, nitrification, nitrogen transformation, nitrous oxide, oxygen, *Phalaris arundinacea*, plant-mediated gas transport, wetland

Received 2 May 2011 and accepted 15 June 2011

## Introduction

Wetland soils can be significant sources of nitrous oxide (N<sub>2</sub>O) emissions to the atmosphere if conditions for N<sub>2</sub>O production are favourable: high levels of mineral nitrogen (N) in the form of nitrate (NO<sub>3</sub><sup>-</sup>) and low levels of atmospheric oxygen (O<sub>2</sub>) (Liikanen & Martikainen, 2003). Production of N<sub>2</sub>O is predominantly biological and occurs primarily through nitrification (ammonium oxidation and nitrifier denitrification) and denitrification. Dominance of these processes is linked to soil moisture content and O<sub>2</sub> availability, as well as to the presence of labile N and carbon (C) in the soil (Bollmann & Conrad, 1998; Wrage *et al.*, 2001). Condi-

tions favouring N<sub>2</sub>O production in wetland soils are sensitive to seasonal and interannual weather patterns, which affect the soil moisture content, the depth from to the surface to the free-standing water level (WL), and seasonal growth pattern of subsurface aerating wetland macrophytes. Together, these parameters regulate O<sub>2</sub> transport into the soil and determine both the timing and the location of anoxic zones (Askaer *et al.*, 2010; Elberling *et al.*, 2011) and thereby the nature of N-transformation processes and N<sub>2</sub>O production. Following global warming, these conditions will be subject to changes affecting net N<sub>2</sub>O fluxes from the soil to the atmosphere. However, future predictions of N<sub>2</sub>O fluxes are difficult without an improved understanding of the drivers of current flux patterns.

Wetlands are characterized by having the WL near the surface and near-saturated soil water contents

Correspondence: Bo Elberling, tel. +45 3532 2520, fax +45 3532 2501, e-mail: be@geo.ku.dk



resulting in high accumulation rates of organic C and N. Variations in soil water content following WL fluctuations are a strong determinant for conditions favourable for N<sub>2</sub>O production, consumption and transport (Heincke & Kaupenjohann, 1999; Clough *et al.*, 2005), and exerts a major control on N<sub>2</sub>O emissions from soil by regulating subsurface O<sub>2</sub> availability and N-transformation processes (Firestone & Davidson, 1989; Bollmann & Conrad, 1998; Khalil *et al.*, 2004).

The position of the WL in wetlands has a direct effect of subsurface gas exchange by limiting the diffusion rates of both O<sub>2</sub> and N<sub>2</sub>O when transport pathways become water-filled (Heincke & Kaupenjohann, 1999; Clough *et al.*, 2005). Certain wetland macrophytes are capable of aerating the subsoil through aerenchymous plant tissue (Colmer, 2003). As alternate oxic and anoxic conditions may promote the production of N<sub>2</sub>O in the subsoil through sequential nitrification–denitrification reactions (Patrick & Reddy, 1976; Smith & Patrick, 1983; Firestone & Davidson, 1989) changes in seasonal WL dynamics and plant growth of subsurface aerating macrophytes are likely to affect subsurface N<sub>2</sub>O production and surface emissions. In Northern Europe, climate change is predicted to cause a general intensification of rainfall events (IPCC, 2007) resulting in an amplification of seasonal WL dynamics, which will influence the environmental drivers for subsurface N-transformation processes. While the current state of knowledge on the spatio-temporal nature of N<sub>2</sub>O flux dynamics from nonmanaged wetlands is derived from either controlled laboratory experiments or low temporal resolution flux chamber measurements (weekly to biweekly sampling frequency), significant uncertainty exists concerning the spatio-temporal nature of current N<sub>2</sub>O emission dynamics from these potentially important N<sub>2</sub>O sources, as well as the role of plant-mediated N<sub>2</sub>O transport across the soil–atmosphere interface. To understand the potential impacts and feedbacks on N<sub>2</sub>O fluxes from natural wetlands to global warming, both the timing and magnitude of N<sub>2</sub>O fluxes need to be determined in a variety of relevant ecosystems at a higher temporal resolution than is currently available.

The aims of this work were to (i) determine the spatio-temporal dynamics and gas transport mechanisms of current N<sub>2</sub>O flux patterns in high temporal resolution over a full growing season in a protected and nonmanaged wetland; (ii) explore the linkages between surface fluxes and subsurface gas concentrations of N<sub>2</sub>O, O<sub>2</sub> and dissolved mineral-N in response to seasonal variations in WL; and (iii) relate the flux dynamics to the position of the WL and seasonal variations in plant growth of a subsurface aerating macrophyte *Phalaris arundinacea*.

The aims are achieved by comparing continuously measured fluxes of N<sub>2</sub>O across the soil–atmosphere

interface with subsurface N<sub>2</sub>O, O<sub>2</sub> and mineral-N concentration profiles over a full growing season in a nonmanaged Danish wetland overgrown with *P. arundinacea*.

## Materials and methods

### Site description

The Maglemøsen experimental site is a nonmanaged minerotrophic wetland located ca. 20 km north of Copenhagen, Denmark (55°51'N, 12°32'E) with *P. arundinacea* as the dominating vegetation cover at the selected study site. A description of the annual life cycle of *P. arundinacea* at the particular site can be found in (Askaer *et al.*, 2011). Mean annual temperature and precipitation are 8 °C and 613 mm, respectively. Sample collections and field measurements were conducted from mid-April to mid-October 2010 over a full growing season, defined as a 7 day moving average of daily air temperature >5 °C (Jin *et al.*, 2010).

### Soil characteristics

Histosols cover the majority of the area with peat depths ranging from 0 to 3 m. At the experimental site, the peat thickness is between 45 and 55 cm with the main root zone occupying the upper 25–30 cm. Soil porosity in the peat layers ranges from 70% to 80% by volume. Bulk density decreases gradually from 0.25 at the surface to 0.40 g cm<sup>-3</sup> at 60 cm depth. Total organic C content in the peat ranges from 23% to 29%, while total N ranges from 1.8% to 2.4% resulting in peat C : N ratios of 10 : 12 (see also Fig. S1a–e, Supporting Information).

### Environmental parameters

The position of the WL, defined as the depth from the surface to the free-standing position of the secondary groundwater body closest to the surface, was measured using a pressure sensor (PCR 1830 series, Druck; ThermX, San Diego, CA, USA) submerged in a 2 m long perforated plastic tube placed in a sand cast drill hole. The sensor was mounted on a horizontal bar attached to 3 m long stainless steel rods inserted into the underlying mineral soil, to avoid potential measurement errors caused by seasonal displacement of the surface following swelling and shrinkage of the peat soil.

Incoming radiation in the wavelength spectrum of photosynthetically active radiation (PAR), i.e. 400–700 nm, was measured in 30 s time resolution with an energy sensor (SKE 510; Skye Instruments, Powys, UK) mounted at 1.5 m above the peat surface and equal to maximum vegetation height. Vegetation height was measured continuously on a 10 min temporal resolution by a sonic range sensor (SR50a; Campbell Sci, Loughborough, UK) mounted on a horizontal bar 3.5 m above the peat surface. Automated measurements were verified by manual measurements on a weekly basis.

Soil temperature and soil moisture were measured in the soil profile by zero-off corrected thermistors (Campbell Scien-

tific 107) and site-specific calibrated soil moisture impedance probes (Theta Probe ML2x; Delta-T Devices, Cambridge, UK) inserted horizontally in 2–10 cm depth increments, to a depth of 50 cm below the peat surface. In addition, a soil moisture probe was inserted vertically into the top soil for seasonal measurements of soil moisture content at the soil–atmosphere interface. Due to the physical design of the impedance probes, volumetric soil moisture contents are rendered as average values over a 3.5 cm depth interval. Conversion of volumetric soil moisture contents into saturation degree was based on depth-specific bulk density measurement and calculated porosity at full water saturation assuming a particle density of 1.2 g cm<sup>-3</sup> (Redding & Devito, 2006).

#### Subsurface gas measurements

Subsurface oxygen concentrations were measured at 5, 10, 15, 20, 25, 30, 35, 40, 45, 50 and 60 cm depth using O<sub>2</sub>-optodes (O<sub>2</sub>-Dipstick; PreSens GmbG, Regensburg, Germany) connected to a multi channel fibre-optic O<sub>2</sub> meter (OXY-10; PreSens GmbG). The O<sub>2</sub>-optodes were calibrated in O<sub>2</sub>-free and O<sub>2</sub>-saturated water before permanent installation in the soil profile. Raw phase angle outputs were converted into temperature-corrected O<sub>2</sub> concentrations (% atmospheric saturation) using soil temperature values measured at the respective depths (Askaer *et al.*, 2010).

Subsurface N<sub>2</sub>O concentrations were sampled on a weekly basis in 5 cm depth increments to a maximum depth of 60 cm using buried silicon probes (Jacinte & Dick, 1996; Kammann *et al.*, 2001). Gas samples were collected with 60 mL plastic syringes and transferred to evacuated soda-glass vials (5.9 mL Exetainer; LabCo, UK) and kept at 5 °C until analysis. Gas samples were analysed by gas chromatography (HP 7890; Agilent, Santa Clara, CA, USA). Following separation on gas column (1/8" × 4 m Haysep Q 80/100 mesh), the sample gas was analysed for N<sub>2</sub>O by  $\mu$ ECD. Dinitrogen (N<sub>2</sub>) was used as carrier gas and Ar : CH<sub>4</sub> (10 : 90) as makeup for  $\mu$ ECD. The GC was calibrated prior to each run by analysing a dilution series of a certified greenhouse gas mixture in synthetic air (N<sub>2</sub>O : 15  $\mu$ L L<sup>-1</sup>; Air Products, Brussels, Belgium).

#### Soil sampling

Weekly soil samples for chemical analysis were collected by soil coring (Eijkelkamp auger). The intact cores were split into mixed subsamples for every 5 cm and packed in gas tight ziploc bags. *In situ* pH was measured by inserting a pH electrode (Mettler Toledo MP220) directly into the moist sub sample and a stable reading was taken after 2–3 min. Total nitrate (NO<sub>3</sub><sup>-</sup>), nitrite (NO<sub>2</sub><sup>-</sup>) and ammonium (NH<sub>4</sub><sup>+</sup>) were determined as water extractable NO<sub>3</sub><sup>-</sup> and NO<sub>2</sub><sup>-</sup> (1 : 5 soil-water ratio) and 2 M KCl extractable NH<sub>4</sub><sup>+</sup> (1 : 10 soil-water ratio). NO<sub>3</sub><sup>-</sup> and NO<sub>2</sub><sup>-</sup> were determined by ion chromatography (Metrohm IC system 761, ASUPP 150 column, 3.2 mM Na<sub>2</sub>CO<sub>3</sub>/1.0 mM NaHCO<sub>3</sub> Eluent and 0.05 M H<sub>2</sub>SO<sub>4</sub><sup>2-</sup> regenerant). NH<sub>4</sub><sup>+</sup> was determined according to AN 5226 using a FIAstar 5000 flow injection analyser (FOSS tecator Höganäs).

#### Potential N<sub>2</sub>O consumption rates

Batch experiments with addition of N<sub>2</sub>O and/or acetylene to peat soil from the Maglemosen field site were conducted to estimate potential N<sub>2</sub>O consumption rates in soil samples from the main root zone (10–20 cm below the surface) and the soil layers below the main root zone (40–50 cm). Ten grams of mixed peat soil sampled on 28 September 2009 from and below the main root zone (10–20 and 40–50 cm respectively) were incubated at 20 °C in triplicate in 118 mL Venject tubes after addition of 20 mL demineralized water. The tube headspaces were flushed with N<sub>2</sub> for 1 min to achieve anoxic conditions. N<sub>2</sub>O was then injected to reach a final headspace concentration of 25  $\mu$ L L<sup>-1</sup>. An identical parallel batch was prepared where the consumption of N<sub>2</sub>O was inhibited by addition of 10% acetylene. Changes in headspace concentrations of N<sub>2</sub>O over the first 24 h were measured by analysing 3 mL headspace gas on the gas chromatograph. Prior to sampling, 3 mL N<sub>2</sub> was added to the test tubes to avoid pressurizing the tubes following sampling. Potential N<sub>2</sub>O consumption rates per gram soil in the presence and absence of N<sub>2</sub>O reductase inhibitor were calculated by the changes in volume-corrected headspace concentrations over time.

#### Field monitoring of CO<sub>2</sub> and N<sub>2</sub>O fluxes

Five replicate automated flux chambers (D: 60 cm × W: 60 cm × H: 60 cm ± 50 cm extender) made of transparent 6 mm polycarbonate sheets were installed in steel base frames inserted 10 cm into the soil. Transmission of radiation in the PAR spectrum through the chamber walls was measured to be above 80% of incoming PAR. The chambers were permanently installed in steel in an area with a uniform stand of *P. arundinacea*, at an average elevation of 2.5 m above mean sea level. The chambers were fitted with both inlet and outlet tube connectors. During measurements, air from the chamber headspace was circulated through R.S. 293-2000 tubing (inner diameter 0.5 mm/outer diameter 0.9 mm) from the chamber to the gas analysers in a closed and pressure tight loop at ca. 2.5 L min<sup>-1</sup>. During measurement, the air volume inside the closed chamber headspace was circulated using a 12 V fan to prevent build up of concentration gradients of the measured gasses across the height of the chambers.

Real-time concentrations of carbon dioxide (CO<sub>2</sub>), N<sub>2</sub>O and water vapour (H<sub>2</sub>O) were determined using both a nondispersive infrared gas analyser (LI-840; LiCor, Lincoln, NE, USA) and an in-line photoacoustic trace gas analyser (INNOVA 1312; LumaSense Technology Inc, Denmark) similar to other automated N<sub>2</sub>O flux measurements studies (Ambus & Robertson, 1998; Yamulki & Jarvis, 1999; Flechard *et al.*, 2005). Simultaneous measurements of CO<sub>2</sub> and H<sub>2</sub>O concentrations were performed by both the LI-840 and the INNOVA 1312 to achieve a 30 s temporal resolution of CO<sub>2</sub> concentrations by the LI-840 and to provide an independent CO<sub>2</sub> control on the status of the low concentration measurements (nL L<sup>-1</sup> region) of N<sub>2</sub>O by the photoacoustic gas analyser. To achieve an acceptable signal strength for N<sub>2</sub>O, the flux chamber closing period was 30 min. Gas concentrations of H<sub>2</sub>O, CO<sub>2</sub> and N<sub>2</sub>O

in the chamber headspace were determined every 4 min with the INNOVA (sample integration time of 50 s for each gas) with corrections made for water vapour and CO<sub>2</sub> interferences. To stabilize the water vapour pressure in the measurement cell, the sample gas was dried prior to analysis using a noninterfering Nafion dryer (MD110; PermaPure Inc., Toms River, NJ, USA) with continuous purging of dry air. The noise level in ambient N<sub>2</sub>O concentrations under the applied settings was about 10 nmol mol<sup>-1</sup>. According to Flechard *et al.* (2005), a conservative N<sub>2</sub>O flux detection limit estimate over 30 min will be ca. 6.5 µg N<sub>2</sub>O–N m<sup>2</sup> s<sup>-1</sup> (chamber height: 0.6 m) and 12 µg N<sub>2</sub>O–N m<sup>2</sup> s<sup>-1</sup> (chamber height: 1.1 m). All real-time field data were transmitted by a cell phone modem to the department server for daily data quality control.

#### Flux calculation procedure

Surface flux estimates were calculated using quadratic regression to account for potential nonlinearity in the headspace gas increase over 30 min providing a more accurate estimate of CO<sub>2</sub> and N<sub>2</sub>O fluxes while returning the same estimate as the linear regression model in case of perfect linearity in headspace concentration increase/decrease (Wagner *et al.*, 1997). Flux estimates were temperature- and pressure-corrected according to Askaer *et al.* (2011). A total of 3903 flux measurements of CO<sub>2</sub> and N<sub>2</sub>O were made during the measurement period (from 1 May 2010 to 10 October 2010). A significance test was made to remove flux estimates below a significance level of 95%. Approximately 70% of the total numbers of N<sub>2</sub>O flux measurements were below the detection limit. Frequency distributions of significant N<sub>2</sub>O fluxes ( $P < 0.05$ ) vs.  $R^2$  for each of the five replicate flux chambers are shown in Fig. S2.

#### Plant emissions of N<sub>2</sub>O

A microchamber was constructed using a transparent PVC tube (100 cm long; ID: 30 mm) to measure the N<sub>2</sub>O flux directly from the plants, excluding the soil flux contribution. The microchamber was placed over a number of single *P. arundinacea* straws, closed at the top with a plastic plug and sealed at the foot of the straw by a gas impermeable Rilsan polymer membrane (PA11; Arkema Inc, Birdsboro, PA, USA). The change in headspace concentrations of N<sub>2</sub>O over a span of 20 min was determined using an in-line photoacoustic trace gas analyser (INNOVA 1312; LumaSense Technology Inc) after dehumidification of the air stream by a noninterfering Nafion dryer (MD110, PermaPure Inc.) with continuous purging of dry air. To avoid build up of concentration gradients in the headspace during measurements, the headspace air volume was circulated in a closed loop using a battery-driven air pump at a rate of 0.5 L min<sup>-1</sup> (Fig. S3a). The effect of illumination on N<sub>2</sub>O emissions was tested during mid-day on 22 September 2009 with the microchamber placed in natural illumination (PAR ≈ 300–400 W m<sup>-2</sup>) and in simulated darkness, which was obtained by covering the chamber in a black plastic (PAR = 0 W m<sup>-2</sup>) immediately prior to measurements (Fig. S3b).

#### Contour plots

Contour plots of subsurface concentrations of O<sub>2</sub>, N<sub>2</sub>O, NO<sub>3</sub><sup>-</sup>, NH<sub>4</sub><sup>+</sup> and pH were constructed by kriging interpolation (Surfer Version 8.05; Golden Software Inc., USA). Temporal resolution of input data for the high resolution O<sub>2</sub> plot was 10 min ( $n = 235.061$ ), whereas the plots of N<sub>2</sub>O, NO<sub>3</sub><sup>-</sup>, NH<sub>4</sub><sup>+</sup> and pH were based on weekly profile measurements ( $n = 312$ ).

## Results

#### Water level dynamics

The annual amplitude of the WL was ca. 80 cm in the growing season of 2010 (see Fig. 1a). Generally, the WL was located near the surface (ca. 0–10 cm) during the late autumn, winter and early spring. Maximum depths of the WL were observed during the peak of the growing season in the end of July after an average decrease in WL position up to 2.7 cm day<sup>-1</sup> over a 5 week period (Fig. 1a).

Rapid responses in the position of the WL were observed following precipitation events of more than 10 mm day<sup>-1</sup>, e.g. 14 August 2010 (112 mm precipitation in 7 h) where the WL rose from –50 to +20 cm in 3 h leading to a near-surface WL through the remaining part of the measurement period (Fig. 1a).

#### Temperature

In the growing season 2010, daily mean air temperatures varied between 5 and 20 °C (Fig. 1b) and daily mean soil temperatures in the upper 60 cm varied between 5 and 17 °C. Maximum daily variations in air (2 m) and top soil (–2 cm) temperature were ca. 15 and 4 °C respectively (see Figs 7b and 8b). The relative modest maximum temperature variations in the top soil were caused by effective shading by the dense vegetation cover.

#### Soil moisture content

Soil moisture contents were close to saturation over the entire soil profile in both early and late seasons. In mid-season from late June to mid-August, the degree of water saturation was observed to decrease in response to a decreasing WL. The degree of water saturation was ca. 45–60% in the upper 5 cm and 80% at a depth of 20 cm (Fig. 1c) when the WL was at its lowest. At a depth of 50 cm, the degree of water saturation was above 95% throughout the measurement period. The largest variations in water saturation degrees were observed in the top soil following precipitation events at the end of July and at the start of August 2010. Here, the degree of water saturation was observed to increase

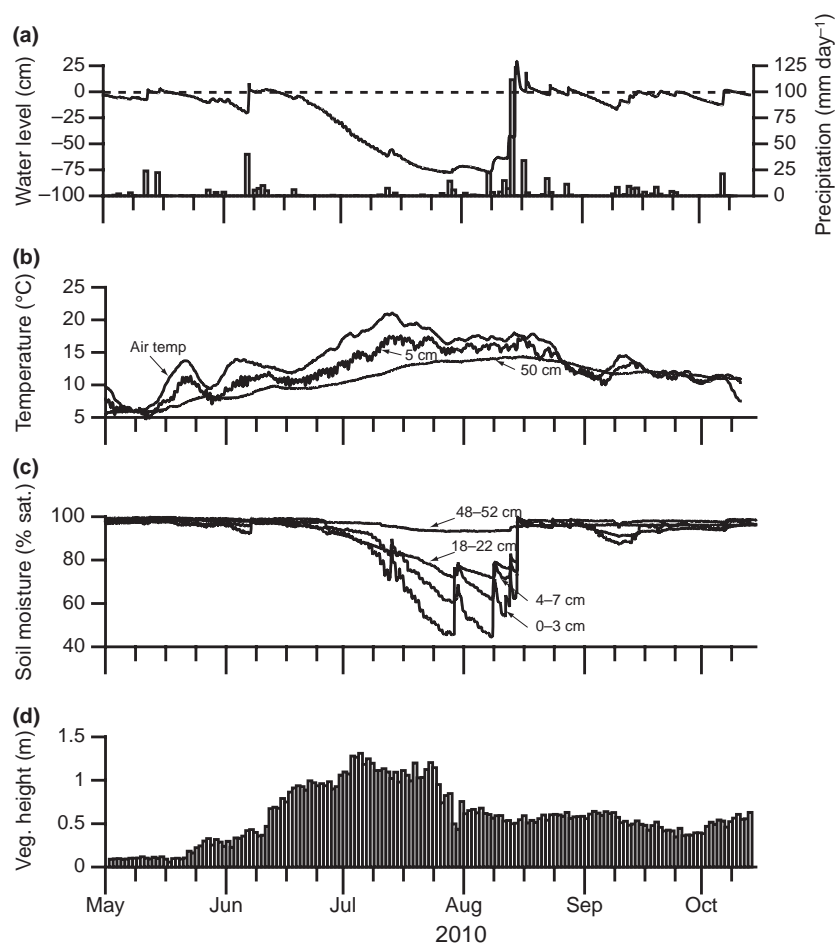


**Fig. 1** Overview of environmental parameters and vegetation height at the Maglemosen field site (from 1 May 2010 to 10 October 2010). (a) Water level (line) and daily precipitation (bars). (b) Seven day moving average air temperature, soil temperature 5 cm and soil temperature 50 cm. (c) Soil moisture content in per cent saturation degrees in 0–3, 4–7, 18–22 and 48–52 cm. (d) Average daily vegetation height (m).

from 45% to 70% within a few hours after rainfall (Fig. 1c).

#### Vegetation height

The daily average height of *P. arundinacea* at the field site in 2010 varied from ca. 0.1–0.2 m prior to the growing season to a seasonal maximum of 1.2–1.5 m in the beginning of July after onset of flowering in mid-June (Fig. 1d). Mid-summer dormancy was observed by the end of July. After this time, the stems lodged and grew more parallel to the ground before beginning of the second growth peak in late August.

#### Subsurface O<sub>2</sub> concentrations

Subsurface O<sub>2</sub> concentrations ranged from fully oxygenated conditions in the surface layers to completely O<sub>2</sub>-depleted conditions below 40 cm. Shorter periods of anoxic conditions in the upper 5–10 cm were only

observed in the hours following increases in the WL to a position at or above the peat surface. When the position of the WL was in the range of 0–50 cm below the surface, the transition between fully oxygenated and anoxic conditions was observed to take place over smaller distances than the depth interval of the buried optodes, i.e. <5 cm. At times when the WL was below ca. 60 cm, a zone of gradual transition between oxic and anoxic conditions was observed over a depth of 10–15 cm (see Figs 2a and 3d).

In the period of lowest WL, the zone of complete oxygenation extended to a depth of 20–30 cm below the surface corresponding to the lower boundary of the root zone, while the lower soil depths remained O<sub>2</sub> depleted or fully anoxic.

#### Subsurface mineral-N concentrations

Soil sample concentrations of water extractable NO<sub>3</sub><sup>-</sup> were in the range of 0–10 mg kg<sup>-1</sup> NO<sub>3</sub><sup>-</sup>-N with only a



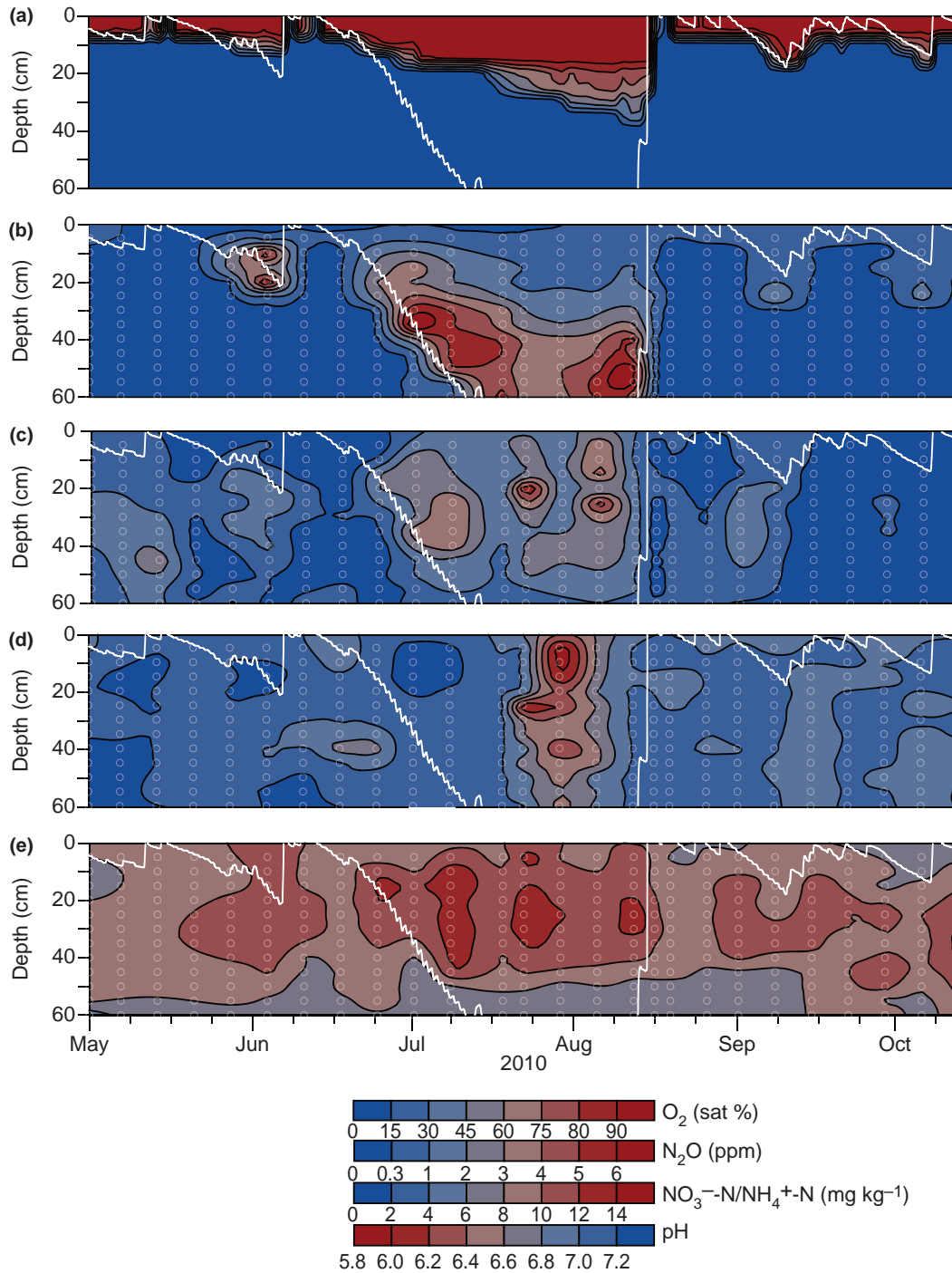


**Fig. 2** Overview of subsurface parameters in response to variations in the position of the water level (WL) over the growing season of 2010. Contour plots of (a) oxygen concentration (atmospheric saturation%), (b)  $N_2O$  concentrations (ppm), (c)  $NO_3^-$  concentrations ( $mg\ NO_3^-N\ kg^{-1}$ ), (d)  $NH_4^+$  concentrations ( $mg\ NH_4^+-N\ kg^{-1}$ ) and (e) pH. The position of the WL is shown by a white line in all contour plots. Open white circles in (b) to (e) show depth and time of individual sample profiles.

few samples above  $10\ mg\ kg^{-1}$ . The lowest  $NO_3^-$  concentrations were measured in periods where the WL was near the surface, whereas increasing  $NO_3^-$  concentrations were observed in periods following decreasing

WL depths (Fig. 2c). Rapid decreases in  $NO_3^-$  concentrations were observed in the samples obtained immediately after the events of rapidly increasing WL and decreasing  $O_2$  availability (Figs 1a and 2a). The highest

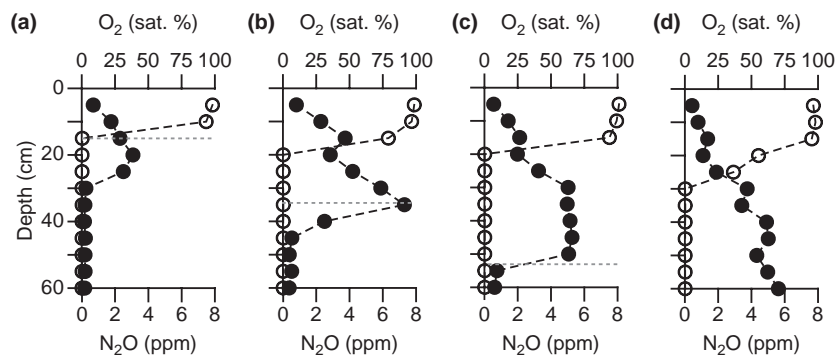


**Fig. 3** Profiles of N<sub>2</sub>O and O<sub>2</sub> concentrations during a period of falling water level (WL) with profiles from (a) 25 June 2010 (WL = 15 cm), (b) 2 July 2010 (WL = 35 cm), (c) 9 July 2010 (WL = 53 cm), (d) 19 July 2010 (WL = 69 cm). Open circles show O<sub>2</sub> concentrations (atm. sat%) and filled circles show N<sub>2</sub>O concentrations (ppm). The position of the WL is shown by horizontal dashed lines.

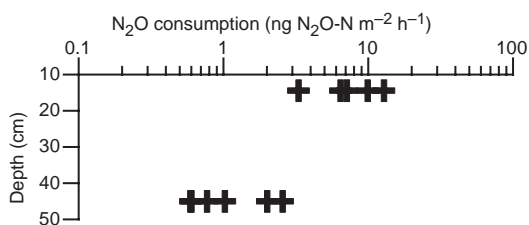


**Fig. 4** Potential N<sub>2</sub>O consumption rates within the main root zone (10–20 cm) and below the root zone (40–50 cm).

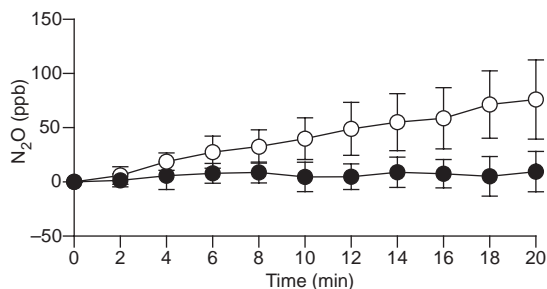


**Fig. 5** Plant-mediated N<sub>2</sub>O emissions. Normalized average headspace increase of N<sub>2</sub>O in single straws of *Phalaris arundinacea* in illuminated (open circles;  $n = 11$ ) and dark conditions (closed circles,  $n = 5$ ) over 20 min with standard deviations shown by vertical error bars.

NO<sub>3</sub><sup>-</sup> concentrations were measured at depth of 20–30 cm in late July and early August corresponding to the time of lowest WL and maximum O<sub>2</sub> penetration depth (Fig. 2a). Total nitrite (NO<sub>2</sub><sup>-</sup>) concentrations were at all times below the detection limit.

Soil sample concentrations of extractable NH<sub>4</sub><sup>+</sup> were in the range of a few mg NH<sub>4</sub><sup>+</sup>-N kg<sup>-1</sup> over the entire soil profile throughout the growing season, with the exception of elevated concentrations in the upper 30 cm in the last weeks of July 2010 (Fig. 2d) where the WL was at its lowest.

### Soil pH

Measured *in situ* values of soil pH were in the lower neutral range (6.0–6.5) throughout the measurement period with variations <1.5 pH unit between minimum and maximum observations (Fig. 2e). Highest pH values in the top 20–40 cm of the soil profile were observed at times of high WL positions as well as following rapid rising WL events. Lowest pH values were observed during the periods of decreasing and low WL in combination with fully oxygenated soil conditions in the top soil.

### Subsurface N<sub>2</sub>O concentrations

Increasing N<sub>2</sub>O concentrations at progressively lower depths were observed over time in periods of falling WL (Fig. 2b). Maximum N<sub>2</sub>O concentrations were observed in both the first week of June/July and the beginning of August at soil depths immediately below the depth of maximum O<sub>2</sub> penetration (see also Fig. 3). Peak N<sub>2</sub>O concentrations in the individual profiles were found either at the depth of the WL, when this was near the surface, or in a zone at the capillary fringe ca. 0–25 cm above the position of the WL when located at depths below 40–50 cm (see example in Fig. 3c and d).

The depth interval of maximum subsurface N<sub>2</sub>O concentrations (Fig. 2b) was located at the capillary fringe with mixed aerobic and anaerobic soil conditions between the lower extent of the oxidized soil layers (Fig. 2a) and the position of the WL (Fig. 1a). Sharp decreases in subsurface N<sub>2</sub>O concentrations were observed following the rapid WL increases in early June and mid-August when the soil profile was re-saturated. In the periods dominated by high WL, subsurface N<sub>2</sub>O concentrations were low-to-sub-ambient over the entire soil profile.

### Potential N<sub>2</sub>O consumption capacity

Significant N<sub>2</sub>O consumption capacities were found in the investigated soil profile (Fig. 4). Average potential N<sub>2</sub>O consumption capacities for the soil layers from the main root zone (10–20 cm) were ca. 5–6 times greater than the average potential N<sub>2</sub>O consumption capacities from soil layers below the main root zone (40–50 cm).

### N<sub>2</sub>O emissions from *P. arundinacea*

Significant increases ( $P < 0.05$ ) in average headspace N<sub>2</sub>O concentrations were observed in all of the illuminated measurements (PAR = 300–400 W m<sup>-2</sup>) when the soil flux contribution was excluded (Fig. 5). In simulated darkness (PAR = 0 W m<sup>-2</sup>), the changes in headspace concentrations were markedly lower with average headspace concentrations being nonsignificantly different from the ambient concentrations.

### Spatio-temporal flux dynamics of N<sub>2</sub>O and CO<sub>2</sub>

Seasonal N<sub>2</sub>O and CO<sub>2</sub> flux levels across the soil–atmosphere interface were characterized by both large temporal and spatial variations in flux magnitude and flux direction (Fig. 6a and b). The temporal pattern in the CO<sub>2</sub> flux dynamics showed a significant correlation ( $P < 0.01$ ) with incoming PAR in response to photosynthesis and soil respiration, with maximum negative fluxes during the day (C-uptake) and positive fluxes during the night (C-release). The CO<sub>2</sub> fluxes were related to seasonal variations in plant growth and WL changes, with decreasing positive fluxes when the position of the WL was near surface (Fig. 6b).

Negative CO<sub>2</sub> fluxes were observed when PAR was above 10–30 W m<sup>-2</sup> and positive fluxes below.

The magnitudes of both the hourly negative and positive CO<sub>2</sub> fluxes differed in response to seasonal differences in soil moisture and soil temperature for microbial respiration, as well as growth stage of the vegetation for photosynthetic CO<sub>2</sub> assimilation (see also Fig. 1b–d).

The N<sub>2</sub>O fluxes were generally characterized by positive N<sub>2</sub>O fluxes lower than 25 µg N<sub>2</sub>O–N m<sup>-2</sup> h<sup>-1</sup> during periods with near-surface WL. The magnitudes of the N<sub>2</sub>O fluxes were measured to increase in response to a falling WL (Fig. 6a). When the position of the WL was below 50 cm, a period with significant negative fluxes (N<sub>2</sub>O uptake) was observed (Fig. 6a) with pronounced diurnal flux dynamics (Fig. 8a). This period ended with a dramatic increase in WL following a very high precipitation event (>40 mm day<sup>-1</sup>).

Examples of the large temporal and spatial variations in flux dynamics are shown in Figs 7 and 8, where the measured hourly fluxes of both N<sub>2</sub>O and CO<sub>2</sub> over 20 days from all the five flux chambers are shown, together with the synchronous variations in the position of the WL, incoming PAR and top soil (2 cm) and air temperature (2 m), for a period with the WL located at depths between 0 and 20 cm (Period 1) (Fig. 7a and b) and below 50 cm (Period 2) (Fig. 8a and b). Substantial differences in the temporal flux dynamics of N<sub>2</sub>O exist between the two periods. During “Period 1”, positive N<sub>2</sub>O fluxes dominated with fluxes between 50 and 150 µg N<sub>2</sub>O–N m<sup>-2</sup> h<sup>-1</sup> emitted primarily during the illuminated hours (PAR > 0 W m<sup>-2</sup>). At the end of “Period 1” when the WL was at its relative lowest (ca. 20 cm), positive N<sub>2</sub>O fluxes were measured during the dark hours (PAR ≈ 0 W m<sup>-2</sup>) with one of the five chambers showing five to eight times higher flux values than the rest. Both positive and negative N<sub>2</sub>O fluxes were below the detection limit at the end of “Period 1”

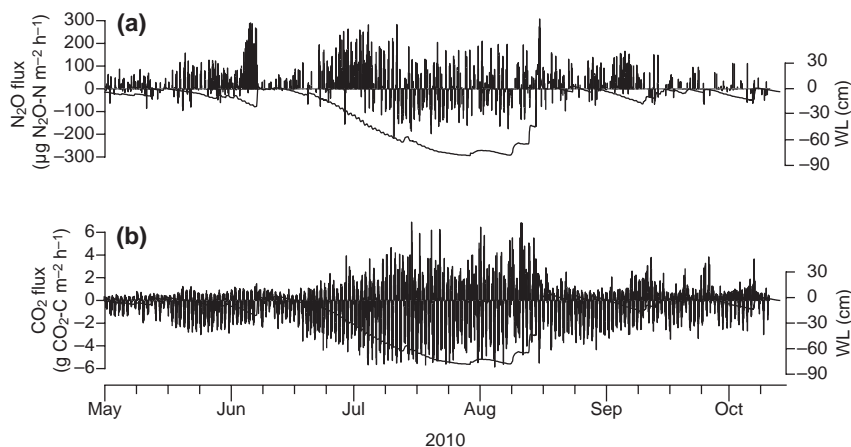
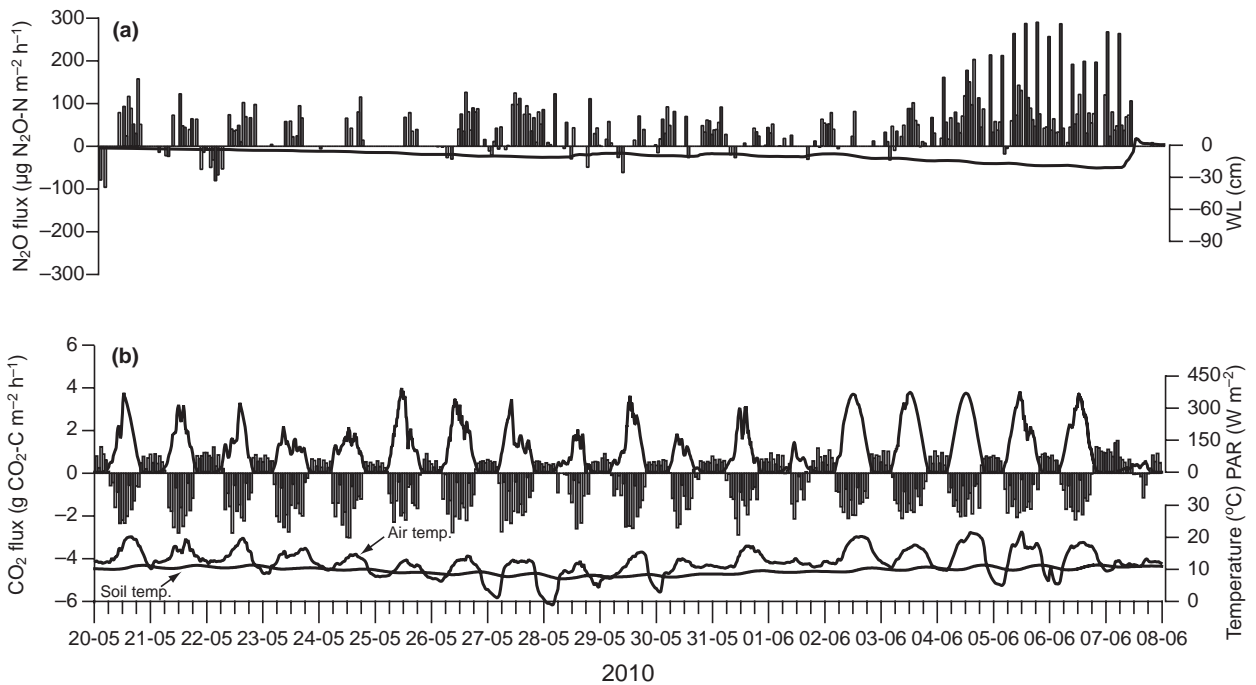
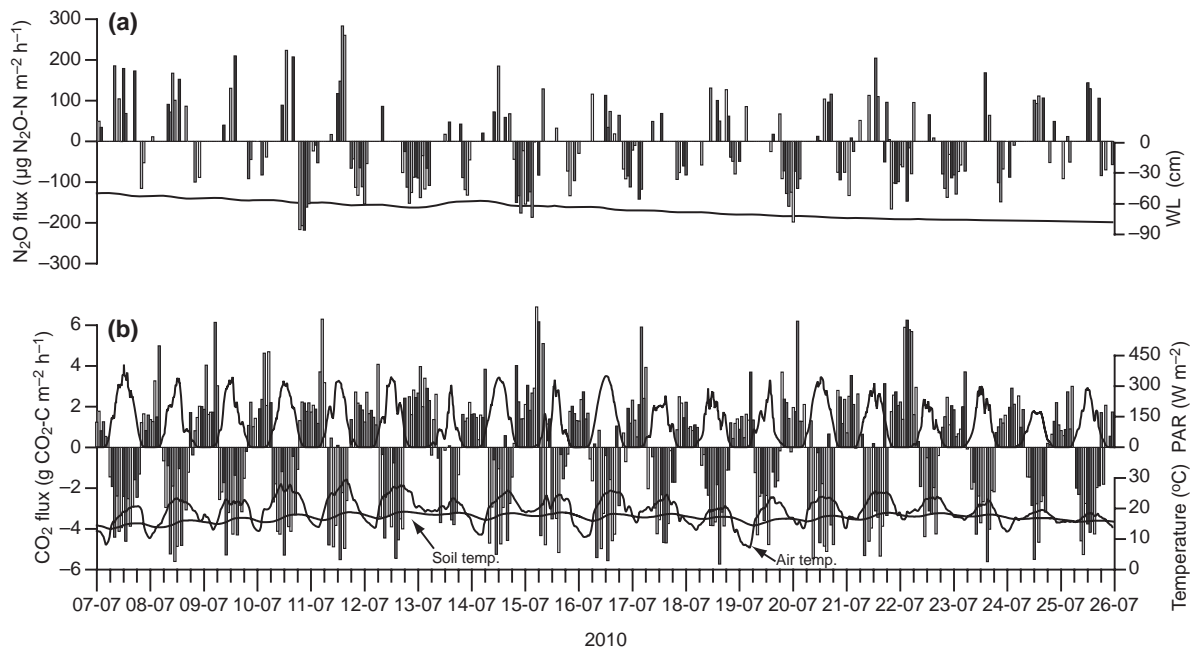


Fig. 6 Significant fluxes ( $P < 0.05$ ) of (a) N<sub>2</sub>O and (b) CO<sub>2</sub> in response to variations in the position of the water level (WL; line) over the growing season of 2010 displayed as individual hourly measurements.



**Fig. 7** Spatio-temporal hourly trends in (a) N<sub>2</sub>O and (b) CO<sub>2</sub> fluxes for each of the five automated flux chamber in “Period 1”. Fluxes from the five chamber replicates are shown by bars of different shades of grey. The individual flux measurements are shown together with the synchronous variations in the position of the (a) water level (WL), (b) incoming photosynthetically active radiation (PAR) and soil (2 cm) and air temperatures (2 m).



**Fig. 8** Spatio-temporal hourly trends in (a) N<sub>2</sub>O and (b) CO<sub>2</sub> fluxes for each of the five automated flux chamber in “Period 2”. Fluxes from the five chamber replicates are shown by bars of different shades of grey. The individual flux measurements are shown together with the synchronous variations in the position of the (a) water level (WL), (b) incoming photosynthetically active radiation (PAR) and soil (2 cm) and air temperatures (2 m).



when the WL increased to a position above the terrain due to a high precipitation event (>40 mm daily precipitation; see Fig. 1a).

In "Period 2", N<sub>2</sub>O fluxes of opposing direction were measured during the illuminated and dark hours. Measured positive fluxes in the illuminated hours were in the same order of magnitude as in "Period 1" (Fig. 7a). Negative N<sub>2</sub>O fluxes in the dark hours of "Period 2" were in the order of 50–200 N<sub>2</sub>O–N m<sup>-2</sup> h<sup>-1</sup>, when the activity was at its highest (Fig. 8a).

## Discussion

### *Temporal dynamics of gas fluxes*

Fluctuating flux gradients between the soil and the atmosphere produce variations in short-term net surface exchange patterns. Subsoil net N<sub>2</sub>O concentrations at any given time are the result of the net balance between production and consumption rates over a certain volume in combination with changes in effective diffusivity. Small changes in the relative magnitude of these process rates may result in short-term concentration variations and fluctuating flux gradients across the soil–atmosphere interface producing irregular flux patterns. In the current study, high temporal variations in N<sub>2</sub>O fluxes were observed both on a daily to weekly time scale and over the entire growing season of 2010. On the basis of characteristic diurnal variations in N<sub>2</sub>O fluxes, a number of distinctive overall flux periods can be identified where: (i) positive surface fluxes dominated during the illuminated hours (Fig. 7a, "Period 1") and (ii) a much stronger diurnal flux dynamics dominated with positive N<sub>2</sub>O fluxes during the illuminated hours and consistent negative N<sub>2</sub>O fluxes during the dark hours (Fig. 8a, "Period 2").

Emission patterns similar to "Period 1" were observed in the middle of May, end of June/beginning of July and beginning of September 2010. Common characteristics for these periods were gradually decreasing WL to a depth of ca. 35 cm below the surface over 2–3 weeks due to evapotranspiration, little precipitation (Fig. 1a), near-saturated soil water conditions in the top soil (Fig. 1c) and maximum O<sub>2</sub> penetration depths of 10–15 cm (Fig. 2a).

The amplitude of the diurnal variation of both PAR, soil and air temperature were similar at ca. 5 °C in both "Period 1" and "Period 2", but the average level of the soil temperature in the upper 5 cm were 6–8 °C higher in "Period 2" (Fig. 8b) than in "Period 1" (Fig. 7b). This difference has probably affected the conditions and activity rates of both nitrification and denitrification processes in the soil profile (Maag & Vinther, 1996) and thereby the net N<sub>2</sub>O emissions (Blackmer *et al.*, 1982;

Dinsmore *et al.*, 2009). The balance between nitrification and denitrification rates responds differently to identical changes in average daily temperature and therefore even though the daily amplitudes in temperature were similar in "Period 1" and "Period 2", the resulting net balance between N<sub>2</sub>O production and consumption could provide contrasting net surface fluxes. Changes in the degree of water saturation added to the complexity as the degree of soil water saturation in the top soil between "Period 1" and "Period 2" differed by up to 40–50% (Fig. 1c), which influenced the balance in N<sub>2</sub>O production and consumption rates and the diffusive resistance of gasses across the soil–atmosphere interface.

Another key difference between the dominating flux periods was the relative depth of maximum N<sub>2</sub>O concentrations below surface terrain. In the growing season of 2010, peak concentrations of N<sub>2</sub>O were observed within the main root zone when the flux dynamics approximated that observed during "Period 1" (Figs 2b and 3a). In periods of flux dynamics similar to "Period 2", the subsurface concentration peaks of N<sub>2</sub>O were observed at soil depths below the main root zone (Fig. 3c and d).

In previous papers from the same *P. arundinacea* dominated wetland (Askaer *et al.*, 2011; Elberling *et al.*, 2011), it was concluded that the primary gas transport mechanism across the soil–atmosphere interface of methane (CH<sub>4</sub>) was diffusive transport via both the soil matrix and through aerenchymous tissue in *P. arundinacea*. It was observed that extended periods of CH<sub>4</sub> emissions only occurred when the gas was present in the root zone and absent when CH<sub>4</sub> concentration peaks were located below 30–40 cm below the surface. This suggested a substantial CH<sub>4</sub> oxidation capacity by microorganisms within the rhizosphere. The main role of the vegetation for greenhouse gas transport was therefore to serve as a passive conduit for increased gas exchange between the soil/rhizosphere and the atmosphere (Mosier *et al.*, 1990; Rusch & Rennenberg, 1998).

### *N<sub>2</sub>O sink activity*

The conditions promoting N<sub>2</sub>O consumption in the soil and the environmental drivers for N<sub>2</sub>O deposition from the atmosphere to the soil are yet to be consistently identified. Denitrification is considered the most important process for N<sub>2</sub>O uptake, while the roles of NO<sub>3</sub><sup>-</sup> availability, soil pH, temperature and water content as well as O<sub>2</sub> pressure are much less clear (Chapuis-Lardy *et al.*, 2007). Potential N<sub>2</sub>O consumption rates in both the main root zone (10–20 cm below the surface) and below the root zone (40–50 cm) were estimated by incubation experiments using site- and

depth-specific soil samples. The range in potential N<sub>2</sub>O consumption rates in the main root zone between 3 and 15 ng N<sub>2</sub>O–N cm<sup>-3</sup> h<sup>-1</sup> (Fig. 4) is unlikely to reflect *in situ* N<sub>2</sub>O consumption rates, but, nevertheless, shows a substantial inherent N<sub>2</sub>O consumption capacity in site-specific soil samples. For example, a peat volume of 0.025 m<sup>3</sup> (corresponding to a depth of 25 mm over a 1 m<sup>-2</sup> area) would be sufficient to produce an hourly negative N<sub>2</sub>O flux of 200 µg N<sub>2</sub>O–N m<sup>-2</sup> h<sup>-1</sup> assuming an average N<sub>2</sub>O consumption capacity of 8 ng N<sub>2</sub>O–N cm<sup>-3</sup> h<sup>-1</sup>.

The marked diurnal flux direction shifts observed under conditions similar to “Period 2” are most likely linked to nonlinear variations in N<sub>2</sub>O production and consumption rates within the root zone, responding to rapid changes in subsurface O<sub>2</sub> and NO<sub>3</sub><sup>-</sup> availability dynamics related to diurnal variations in plant release of O<sub>2</sub> in the rhizosphere (Bollmann & Conrad, 1998; Khalil *et al.*, 2004). This will affect microbial N-transformation processes and plant uptake and reallocation of mineral-N in the rhizosphere. A sampling frequency on a higher spatial and temporal resolution would be needed to elucidate the processes and drivers of simultaneous N<sub>2</sub>O production and consumption on a microscale within the rhizosphere, as well as the short-term effect of resource competition between vegetation and soil microbes in response to light-driven changes in O<sub>2</sub> availability.

While speculative, we hypothesize that the combined effect in the top soil of seasonally high soil temperatures, nonlimited O<sub>2</sub> availability, intermediate water saturation degrees and high mineral-N availability could produce conditions where the rates of N<sub>2</sub>O consumption exceed the N<sub>2</sub>O production rates, producing negative flux gradients across the soil–atmosphere interface. According to the measured potential N<sub>2</sub>O consumption capacities (Fig. 4), the net N<sub>2</sub>O sink effect would be largest in the top soil and rhizosphere through which all N<sub>2</sub>O produced at deeper soil depths will have to pass before being emitted, unless gas transport through plants occurs.

#### *Plant transport of N<sub>2</sub>O and O<sub>2</sub>*

Plant-driven subsoil aeration (Brix *et al.*, 1994; Colmer, 2003) has been suggested to modify field scale N-cycling processes and potentially the production, consumption and emissions of N<sub>2</sub>O in wetlands, where N-transformation processes in the root zone will be influenced by O<sub>2</sub> entering the soil via aerenchymous plant tissue (Reddy *et al.*, 1989; Rückauf *et al.*, 2004; Hyvoenen *et al.*, 2009). Significant correlations ( $P < 0.001$ ) between O<sub>2</sub> concentration in the root zone and diurnal variations in incoming PAR were observed throughout the growing season in soil layers above the WL as a

result of plant-transported O<sub>2</sub> into the soil (see example in Fig. S4). In this context, plant-driven subsoil aeration appears to provide the capacity for keeping parts of the root zone oxidized despite a high WL, where the soil in the absence of roots will quickly become anaerobic as observed in the nonsaturated but anoxic soil layers below the root zone (Fig. 2a).

Field measurements of N<sub>2</sub>O using a plant-only microchamber (Fig. 5) show N<sub>2</sub>O emissions ( $P < 0.05$ ) to the atmosphere directly through the vegetation canopy of *P. arundinacea* when the vegetation is exposed to sunlight. Under conditions of simulated darkness, the absence of significant increases in headspace N<sub>2</sub>O concentrations suggests a light-dependent plant internal gas transport mechanism or possible light-dependent plant internal N<sub>2</sub>O production as hypothesized in the study of Yu & Chen (2009). While these measurements are unlikely to reflect net *in situ* fluxes from the ecosystem due to the exclusion of soil emitted fluxes, data indicate that the inclusion of the vegetation in the flux chambers are essential for achieving the most accurate N<sub>2</sub>O flux estimates on both a diurnal and seasonal time scale.

Previous studies on other vegetation types have shown that N<sub>2</sub>O can be transported from the soil to the atmosphere by plants via internal gas transport of gas venting macrophytes (Reddy *et al.*, 1989) or as dissolved gas via the transpiration stream (Chang *et al.*, 1998), and that changes in illumination could affect N<sub>2</sub>O emissions (Yu & Chen, 2009). The plant transport pathway appears to be especially relevant when soil moisture contents in the top soil are high and the formation of discontinuous pore spaces and restricted diffusive exchange promotes entrapment of N<sub>2</sub>O, longer residence time and higher potential for full reduction to N<sub>2</sub> (Heincke & Kaupenjohann, 1999).

We conclude that *P. arundinacea* has the ability to facilitate N<sub>2</sub>O transport from the root zone to the atmosphere and thereby effectively bypassing the soil characterized by lower diffusion rates. At present, the mechanism by which this N<sub>2</sub>O transport occurs remains to be determined. Additional experiments are needed to determine the quantitative importance of the plant transport as well as the actual transport mechanisms, potential transport drivers and seasonal timing. Adding to the complexity, N<sub>2</sub>O production during N-assimilation within the above-ground biomass of certain higher plants has been hypothesized (Yu & Chen, 2009). The potential ramifications of this leaf internal N<sub>2</sub>O production or consumption in *P. arundinacea* could be a parallel N<sub>2</sub>O source and sink system detached from the soil and belowground biomass, modifying the net N<sub>2</sub>O fluxes from this type of wetland ecosystem.

Results presented here emphasize the importance of including the vegetation itself in the flux chambers

when measuring the seasonal flux dynamics pattern from ecosystems with subsurface aeration macrophytes such as *P. arundinacea*. This leads to a key conclusion that exclusion of the aboveground biomass in flux chamber measurements may lead to significant underestimations of net N<sub>2</sub>O fluxes.

#### *Potential N<sub>2</sub>O emission feedbacks to global warming*

Near-continuous measurement of N<sub>2</sub>O fluxes over the growing season of 2010 showed high temporal variability with significant changes in flux magnitudes and shifts in flux directions within hours. Periods characterized by N<sub>2</sub>O emissions during the illuminated hours of the day were associated with the presence of N<sub>2</sub>O in the upper 35 cm, which corresponded to the vertical extent of the main root zone. Maximum concentrations of subsurface N<sub>2</sub>O were observed within the root zone in all periods with positive fluxes, while maximum concentrations of subsurface N<sub>2</sub>O were located at depth below the main root zone in the nocturnal negative flux periods. The significant relationship between diurnal variations in O<sub>2</sub> concentrations and incoming solar radiation in the PAR spectrum highlights the importance of plant-driven oxygenation of the rhizosphere and the associated controls on coupled nitrification/denitrification processes.

Incubation experiments of potential N<sub>2</sub>O consumption capacities demonstrated a significant N<sub>2</sub>O consumption potential both in and below the root zone, indicating that the net N<sub>2</sub>O surface flux may be subject to rapid shifts in rates and direction on a short time scale, according to the relative balance between simultaneously acting N<sub>2</sub>O production and consumption processes.

Weekly concentration profiles showed that subsurface build up of N<sub>2</sub>O was directly linked to changes in the position of the WL and thereby soil moisture content and associated O<sub>2</sub> availability at the capillary fringe. The observed peak N<sub>2</sub>O concentrations at the capillary fringe are consistent with optimal conditions for N<sub>2</sub>O production as measured water saturation degrees are in the critical range between 60% and 85% (Davidson, 1991; Skiba & Smith, 2000) and a supply of NO<sub>3</sub><sup>-</sup> was readily available by diffusive transport from oxidized soil layers above (Regina *et al.*, 1996). In combination with plant-transported O<sub>2</sub> into the root zone, the extent and duration of soil oxygenation influenced N-transformation as measured in increasing concentrations of extractable NO<sub>3</sub><sup>-</sup> and NH<sub>4</sub><sup>+</sup> after prolonged periods of oxic soil conditions in the root zone.

A comparison between depth and duration of O<sub>2</sub>-penetration and mineral-N availability documents that prolonged soil oxygenation was needed for increasing concentrations of NO<sub>3</sub><sup>-</sup> by N-mineralization processes

during a dry summer period. It can be concluded that the complex interactions between O<sub>2</sub> and mineral-N availability following near-surface WL fluctuations and plant growth of *P. arundinacea* controlled the observed subsurface N<sub>2</sub>O concentrations and gas transport mechanisms responsible for N<sub>2</sub>O fluxes across the soil-atmosphere interface.

While periods of different temporal N<sub>2</sub>O flux dynamics were distinguished by the seasonal position of the WL, this driver could not explain the contrasting flux dynamics on a diurnal to weekly time scale indicating that the linkages between subsurface N<sub>2</sub>O concentration and surface flux dynamics are more complicated. Future research in the dynamics of N-transformation processes in both plant internals and the root zone of subsurface aerating macrophytes such as *P. arundinacea* is needed to address the knowledge gap between the controls on subsurface N<sub>2</sub>O production/consumption and net surface emissions. The results presented in this work emphasize the risk of substantial underestimations of net N<sub>2</sub>O fluxes from wetland ecosystems if the sampling frequency is too low, or if the plant-transported N<sub>2</sub>O contribution is omitted, and stress the importance for high temporal resolution flux measurements in future investigations.

While N<sub>2</sub>O is predominantly formed via denitrification of NO<sub>3</sub><sup>-</sup>, which net availability may depend on O<sub>2</sub>-limited nitrification and dissimilatory NO<sub>3</sub><sup>-</sup> reduction to NH<sub>4</sub><sup>+</sup> (DNRA), future changes in the seasonal WL dynamics with longer periods of drought may produce longer periods of oxidized soil conditions during the summer months. This could influence the rates of N-transformation and NO<sub>3</sub><sup>-</sup> availability, with the potential result of greater subsoil production rates of N<sub>2</sub>O. On the other hand, improved conditions for plant growth and microbial respiration under warmer and more nutrient-rich conditions as well as elevated ambient CO<sub>2</sub> pressure may counterbalance the accelerated N-mineralization rate by increased resource competition for mineral-N between plants and soil microbes or increased rates of DNRA, increasing the current net N<sub>2</sub>O sink capacity when N availability is limited.

#### **Acknowledgements**

This work was conducted within the framework of the projects "Oxygen availability controlling the dynamics of buried organic carbon pools and greenhouse gas emissions" and "Nitrous oxide dynamics: The missing links between controls on subsurface N<sub>2</sub>O production/consumption and net atmospheric emissions" financed by the Danish Natural Science Research Council (PI: B. E.). The authors thank Paul Christiansen and Rune Skalborg for help with fieldwork, Bo Holm-Rasmussen for technical support and programming assistance, Per Ambus (Risø DTU) for help with GC analyses, the Geological Survey of Denmark and Greenland for C & N analyses, and Joshua Schimel (Univer-

city of California, Santa Barbara, USA), Tim Clough (Lincoln University, New Zealand) and three anonymous journal referees for many helpful comments and discussions.

## References

- Ambus P, Robertson GP (1998) Automated near-continuous measurement of carbon dioxide and nitrous oxide fluxes from soil. *Soil Science Society of America Journal*, **62**, 394–400.
- Askaer L, Elberling B, Glud RN, Kuhl M, Lauritsen FR, Joensen HP (2010) Soil heterogeneity effects on O<sub>2</sub> distribution and CH<sub>4</sub> emissions from wetlands: in situ and mesocosm studies with planar O<sub>2</sub> optodes and membrane inlet mass spectrometry. *Soil Biology and Biochemistry*, **42**, 2254–2265.
- Askaer L, Elberling B, Friberg T, Jørgensen CJ, Hansen B (2011) Plant-mediated CH<sub>4</sub> transport and C gas dynamics quantified in-situ in a *Phalaris arundinacea* dominant wetland. *Plant and Soil*, **343**, 287–301.
- Blackmer AM, Robbins SG, Bremner JM (1982) Diurnal variability in rate of emission of nitrous-oxide from soils. *Soil Science Society of America Journal*, **46**, 937–942.
- Bollmann A, Conrad R (1998) Influence of O<sub>2</sub> availability on NO and N<sub>2</sub>O release by nitrification and denitrification in soils. *Global Change Biology*, **4**, 387–396.
- Brix H, Lorenzen B, Morris JT, Schierup HH, Sorrell BK (1994) Effects of oxygen and nitrate on ammonium uptake kinetics and adenylate pools in *Phalaris arundinacea* L and *Glyceria maxima* (Hartm) Holmb. *Proceedings of the Royal Society of Edinburgh Section B-Biological Sciences*, **102**, 333–342.
- Chang C, Janzen HH, Cho CM, Nakonechny EM (1998) Nitrous oxide emission through plants. *Soil Science Society of America Journal*, **62**, 35–38.
- Chapuis-Lardy L, Wrage N, Metay A, Chotte JL, Bernoux M (2007) Soils, a sink for N<sub>2</sub>O? A review. *Global Change Biology*, **13**, 1–17.
- Clough TJ, Sherlock RR, Rolston DE (2005) A review of the movement and fate of N<sub>2</sub>O in the subsoil. *Nutrient Cycling in Agroecosystems*, **72**, 3–11.
- Colmer TD (2003) Long-distance transport of gases in plants: a perspective on internal aeration and radial oxygen loss from roots. *Plant, Cell and Environment*, **26**, 17–36.
- Davidson EA (1991) Fluxes of nitrous oxide and nitric oxide from terrestrial ecosystems. In: *Microbial Production and Consumption of Greenhouse Gases: Methane, Nitrogen Oxides, and Halomethanes* (eds Rogers JE, Whitman WB), pp. 219–235. American Society of Microbiology, Washington, DC.
- Dinsmore KJ, Skiba UM, Billett MF, Rees RM (2009) Effect of water table on greenhouse gas emissions from peatland mesocosms. *Plant and Soil*, **318**, 229–242.
- Elberling B, Askaer L, Jørgensen CJ, Kuhl M, Glud RN, Lauritsen FR (2011) Linking soil O<sub>2</sub>, CO<sub>2</sub>, and CH<sub>4</sub> concentrations in a wetland soil: implications for CO<sub>2</sub> and CH<sub>4</sub> fluxes. *Environmental Science & Technology*, **45**, 3393–3399.
- Firestone MK, Davidson EA (1989) Microbiological basis of NO and N<sub>2</sub>O production and consumption in soil. *Exchange of Trace Gases Between Terrestrial Ecosystems and the Atmosphere*, **47**, 7–21.
- Flecharl CR, Neftel A, Jocher M, Ammann C, Fuhrer J (2005) Bi-directional soil/atmosphere N<sub>2</sub>O exchange over two mown grassland systems with contrasting management practices. *Global Change Biology*, **11**, 2114–2127.
- Heincke M, Kaupenjohann M (1999) Effects of soil solution on the dynamics of N<sub>2</sub>O emissions: a review. *Nutrient Cycling in Agroecosystems*, **55**, 133–157.
- Hyyonen NP, Huttunen JT, Shurpali NJ, Tavi NM, Repo ME, Martikainen PJ (2009) Fluxes of nitrous oxide and methane on an abandoned peat extraction site: effect of reed canary grass cultivation. *Bioresource Technology*, **100**, 4723–4730.
- IPCC (2007) The physical science basis. In: *Contribution of Working Group I to the Fourth Assessment Report of the Intergovernmental Panel on Climate Change* (eds Solomon S, Qin D, Manning M, Chen Z, Marquis KB, Tignor M, Miller HL). Cambridge University Press, Cambridge.
- Jacinto PA, Dick WA (1996) Use of silicone tubing to sample nitrous oxide in the soil atmosphere. *Soil Biology and Biochemistry*, **28**, 721–726.
- Jin T, Shimizu M, Marutani S, Desyatkin AR, Iizuka N, Hata H, Hatano R (2010) Effect of chemical fertilizer and manure application on N<sub>2</sub>O emission from reed canary grassland in Hokkaido, Japan. *Soil Science and Plant Nutrition*, **56**, 53–65.
- Kammann C, Grünhage L, Jäger HJ (2001) A new sampling technique to monitor concentrations of CH<sub>4</sub>, N<sub>2</sub>O and CO<sub>2</sub> in air at well-defined depths in soils with varied water potential. *European Journal of Soil Science*, **52**, 297–303.
- Khalil K, Mary B, Renault P (2004) Nitrous oxide production by nitrification and denitrification in soil aggregates as affected by O<sub>2</sub> concentrations. *Soil Biology and Biochemistry*, **36**, 687–699.
- Liikanen A, Martikainen PJ (2003) Effect of ammonium and oxygen on methane and nitrous oxide fluxes across sediment-water interface in a eutrophic lake. *Chemosphere*, **52**, 1287–1293.
- Maag M, Vinther FP (1996) Nitrous oxide emission by nitrification and denitrification in different soil types and at different soil moisture contents and temperatures. *Applied Soil Ecology*, **4**, 5–14.
- Mosier AR, Mohanty SK, Bhadrachalam A, Chakravorti SP (1990) Evolution of di-nitrogen and nitrous-oxide from the soil to the atmosphere through rice plants. *Biology and Fertility of Soils*, **9**, 61–67.
- Patrick WH, Reddy KR (1976) Nitrification-denitrification reactions in flooded soils and water bottoms – dependence on oxygen-supply and ammonium diffusion. *Journal of Environmental Quality*, **5**, 469–472.
- Redding TE, Devito KJ (2006) Particle densities of wetland soils in northern Alberta, Canada. *Canadian Journal of Soil Science*, **86**, 57–60.
- Reddy KR, Patrick WH, Lindau CW (1989) Nitrification-denitrification at the plant root-sediment interface in wetlands. *Limnology and Oceanography*, **34**, 1004–1013.
- Regina K, Nykanen H, Silvola J, Martikainen PJ (1996) Fluxes of nitrous oxide from boreal peatlands as affected by peatland type, water table level and nitrification capacity. *Biogeochemistry*, **35**, 401–418.
- Rückauf U, Augustin J, Russow R, Merbach W (2004) Nitrate removal from drained and reflooded fen soils affected by soil N transformation processes and plant uptake. *Soil Biology and Biochemistry*, **36**, 77–90.
- Rusch H, Rennenberg H (1998) Black alder (*Alnus glutinosa* (L.) Gaertn.) trees mediate methane and nitrous oxide emission from the soil to the atmosphere. *Plant and Soil*, **201**, 1–7.
- Skiba U, Smith KA (2000) The control of nitrous oxide emissions from agricultural and natural soils. *Chemosphere – Global Change Science*, **2**, 379–386.
- Smith CJ, Patrick WH Jr (1983) Nitrous oxide emission as affected by alternate anaerobic and aerobic conditions from soil suspension enriched with ammonium sulfate. *Soil Biology and Biochemistry*, **15**, 693–697.
- Wagner SW, Reicosky DC, Alessi RS (1997) Regression models for calculating gas fluxes measured with a closed chamber. *Agronomy Journal*, **89**, 279–284.
- Wrage N, Velthof GL, van Beusichem ML, Oenema O (2001) Role of nitrifier denitrification in the production of nitrous oxide. *Soil Biology and Biochemistry*, **33**, 1723–1732.
- Yamulki S, Jarvis SC (1999) Automated chamber technique for gaseous flux measurements: evaluation of a photoacoustic infrared spectrometer-trace gas analyzer. *Journal of Geophysical Research-Atmospheres*, **104**, 5463–5469.
- Yu K, Chen G (2009) Nitrous oxide emissions from terrestrial plants: observations, mechanisms and implications. In: *Nitrous Oxide Emissions Research Progress* (eds Sheldon AI, Barnbart EP), pp. 85–104. Nova Science Publishers, Hauppauge.

## Supporting Information

Additional Supporting Information may be found in the online version of this article:

**Figure S1.** Overview of soil properties and soil profile picture (sample date: 05-03-2010): (a) soil moisture profile (vol %) under fully flooded conditions, (b) bulk density profile (g cc<sup>-1</sup>), (c) calculated total porosity (%), (d) C/N ratio and (e) picture of soil profile. The upper 50–55 cm is dominated by peat with the main root zone occupying the top 25–30 cm. Carbonate rich organic silt is the dominating deposit at a depth of 55–60 cm.

**Figure S2.** Frequency distributions of significant N<sub>2</sub>O fluxes ( $P < 0.05$ ) in the period from 01-05-2010 to 10-10-2010.

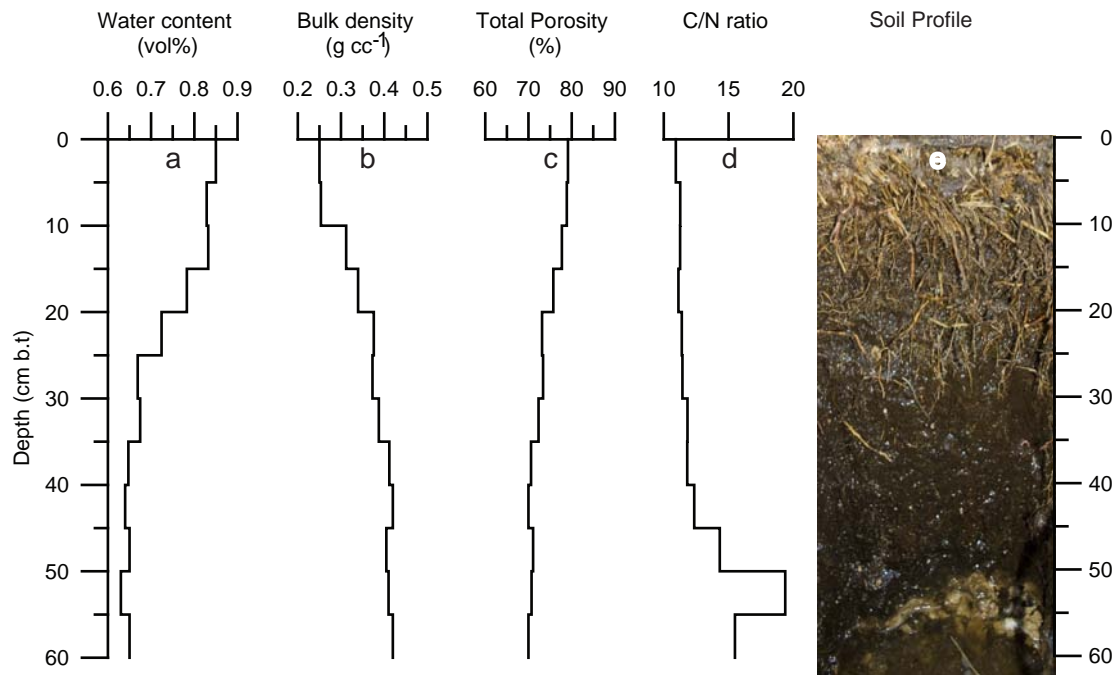
**Figure S3.** Pictures of microchamber used for testing the plant transport pathway as possible N<sub>2</sub>O conduit from the soil to the atmosphere. (a) Chamber under illuminated conditions (PAR = 300–400 W m<sup>-2</sup>), (b) chamber under simulated dark conditions (PAR = 0 W m<sup>-2</sup>).

**Figure S4.** Example of oxygen (O<sub>2</sub>) transport via plants in the period from 20 May 2010 to 01-06.2010.

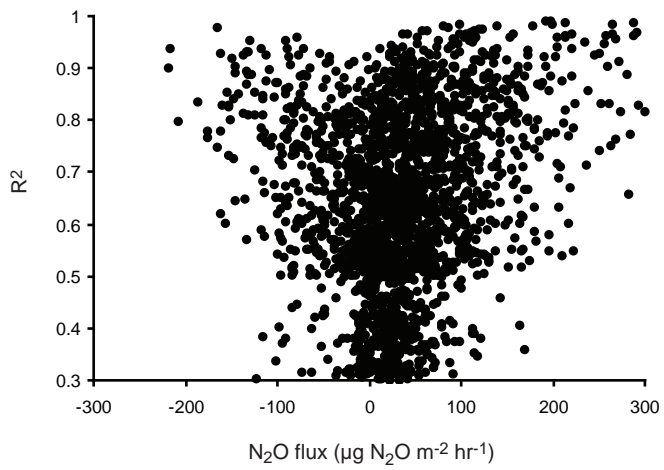
Please note: Wiley-Blackwell are not responsible for the content or functionality of any supporting materials supplied by the authors. Any queries (other than missing material) should be directed to the corresponding author for the article.





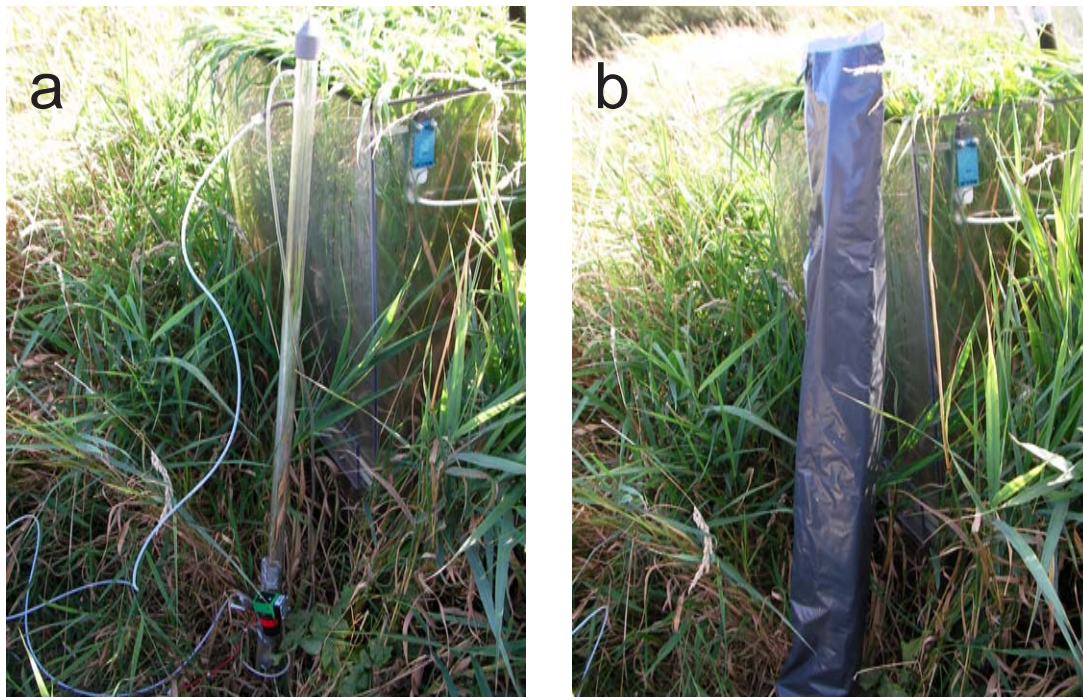


**SI Fig. 1.** Overview of soil properties and soil profile picture (Sample date: 05-03-2010): (a) Soil moisture profile (vol %) under fully flooded conditions, (b) Bulk density profile ( $\text{g cc}^{-1}$ ), (c) Calculated total porosity (%), (d) C/N ratio and (e) picture of soil profile. The upper 50-55 cm is dominated by peat with the main root zone occupying the top 25-30 cm. Carbonate rich organic silt is the dominating deposit at a depth of 55-60 cm.

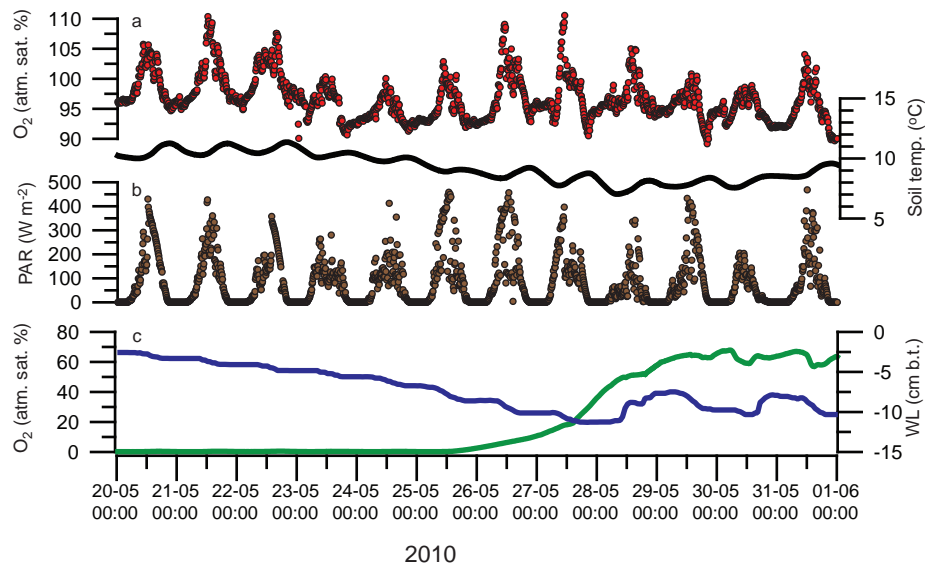


**SI Fig. 2.** Frequency distributions of significant  $N_2O$  fluxes ( $p < 0.05$ ) in the period 01-05-2010 to 10-10-2010.





**SI Fig. 3.** Pictures of micro chamber used for testing the plant transport pathway as possible N<sub>2</sub>O conduit from the soil to the atmosphere. (a) Chamber under illuminated conditions (PAR = 300 - 400 W m<sup>-2</sup>), (b) Chamber under simulated dark conditions (PAR = 0 W m<sup>-2</sup>).



**SI Fig. 4.** Example of oxygen (O<sub>2</sub>) transport via plants in the period 20-05-2010 to 01-06-2010. (a) O<sub>2</sub> concentrations in 5 cm (red circles) and soil temperature (black line), (b) PAR radiation (brown circles), (c) O<sub>2</sub> concentrations in 10 cm (green line) and water level (blue line). Significant correlation ( $p < 0.001$ ) between diurnal variations in PAR radiation ( $\text{W m}^{-2}$ ) indicates plant transport O<sub>2</sub> into the root zone as a result of active photosynthesis. The timing of the daily maximum soil temperature (5 cm) are on average delayed about 3 to 5 hours compared to maximum incoming radiation. In the first half of the period, O<sub>2</sub> concentration varies from full oxygenation at a depth of 5 cm to fully O<sub>2</sub> depleted at a depth of 10 cm b. t. Partial oxygenation of the soil at a depth of 10 cm b.t. is observed only when the WL decreases to a depth below 8-10 cm b.t. It therefore likely that the rate of plant transported O<sub>2</sub> into the soil, which presumably takes place over the majority of the root zone which occupies the upper 25-30 cm, does not appear to be high enough to exceed the respiratory O<sub>2</sub> consumption of roots and rhizomes under saturated conditions which would lead to an overall oxygenation of the saturated bulk soil.





# Annex IV





# Flooding-induced N<sub>2</sub>O production, consumption and emission dynamics in wetland soil

Christian Juncher Jørgensen<sup>1,\*</sup> & Bo Elberling<sup>1</sup>

<sup>1</sup> Department of Geography and Geology, University of Copenhagen, Øster Voldgade 10, Copenhagen, Denmark, Phone: +45 3532 2500, Fax: +45 3532 2501.

\* = corresponding author (cjj@geo.ku.dk; Phone: +45 3532 4180; Fax: +45 3532 2501)

## Abstract

Changes in flooding frequency of wetland soil following future climate change will likely affect the timing and magnitude of nitrous oxide (N<sub>2</sub>O) emissions. Rapid flooding of wetland soil promotes subsurface N<sub>2</sub>O production in the soil and potential emission to the atmosphere in distinctive emission pulses. From October 2009 to October 2010, rapid flooding of the studied wetland was observed twice in response to high precipitation events. A flooding induced N<sub>2</sub>O emission pulse (delay ~16 hrs; duration ~12 hrs; total emission 1.83 mg N<sub>2</sub>O-N, max. emissions ~250 µg N<sub>2</sub>O-N m<sup>-2</sup> hr<sup>-1</sup>) was observed after the soil conditions in the top soil had been oxidized for more than 2-3 weeks prior to flooding constituting ~2.5% of annual net N<sub>2</sub>O emissions of 0.74 kg N<sub>2</sub>O-N ha<sup>-1</sup> yr<sup>-1</sup>. Net uptake of atmospheric N<sub>2</sub>O was observed during mid-summer where the WL was at its seasonally lowest counterbalancing ~6.4% of the total annual net N<sub>2</sub>O emission budget. Main surface emission periods of N<sub>2</sub>O were observed when the water level and associated peaks in subsurface N<sub>2</sub>O concentrations were gradually decreasing to soil depths down to 40 cm below the surface. Soil flooding experiments using high-resolution N<sub>2</sub>O microsensors demonstrate very large N<sub>2</sub>O production and consumption capacities where >500 nmol N<sub>2</sub>O cm<sup>-3</sup> were sequentially produced and consumed in less than 24 hrs. Results indicate that 0.5-2.5% of the soil NO<sub>3</sub><sup>-</sup> present at the time of flooding was being emitted as N<sub>2</sub>O when the aerenchymous roots were removed, whereas this fraction was in the order of 1/3 of the NO<sub>3</sub><sup>-</sup> concentration present in the soil profile before and after flooding under natural field conditions. The observed difference highlights the importance of plant-specific N<sub>2</sub>O studies, as plant-mediated gas transport can be very important for the net annual N<sub>2</sub>O emission budget.

Keywords: Nitrous oxide, soil nitrogen transformation, denitrification, oxygen, flooding, water level, wetland, emission budget, microsensor.

*Submitted to Global Change Biology 22<sup>th</sup> August 2011.*

## Introduction

Future changes in precipitation patterns and fluctuating positions of the water level (WL) including increased flooding frequencies are likely to modify the current N<sub>2</sub>O emission dynamics from wetlands. Changes in precipitation patterns with increased frequency and intensity of rainfall events is one of the primary consequences of climate change (IPCC, 2007). Rapid natural shifts from drained to fully flooded soil conditions in wetland soil limit subsurface oxygen (O<sub>2</sub>) availability and provide improved conditions for

N<sub>2</sub>O production via denitrification by depletion of the soil nitrate (NO<sub>3</sub><sup>-</sup>) pool (Firestone and Davidson, 1989; Davidson, 1991; Martikainen *et al.* 1993; Kliewer and Gilliam, 1995).

Wetlands are often characterized by a large seasonal variation in the position of the WL and O<sub>2</sub> penetration depths resulting in contrasting environmental conditions for N<sub>2</sub>O production and consumption over time. The existence of a delicate N<sub>2</sub>O regulatory mechanism influenced by the position of the WL has been demonstrated in a number of studies (Kliewer and Gilliam, 1995; Aerts and Ludwig, 1997; Jungkunst *et al.* 2008;

Dinsmore *et al.* 2009; Berglund and Berglund, 2011; Regina *et al.* 1999). Results show that N<sub>2</sub>O emissions can occur following both falling and rising WL and highlight the potential importance and implications of flooding induced N<sub>2</sub>O emission pulses on the net ecosystem N<sub>2</sub>O emission budget.

Studies presenting surface flux data with a sufficiently high temporal resolution to capture real time dynamics from natural field conditions are very limited, and both the duration and magnitude of flooding induced N<sub>2</sub>O emissions remain unclear. Also the temporal linkages between the surface emission dynamics of N<sub>2</sub>O in response to rapid changes in WL and subsurface N<sub>2</sub>O concentrations need to be determined. Underestimation of net N<sub>2</sub>O surface emission from the soil to the atmosphere is likely if these N<sub>2</sub>O pulses are of significant proportions in relation to net annual surface emissions under both current and future climatic conditions.

Specific aims of this study were (i) to relate temporal WL variations to belowground N<sub>2</sub>O concentrations and net N<sub>2</sub>O surface emission patterns, (ii) to evaluate the temporal nature and total contribution of flooding induced N<sub>2</sub>O emissions to net annual N<sub>2</sub>O emissions from a non-managed Danish wetland and (iii) evaluate the temporal effects of changes in subsurface N<sub>2</sub>O production and consumption on net N<sub>2</sub>O emissions. The aims were achieved by a combination of field and laboratory experiments, where the linkages between simultaneous surface flux measurements and subsurface N<sub>2</sub>O concentration profiles were determined in the field using automated high temporal resolution flux chambers, subsurface gas concentration profiles and high spatial and temporal resolution N<sub>2</sub>O microsensor profiling in the laboratory.

## Materials and methods

### *Study site and soil description*

The Maglemeden experimental site is a non-managed minerotrophic wetland located approximately 20 km north of Copenhagen, Denmark (55°51'N, 12°32'E) with *P. arundinacea* as the dominating vegetation cover at the selected study site. Mean annual air temperature and precipitation is 8°C and 613 mm, respectively (Askaer *et al.* 2011). Histosols cover

the majority of the area with peat depths ranging from 0-3 m. At the experimental site, the soil moisture regime is udic, soil temperature regime is mesic, and the soil can be classified as a Fibric Haplohemist (USDA Soil Taxonomy) with an average peat thickness of 45 to 55 cm with the main root zone occupying the upper 25-30 cm. Soil porosity in the peat layers ranges from 70 to 80% by volume. Bulk density decreases gradually from 0.25 at the surface to 0.40 g cm<sup>-3</sup> at 60 cm depth (Elberling *et al.* 2011). The peat total organic C content ranges from 23 to 29%, while total N ranges from 1.8 to 2.4% resulting in peat C:N ratios of 10 to 12.

### *Environmental parameters*

The depth from the surface to the free standing water level (WL) was measured using a pressure sensor (PCR 1830 series, Druck; ThermX, San Diego, CA, USA) submerged in a 2 m long perforated plastic tube placed in a sand cast drill hole. The sensor was mounted on a horizontal bar attached to 3 m long stainless steel rods inserted into the underlying mineral soil, to avoid potential measurement errors caused by seasonal displacement of the surface following swelling and shrinkage of the peat soil.

Subsurface oxygen (O<sub>2</sub>) concentrations were measured at 5 and 10 cm depth using O<sub>2</sub>-optodes (O<sub>2</sub>-Dipstick, PreSens GmbG, Regensburg, Germany) connected to a multi channel fibreoptic O<sub>2</sub> meter (OXY-10, PreSens GmbG, Regensburg, Germany). The O<sub>2</sub>-optodes were calibrated in O<sub>2</sub>-free and O<sub>2</sub>-saturated water before permanent installation in the soil profile. Raw phase angle outputs were converted to temperature corrected O<sub>2</sub> concentrations (% atmospheric saturation) using soil temperature values measured at respective depths (Askaer *et al.* 2010).

Total nitrate (NO<sub>3</sub><sup>-</sup>) was determined as water extractable NO<sub>3</sub><sup>-</sup> on fresh soil samples (1:5 soil-water ratio) and determined by ion chromatography (IC system 761, Metrohm AG, Herisau, Switzerland) (Jørgensen *et al.* 2011).

Subsurface N<sub>2</sub>O concentrations were sampled on a weekly basis in 5 cm increments to a maximum depth of 60 cm using buried silicon probes (Jacinthe and Dick, 1996; Kammann *et al.* 2001).



### *Measurements of in situ N<sub>2</sub>O fluxes and flux rate calculation*

Surface fluxes of N<sub>2</sub>O were determined using five automated closed static chambers connected in replicate to a photoacoustic trace gas analyser (INNOVA 1312, LumaSense Technology Inc, Ballerup, Denmark)(Jørgensen *et al.* 2011). The five chambers were closed one at a time in a fixed sequence with one chamber being closed for 55 min followed by an open period of 4 hrs. In this way, chamber specific flux estimates could be obtained with a 5 hour temporal resolution.

Flux estimates were calculated using quadratic regression to account for potential non-linearity in the headspace gas increase over 30 min providing a more accurate estimate of N<sub>2</sub>O fluxes while returning the same estimate as the linear regression model in case of perfect linearity in headspace concentration increase/decrease (Wagner *et al.* 1997).

The arithmetic mean was used for calculating both the daily net flux and total annual sum of N<sub>2</sub>O fluxes because the method is both unbiased, robust and allows for the inclusion of negative fluxes (Velthof and Oenema, 1995). Daily averages of flux estimates from the five replicate chambers were chosen as method for estimating net ecosystem N<sub>2</sub>O flux magnitude and direction.

### *Laboratory flooding of soil columns*

An intact soil core of the top soil (dimensions L-W-D: 40-30-25 cm) was extracted on May 12<sup>th</sup> 2010 and left to drain freely at ambient temperature for 10 days. The soil core was split, homogenized and passed through a 2 mm mesh to remove the aboveground vegetation roots larger than 2 mm. Two experimental columns were constructed from a heavy walled PVC tube (Inner diameter: 70 mm, outer diameter: 90 mm; height: 100 mm) and closed at the bottom with a butyl rubber plug (height: 30 mm) to avoid diffusive gas loss at the lower boundary. Rhizon samplers (Rhizosphere Research Products, Wageningen, Netherlands) were inserted vertically in the wall of the column to facilitate depth-specific and sterile filtered water samples (2.5 mL water) for immediate pH and NO<sub>3</sub><sup>-</sup> concentration determinations (Shotbolt, 2010). Two columns were filled stepwise with homogenized peat soil (~100 g each) to achieve a similar porosity with depth. MilliQ water was added to both columns

ensuring an approximate 10 mm of free standing water above peat surface. Soil temperature at the flooding experiment was 20°C.

### *Microsensor profiles of N<sub>2</sub>O and O<sub>2</sub>*

Vertical concentration profiles of N<sub>2</sub>O and O<sub>2</sub> were measured in the soil columns on an hourly basis in 500 µm depth increments to a final soil depth of 22 mm using commercial N<sub>2</sub>O and O<sub>2</sub> microsensors with an outside tip diameter of 100 µm (Unisense, Denmark). The sensors were mounted side by side on a motorized micromanipulator and connected to a picoammeter (PA2000, Unisense, Denmark). The O<sub>2</sub> sensor was two-point calibrated in O<sub>2</sub> free and air saturated water. The N<sub>2</sub>O sensor was calibrated in water with 0, 100 and 200 µmol dissolved N<sub>2</sub>O and operated with a 50 sec equilibration time between measurements. An electrical failure caused corruption of the profiles between 23 and 25 hrs after flooding. Sensor calibration before and after the failure showed less than 2% drift. The integrated concentration of N<sub>2</sub>O was calculated as the cumulative N<sub>2</sub>O concentration in all measured depth per time step.

A contour map of subsurface N<sub>2</sub>O concentrations was constructed by kriging interpolation (Surfer Version 8.05, Golden Software Inc., Colorado, USA) of the measured N<sub>2</sub>O concentrations (n = 2440).

### *N<sub>2</sub>O flux estimates from flooded soil columns*

Hourly N<sub>2</sub>O fluxes were calculated using two independent methods: standard closed static chamber methodology and diffusive gas exchange across the diffusive boundary layer (DBL) at the interface between the oxic water layer and the top of the submerged peat surface, assuming no production or consumption of N<sub>2</sub>O at the DBL. Across the DBL, flow velocity is so low that molecular diffusion becomes the dominant form of mass transport. The flux of N<sub>2</sub>O across the DBL can be estimated by the linear slope of the measured concentration profile across the DBL using a modified version of Fick's 1<sup>st</sup> law of diffusion (Elberling and Damgaard, 2001; Beer and Stoodley, 2006) with an effective diffusion coefficient (D<sub>eff</sub>) of 2.2295 x 10<sup>-5</sup> cm<sup>2</sup> s<sup>-1</sup> for N<sub>2</sub>O in water at 20°C. First time of sampling (t<sub>0</sub>) was 30 min after flooding.

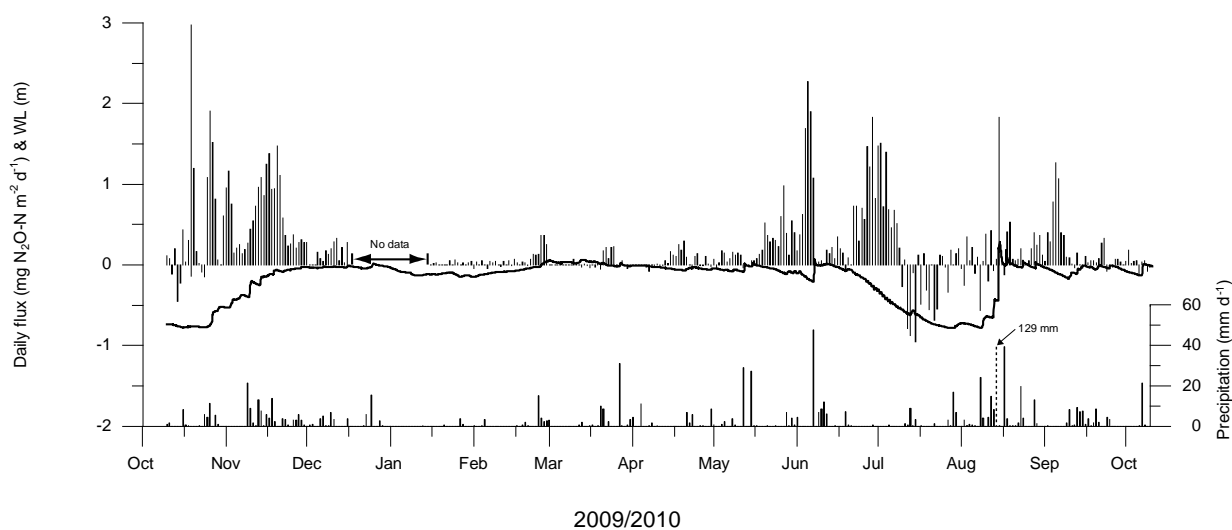


**Fig 1** N<sub>2</sub>O fluxes, precipitation and position of the water level (WL) in the period October 2009 to October 2010. Daily average N<sub>2</sub>O fluxes (left y-axis; mg N<sub>2</sub>O-N m<sup>-2</sup> d<sup>-1</sup>) are shown in the upper bar diagram (positive flux = emission and negative flux = uptake). The position of the WL (left y-axis; cm. below the surface) is shown by the solid line. Daily cumulative precipitation (right y-axis; mm d<sup>-1</sup>) is shown in the lower bar diagram (Note: Daily cumulative precipitation was of the scale with 129 mm on the 14<sup>th</sup> August 2010 and indicated by a dashed bar)

### *Modelling of depth-specific N<sub>2</sub>O production and consumption*

Production and consumption rates of N<sub>2</sub>O as a function of depth was estimated using the numerical model PROFILE (Berg *et al.* 1998; Elberling *et al.* 2010) under the assumption of near steady-state conditions at the time measurements. The model returns the simplest statistically significant ( $p < 0.05$ ) net production profile that approximates the measured concentration profile according to Fick's 2<sup>nd</sup> law of diffusion.

## **Results**

### *Precipitations and water level dynamics*

From October 2009 to October 2010, the amplitude of the observed WL variations was approximately 100 cm ranging from 80 cm below the surface in October 2009 and August 2010 to 20 cm above the surface following a large flooding event on 14<sup>th</sup> August 2010 (Fig. 1). The position of the WL was close to the surface during winter and spring and below 60 cm during summer and early autumn (Fig. 1).

The distance from the surface to the WL varied over the season in response to variations in evapotranspiration and precipitation events. Daily variations in the position of the WL of more than 5 cm day<sup>-1</sup> were only observed following precipitation events of more than 10 mm precipitation day<sup>-1</sup> (Fig. 1). Two natural flooding events were observed at the field site during the measurement periods, i.e. on June 07<sup>th</sup> 2010 and August 14<sup>th</sup> 2010. In both cases, extreme weather events with precipitation of 51 and 129 mm day<sup>-1</sup> caused the WL to rise in the range of 25-70 cm within 3-6 hrs (Fig. 1).

### *Subsurface N<sub>2</sub>O distribution*

Subsurface concentration profiles of N<sub>2</sub>O normalized to the position of the WL on the day of sampling show that maximum concentrations were observed at the capillary fringe -5 to 40 cm above the WL (Fig. 2). N<sub>2</sub>O concentrations were below ambient concentrations when position of the WL was close to the surface. During the autumn of 2009, the gradual increase in the position of the WL resulted in maximum subsurface N<sub>2</sub>O concentrations higher than 10 ppm, which were approximately 2-3 times the

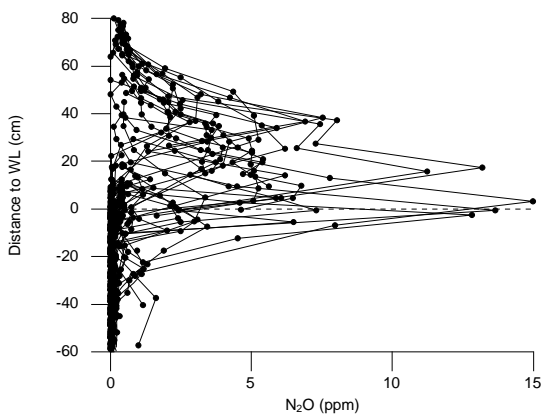


**Fig 2** Subsurface  $N_2O$  concentrations normalized to the position of the WL at the time of sampling.

concentrations observed when the WL was gradually decreasing.

#### *$N_2O$ flux dynamics*

Daily average net flux estimates of  $N_2O$  were in the range of  $-1$  to  $3 \text{ mg } N_2O\text{-N } m^{-2} d^{-1}$  (Fig. 1). Lowest fluxes were observed during winter and early spring. Pronounced daily and seasonal variations in both flux magnitude and direction were observed with the highest fluxes during the summer and early autumn (Jørgensen *et al.* 2011). Positive daily net fluxes of  $N_2O$  (emission) were dominating during the measurement period.

Periods with negative daily net fluxes (uptake) were primarily observed during October 2009 and July/August 2010. Four emission periods with consecutive daily positive fluxes above  $0.2 \text{ mg } N_2O\text{-N } m^{-2} d^{-1}$  were identified in November 2009, early June 2010, end July 2010 and early September 2010. The timing of these emissions periods were all linked to the gradual movements of the WL in soil depths of 5 to 35 cm below the surface (Fig. 1). Isolated emission pulses of 2 to  $3 \text{ mg } N_2O\text{-N } m^{-2} d^{-1}$  were observed on 19<sup>th</sup> Oct 2009 and 15<sup>th</sup> August 2010.

#### *$N_2O$ & $NO_3^-$ dynamics following field flooding*

The position of the WL, subsurface concentrations of  $N_2O$ ,  $NO_3^-$  and  $O_2$  as well as hourly net  $N_2O$  surface emissions before and after the June and August flooding events are shown in Figs. 3 & 4. Average daily soil temperatures at a depth of 10 cm were  $10.7 \pm 0.1^\circ C$  on June 7<sup>th</sup> 2010 and  $16.0 \pm 0.4^\circ C$  on August 14<sup>th</sup> 2010.

Three days before the June 7<sup>th</sup> flooding event, peak subsurface  $N_2O$  concentrations were located at the capillary fringe between 10 and 20 cm below the surface. Concentrations decreased to sub-ambient levels ( $<300$  ppb) below the position of the WL (Fig. 3a). Concentrations of  $NO_3^-$  increased with depth from a few  $\mu g \text{ } NO_3^-\text{-N } L^{-1}$  at 5 cm to approximately  $20\text{-}40 \mu g \text{ } NO_3^-\text{-N } L^{-1}$  between 15 and 40 cm below the surface (Fig. 3a). Four days after the first flooding event,  $N_2O$  concentrations were sub-ambient across the entire profile and  $NO_3^-$  concentrations between  $0\text{-}20 \mu g \text{ } NO_3^-\text{-N } L^{-1}$  (Fig. 3b). At the time of flooding, the WL increased from 20 cm below the surface to 5 cm above the surface within 6 hrs (Fig. 3c).

The average surface emission level was approximately  $90 \mu g \text{ } N_2O\text{-N } m^{-2} hr^{-1}$  in the days preceding the flooding event (Fig 3c). After the flooding event, emissions of  $N_2O$  decreased to below the detection limit.

Rapid responses in soil oxygenation status were observed following the WL rise, where the oxygen saturation degrees in 5 cm below the surface changed from 100% atm. saturation to  $<10\%$  atm. saturation within 6 hr, and from 75 % atm. saturation to fully anoxic within 2.5 hr at a depth of 10 cm below the surface (Fig. 3d).

The day before the August 14<sup>th</sup> flooding event (Fig. 4a), maximum subsurface  $N_2O$  concentrations were measured below the main root zone. In the root zone,  $N_2O$  concentrations were in the range of 0.5 to 2 ppm (Fig. 4a).  $NO_3^-$  levels increased from approximately  $20 \mu g \text{ } NO_3^-\text{-N } L^{-1}$  at a depth of 5 cm to  $30\text{-}35 \mu g \text{ } NO_3^-\text{-N } L^{-1}$  at a depth of 15-55 cm below the surface (Fig. 4a).

Three days after the second flooding event,  $N_2O$  concentrations were sub-ambient in most parts of the profile (Fig. 4b). At the same time,  $NO_3^-$  concentrations had decreased from an average of  $13.5 \text{ mg } NO_3^-\text{-N } L^{-1}$  before the flooding to an average of  $3.5 \text{ mg } NO_3^-\text{-N } L^{-1}$  (Fig. 4a,b). At the time of flooding, the WL increased from  $\sim 50$  cm below the surface to  $\sim 20$  cm above the surface within 2.5 hrs (Fig. 4c).

A pronounced  $N_2O$  emission pulse was observed approximately 16 hrs after the rapid WL increase on August 14<sup>th</sup> 2010 (Fig. 4c). The duration of the emission pulse was approximately 12 hrs with emission rates in the range of  $25\text{-}250 \mu g \text{ } N_2O\text{-N } m^{-2} hr^{-1}$ .  $N_2O$  fluxes were below  $25 \mu g \text{ } N_2O\text{-N } m^{-2} hr^{-1}$  in the days before and after the flooding event.

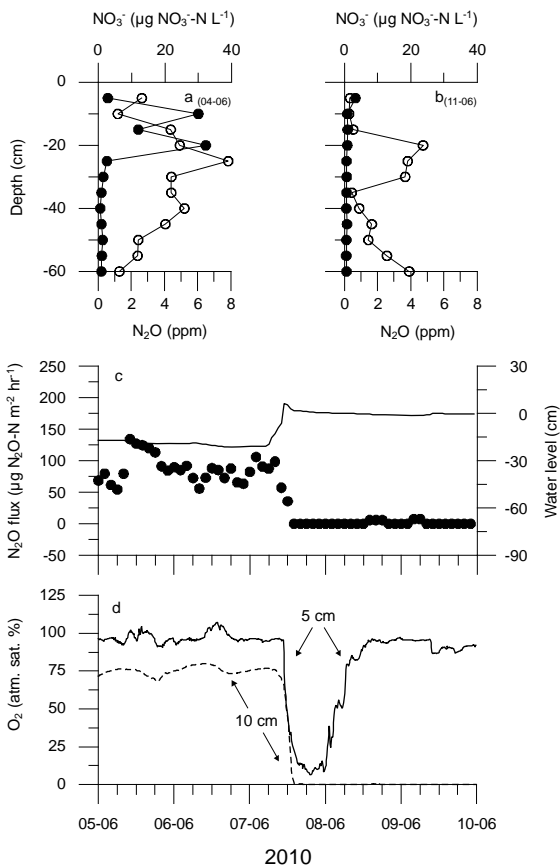


**Fig 3** Water level, subsurface  $N_2O$ ,  $NO_3^-$  and  $O_2$  concentrations and  $N_2O$  fluxes before and after a natural flooding event on 07-06-2010. a) Subsurface concentration profiles of  $N_2O$  (closed circles) and  $NO_3^-$  (open circles) on the 04-06-2010. b) Subsurface concentration profiles of  $N_2O$  (closed circles) and  $NO_3^-$  (open circles) on the 11-06-2010. c) Hourly average  $N_2O$  fluxes (closed circles) and position of the WL (black line; sample frequency resolution = 10 min). d) Subsoil oxygen concentrations (% atmospheric saturation) in 5 (solid line) and 10 (dashed line) cm below the surface (sample frequency resolution = 10 min).

Similar to the first flooding event, the oxygen saturation degrees in 5 and 10 cm below the surface changed from 100 % atm. saturation to anoxic conditions within 2.5 hr after the WL rise (Fig. 4d). Rapid  $O_2$  penetration to a depth of 5 cm was observed approximately 24 hrs after flooding.

#### *N<sub>2</sub>O dynamics following laboratory flooding*

The temporal effect of rapid flooding on  $N_2O$  production, consumption and emission rates was investigated under controlled laboratory conditions, where a previously drained peat soil was inundated and kept water covered with

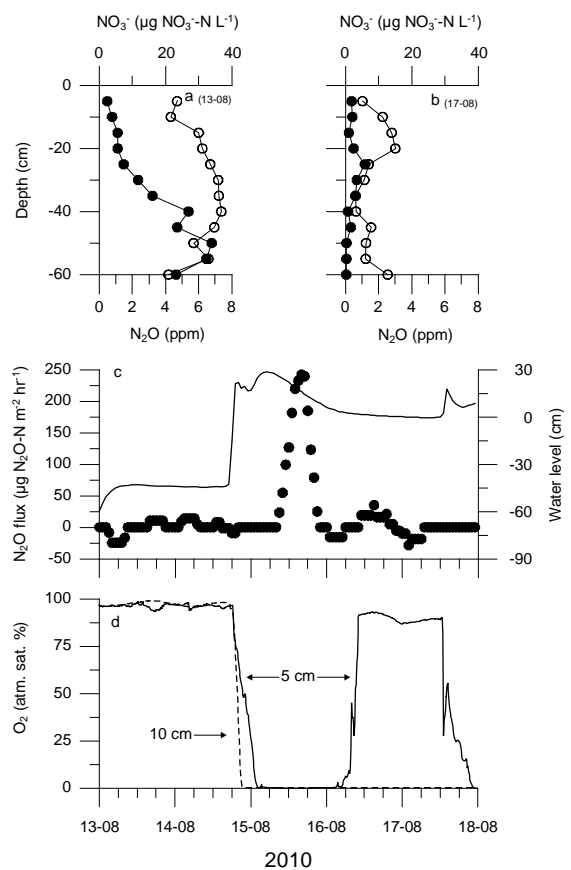


**Fig 4** Water level, subsurface  $N_2O$ ,  $NO_3^-$  and  $O_2$  concentrations and  $N_2O$  fluxes before and after a natural flooding event on 14-08-2010. a) Subsurface concentration profiles of  $N_2O$  (closed circles) and  $NO_3^-$  (open circles) on the 13-08-2010. b) Subsurface concentration profiles of  $N_2O$  (closed circles) and  $NO_3^-$  (open circles) on the 17-08-2010. c) Hourly average  $N_2O$  fluxes (closed circles) and position of the WL (black line; sample frequency resolution = 10 min). d) Subsoil oxygen concentrations (% atmospheric saturation) in 5 (solid line) and 10 (dashed line) cm below the surface (sample frequency resolution = 10 min).

~10mm of water above the soil surface (Fig. 5a-d). Decreasing  $NO_3^-$  concentrations of approx. 55 mg  $NO_3^-$ -N  $m^{-2}$  were observed in the first 14 hrs after flooding (Fig. 5a). In the same period of time, pH values increased gradually by approximately 0.4 pH step (Fig. 5a).

After an initial lag phase of approximately 4-6 hrs,  $N_2O$  concentrations increased with increasing depth (Fig. 5d). At soil depths of 0 to 5 mm below the surface,  $N_2O$  concentrations were observed to peak approximately 15 to 20 hrs after flooding, corresponding to the time of increasing surface fluxes (Fig. 5b,c). The highest subsurface  $N_2O$  concentrations ( $>500$  nmol  $cm^{-3}$ ) were measured

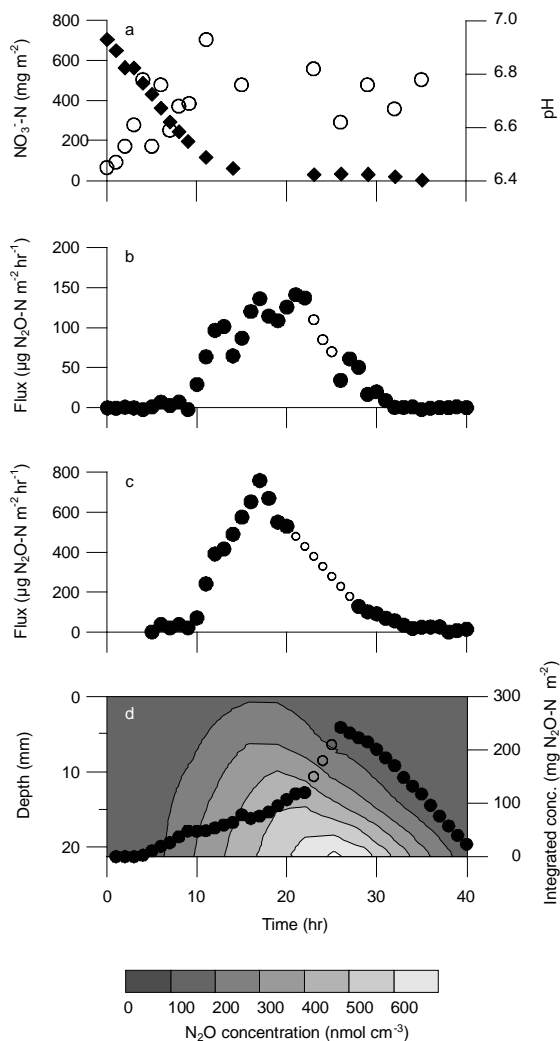


**Fig 5** N<sub>2</sub>O fluxes and N<sub>2</sub>O concentrations, NO<sub>3</sub><sup>-</sup> concentrations and pH during a flooding experiment. a) NO<sub>3</sub><sup>-</sup> concentrations (closed diamond) and pH (open circles) in the porewater over the incubation period. b) Net N<sub>2</sub>O flux estimates determined across the diffusive boundary layer. c) Net N<sub>2</sub>O flux estimate measured by the closed static chamber. d) Subsurface N<sub>2</sub>O concentrations over the incubation period (contour plot) and hourly integrated N<sub>2</sub>O concentration over the full measurement depth (closed circles). Note: open circles in b-d represent best estimate in case of missing data.

at the lowest part of the profile approximately 26 hrs after flooding (Fig. 5d). At the same time, both top soil concentrations and surface fluxes had started to decrease (Fig. 5b).

Integrated N<sub>2</sub>O concentrations over the entire profile showed a net increase in N<sub>2</sub>O concentrations in the first 22 hrs after flooding and a net decrease in N<sub>2</sub>O concentrations between 26 and 40 hrs after flooding (Fig. 5d). The sharp increase in integrated N<sub>2</sub>O concentrations at 26 hrs after flooding was caused by the occurrence of

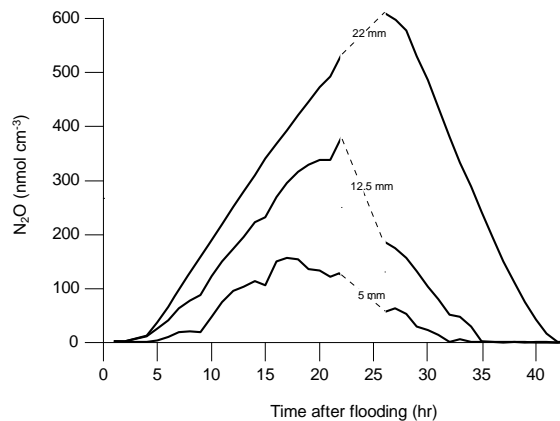


**Fig 6** Three depth specific N<sub>2</sub>O concentration profiles during the measurement period.

N<sub>2</sub>O concentrations above 500 nmol cm<sup>-3</sup> in the lower parts of the profile. Approximately 42 hrs after flooding, N<sub>2</sub>O concentrations were below the detection limit over the entire soil profile (data not shown).

Subsurface N<sub>2</sub>O concentrations at individual depths below 5 mm from the surface showed significant linear developments ( $p < 0.05$ ) from the first depth specific observation above/below a threshold of 10 nmol cm<sup>-3</sup> ( $C_{start}/C_{end}$ ) to/from the depth-specific maximum concentration ( $C_{max}$ ) (see Fig. 6). Depth-specific net N<sub>2</sub>O production rates were calculated from the slope of the linear line fit showing increasing net rates in both positive and negative directions with increasing depth below the surface (Table 1). At all profiled soil depths, the first observations above  $C_{start}$  were observed with a separation of just a few hrs. In contrast, the time of  $C_{max}$  and  $C_{end}$  differed by up to 10 hrs depending on the position in the profile.

Significant surface fluxes of N<sub>2</sub>O ( $p < 0.05$ ) were observed 10 to 32 hrs after the first measurement, using both the closed static chamber and DBL method (Fig. 5b,c). Maximum flux rates in both replicate columns were measured after approximately  $20 \pm 3$  hrs. Fluxes determined using the closed static chamber were on average 4 to 5 times greater than the corresponding point-based fluxes determined based on the measurements across the diffusive boundary layer.

#### *N<sub>2</sub>O production and consumption*

Figure 7 shows two examples of the concentration profiles from the time periods dominated by either net increasing integrated concentrations (IC)

( $t_0$  to  $t_{22}$ ) (Fig. 7a) or net decreasing integrated concentrations ( $t_{22}$  to  $t_{40}$ ) (Fig. 7b). Based on the significant fits ( $p < 0.01$ ) between the measured  $N_2O$  concentrations and modelled  $N_2O$  concentrations in the given examples, the numerical model PROFILE returns a net  $N_2O$  production best fit profile at  $t_{15}$  and net  $N_2O$  reduction best fit profile at  $t_{27}$  (Fig. 7c). Similar modelling have been conducted for the remaining concentration profiles showing an overall subsurface dominance of  $N_2O$  production processes in the period of net increasing IC ( $t_0$  to  $t_{22}$ ) and overall dominance of  $N_2O$  consumption processes in the period of net decreasing IC ( $t_{26}$  to  $t_{40}$ ).

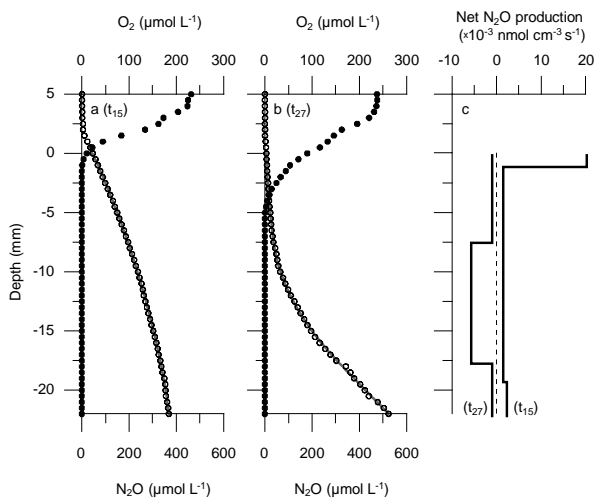


**Fig 7** Concentration profiles of  $N_2O$  and  $O_2$  at times of dominating  $N_2O$  production and consumption. a)  $N_2O$  (open circles) and  $O_2$  (closed circles) concentrations 15 hours after flooding normalized to the position of the surface (depth: 0 mm). b)  $N_2O$  (open circles) and  $O_2$  (closed circles) concentrations 27 hours after flooding normalized to the position of the surface (depth: 0 mm). c) Depth zonation of net  $N_2O$  production rates as modelled by PROFILE. Positive sign show net  $N_2O$  production and negative sign show net  $N_2O$  consumption. Modelled  $N_2O$  concentration profiles are shown by the black lines in a and b.

Depth (mm)	$C_{start}$ (hr)	$C_{max}$ (hr)	$C_{end}$ (hr)	Net positive rate (nmol cm <sup>-3</sup> hr <sup>-1</sup> )	Net negative rate (nmol cm <sup>-3</sup> hr <sup>-1</sup> )
5.0	6	17	31	14.19	-10.62
7.5	5	17	33	17.41	-14.14
10.0	5	18	33	20.52	-18.76
12.5	4	20	34	22.04	-23.38
15.0	4	21	35	24.25	-27.30
17.5	4	21	38	26.54	-29.34
20.0	4	26	40	26.39	-39.73
22.0	4	26	42	28.55	-43.99

**Table 1** Apparent net  $N_2O$  production rates in 8 depths over the duration of the flooding experiment.  $C_{start}$  and  $C_{end}$  denotes the hour after flooding where the concentrations were above/below a threshold concentration of 10 nm cm<sup>-3</sup>

## Discussion

### Hydrological controls on $O_2$ availability and redox conditions

The temporal trends in  $O_2$  depletion were observed to be of similar proportions in both the presence of aerenchymous roots under field conditions (Figs. 3 & 4), and in the absence of roots in the experimental soil columns. This indicates that the rates of respiratory oxygen consumption were much greater than the diffusive influx of  $O_2$  via plant roots or across the soil surface when soils were rapidly flooded and a likely indicator of non-limiting availability of dissolved carbon (C) in the peat soil.

### Flooding induced $N_2O$ production and consumption

A lag phase of approximately 4-5 hrs between the onset of  $NO_3^-$  reduction and  $N_2O$  production was observed in the flooding experiment and is considered a result of the time period needed for the expression of relevant  $NO_x$ -reducing enzymes eventually leading to  $N_2O$  formation.

The average  $NO_3^-$  concentration in the first water samples taken 30 min after flooding of the soil columns in the laboratory was  $\sim 700$  mg  $NO_3^-$ -N m<sup>-2</sup> (Fig. 5a). Under the assumption that this concentration is representative for the entire homogenized soil volume, a complete reduction of this  $NO_3^-$  into  $N_2O$  without any further reduction to  $N_2$  would result in a potential  $N_2O$  production  $\sim 350$  mg  $N_2O$ -N m<sup>-2</sup>. Approximately 26 hrs after flooding,  $NO_3^-$  concentrations were below 10 mg  $NO_3^-$ -N m<sup>-2</sup>. At the same time, the integrated subsurface  $N_2O$  concentration was 243.8 mg  $N_2O$ -N m<sup>-2</sup>, corresponding to  $\sim 70\%$  of the potential  $N_2O$  production under the stated assumption. At 42 hrs after flooding, integrated  $N_2O$  concentrations were below the detection limit. Cumulative surface fluxes measured across the DBL and by the closed static chamber over the entire incubation period (Fig. 5b,c) were 1.76 and 8.35 mg  $N_2O$ -N m<sup>-2</sup>, equal to approximately 0.5 and 2.5% of the potential  $N_2O$  production after complete reduction of initial  $NO_3^-$  to  $N_2O$ , or 0.7 and 3.4% of the measured integrated  $N_2O$  concentrations. Two main conclusions can be made from these calculations: First, since the complete amount of the initial  $NO_3^-$  was reduced over the duration of the flooding experiment and



approximately 70% can be explained by the observed N<sub>2</sub>O production, it follows that the remaining 30% of the initial NO<sub>3</sub><sup>-</sup> may either have been transformed into ammonium (NH<sub>4</sub><sup>+</sup>) by dissimilatory NO<sub>3</sub><sup>-</sup> reduction to NH<sub>4</sub><sup>+</sup> (DNRA) (Kelso *et al.* 1997; Scott *et al.* 2008), have been transformed into organic-N compounds or have been reduced to N<sub>2</sub> before the calculated maximum in integrated N<sub>2</sub>O concentrations. Secondly, the unaccounted fractions between both the potential N<sub>2</sub>O production and measured integrated concentration versus the measured cumulative surface fluxes must have been consumed within the soil profile in the process of complete denitrification to N<sub>2</sub> similar to the observation in (Rückauf *et al.* 2004), as no other N<sub>2</sub>O consumption process is currently known.

N<sub>2</sub>O production-consumption reaction dynamics in which positive rates of N<sub>2</sub>O production is switched off by the depletion of NO<sub>3</sub><sup>-</sup> has previously been demonstrated using production rate modelling with a calibrated mechanistic diffusion-reaction model (Markföged *et al.* 2011). This model accounts for the diffusive mass loss across the soil-atmosphere interface and explains the shift in the production rate by NO<sub>3</sub><sup>-</sup> depletion (Markföged *et al.* 2011). In the current study, a similar production-consumption sequence was observed, where the periods of net N<sub>2</sub>O production and net N<sub>2</sub>O consumption were clearly separated within just a few hrs (Fig. 6).

#### *N<sub>2</sub>O emission pulses following soil flooding*

Emission pulses of N<sub>2</sub>O were observed in the hrs following the rapid rises in WL under field conditions on August 14<sup>th</sup> 2010 (maximum emission rates ~250 µg N<sub>2</sub>O-N m<sup>-2</sup> hr<sup>-1</sup>) (Fig. 4c) and in the controlled laboratory experiment (max. emission rates ~150-800 µg N<sub>2</sub>O-N m<sup>-2</sup> hr<sup>-1</sup>) (Fig. 5b,c). In both cases, the onset of the N<sub>2</sub>O emission pulse was observed approximately 10-12 hrs after flooding or approximately 6 hrs after complete O<sub>2</sub> depletion of the top soil.

The durations of the flooding induced emission pulses were approximately 20-24 hrs in the laboratory and 12 hrs under field conditions and linked to initial NO<sub>3</sub><sup>-</sup> concentrations prior to flooding. The total amount of NO<sub>3</sub><sup>-</sup> accumulated in the field across the measured soil depth (0-60 cm) at a given sample point was calculated as the sum of NO<sub>3</sub><sup>-</sup> concentrations in each sample depth

corrected for depth-specific variations in bulk density, porosity and soil moisture content. In this way, the total NO<sub>3</sub><sup>-</sup> amount in the soil profile were 13.45 mg NO<sub>3</sub><sup>-</sup>-N m<sup>-2</sup> and 3.58 mg NO<sub>3</sub><sup>-</sup>-N m<sup>-2</sup> on the August 13<sup>th</sup> and 17<sup>th</sup> 2010, respectively. If the difference in NO<sub>3</sub><sup>-</sup> concentrations between these two dates were transformed into N<sub>2</sub>O without further reduction into N<sub>2</sub>, an approximate 5 mg N<sub>2</sub>O-N m<sup>-2</sup> would be produced, which could be emitted in the hrs and days following the natural flooding event. Cumulative surface fluxes measured in the field in the hrs following flooding (Fig. 4c) were 1.83 mg N<sub>2</sub>O-N m<sup>-2</sup>. If this surface flux originates from the reduction of the soil NO<sub>3</sub><sup>-</sup>, as much as 1/3 of the calculated difference in soil NO<sub>3</sub><sup>-</sup> across the entire soil profile was emitted as N<sub>2</sub>O following flooding.

An important difference between field and laboratory conditions is the presence or absence of the above-ground biomass and aerenchymous roots and rhizosphere, which serves as potential gas transport pathway via aerenchymous plant tissue (Yu and Chen, 2009). Also, coupled nitrification-denitrification in the root zone can be maintained under submerged conditions via rhizosphere oxygenation (Patrick and Reddy, 1976; Engelaar *et al.* 1995; Bodelier *et al.* 1996) while photosynthetically assimilated labile C can be provided to the soil microbial biomass by internal translocation and excretion from the roots (Edwards *et al.* 2006). These differences are likely reflected in the marked difference between laboratory and field ratios of the potential amount of N<sub>2</sub>O being produced and emitted (assuming full NO<sub>3</sub><sup>-</sup> reduction to N<sub>2</sub>O) versus the measured cumulative N<sub>2</sub>O surface flux. In the current study, main N<sub>2</sub>O emissions and subsurface N<sub>2</sub>O concentrations were observed during the growing season of *Phalaris arundinacea* when the position of the WL and associated peak N<sub>2</sub>O concentrations at the capillary fringe were located at depths corresponding to the root zone. A comparison between the depth of maximum N<sub>2</sub>O concentrations and observed surface fluxes indicates that a certain limiting depth of approximately 30-40 cm exists in the field. When the maximum concentrations of N<sub>2</sub>O are above the limiting depth, surface emissions occur while the opposite occurs when maximum concentrations are below. This indicates the importance of root zone processes in regulating O<sub>2</sub> and NO<sub>3</sub><sup>-</sup> availability for N<sub>2</sub>O producing and consuming processes, modified by seasonal variation in root

exudation of C compounds in response to plant growth stage (Edwards *et al.* 2006). However, contrasting results have been reported on how the presence of *P. arundinacea* potentially modifies net emission rates: No significant alterations on N<sub>2</sub>O emissions by *P. arundinacea* was reported by (Rückauf *et al.* 2004) whereas the presence of the *P. arundinacea* increased the annual N<sub>2</sub>O emissions 10-fold from approximately 65 to 650 g N<sub>2</sub>O-N ha<sup>-1</sup> year<sup>-1</sup> compared to unplanted peat soil in (Hyvoenen *et al.* 2009), but approximately halved the daily emission rates from unplanted peat soil from 0.04 to 0.02 mg N<sub>2</sub>O-N m<sup>-2</sup> day<sup>-1</sup> in (Maltais-Landry *et al.* 2009).

#### *Field scale linkages between subsurface N<sub>2</sub>O concentrations and net emissions*

At the capillary fringe above the WL, the soil was characterised by having close to sub-saturated soil moisture degrees and mixed aerobic/anaerobic conditions, promoting the environmental conditions favourable for both N<sub>2</sub>O production via denitrification and NO<sub>3</sub><sup>-</sup> reduction via DNRA (Magonigal *et al.* 2003). Combined data on WL position, O<sub>2</sub>-penetration depth and NO<sub>3</sub><sup>-</sup> concentrations in the soil indicate that WL changes within the root zone is an important driver for sustained N<sub>2</sub>O emissions above 0.2 mg N<sub>2</sub>O-N m<sup>-2</sup> day<sup>-1</sup>. In contrast, very rapid WL changes following flooding only produced N<sub>2</sub>O emission pulses when soil conditions had been oxidized in more than 2-3 weeks before the flooding, allowing NO<sub>3</sub><sup>-</sup> concentrations to increase to levels above ~20 µg NO<sub>3</sub><sup>-</sup>-N L<sup>-1</sup>. The importance of this temporal aspect of subsoil oxygenation and NO<sub>3</sub><sup>-</sup> generation can be seen by comparison of the June and August flooding events (Fig. 1), where an emission pulse only occurred when the top soil had been oxidized in the weeks before the changing WL position. Similar contrasting effect on rapid WL increases has been demonstrated in (Regina *et al.* 1999) and (Dinsmore *et al.* 2009). In the first study it was concluded, that raising the WL caused a cessation of the N<sub>2</sub>O fluxes from the peat soil, whereas the latter observed a N<sub>2</sub>O emission pulse approximately 2 days after manually raising the WL.

#### *Annual N<sub>2</sub>O flux budget*

The annual N<sub>2</sub>O flux sum based on cumulated daily N<sub>2</sub>O fluxes was 74 mg N<sub>2</sub>O-N m<sup>-2</sup> year<sup>-1</sup> over the investigated time period (October 2009 to October 2010) and was of similar proportions to what has been reported from other *Phalaris arundinacea* dominated areas (Hyvönen *et al.* (2009) ~ 64 mg N<sub>2</sub>O-N m<sup>-2</sup> year<sup>-1</sup>; Jin *et al.* (2010) unfertilized control plot ~60 mg N<sub>2</sub>O-N m<sup>-2</sup> year<sup>-1</sup>). In the period July 10<sup>th</sup> and August 10<sup>th</sup> 2010 where net N<sub>2</sub>O sink activity was dominating, the total sum of daily surface fluxes was approximately -4.7 mg N<sub>2</sub>O-N m<sup>-2</sup>, counterbalancing approx. 6.4% of the annual N<sub>2</sub>O flux sum. In the same way, the cumulative sum of the flooding induced N<sub>2</sub>O emissions of approximately 1.83 mg N<sub>2</sub>O-N m<sup>2</sup> on the 14<sup>th</sup> August 2010 (Fig. 4c), constituted approximately 2.5% of the annual N<sub>2</sub>O flux sum.

A conservative estimate of the average annual sum of dry and wet deposition of N to Danish land areas is approximately 17 kg N ha<sup>-1</sup> year<sup>-1</sup> (Asman, 2001). Under the assumption that this deposition rates is representative for the Maglemosen study site, and that no other local N-source contribute to the annual N-input, roughly 4-5% of the N deposition input to the ecosystem would be sufficient to fuel the measured annual net N<sub>2</sub>O-N emission of 0.74 kg N<sub>2</sub>O-N ha<sup>-1</sup> year<sup>-1</sup>. A comparison between this annual N<sub>2</sub>O load from the studied non-managed wetland and the estimated total annual N<sub>2</sub>O emissions from Danish agricultural land areas of 7.3 kg N<sub>2</sub>O-N ha<sup>-1</sup> year<sup>-1</sup> (Boeckx and Van Cleemput, 2001) shows that the mean annual N<sub>2</sub>O emission rate from a natural ecosystem as Maglemosen could be roughly 10% of the average emission from agricultural areas. While this fraction may appear surprisingly high, the climatic impact of N<sub>2</sub>O emissions from this type of non-managed minerotrophic wetland will be limited, due to the relative low land area coverage percentage compared to agricultural areas. Nonetheless, the results show that natural wetland ecosystems have the potential of modifying atmospheric N<sub>2</sub>O concentrations by having substantial net source and sink capacities, which relative distribution is governed by the seasonal changes in NO<sub>3</sub><sup>-</sup> availability following changes in subsoil oxygenation status and WL variations.

## Summary and perspectives

The highest subsurface N<sub>2</sub>O concentrations were observed at the capillary fringe just above the WL, while the lowest concentrations were observed below the position of the WL. Very low net surface emission were observed during the winter and early spring when the position of the WL was close to the surface and subsurface N<sub>2</sub>O concentrations close to or below ambient concentration. Main surface emission periods of N<sub>2</sub>O were observed at times when the WL and associated peaks in subsurface N<sub>2</sub>O concentrations were gradually decreasing to soil depths down to 40 cm below the surface, corresponding to the vertical extent of the root zone of the subsurface aerating macrophyte *Phalaris arundinacea*. Sustained N<sub>2</sub>O emissions were primarily observed in response to gradual movements of the WL through the root zone. Rapid flooding of the soil profile was observed twice during the season in response to high precipitation events. A flooding induced N<sub>2</sub>O emission pulse was only observed when the soil conditions had been oxidized to soil depths below approximately 30 cm in more than 2-3 weeks before the flooding.

The majority of the net annual N<sub>2</sub>O surface fluxes were observed during the growing season in the summer and autumn months where the combination of seasonally highest soil and air temperatures, highest evapotranspiration, greatest O<sub>2</sub> penetration depths and root exudation of labile organic carbon stimulates microbial N-transformation leading to high potential N<sub>2</sub>O production and consumption rates affecting the net emissions of N<sub>2</sub>O across the soil-atmosphere interface. A net N<sub>2</sub>O sink capacity counterbalancing of approximately 6.4% of the total annual net N<sub>2</sub>O emission was observed during mid-summer, whereas the short-lived flooding induced N<sub>2</sub>O pulse constituted approximately 2.5% of annual net N<sub>2</sub>O emissions.

Microsensor production and consumption profiles demonstrate very large and rapid N<sub>2</sub>O production and consumption capacities in the peat soil where concentrations of more than 500 nmol N<sub>2</sub>O cm<sup>-3</sup> were produced or consumed in the soil in less than 24 hrs. The presence of this large inherent N<sub>2</sub>O consumption capacity in the top soil is a likely explanation for the observed net sink activity under field conditions in mid-summer and the low net N<sub>2</sub>O fluxes when peak concentrations of subsurface N<sub>2</sub>O were observed at soil depths

lower than 30-40 cm. Under these conditions, the length of the diffusion path from the soil depths of production to the soil-atmosphere interface leads to high residence times in the soil and an increased potential for full reduction to N<sub>2</sub>. The incubation experiments further showed that approximately 0.5-2.5% of the soil NO<sub>3</sub><sup>-</sup> present at the time of flooding was being emitted as N<sub>2</sub>O when the aerenchymous roots were removed. By comparison, this fraction was approximately 1/3 of the NO<sub>3</sub><sup>-</sup> concentration present in the soil profile before and after flooding under natural field conditions, highlighting the potential importance of plant-mediated gas transport for the net annual N<sub>2</sub>O emission budget across the soil-atmosphere interface and the interactions between plants and microbes.

Under current climatic conditions, flooding-induced N<sub>2</sub>O emission pulses constitute only a small percentage of the net annual N<sub>2</sub>O emission budget and the relative contribution of such pulses to the net annual emission is not considered important. Given the large N<sub>2</sub>O consumption capacity in the peat soil, future increases flooding frequency is not expected to increase net annual N<sub>2</sub>O emissions significantly unless future rates on NO<sub>3</sub><sup>-</sup> formation in the soil are increased. In this way, the shown linkages between WL variations, plant growth of *P. arundinacea* and root zone transformation of O<sub>2</sub>, NO<sub>3</sub><sup>-</sup> and N<sub>2</sub>O call for future studies focusing on N<sub>2</sub>O production, consumption and surface emission following future changes in plant growth, root zone oxidation, C excretion and NO<sub>3</sub><sup>-</sup> resource competition between soil microbes and a wider range in species of subsurface aerating macrophytes.

## Acknowledgements

This work was conducted within the framework of the project "Nitrous oxide dynamics: The missing links between controls on subsurface N<sub>2</sub>O production/consumption and net atmospheric emissions" financed by the Danish Natural Science Research Council (PI: B.E.) The authors wish to thank Rune Skalborg for help with fieldwork, Paul Christiansen for help building and installing the flux chambers, Bo Holm-Rasmussen for technical support and programming assistance, Per Ambus (Risø DTU) for with help GC analyses and to Sten Struwe (University of Copenhagen, Department of Microbiology) for supplying the trace gas analyzer.

## Reference List

- Aerts R, Ludwig F (1997) Water-table changes and nutritional status affect trace gas emissions from laboratory columns of peatland soils. *Soil Biology & Biochemistry*, **29**, 1691-1698.
- Askaer L, Elberling B, Glud RN, Kuhl M, Lauritsen FR, Joensen HP (2010) Soil heterogeneity effects on O<sub>2</sub> distribution and CH<sub>4</sub> emissions from wetlands: In situ and mesocosm studies with planar O<sub>2</sub> optodes and membrane inlet mass spectrometry. *Soil Biology and Biochemistry*, **42**, 2254-2265.
- Asman WAH (2001) Modelling the atmospheric transport and deposition of ammonia and ammonium: an overview with special reference to Denmark. *Atmospheric Environment*, **35**, 1969-1983.
- Beer D, Stoodley P (2006) Microbial Biofilms. In: *The Prokaryotes* (eds Dworkin M, Falkow S, Rosenberg E, Schleifer KH, Stackebrandt E), pp. 904-937. Springer New York.
- Berg P, Risgaard-Petersen N, Rysgaard S (1998) Interpretation of measured concentration profiles in sediment pore water. *Limnology and Oceanography*, **43**, 1500-1510.
- Berglund Í, Berglund K (2011) Influence of water table level and soil properties on emissions of greenhouse gases from cultivated peat soil. *Soil Biology and Biochemistry*, **43**, 923-931.
- Bodelier PLE, Libochant JA, Blom CWPM, Laanbroek HJ (1996) Dynamics of nitrification and denitrification in root-oxygenated sediments and adaptation of ammonia-oxidizing bacteria to low-oxygen or anoxic habitats. *Applied and Environmental Microbiology*, **62**, 4100-4107.
- Boeckx P, Van Cleemput O (2001) Estimates of N<sub>2</sub>O and CH<sub>4</sub> fluxes from agricultural lands in various regions in Europe. *Nutrient Cycling in Agroecosystems*, **60**, 35-47.
- Davidson EA (1991) Fluxes of Nitrous Oxide and Nitric Oxide from Terrestrial ecosystems. In: *Microbial Production and Consumption of Greenhouse Gases: Methane, Nitrogen Oxides, and Halomethanes* (eds Rogers JE, Whitman WB), pp. 219-235. American Society of Microbiology, Washington, D.C.
- Dinsmore KJ, Skiba UM, Billett MF, Rees RM (2009) Effect of water table on greenhouse gas emissions from peatland mesocosms. *Plant and Soil*, **318**, 229-242.
- Edwards KR, Cizkova H, Zemanova K, Santruckova H (2006) Plant growth and microbial processes in a constructed wetland planted with *Phalaris arundinacea*. *Ecological Engineering*, **27**, 153-165.
- Elberling B, Christiansen HH, Hansen BU (2010) High nitrous oxide production from thawing permafrost. *Nature Geoscience*, **3**, 332-335.
- Elberling B, Askaer L, Jørgensen CJ, Joensen HP, Kuhl M, Glud RN, Lauritsen FR (2011) Linking Soil O<sub>2</sub>, CO<sub>2</sub>, and CH<sub>4</sub> Concentrations in a Wetland Soil: Implications for CO<sub>2</sub> and CH<sub>4</sub> Fluxes. *Environmental Science & Technology*, **45**, 3393-3399.
- Elberling B, Damgaard LR (2001) Microscale measurements of oxygen diffusion and consumption in subaqueous sulfide tailings. *Geochimica et Cosmochimica Acta*, **65**, 1897-1905.
- Engelaar WMHG, Symens JC, Laanbroek HJ, Blom CWPM (1995) Preservation of Nitrifying Capacity and Nitrate Availability in Waterlogged Soils by Radial Oxygen Loss from Roots of Wetland Plants. *Biology and Fertility of Soils*, **20**, 243-248.
- Firestone MK, Davidson EA (1989) Microbiological Basis of NO and N<sub>2</sub>O Production and Consumption in Soil. *Exchange of Trace Gases Between Terrestrial Ecosystems and the Atmosphere*, **47**, 7-21.
- Hyvoenen NP, Huttunen JT, Shurpali NJ, Tavi NM, Repo ME, Martikainen PJ (2009) Fluxes of nitrous oxide and methane on an abandoned peat extraction site: Effect of reed canary grass cultivation. *Bioresource Technology*, **100**, 4723-4730.
- IPCC (2007) *The Physical Science Basis. Contribution of Working Group I to the Fourth Assessment Report of the Intergovernmental Panel on Climate Change*. Cambridge University Press, Cambridge.
- Jacinte PA, Dick WA (1996) Use of silicone tubing to sample nitrous oxide in the soil atmosphere. *Soil Biology & Biochemistry*, **28**, 721-726.
- Jørgensen CJ, Struwe S, Elberling B (2011) Temporal trends in N<sub>2</sub>O flux dynamics in a Danish wetland. Effects of plant-mediated gas transport of N<sub>2</sub>O and O<sub>2</sub> following changes in water level and soil mineral-N availability. *Global Change Biology*. In Press, doi:10.1111/j.1365-2486.2011.02485.x.
- Jungkunst HF, Flessa H, Scherber C, Fiedler S (2008) Groundwater level controls CO<sub>2</sub>, N<sub>2</sub>O and CH<sub>4</sub> fluxes of three different hydromorphic soil types of a temperate forest ecosystem. *Soil Biology and Biochemistry*, **40**, 2047-2054.
- Kammann C, Grünhage L, Jäger HJ (2001) A new sampling technique to monitor concentrations of CH<sub>4</sub>, N<sub>2</sub>O and CO<sub>2</sub> in air at well-defined depths in soils with varied water potential. *European Journal of Soil Science*, **52**, 297-303.
- Kelso BHL, Smith RV, Laughlin RJ, Lennox SD (1997) Dissimilatory nitrate reduction in anaerobic sediments leading to river nitrite accumulation. *Applied and Environmental Microbiology*, **63**, 4679-4685.
- Kliewer BA, Gilliam JW (1995) Water-Table Management Effects on Denitrification and Nitrous-Oxide Evolution. *Soil Science Society of America Journal*, **59**, 1694-1701.
- Maltais-Landry G, Maranger R, Brisson J, Chazarenc F (2009) Greenhouse gas production and efficiency of planted

and artificially aerated constructed wetlands. *Environmental Pollution*, **157**, 748-754.

Markfoged R, Nielsen LP, Nyord T, Ottosen LDM, Revsbech NP (2011) Transient N<sub>2</sub>O accumulation and emission caused by O<sub>2</sub> depletion in soil after liquid manure injection. *European Journal of Soil Science*, **62**, 1-10.

Martikainen PJ, Nykanen H, Crill P, Silvola J (1993) Effect of A Lowered Water-Table on Nitrous-Oxide Fluxes from Northern Peatlands. *Nature*, **366**, 51-53.

Megonigal JP, Hines ME, Visscher PT (2003) Anaerobic Metabolism: Linkages to Trace Gases and Aerobic Processes. In: *Treatise on Geochemistry* (eds Heinrich DH, Karl KT), pp. 317-424. Pergamon, Oxford.

Patrick WH, Reddy KR (1976) Nitrification-Denitrification Reactions in Flooded Soils and Water Bottoms - Dependence on Oxygen-Supply and Ammonium Diffusion. *Journal of Environmental Quality*, **5**, 469-472.

Regina K, Silvola J, Martikainen PJ (1999) Short-term effects of changing water table on N<sub>2</sub>O fluxes from peat monoliths from natural and drained boreal peatlands. *Global Change Biology*, **5**, 183-189.

Rückauf U, Augustin J, Russow R, Merbach W (2004) Nitrate removal from drained and reflooded fen soils affected by soil N transformation processes and plant uptake. *Soil Biology and Biochemistry*, **36**, 77-90.

Scott J, McCarthy M, Gardner W, Doyle R (2008) Denitrification, dissimilatory nitrate reduction to ammonium, and nitrogen fixation along a nitrate concentration gradient in a created freshwater wetland. *Biogeochemistry*, **87**, 99-111.

Shotbolt L (2010) Pore water sampling from lake and estuary sediments using Rhizon samplers. *Journal of Paleolimnology*, **44**, 695-700.

Velthof GL, Oenema O (1995) Nitrous oxide fluxes from grassland in the Netherlands .1. Statistical analysis of flux-chamber measurements. *European Journal of Soil Science*, **46**, 533-540.

Wagner SW, Reicosky DC, Alessi RS (1997) Regression models for calculating gas fluxes measured with a closed chamber. *Agronomy Journal*, **89**, 279-284.

Yu K, Chen G (2009) Nitrous Oxide Emissions from Terrestrial Plants: Observations, Mechanisms and Implications. In: *Nitrous Oxide Emissions Research Progress* (eds Sheldon AI, Barnbart EP), pp. 85-104. Nova Science Publishers.

